IRON NICKEL SEPARATION AT HIGH CONCENTRATION SOLUTIONS USING ION EXCHANGE

by © René Alberto Silva Jimenez

A Thesis submitted to

School of Graduate Studies in partial fulfilment of the

requirements for the degree of

Doctor of Philosophy

Department of Process Engineering

Faculty of Engineering and Applied Science

Memorial University of Newfoundland

August 23, 2021

St. John's, Newfoundland and Labrador

Abstract

Separation of iron from nickel and other base metals is an indispensable step of leach liquor purification in hydrometallurgy. Currently, the removal of Fe^{3+} is carried out by precipitation increasing pH of leach liquor to the limits of iron solubility. Depending on the process conditions Fe^{3+} precipitates into jarosite, hematite, goethite, or magnetite. Mechanical filtration processes separate the Fe-precipitates from nickel leach solutions. The disposal of precipitate requires strict measures of waste management to reduce the potential of pollution. Iron removal through precipitation is a resource intensive process. Therefore, the pursuit of alternative processes for iron removal signify an opportunity for overall process improvements.

Ion exchange is a potential alternative for Fe removal. Hydrometallurgy currently uses ion exchange resin at industrial scale for removal and purification of non-ferrous metals. However, the industry remains reluctant in applying ion exchange for iron removal. Partly due to relatively simplicity of Fe precipitation processes and the lack of environmental regulation related to waste disposal. Previous research on Fe removal by ion exchange focuses on systems at low concentrations (>0.1 M) and research related to Fe removal from electrolytes at high metal concentration is scarce. At large, most of the work is unavailable. It is protected by intellectual properties and company secrecy. Although selectivity of resins is stablished at low concentration systems, theory suggest that

selectivity trends and adsorption potential change as metal concentration increases. Therefore, there is a need for investigation to confirm resins technical feasibility at electrolytes of high metal concentration.

In this work, the adsorption capabilities and selectivity for Fe^{3+} over Ni^{2+} were evaluated using 30 commercial ion exchange resins of cross-linked polystyrene with divinylbenzene body with 16 different functional groups. The selected resins were classified into strong cationic exchangers (i.e., sulfonic resins), weak cationic exchangers (i.e., carboxylic resins), chelating resins (i.e., N-methyl-glucamine, amidoxime, iminodiacetic, bis-picolylamine, phosphinic, phosphoric, thiol, thiourea and isothiouronium, aminophosphonic, and combination of sulfonic and phosphonic resins), and mixed bed resin (i.e., combination of sulfonic and quaternary ammonium groups). Additionally, resin containing strong anion exchange characteristics (i.e., quaternary ammonium resins) acted as control experiments while non-functionalized resin acted as blank experiments. The potential for Fe^{3+} adsorption and selectivity was evaluated in bimetallic (Fe:Ni) and polymetallic (Fe:Ni:Co:Cu) systems. The bimetallic systems contained equimolar concentration of Fe^{3+} and Ni^{2+} satisfying rough averages of common concentration found in Ni-bearing sulfide and laterite ore leach liquors. The polymetallic systems contained excess of Ni^{2+} to represent leach liquors obtained from Ni-bearing sulfide ores.

Among the resins tested, resins containing aminophosphonic acid groups (up to 94% removal), a combination of phosphonic and sulfonic (93%), iminodiacetic acid (92%), methylglucamine (91%), carboxylic acid (78%), quaternary ammonium (62%), amidoxime

(67%), phosphoric acid (92%), and phosphinic acid (84%) were the best performing resins obtaining satisfactory results for the selective adsorption of Fe^{3+} from bimetallic and polymetallic systems. The best performing resins underwent systematic studies of single factor optimization to elucidate the parameters that most affect the efficiency of Fe^{3+} separations. Metal concentrations above 20 g/L and solution pH between 1.0 and 2.3 were dominant solution factors affecting the adsorption trends. Adsorption selectivity changed in time. Adsorption of Fe^{3+} increased with time up to a maximum of 120 min. Thereafter, the adsorption of Fe^{3+} was negligible. In periods under 10 min, resins obtained significant co-adsorption of base metals. After that, the co-adsorption of base metal decreased suggesting a base metal displacement by Fe^{3+}. Conversely, temperature had little effect on the metal adsorption trends suggesting that ion exchange do perform appropriately at temperatures ranging from 20°C to 90°C.

Not all best performing resins sustained Fe^{3+} adsorption selectivity after modification of process variables. Among the best performers, the resins sustaining Fe^{3+} adsorption selectivity were resins with a combination of phosphonic and sulfonic groups, resins with aminophosphonic acid, with carboxylic acid, iminodiacetic acid, phosphoric acid, quaternary ammonium, and methylglucamine. These best performing resins underwent a series of elution studies in H_2SO_4 and HCl solutions of 0.2, 0.5, 1, 5, and 10% v/v. Resins with a combination of phosphonic and sulfonic group showed the best elution performance amidst the resins analyzed and underwent a systematic analysis to determine the best conditions to enhance metal elution. A combination of primary and secondary

elution using solutions of H_2SO_4 5% v/v and EDTA 5% w/w resulted in almost 100% elution of Fe^{3+} and Ni^{2+}.

The thermodynamic characteristics of the metal adsorption on ion exchange resins with a combination of phosphonic and sulfonic groups confirmed preference for Fe^{3+} over Ni^{2+}. The calculation of heat of adsorption, entropy, and the degree of spontaneity of the adsorption reaction was difficult due to the high metal concentration in electrolyte. However, the results showed that the adsorption of Fe^{3+} in ion exchange resins was favourable with exothermic and exergonic characteristics and positive changes in entropy. Conversely, Ni^{2+} adsorption was not favourable having negative changes in entropy while the change in Gibbs energy was positive. These observations confirmed the low adsorption percentages of Ni^{2+} compared to that of Fe^{3+}. None of the kinetic models employed described satisfactory the adsorption rate of Fe^{3+} as they failed to achieve correlations above 90%. This suggest that the adsorption rate of Fe^{3+} on resins with a combination of phosphonic and sulfonic groups may be governed by unknown transport phenomena not accounted on the kinetic models used.

Overall, the results obtained suggest ion exchange can potentially be an alternative to iron precipitation as an iron removal process in nickel purification. However, economic studies are still required to determine the cost benefit of ion exchange resins against precipitation.

Acknowledgements

Para Emilia y Rafael, la trayectoria es irrelevante, más imprescindible es el estado final.

I would like to express my sincere gratitude to my supervisors Dr. Yahui Zhang and Dr. Kelly Hawboldt for their assertive advice, continuous support, and timely instruction during my PhD studies. Without their help, none of this would have been possible. In addition, I would like to extend my appreciation to Dr. Yan Zhang, who is a member of my Ph.D. committee, for her feedback, and assistance.

I am also grateful to all members of the Hydrometallurgy lab for their cooperative work and patience. The financial support from Memorial University of Newfoundland and the Natural Sciences and Engineering Research Council of Canada (NSERC) for funding my research related area. Also, to Prof. Hyunjung Kim Ph.D., Prof. José Andres Hernández, Amin GhavamiNejad Ph.D., and Melissa Brothers for believing in my potential, provide me with recommendations to enter this house of studies, and their continuous support.

I would like to extend my sincere gratitude to Karyn, for her patience, support, and understanding. Any laudatory and appreciation words are not excessive to express my gratitude to her. My siblings, Jaime Rafael and Edda Dilenia for their encouragement and example. Last but not least, to my parents, for being an extraordinary example of relentless self-improvement, love, generosity, and unconditional support along the road.

¡Gracias por todo, papás!

Table of Contents

List of Tables

List of Figures

List of Abbreviations and Symbols

$\Delta G°$	Change in Gibbs energy
$\Delta H°$	Change in Enthalpy
$\Delta S°$	Change in Entropy
A	Constant A for Debye-Huckel equation
a	Chemical activity
B	Constant B for Debye-Huckel equation
C	Constant related to thickness of boundary layer for IPD equation
C_E	Final concentration [g/L]
$C_M^{\pm}$	Metal ion molar concentration
C_o	Initial concentration [g/L]
d	Effective hydrated diameter
D2EHPA	Di-2-ethylhexyl-phosphoric acid
DHLL	Debye Huckel Limiting Law equation
DTMPPA	Di(2,4,4-trimethylpentyl)-phosphinic acid
E(%)	Metal eluted in primary elution
E_2(%)	Metal eluted in secondary elution
EDH	Extended Debye Huckel
E_O(%)	Overall metal eluted

Fe_{Ni}	Bimetallic systems containing similar concentrations of Fe^{3+} and Ni^{2+}
$Fe_{Ø}$	Monometallic systems containing exclusively Fe^{3+}
ICP-EOS	Inductively Couple Plasma Optical Emission Spectroscopy
IPD	Intra-particle diffusion equation
K_a	Thermodynamic equilibrium constant
K_D	Distribution constant
K_L	Langmuir equilibrium constant
k_1	First order rate constant
k_2	Second order rate constant
k_p	rate constant of IDP
$L(\%)$	Metal adsorption
M^+	Metal ion
MBR	Mixed bed resins
Ni_{Fe}	Bimetallic systems containing similar concentrations of Ni^{2+} and Fe^{3+}
$Ni_{Ø}$	Monometallic systems containing exclusively Ni^{2+}
PFO	Pseudo First Order equation
PL	Pressure Leaching Process
PSO	Pseudo Second Order equation
q_e	Adsorption capacity of adsorbent at equilibrium
$q_{e\ exp}$	Adsorption capacity at equilibrium obtained experimentally
q_{max}	Maximum adsorption capacity of adsorbent
q_t	Adsorbate uptake per mass of adsorbent at given time

R	Ideal gas constant [8.315 J/mol K]
SAR	Strong anion exchange resins
SCR	Strong cation exchange resins
SIR	Solvent impregnated resin
T	Temperature (K)
TBP	Tri-n-butylphosphate
TIPS	Tri-isobutyl-phosphine sulfide
TOPO	Tri-n-octyl-phosphine oxide
v_L	Volume of sample in adsorption experiments [L]
WAR	Weak anion exchange resins
WCR	Weak cation exchange resins
w_E	Amount of resin used in elution experiments [g]
w_R	Amount of resin used in adsorption experiments [g]
X_l	Amount of metal eluted [g]
x_R	Amount of metal per gram of resin [g M^+/ g $_{resin}$]
z	Integer charge of metal ion
α	Elovich equation initial rate constant
β	Elovich equation desorption constant
θ_E	Fraction of occupied adsorption sites
$\gamma_M^{\pm}$	Activity coefficient of the metal in solution

Chapter 1 Introduction

1.1 Problem statement

Separation of iron from nickel and other base metals is a common hydrometallurgy. Iron coexists with base metals in ore mineral with mass fractions often larger than the metals of interest. The main sources for primary nickel production worldwide are Ni-bearing sulfide and lateritic ores (Bacon and Mihaylov, 2002; Chang et al., 2010; Zhang et al., 2015). The Ni-bearing sulfide ores, typically contain between 1-3% of Ni while nickeliferous lateritic ores contain about 1-2% of Ni (Agatzini-Leonardou et al., 2009; Mudd, 2010). After pressure leaching operations, iron is leached together with nickel and other base metals. Then, the removal of iron is by norm the first step in hydrometallurgy (Monhemius, 2016). Currently, Fe is removed mechanically after induced precipitation. Increments in leachate pH promote the formation of Fe^{3+} precipitates in the form of jarosite ($MFe_3(SO_4)_2(OH)_6$ where M can be K^+, Na^+, or NH_4^+, etc.), hematite (Fe_2O_3), goethite (FeOOH), or magnetite (Fe_3O_4). Although this process is an effective technique, it requires extensive use of alkali materials requiring complex logistics, unwanted by-products in the downstream process, and the disposal of the precipitate formed. Mechanic filtration process typically remove Fe-precipitate from nickel leach solution. Disposal of precipitate may pose environmental risks if not well managed (Zhang et al., 2016). The removal of iron from pressure leaching solutions is a resource intense process resulting in large amounts of hazardous waste. Therefore, the pursuit of alternative processes for iron removal signify

an opportunity for overall process improvements and address the growing trend of zero waste production and green mining approaches.

Potential alternatives for Fe removal are solvent extraction and ion exchange. Industrial hydrometallurgy for non-ferrous metals currently use solvent extraction and ion exchange, as shown in Figure 1.1. Before the introduction of solvent extraction and ion exchange in non-ferrous hydrometallurgy, precipitation processes achieved the base metal separation and purifications showed in Figure 1.1. Nonetheless, the industry has remained reluctant to adopt these technologies for Fe removal due to the simplicity in Fe precipitation process, and lack of environmental regulations related to disposal of waste precipitates.

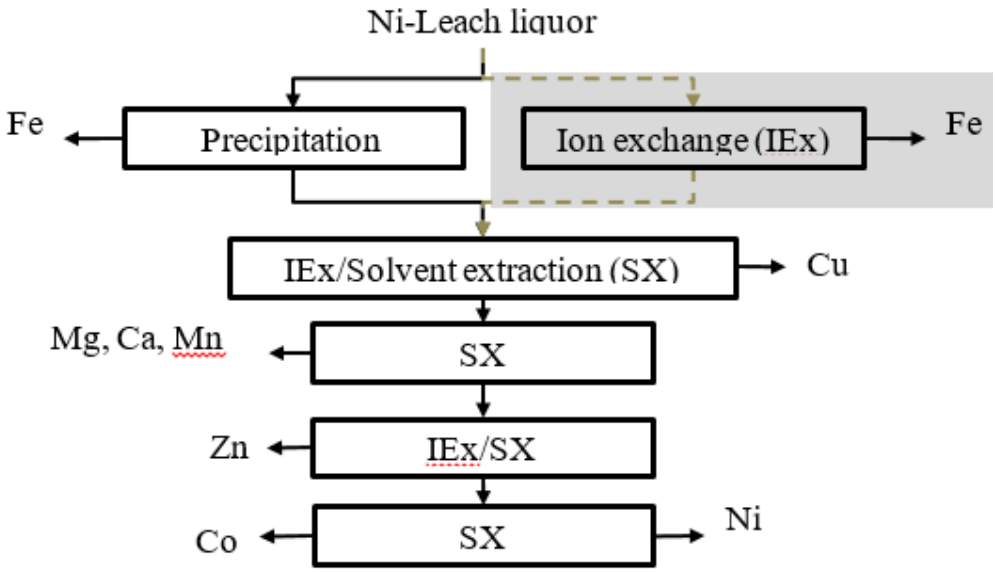

Figure 1.1 Simplified flow sheet of Ni recovery from laterites using precipitation process and its alternative of ion exchange (IEx) for iron separation (adapted from Silva et al., 2019)

Both solvent extraction and ion exchange technologies rely on the complexation of metal ions by organic ligands. The differences in complex formation amongst different

ligand-metal systems is one of the main factors for selective ionic bonding. The United States National Institute of Standards and Technology (NIST) identifies more than 6166 ligands which have potential for a specific metal preference. However only few ligands have reached the market of solvent extraction and fewer ligands have made it to ion exchange resins (NIST, 2013). Manufacturers marketing strategies, complex synthesis, toxicity of ligands, and lack of research are among the reasons for low diversity of ligands in the market. Example of this are thiocarbamate groups with S and N as electron donor atoms, which have shown special attraction for precious, and platinum group metals (PGM) with high economic value. Nonetheless, the commercial production of thiocarbamate resins was discontinued due to its toxicity and no commercial equivalent is available.

Although there are thousands of commercial ion exchange resins, there are less than 30 functional groups available. The majority of commercial ion exchange resins have several variations of the same functional group. One functional group has a number of physical variations with different particle size, degree of crosslinking, and different purity grade. The grade of purity of a resin dictates whether the resin is intended for the manufacturing of products for human consumption (e.g., water treatment, food industry, make-up industry, etc.) or for the chemical or analytical industry. In some specific cases, the functional group is altered to provide specific metal adsorption s (e.g., chain length between of two aminophosphonic acid groups being aminomethylphosphonic or aminopropylphosphonic) but this remain under manufacturer secrecy (Silva et al., 2018). Fifteen manufacturing companies produce ion exchange for the Canadian market. Six

companies lead the market producing the majority of ion exchange resins. Other nine companies focus on the production of specialized resins.

Mostly all research related to ion exchange resins focus on separation of metals in solutions at low concentration. Manufacturers report resins' general selectivity trends based on adsorption experiments at single metal systems and low concentration. Similarly, comparisons of adsorption efficiencies of commercial IEx-resin with analogue functional groups (e.g., two different commercial resins containing aminophosphonic acid groups) at low metal concentrations are common among scientific literature. The development of new resins satisfies the demand of specific separations otherwise unattainable with current technologies. Nonetheless, new developed resins rarely challenge the application of existing resins, meaning that stablished process do not seek for novel resins with improved separation yields. Better separation efficiencies mean better opportunities to replace current precipitation processes as Fe removal strategy. However, research comparing metal selectivity among different functional groups at high metal concentrations is required to assess properly the best performing resins for Fe separation in hydrometallurgy of Ni beneficiation. Therefore, a study on the adsorption properties and preferences to Fe adsorption by resins with different functional groups is beneficial for a better resin selection at laboratory and industrial scales.

1.2 Objective and scope of study

The final objective of the research is to identify the most efficient ion exchange resin for the separation of Fe^{3+} from Ni^{2+} leach solutions. The adsorption capabilities and

selectivity of Fe^{3+} over Ni^{2+} were evaluated in 16 different functionalities represented in 30 commercial ion exchange resins. This as part of the initial studies considering ion exchange as a potential alternative for Fe^{3+} removal from Ni^{2+} hydrometallurgy plants providing opportunities for Fe^{3+} co-beneficiation.

The functional groups employed for analyses were identified the most common commercial IEx-resins in Canadian market. The selected resins were classified into strong cationic exchangers (i.e., sulfonic resins), weak cationic exchangers (i.e., carboxylic acid resins), chelating resins (i.e., N-methyl-glucamine, amidoxime, iminodiacetic, bis-picolylamine, phosphinic, phosphoric, thiol, thiourea and isothiouronium, aminophosphonic, and combination of sulfonic and phosphonic resins), and mixed bed resin (i.e., combination of sulfonic and quaternary ammonium groups). Additionally, resin containing strong anion exchange characteristics (i.e., quaternary ammonium resins) acted as control and non-functionalized resin as blank experiments.

The separation of Fe from Ni occurred in solution containing equimolar concentrations of Fe^{3+} and Ni^{2+}. In consequence, the analysis equally satisfied a rough average of Fe and Ni concentrations commonly found in liquors after pressure leaching of Ni-bearing sulfide and laterite ores. To emulate leach liquors obtained from sulfide nature, resins were tested in presence of Ni^{2+}, Cu^{2+}, and Co^{2+} using conditions resembling conditions of a Ni hydrometallurgy plant. Supplementary systematic studies of single factor optimization highlighted the factors affecting Fe^{3+} separations' efficiency among the best performers and confirmed the most efficient process. The most efficient resins underwent exploration studies to identify its potential for primary elution. The resin

showing the best properties for primary elution underwent a systematic study to study the effects of time and temperature on primary elution. Likewise, underwent a systematic study for secondary elution using different strong acid concentrations and complexing agents. Lastly, best performer resins underwent thermodynamic and kinetic studies to define the Fe adsorption characteristics.

1.3 Thesis outline

This thesis includes seven chapters. Chapter 1 is an introduction to this study including relevant background information, the scope, and the objectives of the research. Chapter 2 includes a review of the literature of ion exchange technologies in hydrometallurgy. It identifies the most common functional groups employed in metal ion separations at laboratory and industrial scale. Also, identifies the most common ion exchange brands for each available functional group. Chapter 3 includes an exploratory Fe^{3+}-Ni^{2+} separation in bi-metallic systems with the commercial resins available in the Canadian market including a systematic analysis of single factor optimization with best performers. The resins' performance for Fe^{3+} separation in presence of Ni^{2+}, Cu^{2+}, and Co^{2+} is included in Chapter 4 with respective single parameter optimization analysis. Chapter 5 discusses the separations at multiple batch systems, and subsequent elution analyses for the most promising resins in the Fe^{3+}-Ni^{2+} separation. Chapter 6 contains thermodynamic and kinetic analysis for best performers. Chapter 7 summarizes the potential for future studies and includes the overall conclusions.

Chapter 2 Literature Review and critique

This chapter includes information based on the published paper:

R.A. Silva, K. Hawboldt, & Y. Zhang. (2018). Application of resins with functional groups in the separation of metal ions/species – a review. Mineral Processing and Extractive Metallurgy Review 39, 395–413 having the following roles:

Rene A. Silva designed, gathered the information, and conducted the literature review. Dr. Kelly Hawboldt and Dr. Yahui Zhang supervised the design of the literature review and reviewed the manuscript.

2.1 Ion exchange resins definition and classifications

Ion exchange resins are cross-linked polymers (a.k.a., synthetic resins) acting as sorbent media for ion exchange in solid-liquid separations. This technology has a wide range of applications and represent an alternative to solvent extraction technologies (Alexandratos, 1988; Aly and Hamza, 2013). Ion exchange is employed for: (i) water and waste water treatments (Dabrowski et al., 2004) concentration of valuable trace metals like uranium harvesting from sea waters (Aly and Hamza, 2013; Chouyyok et al., 2016), extraction of valuable metals from hydrometallurgical leachates (Bregunccі, 2001; Cortina et al., 1998), and separation and purification of chemical species (Alexandratos, 1988; Miesiac, 2005).

Ion exchange resins contain two main parts: (i) an inert hydrophobic cross-linked polymer acting as supporting body and porous media, e.g., cross-linked polystyrene; and (ii) an active organic functional group capable of dissociation or coordinating bonding for ion sequestration. Each part tailored to enhance adsorption selectivity in specific processes (Aly and Hamza, 2013; Cortina et al., 1998). The most common polymeric matrix used in commercial resins are polystyrene cross-linked with divinylbenzene (PS-DVB), polyacrylic divinylbenzene (PA-DVB), polystyrene (PS), and divinylbenzene (DVB). Although the polymeric matrix has multitude of combinations of crosslinking degree, the functional group that provides the characteristics for specific extractions.

The versatility of resins lies in the easy altering of the surface during or after synthesis to match specific process conditions by adding or substituting organic functional groups (Alexandratos, 1988; Cortina et al., 1998). This solid-liquid extraction provides a

number of advantages over liquid-liquid processes, as the latter requires additional mixing and settling before the recovery and regeneration of extractants (Bachiller et al., 2004; Benamor et al., 2008; Iglesias et al., 1999). The body of the resins provides a higher physical and chemical stability simplifying the desorption operation (Akkaya and Ulusoy, 2008; Alexandratos and Smith, 2004; René A Silva et al., 2018), also reduces losses through entrainment and allows a higher number of adsorption/desorption cycles (Iglesias et al., 1999; Zhang et al., 2016). The drawbacks of resins lie in the high cost and low reaction kinetics (Benamor et al., 2008; Benkhedda et al., 2005). Ion exchange is a feasible alternative for metal separation at industrial scale despite its high cost. It provides high metal recovery with greater physicochemical stability than solvent extraction (Breguncci, 2001).

Depending on the synthesis method, resins are classified as Levextrel type, Solvent Impregnated Resin (SIR), and grafted resins (Zagorodni, 2006). The additions of functional groups during synthesis produce Levextrel type resins, whereas a resin obtained from the substitution or addition of functional groups after synthesis is known as Solvent Impregnated Resin (SIR). This two types of resins follow the principles of ion exchange/substitution reactions to separate the target species. Contrarily, grafted resins contain a specific molecular geometry capable selective recovery based on the geometrical configurations of the target species. Levextrel and SIR resins adopt the background knowledge of solvent extraction to include specific organic functional groups for specific metal sorption. However, unlike solvent extraction, the ion exchange reactions occur in the

porous media of the resins allowing the retention and concentration of the target species (Free, 2013).

2.2 Principles of reaction mechanism

The ion exchange characteristics of a resin depend on the physicochemical nature of its functional groups. That is, dissociation characteristics, the charge of the ionized groups, and bonding preferences. All these determine the applications of the resin (Helfferich, 1962; Zagorodni, 2006). Literature suggest that solution pH, active functional groups, and metal species in solution as the most influential variables for specific metal adsorption (Harland, 1994).

There are two general categories of interactions between the functional groups and the target ionic species: (i) ion pairing or ion substitution and (ii) coordination bonding or chelating interactions:

2.2.1 Ion exchange by ionic substitution

Ionic substitution operates on the principle of pairing ionized species of opposite charge. A polymeric support (Pol) with functional group ($Fg^{\pm}$) exchanges its mobile ion ($M^{\pm}$) with the ionized target species ($T^{\pm}$):

$$Pol\text{-}Fg^{\pm}\,M^{\pm} + T^{\pm} \leftrightarrow Pol\text{-}Fg^{\pm}\,T^{\pm} + M^{\pm} \qquad \text{Eq. (2.1)}$$

Where $M^{\pm}$ and $T^{\pm}$ have either a positive or negative charge but are opposite to that of $Fg^{\pm}$. The selection of $Fg^{\pm}$ charge depends on the ionization characteristics of the target species $T^{\pm}$. A sub-classification of ion exchange depends on the charge of their ionizable groups $Fg^{\pm}$ dividing resins into cationic and anionic exchange resins. Cationic exchangers have anionic groups attached to the polymer frame. Therefore, have mobile cations that exchange for the target cations in solution. Anion exchangers, have cations attached to the polymer frame with mobile anions. Therefore, exchange for the target anions in solution. To proceed with the general ion exchange reaction (Equation 2.1), cation exchange resins are required to follow an initial deprotonation or dissociation reaction to create negatively charged sites for the attraction of the positive target species (Zagorodni, 2006). Contrarily, anion exchange resins having conjugated acids groups or free bases requiring an initial protonation attract negative charged complexes. The general deprotonation reaction for cation exchangers is follows:

$$\text{Pol-Fg}^{-}\,\text{H}^{+} \leftrightarrow \text{Pol-Fg}^{-} + \text{H}^{+} \qquad \text{Eq. (2.2)}$$

Once the resin has its negative site available, the uptake of the free cation species in solution follows the reaction:

$$\text{Pol-Fg}^{-} + \text{T}^{+} \leftrightarrow \text{Pol-Fg}^{-}\,\text{T}^{+} \qquad \text{Eq. (2.3)}$$

Anion exchangers in free base (e.g., tertiary amines) follow a general protonation reaction as follows:

$$\text{Pol-Fg} + \text{H}^{+} \leftrightarrow \text{Pol-FgH}^{+} \qquad \text{Eq. (2.4)}$$

Anion exchangers as conjugated acid in salt form (e.g., quaternary ammonium) lose their anion (e.g., SO_4^{2-} OH^-, Cl^-, etc.) to obtain its positive site:

$$Pol\text{-}Fg^+OH^- \leftrightarrow Pol\text{-}Fg^+ + OH^- \quad \text{Eq. (2.5)}$$

Once the anion exchanger has its positive site available, it allows the sorption of negatively charged metal complexes following the reactions:

$$Pol\text{-}FgH^+ + CplxT^- \leftrightarrow Pol\text{-}FgH^+CplxT^- \quad \text{Eq. (2.6)}$$

Or

$$Pol\text{-}Fg^+ + CplxT^- \leftrightarrow Pol\text{-}Fg^+CplxT^- \quad \text{Eq. (2.7)}$$

Where $CplxT^-$ represents a metal complex anion. Resins containing functional groups in salt form tend to hydrolyze accordingly to the strength characteristics of the associated acid/base form (Rodrigues, 1986), following the reaction:

$$Pol\text{-}Fg^-Na^+ + T^+ \leftrightarrow Pol\text{-}Fg^-T^+ + Na^+ \quad \text{Eq. (2.8)}$$

Equations 2.2-2.8 state that the dissociation of the organic acids, bases, and salts contained as active functional groups governs ion exchange reactions. The resins' ionization equilibrium is strongly pH dependent. Therefore, the terminology of strong and weak acid/base has also been adapted to classify the ionization strength of the resins. As cation exchangers can be classified as Lewis acids and anion exchangers as bases, the classification of strong and weak ion exchange resins also provides information about the pH range in which the resin is capable of ionizing (Helfferich, 1962). Strong cationic resins (SCR) and strong anionic resins (SAR) can dissociate over the entire pH range. Weak

cation resins (WCR) and weak anion resins (WAR) have limitations for dissociation. WCR dissociate at solution pH higher than their pK_a. Meanwhile, WAR dissociate at solution pH lower than pK_a values. Figure 2.1 shows a schematic representation of the operating pH ranges of ion exchange resins. Both, WCR and WAR have compromised exchange capacities when operating in solution pH that do not allow dissociation.

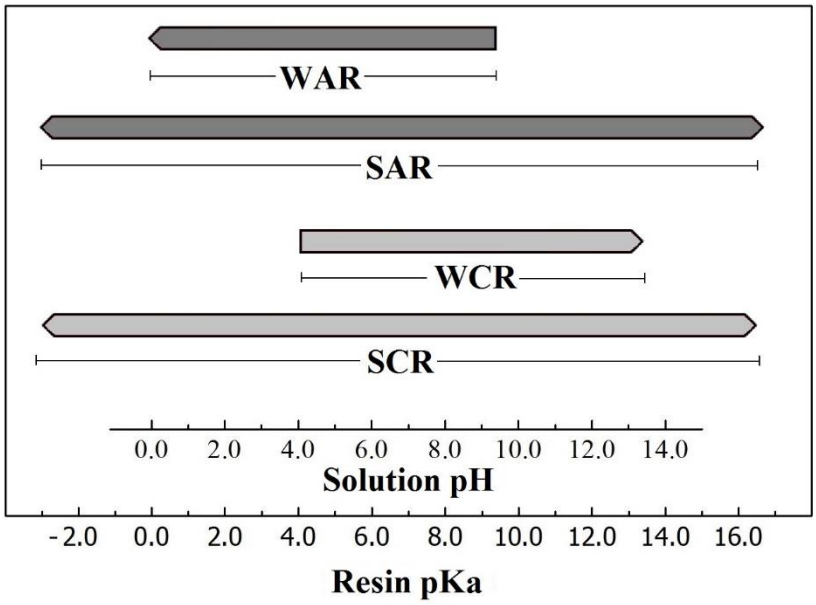

Figure 2.1: Operating pH range for ionization of active groups in weak (W-) and strong (S-) anionic (-AR) and cationic (-CR) resins as presented in (Silva et al., 2018)

2.2.2 Ion exchange by coordination bonding

Coordination bonding results from the interaction between metal ions and the ligands of a functional group. Generally the ligands are electron donor atoms from the elements of groups 5, 6, and 7 of the periodic table, being the most common ones N, P, O, and S (Zaganiaris, 2013). Bonding by coordination through multiple functionalities on a

single ligand (polydentate ligand) is more stable than simple single ionic or covalent bond (Martell and Hancock, 2013).This stability is known as chelation effect which is attributed to favourable entropy changes relative to monodentate ligands (Lawrance, 2013; Martell and Hancock, 2013). Chelating resins are ion exchange resins that selectively adsorb a metal ion by chelating interactions. Unlike resin following substitution reactions, chelating resins do not require dissociation of the functional group as long as the electron donor has free electrons available for interaction (e.g., S and N in thiourea groups).

The preference of specific metal-ligand bonding and stability on chelating resins depends on formation constant, charge of ligand and metal ion, electronegativity, molecular geometry, and ionic diameter (Martell and Hancock, 2013). Besides formation constants, the rest of the properties influencing the metal-ligand bonding follow the Pearson Hard and Soft Acids and Bases (HSAB) theory (Pearson, 1963). This, as the ligands of the functional groups in resins behave as bases (i.e., electron donors) and the metal ions as acids (i.e., electron acceptors) following Lewis theory of acids and bases (see Table 2.1).

Hard acids favour the interaction with hard bases, soft acids favour soft bases, and intermediate or borderline acids can interact with either soft or hard bases complying to HSAB theory (Martell and Hancock, 2013; Zaganiaris, 2013). Hard acids are ions with low electronegativity, weakly polarizable, with high charge to ionic radius ratio, and are attracted to hard bases of high electronegativity. Soft acids are polarizable ions with low charge to ionic radius ratio and with relatively high electronegativity that matches the

relatively low electronegativity of soft bases (Martell and Hancock, 2013; Zaganiaris, 2013).

Table 2.1: Classification of ions according to Lewis theory of acids and bases (electron donor/acceptor) and Pearson's Hard and Soft Acids and Bases (HSAB) theory as suggested by (Silva et al., 2018)

	Acids	**Bases**
Hard	H^+, Li^+, Na^+, Rb^+, Sr^{2+}, Mg^{2+}, Ca^{2+}, UO_2^{2+}, VO^{2+}, Ti^{3+}, Cr^{3+}, Mn^{3+}, Fe^{3+}, Co^{3+}, Al^{3+}, Sc^{3+}, U^{4+}, Si^{4+}, Ti^{4+}	NH_3, R-NH_2, H_2O, OH^-, O^{2-}, R-OH, -COO^-, CO_3^{2-}, NO_3^-, SO_4^{2-}, F^-, O, N, PO_4^{3-}, -PO_3^{2-}, -OPO_3^{2-}, -PO_2^{2-}, Phosphonic, Phosphinic
Intermediate or Borderline	Fe^{2+}, Co^{2+}, Ni^{2+}, Cu^{2+}, Zn^{2+}, Pb^{2+}, Mn^{2+}, Bi^{2+}, In^{3+}	NO_2^-, SO_3^{2-}, Cl^-, SCN^-, SO_4^{2-}, Aromatic amines, Pyridine, Aniline
Soft	Cu^+, Ag^+, Au^+, Tl^+, Cd^{2+}, Hg^+, Hg^{2+}, Au^{3+}, Pd^{2+}, Pt^{2+}	CN^-, CO, S^{2-}, Te^{2-}, $S_2O_3^{2-}$, R-SH, I^-, P, R_2S, RS^-, $S{=}C(NH_2)_2$, Phosphine

2.3 Common types of functional groups in ion exchange resins

The most common functional groups found in ion exchange resins are based on nitrogen, phosphorus, sulfur, oxygen, and a combination of them as electron donors or active atoms (Zagorodni, 2006). Although there are countless configuration of functional groups, following is a description of the most common employed in ion exchange technologies:

2.3.1 Ion exchange resins with nitrogen containing groups:

The most common nitrogen containing groups found in ion exchange resins are: quaternary ammonium groups, tertiary and secondary amino groups, bis-picolylamine

groups, and guanidine groups (Zaganiaris 2013; Kagaya et al. 2015). Nitrogen based ion exchange resins commonly require a preliminary protonation to activate the anionic exchange characteristics. The classification of the amino groups depends on the number of hydrogen atoms replaced by alkyl or aryl groups. The replacement of one hydrogen atom in the amino group produces a primary amine. Two hydrogen atoms replaced produces a secondary amine, and three replacements produces a tertiary amine (Wade, 2006). Quaternary ammonium groups occur by the protonation of the amine group with a fourth alkyl or aryl group. Given that the strength of protonation is not equal for all nitrogen groups, some groups are unable to load metal ions at strong alkaline conditions. Others, base their preference on such limitations by only allowing protonation at specific pH conditions appropriate for a particular anion adsorption. Following is a brief description of the nitrogen groups found.

2.3.1.1 Resins containing quaternary ammonium functional groups

Quaternary ammonium groups are SARs and dissociate over the entire pH range. In consequence, favour the recovery and removal of a wide variety of anion complexes in solution (Dabrowski et al., 2004). Resins with quaternary groups are the most used SAR in commercial resins. Exist under several brands produced by almost all ion exchange manufacturers (See Table 2.2).

In hydrometallurgy, quaternary ammonium resins found its application as an alternative to activated carbon recovering precious and base metals in the cyanide form. However, the high strength of quaternary ammonium groups cannot achieve high

selectivity over specific anion species. In alkaline cyanide solutions precious and base metal exist as aurocyanide ($Au(CN)_2^-$), silver cyanide ($Ag(CN)_2^-$), and general base-metal cyanides species as $Cu(CN)_3^{2-}$, $Zn(CN)_4^{2-}$, $Ni(CN)_4^{2-}$, $Co(CN)_5^{3-}$, $Fe(CN)_6^{4-}$ (Kotze et al., 2005). High value metal species (e.g., $Au(CN)_2^-$ and $Ag(CN)_2^-$) compete with base metals for the finite number of adsorption sites in the resin. Hence quaternary ammonium resins are inconvenient for purification of metal solutions (Fedyukevich and Vorob'ev-Desyatovskii 2016; X Dai et al. 2010). Instead, these resins achieve great purifications removing and concentrating anions from liquid media. Some scholars state that quaternary ammonium resins may achieve certain degree of selectivity based on the geometrical configuration of the target species. Based on its geometrical configuration, quaternary ammonium groups show adsorption preference for metal complexes with linear geometry over other configurations like trigonal planar or tetrahedral alignments (Kotze et al., 2005). Based on this principle, some commercial resins like Dowex Minix produce satisfactory recoveries of gold cyanide at industrial scale.

There are two common types of quaternary ammonium groups in resins. Type 1 containing three methyl groups attached to the nitrogen atom that is fixed to the reticular body of the resin and type 2 with one methyl group substituted by ethanol. Table 2.3 contains examples of resins containing quaternary ammonium groups. The introduction of ethanol group reduces the basic strength of the resin, but it facilitates the resin regeneration process improving the elution yields (Wachinski, 2016).

Table 2.2: Examples of commercial resins containing quaternary ammonium groups. Data obtained from listed references and datasheet specifications available in each resin manufacturer's website.

Example of commercial resin		
Brand name	**Group / Form**	**Reference**
Amberjet 4400 Cl	$-N^+(CH_3)_3$ / Cl^-	(Dai et al. 2010)
Amberlite IRA 402Cl	$-N^+(CH_3)_3$ / Cl^-	(Dai et al. 2010)
Amberlite IRA-458	$-N^+(CH_3)_3$ / ns[1]	(Grosse et al. 2003) (Leao et al. 1998)
Amberlite IRA-400	$-N^+(CH_3)_3$ / ns	(Grosse et al. 2003) (Leao et al. 1998)
Dowex MAS-1	$-N^+R_3$ / ns	(Leao et al. 1998) (Diniz et al. 2000)
Dowex Minix	$-N^+((CH_2)_3CH_3)_3$ / ns	(Fedyukevich et al. 2015) (Fedyukevich and Vorob'ev-Desyatovskii 2016) (Petersková et al. 2012) (Van Deventer 2011)
Duolite A191 L	$-N^+(CH_3)_3$ / Cl^-	(Glover et al. 1990)
IMAC HP 555s	$-N(CH_2CH_3)_3^+$ / Cl^-	(Leao et al. 1998)
Indep. A16LL	$-N^+R_3$ / ns	(Leao et al. 1998)
Indep. NOTREN	$-N^+R_3$ / Cl^-	(Dicinoski 2000) (Grosse et al. 2003)
Indep. TEA-BE	$-N^+R_3$ / Cl^-	(Dicinoski 2000)
Purolite A850DL	$-N^+R_3$ / Cl^-	(Petersková et al. 2012)
Purolite A520E	$-N^+R_3$ / Cl^-	(Leao et al. 1998)

[1]ns: not specified

Table 2.3: Examples of commercial resins with quaternary ammonium type 1 & type 2 groups. Data obtained from listed references and datasheet specifications available in each resin manufacturer's website.

Example of commercial resin			
Type	**Brand name**	**Group / Form**	**Reference**
Type 1	TOKEM AV17	$-N^+R_3$ / Cl^-	(Grosse et al. 2003) (Kononova et al. 2007)
Type 1	Ambersep 400 SO_4	$-N^+(CH_3)_3$ / ns[1]	(Kim et al. 2001)
Type 1	Amberlite IRA 900RF	$-N^+(CH_3)_3$ / ns	(Fernando et al. 2002)
Type 1	Purolite A500/2788	$-N^+(CH_3)_3$ / ns	(Dai et al. 2010)
Type 1	Purolite A500/2788	$-N^+(CH_3)_3$ / Cl^-	(Dai et al. 2010)
Type 2	Lewatit S 7468	$-N(CH_3)_2(C_2H_5OH)$ / Cl^-	na[2]
Type 2	Lewatit MONOPLUS MP 600	$-N(CH_3)_2(C_2H_5OH)$ / Cl^-	na
Type 2	Purofine PFA300	$-N(CH_3)_2(C_2H_5OH)$ / Cl^-	na
Type 2	Purolite A300OH	$-N(CH_3)_2(C_2H_5OH)$ / OH^-	na

[1]ns: not specified; [2]na: not available/not found in scientific literature

2.3.1.2 Resins containing secondary and tertiary amino functional groups

Resins containing tertiary and secondary amino groups are WARs with average pK_a values of 9.7 and 10.7, respectively (Wade, 2006). Resins containing tertiary amino groups are the most common among amino groups in the market. Resins with secondary amino groups are scarce being more common as a combination with tertiary groups (Silva et al., 2018). The applications of resins with amino groups include the recovery of Rhenium from low-grade solutions using the commercial resins IRA-67, Purolite A170, and Purolite A172 (Van Deventer, 2011; Virolainen et al., 2015). Also, the removal of different metal complex (e.g., $HCrO_4^-$) in water purification systems at neutral pH (Dabrowski et al., 2004). Table 2.4 includes examples of commercial resins containing amino groups.

Table 2.4: Examples of commercial resins containing secondary and tertiary amino groups

Example of commercial resin			
Brand name	**Group / Form**	**Type**	**Reference**
Indep. AM2B	-NR; $-NR_2$ / ns[1]	2nd&3rd; [2]	(Fedyukevich et al. 2015) (Grosse et al. 2003) (Van Deventer 2011)
Purogold S992	-NR; $-NR_2$ / FB[3]	2°&3°; [2]	(Fedyukevich et al. 2015) (Fedyukevich and Vorob'ev-Desyatovskii 2016)
TOKEM AN-85	Acrylonitrile / ns	2°&3°	(Kononova et al. 2007)
Amberlite IRA 96	$-NR_2$ / FB	3°; [4]	(Dai et al. 2010)
Amberlite IRA-68	$-NR_2$ / ns	3°	(Grosse et al. 2003)
Amberlite IRA-67	$-NR_2$ / FB	3°	(Virolainen et al. 2015)
Purolite A100	$-NR_2$ / FB	3°	(Fedyukevich et al. 2015)
TOKEM AN-25	Pyridine / ns	3°	(Kononova et al. 2007)
Purolite A170	Complex amine/FB		(Virolainen et al. 2015)
Purolite A172	Complex amine/FB		(Virolainen et al. 2015)

[1]ns: not specified; [2]2°&3°: combination of secondary and tertiary amino groups; [3]FB: free base; [4]3°: tertiary amino groups

Regardless of the adsorption limitations at pH higher than 10, amino-functionalized resins can recover precious and base metals complexes from cyanide leaching solutions (Dai et al., 2012). At mild alkaline conditions, the commercial resin Lewatit MP62 containing tertiary amino groups showed an order of selectivity of $Fe(CN)_6^{3-/4-}$ > $Cu(CN)_4^{2-}$ > $Ni(CN)_4^{2-}$ > $Zn(CN)_4^{2-}$ > $Cd(CN)_4^{2-}$ (Kurama and Çatalsarik, 2000). However, at pH 10-10.5 amino groups showed a compromised recovery of cyanide complexes underperforming quaternary ammonium groups (Lukey et al., 2000, 1999). Cortina et al. (1998) suggested that WARs containing amino groups in systems with solution pH higher than pKa still adsorb low concentration of metals by coordination interaction between the metal complex and the free electron pair of nitrogen in amino group. The main advantage of the tertiary and secondary amino groups is a pK_a easily adjustable to specific pH and Eh conditions enhancing metal adsorption without complicating the elution process (Cortina et al., 1998; Helfferich, 1962; Zagorodni, 2006). Therefore, these resins provide higher selectivity characteristics than the quaternary ammonium groups counterparts. Figure 2.2 shows an example of enhanced metal adsorption s by WAR pKa's modification.

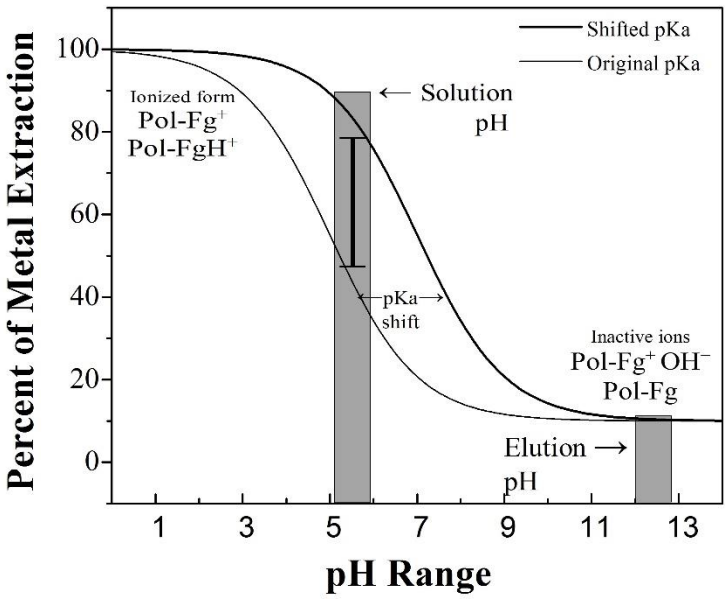

Figure 2.2: Metal extraction rates at different pH for a tertiary amino group described as WAR in Eq. 2.2 and 2.3. The shift in pKa values from 5 to 7 increase metal extractions from 40–50% to values higher than 80% without sacrificing the elution properties as described by (Silva et al., 2018)

2.3.1.3 Resins containing a combination of quaternary ammonium and tertiary amine groups

The combination of tertiary amino groups with quaternary ammonium provide high adsorption rates with high metal selectivity. This combination provides the advantages of the strong anion exchange characteristics of quaternary ammonium groups and the high selectivity of tertiary amine groups. Different mixtures of strong and weak anion exchangers result in resins with different ionization strengths serving specific process conditions. A resin with similar amounts of strong and weak anion exchanger groups is a mixed anion exchanger (MARs). MARs have satisfactory metal selectivity and adsorption capacity. Low strong to weak ratios of anion exchanger groups produces higher selectivity

ratios than the opposite. High strong to weak ratios increases the overall metal adsorption but compromises selectivity. Thus, is more common to see low strong to weak ratios of anion exchanger groups in the market as it provides better selectivity (See Table 2.5).

Table 2.5: Examples of commercial resins containing a combination of tertiary amino groups and quaternary ammonium groups

Example of commercial resin		
Brand name	**Group / Form**	**Reference**
Lewatit MP64	$-N^+R_2$; $-N^+R_3$ / Cl^-	(Galán et al. 2005)
Purolite A100/2412	$-N^+R_2$; $-N^+R_3$ / ns[1]	(Dai et al. 2010)
Resinex HM-WBP-79 BG	$-N^+R_2$; $-N^+R_3$ / FB[2];Cl^-	(Fedyukevich et al. 2015)
Resinex HM-WBP-79 C	$-N^+R_2$; $-N^+R_3$ / FB;Cl^-	(Fedyukevich et al. 2015)

[1]ns: not specified; [2]FB: free base

Applications of resins containing combination of strong and weak anion exchanger groups are industrial scale water treatments and commercial hydrometallurgy plants. Galán et al. (2005) analyzed the removal of CrO_4^{2-} from ground waters to concentration acceptable for human consumption using the commercial resins Lewatit MP64. In hydrometallurgy, serve for precious metal recoveries from cyanide leachates (Fedyukevich et al., 2015; Van Deventer, 2011).

2.3.1.4 Resins containing bis-picolylamine groups

Resins with bis-picolylamine groups (Table 2.6) are WAR with strong chelating properties. This allow efficient metal separation even at the highly acidic environments of acid leaching solutions (Diniz et al., 2000; Van Deventer, 2011). These type of resins have enhanced the selective recovery of nickel and cobalt (Flett, 2004; Nagib et al., 1999) and

commercially are used in Chambishi Metals PLC, Zambia, for Co and Cu production, and in Vale's Ni refinery in Port Colborne, Canada (Van Deventer, 2011; Zaganiaris, 2013). . Resins with bis-picolylamine also show high Mn sorption from the acid leaching solution of MnO_2 batteries with significant concentrations of Cl, Cu, Ni, Co, Pb, and Fe (Diniz et al., 2005, 2002). At mildly acidic conditions, the adsorption preference of resins with bis-picolylamine groups to metal ions follows the order of $Cu^{2+} > Ni^{2+} > Fe^{3+} > Zn^{2+} > Co^{2+} > Cd^{2+} > Fe^{2+} > Mn^{2+}$ (Van Deventer, 2011). Due to their strong chelating properties, bis-picolylamine groups allow higher metal selectivity than resins containing iminodiacetic acid groups and quaternary amines at low pH (Diniz et al., 2000).

Table 2.6: Examples of commercial resins containing bis-picolylamine

Example of commercial resin		
Brand name	**Group / Form**	**Reference**
Dowex M4195	-N(picolyl)$_2$ / ns	(Diniz et al. 2000) (Flett 2004) (Kagaya et al. 2015)
Dowex XUS 43578	-N(picolyl)$_2$ / ns	(Diniz et al. 2000) (Kagaya et al. 2015)
Lewatit MDS TP 220	-N(picolyl)$_2$ / SO_4^{2-}	(Nagib et al. 1999) (Rosato et al. 1984)
Lewatit MONOPLUS TP 220	-N(picolyl)$_2$ / SO_4^{2-}	(Nagib et al. 1999) (Rosato et al. 1984) (Kagaya et al. 2015)
Purolite S960	-N(picolyl)$_2$ / FB; SO_4^{2-}	(Zaganiaris 2013) (Kagaya et al. 2015)
Dowex XFS 43084	-OH(C_3H_6)N(picolyl) / ns	(Kagaya et al. 2015)
Dowex XUS 43605	-OH(C_3H_6)N(picolyl) / ns	(Kagaya et al. 2015)
Dowex M4195	-N(picolyl)$_2$ / ns	(Diniz et al. 2000) (Flett 2004) (Kagaya et al. 2015)

[1]ns: not specified; [2]FB: free base

2.3.1.5 Resins containing guanidine groups

Guanidine groups are chelating ligands with soft Lewis base characteristics and pKa values higher than 13. The high pKa values allow operations in alkaline environments. The soft acid characteristics provide selective adsorption over a broad pH range. Guanidine groups show poor adsorption to base metals, and therefore used in hydrometallurgical processes for the concentration and recovery of the precious metals such as Au, Ag, and platinum group metal (Kramer et al., 2006). This preference is maintained even at base metal concentrations 10 times higher than precious metals and regardless of pH (Jermakowicz-Bartkowiak et al., 2005). Few commercial resins containing guanidine groups are available in the market. One is Aurix, developed by Henkel Australia to recover gold from liquors containing thiosulfate (25–200 mM) and ammonia (>50 mM) at pH 8–10 (Grosse et al. 2003). Other is Purogold MTA9920 (previously known as Purolite S992). However, there are a number of SIR developed at laboratory scale using solvent extractants (e.g., LIX79 - N-N'-bis(2-ethylhexyl)guanidine) for resin-in-pulp and resin-in-leach operations in gold cyanide leaching at pH<10.5 (Cortina et al., 1998).

2.3.2 Ion exchange resins with phosphorous containing groups:

Resins based on phosphorous containing groups operate as Lewis bases and allow chelating interactions in a wide range of pH. Unlike resins with nitrogen or sulfur containing groups, resins with phosphorous groups are scarce in the market. Resins with phosphorous groups are generally hydrophobic with low specific gravity affecting the overall metal recovery. To enhance the reaction kinetics, phosphorous containing resins

often include sulfonic and amino groups to improve the resin's wettability (Chiariza et al., 1997). Phosphonic and aminophosphonic acid groups are the most common phosphorous groups present in commercial resins. In lower numbers are produced as SIR using the most efficient phosphorous based solved extractans. Examples are di(2-ethylhexyl) phosphoric acid (D2EHPA), tri-n-butylphosphate (TBP), di(2,4,4-trimethylpentyl)-phosphinic acid (DTMPPA), tri-n-octyl-phosphine oxide (TOPO), tri-isobutyl-phosphine sulfide, and O-methyldihexyl-phosphine oxide O'-hexyl-2-ethyl phosphoric acid (Bari et al., 2009; Cortina et al., 1997; Juang, 1999; Navarro et al., 2009). These phosphorous containing extractants are immobilized in non-functionalized polymeric matrix such as Amberlite XAD series (e.g., Amberlite XAD-2, Amberlite XAD-4, Amberlite XAD-7), or in other sorbent media such as silica gels and zeolites (Juang, 1999; Navarro et al., 2009). Table 2.7 includes the few examples of resins containing phosphorous groups other than phosphonic and aminophosphonic acid commercially available.

Table 2.7: Detail of commercial resins containing phosphoric, phosphinic, and phosphine groups

	Example of commercial resin		
Group	**Brand name**	**Group / Form**	**Reference**
Phosphoric	Eichrom LN Rsin	D2EHPA / ns	na
Phosphoric	Lewatit VP OC 1026	D2EHPA / ns	(Vaughan et al., 2016a)
Phosphinic	Diaion CRP200	-P(=O)OHR / ns	(Kabay et al. 1998)
Phosphinic	Lewatit TP 272	DTMPPA / ns	(Petersková et al. 2012)
Phosphine	Eichrom RE Resin	CMPO in TBP / ns	na
Phosphine	Eichrom TRU Resin	CMPO in TBP / ns	na

[1]ns: not specified

2.3.2.1 Resins containing phosphonic groups

Phosphonic groups are hard bases with strong, stable, and specific chelating interaction with polyvalent metals. Due to four possible donor atoms with ligand potential phosphonic groups are selective towards actinides in tri-, tetra-, and hexavalent oxidation states (Horwitz et al., 1997). Phosphonic groups provide higher adsorption properties than SCR. However, when combined enhance the overall performance (Chiariza et al., 1997). Resins with phosphonic and sulfonic groups can operate at high ion strength and highly acidic (pH < 1) conditions normally unfavourable for other resins (Sole et al., 2016). In systems at pH 5-8, the combination of sulfonic-phosphonic groups shows high adsorption potential for base metals but do not show any particular preference among them (Chiariza et al., 1997). Due to the strong bonding generated, phosphonic-sulfonic resins are used to control water pollution nearby uranium mining operations (Drozdzak et al., 2015). Table 2.8: includes examples of commercial resins containing phosphonic and a combination of phosphonic-sulfonic resins.

The strong interaction between phosphonic groups and metal ions results in difficult elution processes requiring expensive eluents, highly specific and costly equipment with a general reduced metal recovery rate (Sole et al., 2016; Zhang et al., 2016).

Table 2.8 Examples of commercial resins containing phosphonic groups and a combination of phosphonic and sulfonic groups

Example of commercial resin		
Brand name	**Group / Form**	**Reference**
Permutit XP	$-P(OH)_2$ / ns	(Korkisch 1988)
Cationite PM-52	$-P(OH)_2$ / ns	(Korkisch 1988)
Duolite C-62	$-P(OH)_2$ / ns	(Korkisch 1988)
Bio-Rex 63	$-P(=O)(OH)_2$ / ns	(Korkisch 1988) (Helfferich 1962)
Duolite C-63	$-P(=O)(OH)_2$ / ns	(Korkisch 1988) (Helfferich 1962)
Duolite C-65	$-OP(=O)(OH)_2$ / ns	(Korkisch 1988) (Helfferich 1962)
Duolite ES-463	$-P(=O)(OH)_2$ / ns	(Korkisch 1988)
Duolite ES-467	$-P(=O)(OH)_2$ / ns	(Kabay et al. 1998)
Cationite FV	$-P(=O)(OH)_2$ / ns	(Korkisch 1988)
Cationite KF-1	$-P(=O)(OH)_2$ / ns	(Korkisch 1988)
Cationite KF-2	$-CH_2P(=O)(OH)_2$ / ns	(Korkisch 1988)
Cationite KF-3	$-P(=O)(OH)_2$ / ns	(Korkisch 1988)
Cationite KF-4	$-CH_2P(=O)(OH)_2$ / ns	(Korkisch 1988)
Nalcite X-219	$-P(=O)(OH)_2$ / ns	(Korkisch 1988) (Helfferich 1962)
Cationite SF	$-P(=O)(OH)_2$ / ns	(Korkisch 1988)
Cationite RF	$-OP(=O)(OH)_2$ / ns	(Korkisch 1988)
Mitsui Chemical Co. RCSP	$-P(=O)(OH)_2$ / ns	(Kabay et al. 1998)
Mitsui Chemical Co. RSPO	$-P(=O)(OH)_2$ / ns	(Kabay et al. 1998)
Eichrom Actinide Resin	DEHMPA / ns	na
Purolite S957	$-P(=O)(OH)_2$; $-S(=O)_2-OH$ / H^+	(Drozdzak et al. 2015)
Eichrom Diphonix	$-P(=O)(OH)_2$; $-S(=O)_2-OH$ / Ca^{2+}	(Chiariza et al. 1997) (Drozdzak et al. 2015)

[1]ns: not specified

2.3.2.2 Resins containing phosphoric groups

Phosphoric groups like D2EHPA selectively chelate bivalent metal ions (e.g., Zn^{2+}, Cd^{2+}, Cu^{2+}, Co^{2+}, and Ni^{2+}). Particularly, D2EHPA intends to remove metallic cations from chloride and nitrate media (Akita et al., 1994; Cortina et al., 1994). Commercially, the resins Eichrom LN Resin and Lewatit VP-OC-1026 have included D2EHPA group into the

polymeric matrix and are the only resins available in the market containing this group. Lewatit VP-OC-1026 has shown to favour the adsorption of metal ions at acidic conditions following the order: $Ti^{4+} > Fe^{3+} > In^{3+} > Sn^{2+} / Sn^{4+} > Sb^{3+} > Bi^{3+} > Vo^{2+} > Be^{2+} > Al^{3+} > Zn^{2+} > Pb^{2+} > Cd^{2+} > Ca^{2+} > Mn^{2+} > Cu^{2+} > Fe^{2+} > Co^{2+} > Ni^{2+} > Mg^{2+} > Cr^{3+} >>>$ Alkali (Dabrowski et al., 2004).

2.3.2.3 Resins containing phosphinic groups

Resins with immobilized phosphinic groups successfully extract divalent ions (i.e., Zn^{2+}, Cu^{2+}, Cd^{2+}, and Co^{2+}) from diluted acid solutions (Juang, 1999). DTMPPA (a.k.a., cyanex 272) immobilized in Amberlite XAD-2 produces the most common phosphinic SIR. Besides the physical stability provided by the polymeric resin, the immobilization does not improve or modify the extraction selectivity provided by the solvent extractant (Cortina et al., 1993). Higher operational cost and low separation yields are among the main drawbacks for the adsorption of metals with SIR-DTMPPA systems when compared with solvent extraction processes (Sole et al., 2016). The only commercial resins with phosphinic groups are Daion CRP-200 and Lewatit TP 272 showing metal selectivity orders of $Fe^{3+} > V^{4+} > Zn^{2+} > Al^{3+} > Cu^{2+} > Mn^{2+} > Co^{2+} > Mg^{2+} > Ca^{2+} > Ni^{2+}$. Phosphinic groups are considered in difficult base metal separation such as Co-Ni, Cu-Ni, and Zn-Ni systems (Sole et al. 2016; Vaughan et al. 2016).

2.3.2.4 Resins containing phosphine groups

Phosphine groups are soft Lewis bases with adsorption preferences for soft acids (e.g., Hg, Ag, Au, and PGMs). Commercially, the resins RE Resin and TRU Resin from Eichrom Technologies have included phosphine group as octylphenyl-N,N-di-isobutyl carbamoylphosphine oxide (CMPO) dissolved in tri-n-butyl phosphate (TBP) on inert methacrylic polymeric support. At laboratory scale, phosphine groups immobilized in Amberlite XAD series extracted Fe^{3+} from high chloride concentration environments (Navarro et al., 2009) and Zn^{2+} from solutions containing different concentration of Cu^{2+}, Cd^{2+}, and Cl^{-} (Cortina et al., 1995).

2.3.3 Ion exchange resins with sulfur containing groups:

Resins containing sulfur commonly behave as soft bases producing preferential recoveries of precious metals. However, sulfur-containing resins have remarkable selectivity towards mercury, higher than that of precious metals. The most common type of sulfur based groups in commercial resins are sulfonic groups $(R\text{-}SO_3)^-$ in either H^+ or Na^+ forms (Zagorodni, 2006). Sulfonic groups are also the most common type of strong cation exchanger in the market. In lesser numbers thiol, thiourea, and its tautomeric form isothiouronium are produced as chelating SIR (Nikoloski and Ang, 2014; Okewole et al., 2013).

2.3.3.1 Resins containing sulfonic groups

This group of resins show the strongest adsorption capacity among cation exchangers. However, the group's high strength results in a poor metal selectivity. Therefore, sulfonic acid resins find their application in solution purification processes that do not require selective adsorption requirements. In wastewater treatment, reduce considerably the metal pollutant concentration (Moosavirad et al., 2015). In systems with controlled metal species, allow high percentages of metal recoveries (Mensah-Biney et al., 1995; Van Nguyen et al., 2009). Resin with sulfonic groups exist in Na^+ and H^+ forms. Examples of commercial resins containing sulfonic groups are presented in Table 2.9.

Table 2.9: Examples of commercial resins containing sulfonic groups in H^+ and Na^+ forms

Example of commercial resin		
Brand name	**Group / Form**	**Reference**
Dowex G-23	$-S(=O)_2-OH$ / H^+	(Mensah-Biney et al. 1995)
Dowex G-25	$-S(=O)_2-OH$ / H^+	(Mensah-Biney et al. 1995)
Dowex G-26	$-S(=O)_2-OH$ / H^+	(Van Nguyen et al. 2009)
Dowex M-33	$-S(=O)_2-OH$ / H^+	(Mensah-Biney et al. 1995)
Ionac CFP-110	$-S(=O)_2-ONa$ / Na^+	(Mensah-Biney et al. 1995)
Ionac C-249	$-S(=O)_2-ONa$ / Na^+	(Mensah-Biney et al. 1995)
Amberlite IR 120	$-S(=O)_2-ONa$ / Na^+	(Mensah-Biney et al. 1995)
Amberlite 252	$-S(=O)_2-ONa$ / Na^+	(Monteagudo and Ortiz 2000)
DOWEX 50W X8	$-S(=O)_2-OH$ / H^+	(Moosavirad et al. 2015)
Lewatit S1468	$-S(=O)_2-ONa$ / Na^+	(Müller et al. 2012)
Dowex XZS-1	$-S(=O)_2-OH$ / ns[1]	(Monteagudo and Ortiz 2000)
Dowex XVS	$-S(=O)_2-OH$ / ns	(Monteagudo and Ortiz 2000)
BioRad AG 50W-X8	$-S(=O)_2-OH$ / ns	(Chiariza et al. 1997)
Xi'an LST D001	$-S(=O)_2-OH$ / ns	(Gao et al. 2013)
Xi'an LST DJH003	$-S(=O)_2-OH$ / ns	(Gao et al. 2013)

[1]ns: not specified

Literature suggest that resins with sulfonic acid groups in Na^+ form show on average a 10% higher metal adsorption capacity than the H^+ counterparts. The differences in adsorption capacities are attributed to better ionization properties presented by Na^+ forms (Mensah-Biney et al., 1995). Likewise, present high extraction potential for Hg^{2+} removal (Monteagudo and Ortiz, 2000; Müller et al., 2012).

2.3.3.2 Resins containing thiol groups

Thiol groups, also known as mercaptans, have special affinity for Hg (Dabrowski et al., 2004). Resins with thiol groups are SCR and soft Lewis bases. Also, present chelating properties in solutions at low pH. Resins containing thiol show high adsorption preferences towards soft acids (e.g., Hg, Cu^+, Ag^+, Au^+, and some PGMs) than base metals (Iglesias et al., 1999). Commercially, are employed for metal streams purifications and precious metal concentration (Hubicki and Wołowicz, 2009). The metal ion selectivity of thiol groups reported with Ambersep GT74 follows the order of $Hg^{2+} > Ag^+ > Cu^{2+} > Pb^{2+} > Cd^{2+} > Ni^{2+} > Co^{2+} > Fe^{3+} > Ca^{2+} > Na^+$ and is confirmed by several resins manufacturers (Zaganiaris, 2013). In chloride and nitrate systems at pH < 2, metal ion selectivity follows the order of $Au^{3+} > Pd^{2+} > Cu^{2+} > Ni^{2+}$ (Iglesias et al., 1999). When a system is exclusive of base metals, it follows the order $Cu^{2+} > Pb^{2+} > Cd^{2+} > Zn^{2+}$ (Podkościelna and Kołodyńska, 2013). However, the extent of base metal extraction is pH dependant having the best results at mildly acidic conditions. Using Duolite GT73, the extraction selectivity follow the order $Cu^{2+} > Cd^{2+} > Zn^{2+} > Ni^{2+}$ (Saha et al., 2000). See Table 2.10 for example of commercial resins containing thiol groups. The high affinity of thiol groups with

precious metals also represents its main drawback as the adsorbed metal is difficult to recover during elution process (Kagaya et al., 2014). Thus, use of organic eluents is required to strip the metal from the resin which adds an extra step for metal recovery (Iglesias et al., 1999).

Table 2.10: Examples of commercial resins containing thiol groups

Example of commercial resin		
Brand name	**Group / Form**	**Reference**
Ambersep GT74	-SH / H^+	(Zaganiaris 2013) (Kagaya et al. 2015) (Podkościelna and Kołodyńska 2013)
Purolite S924	-SH / H^+	(Zaganiaris 2013)
Ionac SR4	-CH_3S^- / ns[1]	(Zaganiaris 2013) (Kagaya et al. 2015)
Smopex 111	-SH / ns	(Sole et al. 2016)
Smopex 234	-$C(=O)OC_2H_4SH$ / ns	(Sole et al. 2016)
Duolite ES-465	-RSH / ns	(Dabrowski et al. 2004) (Podkościelna and Kołodyńska 2013)
Duolite GT73	-SH / H^+	(Hubicki and Wołowicz 2009) (Iglesias et al. 1999)
Dowex XUS 43604.00	-RSH / ns	(Dabrowski et al. 2004)
IMAC TRM	-SH / ns	(Podkościelna and Kołodyńska 2013)
Chelite S	-SNa / Na^+	(Podkościelna and Kołodyńska 2013) (Podkościelna and Kołodyńska 2013)

[1]ns: not specified

2.3.3.3 Resins containing thiourea groups

Similar to thiol groups, resins containing thiourea and its conjugate isothiouronium are chelating soft Lewis bases with SCR properties at low pH. As suggested by the manufacturer, thiourea groups contained in Lewatit TP 214 show a metal selectivity order of $Hg^{2+} > Ag^+ > Au^+ = Au^{3+} > Pt^{2+} = Pt^{4+} > Cu^{2+} > Pb^{2+} = Pb^{4+} > Bi^{2+} > Sn^{2+} = Zn^{2+} > Cd^{2+} > Ni^{2+}$. More specifically $Hg^{2+} >> Cu^{2+} >> Pb^{2+}$ (Lezzi and Cobianco, 1994). However,

thiourea and isothiouronium groups show higher adsorption capacities than thiol groups when adsorbing mercury, gold, silver, and PGM ions (Hubicki and Wołowicz, 2009; Zaganiaris, 2013). Also, higher PGM adsorption potential than quaternary ammonium and polyamine groups (Nikoloski et al., 2015). One important characteristic of thiourea and isothiouronium is their low performance on adsorbing base metal ions (Koivula et al., 2000). Also, require large amounts of organic eluents or strong acids for proper metal recuperation in elution processes. Table 2.11 show examples of commercial resins containing thiourea / isothiouronium groups.

Table 2.11: Detail of commercial resins containing thiourea and its tautomeric form isothiouronium groups

Example of commercial resin			
Group	**Brand name**	**Group / Form**	**Reference**
Thiourea	Lewatit TP-214	$-CH_2NHC=SNH_2$ / ns[1]	(Zaganiaris 2013) (Kagaya et al. 2015)
Thiourea	Purolite S-914	ns / ns	(Zaganiaris 2013)
Isothiouronium	Purolite S-920	$-CH_2SC=NHNH_2$ / H^+	(Zaganiaris 2013) (Kagaya et al. 2015) (Hubicki and Wołowicz 2009)
Isothiouronium	Dowex XUS 43600	$-CH_2SC=NHNH_2$ / ns	(Zaganiaris 2013) (Kagaya et al. 2015)

[1]ns: not specified

2.3.4 Ion exchange resins with oxygen containing groups:

Carboxyl and hydroxyl groups are the most recurrent groups in ion exchange resins. These groups are commonly present in several other common functional groups containing N, P, or S. However, only a few resins containing exclusively carboxyl or hydroxyl groups are available in the market as ion exchangers. Carboxylic acid groups are the most common

functional group in commercial resins. In smaller scale, SIR with poly-alcohols (such as Lewatit Monoplus MK51) and poly-phenol groups have been developed but the resin-metal interaction is too weak for considerations in hydrometallurgy.

2.3.4.1 - Resins containing carboxylic acid groups

Resins with carboxylic acid groups are the most common form of WCR. Table 2.12 includes examples of commercial resins containing carboxylic acid groups. These type resins are used for water softening, metal concentration and recuperation (Dabrowski et al., 2004).

Table 2.12: Examples of commercial resins containing thiol groups

Example of commercial resin		
Brand name	**Group / Form**	**Reference**
IMAC HP333	-COOH / ns[1]	na[2]
Wofatit CA-20	-COONa / Na^+	(Dabrowski et al. 2004)
Lewatit S 8528	-COOH / H^+	na
Lewatit CNP-LF NA	-COOH / H^+; Na^+	na
Purolite C106	-COOH / H^+	(Dabrowski et al. 2004)
Purolite C104Plus	-COOH / H^+	na
Duolite C-433	-COOH / H^+	(Gupta et al. 2004)
Dowex MAC-3	-COOH / H^+	(Nomngongo et al. 2013)
Amberlite IRC-50	-COOH / H^+	(Riveros, 2004)
Amberlite IRC-86	-COOH / H^+	(Riveros, 2004)

[1]ns: not specified; [2]na: not available/not found in scientific literature

Resins with carboxylic acid groups show high preference for Fe and Cu adsorption (Nomngongo et al., 2013). Generally operated at pH > 4, show a metal selectivity order of $Fe^{2+} > Cu^{2+} > Zn^{2+} > Pb^{2+} > Ti^{2+} > Mn^{2+} > Cd^{2+} > Cr^{3+}$ in multi metal systems (Nomngongo

et al., 2013). In single metal systems, carboxylic acid groups show high adsorptions of Ni^{2+}, Zn^{2+}, Cd^{2+}, and Cr^{3+} ions (Dabrowski et al., 2004). Other applications of resins with carboxylic acid groups include the removal of heavy metals (e.g., Hg, Pb, and Cd) from industrial waste waters (Gupta et al., 2004; Kaušpėdienė et al., 1998).

2.3.5 Ion exchange resins with more than one atom in the functional group

Modifications of the resin by combining or substituting atoms or functional groups can enhance selectivity. As an example, resins containing quaternary ammonium show enhanced selectivity once one ethanol group substitute one methyl group from type 1 producing type 2. Similarly, is reported that the Cr (VI) extraction is enhanced when the methyl groups of a quaternary ammonium resins are substituted by carbonyl-amide or ketone (Kusku et al., 2014; Wójcik et al., 2011). Examples of the most common groups containing combination of donor atoms are iminodiacetic acid, amoniphosphonic, oxime, thiocarbamate, glucamine, and others.

2.3.5.1 - Resins containing iminodiacetic acid groups

The combination of amino group with carbonyl group produces the iminodiacetic acid with good selectivity for the valuable base metals (e.g., copper, nickel, zinc, cobalt) over calcium and magnesium. Resins with iminodiacetic acid groups are used in metal recovery from wastewaters and water treatments (Stefan and Meghea, 2014; Van Deventer, 2011). Several commercial resins maintain this order of selectivity as included in Table 2.13.

Table 2.13: Examples of commercial resins containing iminodiacetic acid groups

Example of commercial resin		
Brand name	**Group / Form**	**Reference**
BioRad Chellex-100	$-N(CH_2C(=O)ONa)_2$ / ns[1]	(Van Deventer 2011) (Stefan and Meghea 2014) (Kagaya et al. 2015) (Korkisch 1988)
Amberlite IRC748	$-N(CH_2C(=O)ONa)_2 / Na^+$	(Van Deventer 2011) (Stefan and Meghea 2014)
Amberlite IRC-718	$-N(CH_2C(=O)ONa)_2$ / ns	Diniz et al. 2000
Lewatit TP 208	$-N(CH_2C(=O)ONa)_2 / Na^+$	(Stefan and Meghea 2014)
Lewatit TP 207	$-N(CH_2C(=O)OH)_2 / Na^+$	(Van Deventer 2011) (Stefan and Meghea 2014) (Korkisch 1988) (Lee and Lee, 2016)
Lewatit MonoPlus TP 209 XL	$-N(CH_2C(=O)OH)_2$ / ns	na[2]
Lewatit MonoPlus TP 207	$-N(CH_2C(=O)ONa)_2 / Na^+$	(Kagaya et al. 2015)
Purolite S930	$-N(CH_2C(=O)ONa)_2 / Na^+$	(Van Deventer 2011)
Diaion CR11	$-N(CH_2C(=O)ONa)_2 / Na^+$	(Kagaya et al. 2015)
Diaion CR10	$-CH_2N(CH_2C(=O)OH)_2$ / ns	(Korkisch 1988)
Dowex A-1	$CH_2N(CH_2C(=O)ONa)_2 / Na^+$	(Korkisch 1988)
Muromac A-1	$-N(CH_2C(=O)OH)_2$ / ns	(Kagaya et al. 2015)
Muromac B-1	$-N(CH_2C(=O)OH)_2$ / ns	(Kagaya et al. 2015)
Serdolit Chelite CHE	$-N(CH_2C(=O)OH)_2$ / ns	(Kagaya et al. 2015)
Varion CH	$-CH_2N(CH_2C(=O)OH)_2$ / ns	(Korkisch 1988)
Wofatit CM-50	$-CH_2N(CH_2C(=O)OH)_2$ / ns	(Korkisch 1988)
Xi'an LST LSC-100	$-N(CH_2C(=O)OH)_2$ / ns	(Gao et al. 2013)
Zhengguang Industrial Co. D851	$-N(CH_2C(=O)OH)_2$ / ns	(He et al. 2016)
KT-1	$-N(CH_2C(=O)OH)_2$ / ns	(Korkisch 1988)
KT-2 (ANKB-50)	$-CH_2N(CH_2C(=O)OH)_2$ / ns	(Korkisch 1988)
BioRad Chellex-100	$-N(CH_2C(=O)ONa)_2$ / ns	(Van Deventer 2011) (Stefan and Meghea 2014) (Kagaya et al. 2015) (Korkisch 1988)

[1]ns: not specified; [2]na: not available/not found in scientific literature

Similar to resins with carboxylic acid groups, iminodiacetic acid groups have bonding preferences towards Fe and Cu (He et al., 2016). Iminodiacetic acid groups show an ion selectivity in the order of $H^+ > Fe^{3+} > Hg^{2+} > Cu^{2+} > VO^{2+} > UO2^{2+} > Pb^{2+} > Ni^{2+} >$

Zn^{2+} > Co^{2+} > Cd^{2+} > Fe^{2+} > Be^{2+} > Mn^{2+} > Ca^{2+} > Mg^{2+} > Sr^{2+} > Ba^{2+} >>Na^{+} (Van Deventer, 2011). The low selectivity to Ca^{2+} and Mg^{2+}, allows the industrial pH modification with cheap material (e.g., lime) without incurring in Ca/Mg adsorptions on the final product (McKevitt and Dreisinger, 2012). Similarly, this group has a relatively simple desorption process obtaining high elution rates at mild acid solutions.

2.3.5.2 - Resins containing aminophosphonic acid groups

The combination of amino groups with phosphonic acid allows a high number of ligand sites. This provides strong chelating properties even at highly acidic environments (i.e., pH <1). Selectivity orders provided in literature suggest the preference of H^{+} > Fe^{3+} > Pb^{2+} > Cu^{2+} > Zn^{2+} > Al^{3+} > Mg^{2+} > Ca^{2+} > Cd^{2+} > Ni^{2+} > Co^{2+} > Sr^{2+} > Ba^{2+} > Na^{+}. Therefore, allows metal separations like Co^{2+} from Zn^{2+} and Cu^{2+} and Fe^{3+} from Ni^{2+} in highly concentrated leaches (Van Deventer, 2011). Resins with aminophosphonic acid groups are used prior to electrowining processes in the purification of Co and Cu solutions achieving 99.999% of purity (Riveros, 2010; Zaganiaris, 2013). However, aminophosphonic acid groups require organic acids for efficient elution process increasing operation cost and complexity (Kiefer and Höll, 2001). Similarly, aminophosphonic acid groups provide representative adsorptions of Mg^{2+} and Ca^{2+} decreasing the overall separation efficiency in solutions requiring pH adjustments. Table 2.14 includes examples of resins containing aminophosphonic acid groups.

Table 2.14: Examples of commercial resins containing aminophosphonic acid groups

Example of commercial resin		
Brand name	**Group / Form**	**Reference**
Amberlite IRC747	-NH-CH_2-P(=O)$(ONa)_2$ / ns[1]	(Van Deventer 2011)
Amberlite IRC747UPS	-$CH(NH_2)$-P(=O)$(OH)_2$ / ns	Na[2]
Amberlite IRC747	-NH-CH_2-P(=O)$(ONa)_2$ / Na^+	na
Lewatit TP260	-NH-CH_2-P(=O)$(ONa)_2$ / Na^+	na
Lewatit MONOPLUS TP 260	-NH-CH_2-P(=O)$(ONa)_2$ / Na^+	(Kagaya et al. 2015)
Lewatit MDS TP 260	-NH-CH_2-P(=O)$(ONa)_2$ / Na^+	(Van Deventer 2011)
Lewatit OC1060	ns / ns	(Kabay et al. 1998)
Purolite S950	-P(=O)$(ONa)_2$ / Na^+	(Van Deventer 2011) (Kagaya et al. 2015)
Purolite S940	-$CH(NH_2)$P(=O)$(ONa)_2$ / Na^+	(Petersková et al. 2012) (Kagaya et al. 2015)
Purolite PFS951	-NH-CH_2-P(=O)$(ONa)_2$ / Na^+	na
Serdolit Chelite P	-P(=O)$(OH)_2$ / ns	(Kagaya et al. 2015)
Xi'an LST LSC-500	-NH-CH_2-P(=O)$(OH)_2$ / ns	(Gao et al. 2013)

[1]ns: not specified; [2]na: not available/not found in scientific literature

2.3.5.3 - Resins containing oxime groups

Belonging to the imine type of functional groups, oxime groups have an =NOH configuration. This allows amphoteric behaviour depending on solution pH. This group exist as hydroxyoxime, ketoxime, aldoxime, and amidoxime forms in commercial ion exchange resins, being the later the most common in the market. Resins belonging to the oxime groups are rare and related information is scarce in scientific literature. Oxime groups, particularly amidoxime groups, are known to form stable bidentate complexes (Lashley et al., 2016; Rahman et al., 2016) with bivalent cations like Cu, Pb, and U(VI) in uranyl form (DybczyŃski et al., 1988; Rivas et al., 2000). However, show preferential adsorption towards trivalent metals like Ga, Cr, Fe and other or metals with higher oxidation states. This property allows the removal of ferric ions from base metal solutions

(Parus et al., 2010; Zhang et al., 2016). The iron removal potential decreases once reduced from Fe^{3+} to Fe^{2+} (Walsh et al., 1983). Earlier version of resins containing amidoxime groups (i.e.: Duolite ES-346) presented stabilities of metal complexes following the order of $Fe^{3+} > Cu^{2+} > Ni^{2+} > Co^{2+} > Zn^{2+} > Mn^{2+}$. Laboratory synthetized salicylaldoxime has a published order of selectivity of $Pb^{2+} = Zn^{2+} = Ni^{2+} > Cu^{2+} > Cd^{2+} > Pd^{2+} > Mn^{2+} > Fe^{2+} > CO^{2+}$ (Srivastava and Rao, 1990). Meanwhile, resins with phenolic oxime groups allow complex formation with metals V, Cr, Mn, Fe, Co, Ni, Cu, Zn, Ga, Mo, Pd, Sn, and Pt (Smith et al., 2003). Oxime groups also have the potential for selective U and Ga adsorption over several other alkaline-earth metals obtained from sea water (Kabay and Egawa, 1994; Kagaya et al., 2014). Despite the good selectivity properties of oxime groups, there are few ion exchange resins in the market (Table 2.15). The resin Purolite S910, containing amidoxime groups, is commercialized for the selective adsorption of As^{3+}, Fe^{3+}, Cu^{2+}, Pb^{2+}, and Cd^{2+}.

Table 2.15: Examples of commercial resins containing amidoxime groups

Example of commercial resin		
Brand name	**Group / Form**	**Reference**
Purolite 910	$-C(=NOH)NH_2$ / FB[1]	(Zaganiaris 2013) (Gibert et al. 2010) (Petersková et al. 2012)
Eichrom Nickel Resin	DGM / ns[2]	na[3]
Sumichelate MC900	Amidoxime / ns	(Kagaya et al. 2015)

[1]FE: free base; [2]ns: not specified; [3]na: not available/not found in scientific literature

2.3.5.4 - Resins containing methylglucamine groups

Methylglucamine groups, most commonly including N-methylglucamine, are WARs with pKa values close to 9 (Alexandratos, 2007). Nonetheless, it is reported that at acidic conditions, N-methylglucamine groups allow coordination bonding with the oxygen's free electrons of its hydroxyl groups (Yoshimura et al., 1998). These resins are mainly used for the recovery of boric acid and borate ion under alkaline conditions and in waste water treatment (Alexandratos, 2007; Zaganiaris, 2013). It shows high affinity to arsenate anions (AsO_4^{3-}) under neutral to basic conditions (Alexandratos, 2007), Ge in sulfate solutions (Virolainen et al., 2013), and Hg^{2+} in acidic chloride and nitrate solutions (Zhu and Alexandratos, 2005). However this resin has not shown any affinity to base metals such as Pb^{2+}, Cd^{2+}, Cu^{2+}, Ni^{2+}, Co^{2+}, and Zn^{2+}, and therefore its applications in hydrometallurgy are limited (Zhu and Alexandratos, 2005). Resins containing glucamine groups are scarce (see table 2.16) and no order of selectivity is reported.

Table 2.16: Examples of commercial resins containing amidoxime groups

Example of commercial resin		
Brand name	**Group / Form**	**Reference**
Diaion CRB03	Glucamine / ns[1]	(Kagaya et al. 2015)
Amberlite IRA 743	Glucamine / ns	(Zaganiaris 2013) (Kagaya et al. 2015) (Virolainen et al. 2013)
Diaion CRB05	Glucamine / ns	(Kagaya et al. 2015)
Purolite S-108	Glucamine / ns	(Kagaya et al. 2015)

[1]ns: not specified

2.3.5.5 - Resins containing thiocarbamate groups

Thiocarbamate groups include one-nitrogen and two sulfur atoms with electron donor potential for chelating bonding. Similar to other S containing groups, thiocarbamate resins have strong preference for precious and PG metals (Dingman Jr et al., 1974; Hubicki and Wójcik, 2004) and the characteristic attraction to Hg of sulfur groups (Kagaya et al., 2014). Resins containing thiocarbamate groups are mainly SIRs produced at laboratory scale. No references for commercial resins are available in the market. Orders of selectivity for SIR suggest a preference of $Hg^{2+} > Cd^{2+} > Zn^{2+} > Pb^{2+} > Cu^{2+} > Ag^{+} > Cr^{3+} > Ni^{2+}$ (Lezzi and Cobianco, 1994; Zaganiaris, 2013). Orders of selectivity for solvent extractants containing thiocarbamate groups showed a recuperation order of Ni > Zn > Co >> Cd > Fe > Cu (Soylak and Elci, 1997). Some synthesis of SIR included carboxyl groups to form aminodiacetic groups (see Figure 2.2) resulting in stronger coordinated interactions (Jing et al., 2009).

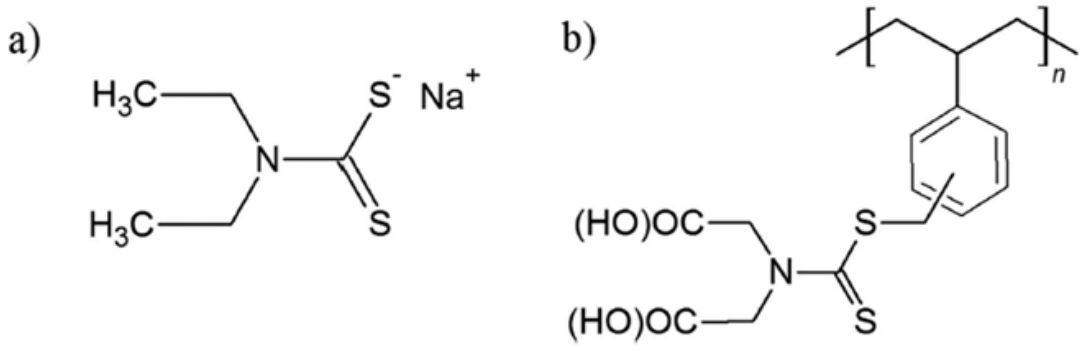

Figure 2.3: Different atomic configuration of thiocarbamate groups presented in (a) the extractant sodium diethyldithiocarbamate (Na-DDTC) used by (Soylak and Elci, 1997) and (b) N,N'-di (carboxymethyl) dithiocarbamate in SIR used by (Jing et al., 2009) that included two carboxyl groups to form iminodiacetic acid and thiocarbamate groups

2.4 Recap

A comprehensive review of polymeric resins used for metal separation/removal in hydrometallurgy and water/waste water treatments was presented in this Chapter. Resins were reviewed and categorized with respect to the principal acting atoms in functional groups, i.e., nitrogen, sulfur, phosphorous, oxygen. There is a large number of functional groups appropriate for ion exchange reactions. However, only a few of them are included in commercial ion exchange resins for applications in hydrometallurgy and water treatment. Nitrogen and sulfur based resins are the most common, whereas phosphorous and oxygen based resins are less so. The low variety of ion exchange resins in the market could be the result of marketing strategies to ease standardized production methods and controls rather than a technical limitation. The majority of macromolecular structures included in resins are based on the polymerization of styrene, acrylic acid, and their crosslinking with divinylbenzene. As a result, the commercial resins commonly have either PS-DVB or PA-DVB as the macromolecule bone structure.

There are two general categories of interactions between the functional groups and the target ionic species: (i) ion pairing or ion substitution and (ii) coordination bonding or chelating interactions between the electron donor species in the ion exchange resins and the target species. Most of resins can have both types of interactions. However, this depends on the characteristics of the functional group. Resins following under the ion pairing or ion substitution category are sub-classified into cationic and anionic resins according to the charge of their ionizable groups. Cationic exchangers, having mobile cationic ions, are resins with a polymer frame containing anionic groups attracting positive

charged ions. Anion exchangers, having mobile anionic ions, are resins with a polymer frame containing cationic groups that substitute for negatively charged species or anions.

Resins based on nitrogen-containing amino groups are anion exchangers used in the recovery of negatively charged metal complex ions. The adsorption power of the amino groups decreases with the order of the amino group (quaternary > tertiary > secondary > primary); while their adsorption selectivity follows the opposite order. Resins with picolylamine groups have strong chelating action with base metals ions, whereas guanidine groups with precious metals. Thus, used in the separation of base metals ions from precious metals complexes.

Resins based on sulfur-containing groups are cation exchangers, sulfonic group is the most common group contained in these resins. Resins with sulfonic groups are employed when the metal ion adsorption does not require specific adsorption selectivity. The high strength of sulfonic groups allows the adsorption of a variety of cations throughout a wide pH range. Chelating groups such as thiol and thiourea are selective for adsorption of PGM, mercury, and other precious metals.

Resins based on phosphorous-containing groups demonstrate high selectivity and can be used over entire pH range. Resins with phosphonic groups favour the adsorption of polyvalent ions. Phosphoric and phosphinic groups favour the adsorption of divalent ions, whereas phosphine groups favour the adsorption of soft acids such as gold, silver, PGMs, and mercury ions. Resins containing phosphorous are scarce being resins with aminophosphonic acid groups the most common in the market.

Resins containing exclusively carboxyl and hydroxyl functionalities are weak cation exchangers with good selectivity and desorption characteristics. The chelating resins based on iminoacetic groups, oxime groups, and glucamine groups maintain the adsorption properties even at acidic conditions allowing a wider range of applications. Few industrial applications were found besides the use of iminodiacetic acid resins for metal recovery from waste waters. Resins with carboxylic acid groups are the only type of resins using exclusively oxygen as the active atom and the most common WCR in the market. Carboxylic acid groups are used in water softening processes and the recuperation of metals in diluted systems.

In general, the adsorption selectivity of a resin to ion metal species depends on the characteristics of the functional group and operation conditions, such as solution pH, temperature, metal concentration, and others. The resin selection criteria depend on the charge and nature of the target metal ion species in solution and their interaction with the functional groups on resins. As such, experiments are required to find the “best” resin for a particular application.

Chapter 3 Adsorption selectivity in Fe-Ni binary metal system

This chapter includes information based on the published papers:

1. R.A. Silva, K. Hawboldt, & Y. Zhang. (2018). Application of resins with functional groups in the separation of metal ions/species – a review. Mineral Processing and Extractive Metallurgy Review 39, 395–413 having the following roles:

Rene A. Silva designed, gather the information, and conducted the literature review. Dr. Kelly Hawboldt and Dr. Yahui Zhang supervised the design of the literature review and reviewed the manuscript.

2. R.A. Silva, Y. Zhang, K. Hawboldt, & L.A. James. (2019). Study on Iron-nickel Separation Using Ion Exchange Resins with Different Functional Groups for Potential Iron Sub-production. Mineral Processing and Extractive Metallurgy Review 39, 1–15 having the following roles:

Rene A. Silva designed experimental conditions, conducted adsorption experiments, and wrote the manuscript. Dr. Yahui Zhang supervised the design of the experiment, reviewed and edited the final version of the manuscript. Dr. Kelly Hawboldt and Dr. Lesley James reviewed and edited the final version of the manuscript.

3. R.A. Silva, Y. Zhang, K. Hawboldt, L.A. James, & W. Saunders (2018). *Selective separation of iron from simulated nickel leach solutions using ion exchange technology. In Extraction 2018 (pp. 2161-2172). Springer, Cham.* having the following roles:

Rene A. Silva designed experimental conditions, conducted adsorption experiments, and wrote the manuscript. Dr. Yahui Zhang supervised the design of the experiment, reviewed and edited the final version of the manuscript. Dr. Kelly Hawboldt and Dr. Lesley James reviewed and edited the final version of the manuscript. Wesley Saunders activated and prepared resins for experiments.

And the unpublished manuscript:

4. R.A. Silva, Y. Zhang, K. Hawboldt, & L.A. James. (Pending submission). Selective Fe(III) loading from base metals using non-traditional ion exchange resins at low pH and high sulfate concentration conditions having the following roles:

Rene A. Silva designed experimental conditions, conducted adsorption experiments, and wrote the manuscript. Dr. Yahui Zhang supervised the design of the experiment, reviewed and edited the final version of the manuscript. Dr. Kelly Hawboldt and Dr. Lesley James reviewed and edited the final version of the manuscript.

3.1 Abstract

Removal of iron is required during base metal purification. This chapter investigates the extent of Fe^{3+}-Ni^{2+} separation using commercially available ion exchange resins in order to determine if this is a technically viable alternative for iron removal in nickel solution purification processes. A synthetic leach liquor containing similar magnitudes of concentration of Fe^{3+} and Ni^{2+} was used. The Fe^{3+} and Ni^{2+} concentrations in bimetallic systems resemble a rough average of concentrations commonly found in leach liquors from Ni-bearing sulfide and laterite ores processing. The study includes the analysis of 30 ion exchange-resins representing 15 different functional groups and a non-functionalized resin. The resins were selected from strong and weak cationic exchangers, chelating, and mixed bed resins. Additionally, anion exchange resins were used as control while non-functionalized resins as blank experiments. The results showed most resins tested favoured Fe^{3+} adsorption over Ni^{2+}. However, only few showed high selectivity. The best Fe^{3+} adsorption resins from "best" to "least" were; aminophosphonic acid > mixed phosphonic and sulfonic > iminodiacetic acid > N-methylglucamine > sulfonic > mixed bed > carboxylic acid > quaternary ammonium > amidoxime > thiourea/isothiouronium > phosphoric acid > non-functionalized resins > phosphinic > bis-picolylamine > thiol. From the resins tested, only those containing bis-picolylamine groups showed higher Ni^{2+} adsorption than Fe^{3+}. Resins with sulfonic, thiourea/isothiouronium, and thiol groups had relatively large Ni^{2+} co-adsorptions. Co-adsorption of Ni^{2+} was almost similar to Fe^{3+} adsorption in resin with sulfonic groups. In resins with thiourea/isothiouronium and thiol Ni^{2+} adsorption reached over half of the adsorption of Fe^{3+}. The rest of the resins had

relatively low Ni^{2+} co-adsorption, obtaining under half of that of Fe^{3+}. Overall, ion exchange resins were able to separate Fe^{3+} in bimetallic systems. Aminophosphonic acid groups and mixed phosphonic and sulfonic resins performed the best.

Selectivity and metal adsorption of ion exchange resins depend on several process variables such as metal concentration, pH, and temperature. To study the impact of these process variables on the adsorption preference of Fe^{3+}, best performing resins underwent a systematic study of single factor optimization. The best performer resins were aminophosphonic acid, a combination of phosphonic and sulfonic groups, iminodiacetic, N-methylglucamine, carboxylic acid, quaternary ammonium, and amidoxime groups. Additionally, studies were conducted on non-functionalized resins as control experiments. In addition, this Chapter includes an analysis of time dependency of the selective adsorption for each of the best performer.

The results show that most of the best performer resins maintained a good performance at different experimental conditions. Only resins with amidoxime groups yielded poor results despite the good performance observed at different resin concentration. The most efficient conditions for selective adsorption are metal concentrations above 20 g/L and a pH under 2.0. Increments in temperature had little effect on the metal adsorption trends maintaining metal selectivity throughout the temperatures tested. Most resins showed little increases of Fe^{3+} adsorption as temperature increased from 20°C to 80°C excepting resins with aminophosphonic acid and iminodiacetic acid groups. Resins with aminophosphonic acid groups showed the highest decrease in Fe^{3+} adsorption as temperature increased up to 80°C. As a general trend, Fe^{3+} adsorption increased with time

while Ni^{2+} adsorptions decreased suggesting a possible displacement by preferred Fe^{3+} adsorption.

3.2 Introduction

Iron co-exists with base metals in mineral ores in concentrations of the same order of magnitude or greater as the metal of interest. Mineral ores for base metal production require the removal of iron to produce high purity material. After initial ore processing, the concentrates undergo a pressure leaching (PL) process to dissolve soluble metals in the leachate for further concentration through hydrometallurgy (Whittington and Muir, 2000). Once metals are available in solution, the first step for base metal purification is the removal of iron in Fe^{3+} form (Kholkin et al., 2000; Meshram et al., 2019). The concentration of Fe^{3+} depends on the nature of the ore and often occur at mass fractions larger than the metals of interest. During nickel production, leach liquors usually contain between 20 - 80 g/L of Fe and <1 - 30 g/L of Ni depending on the type of ore and specifications of leaching process (Bhattacharjee et al., 2005; Dyson and Scott, 1976). Laterite and sulfide ores are the main source of Ni (Çetintaş and Bingöl, 2018). Laterite ores commonly contain higher mass percentage of Fe^{3+} than sulfide ores and therefore, produce a leachate with higher Fe^{3+} content after PL process. However, due to their complex mineralogy, the leach liquors also contain low concentration of Ni. Contrarily, sulfide ores produce leach liquors rich in Ni and Fe (Antola et al., 1995).

Precipitation is the most common process for Fe^{3+} removal after the PL process. This is a simple process requiring increase leach liquor pH to greater than 2.3 to remove

Fe^{3+}. The increase of pH produces insoluble material (solid/slurry) which is removed mechanically. The solids must be treated/disposed of according to regulations resulting in additional environmental and economic costs (Çetintaş and Bingöl, 2018; Zhang et al., 2016). Aside environmental risks posed by waste, the Fe-rich material has added value in terms of Fe co-production. The financial feasibility of Fe co-production relies in achieving high purity Fe sub-products. Options for Fe removal include solvent extraction (Ay et al., 2004; Kholkin et al., 2000; René A Silva et al., 2018) and ion exchange using resins for selective separations. This solid-liquid extraction provides physical and chemical stability during adsorption allowing adsorption-desorption cycles without affecting the chemistry of downstream processes.

An in-depth review of resins available in Canadian market identified 15 brands produced by15 manufacturers (see Table 3.1). Although there is a vast number of commercial resins, an exhaustive classification of the available resins suggest that less than 30 functional groups are available for commercial applications (see Table 3.2). For each functional group, there is a number of variations in the resin such as particle size, degree of crosslinking, polymeric matrix, and final application (e.g., human consumption or in the chemical industry). The most common type of resins are cation exchange resins including 14 main different types functional groups for recovery or removal of metal cations from water streams. Anion exchange resins are the second most common, with eight different types of functional groups. Their application is the removal of metals in oxoacid forms and macromolecules. Lastly, resin with amphoteric properties with two main different types of functional groups and resins containing a combination of cation and anion exchange

properties or mixed bed resins. Resin with amphoteric properties are used for specialized ion removal such as boron, uranium, gallium, and germanium (Silva et al., 2018).

Table 3.1: Main manufacturers in ion exchange industry in Canadian market with their representative commercial brand

	Manufacturer	**Brand**
1	Rohm&Hass	Amberlite
2	Dow	Dowex
3	Purolite	Puromet
4	Lanxess	Lewatit
5	Mitsubishi	Diaion
6	Biorad	IMAC
7	Resinex	Resinex
8	Eichrom	Eichrom
9	Resintech	Resintech
10	Toyopearl	Toyopearl
11	Ionac	Ionac
12	Henckel	Henckel
13	Reillex	Reillex
14	Token	Token
15	Tulsion	Termax

Table 3.2: Main functional groups available in commercial ion exchange resins in Canadian market

Cation exchangers	**Anion exchangers**	**Amphoteric**
Aminophosphonic	Quaternary ammonium type I&II	Amidoxime
Iminmodiacetic	Tertiary amine	Methylglucamine
Sulfonic	Tertiary amine and quaternary ammonium	Mixed bed resins
Thiol	Secondary and tertiary amine	
Phosphoric	Primary amine	
Carboxylic	Complex amine	
Phosphinic	Guanidine	
Polyalchool	Pyridine	
Thiazolidine		
Thiourea		
Isothiouronium		
Phosphonic		
Thiocarbamate		
Picolylamine		

There are a large number of studies comparing the adsorption efficiencies and metal ion selectivity of different commercial IEx-resin. However, most of the studies report adsorption comparisons on resins with analogue functional groups (e.g., comparison of two or more commercial resins containing aminophosphonic acid groups). The metal selectivity of resins has been well reported by manufacturers elsewhere (Silva et al., 2018). However, most of the studies address ionic adsorption behaviour at low metal concentrations and neutral pH, which is not appropriate for hydrometallurgy studies. There is a lack of direct comparisons of different functional groups for specific separations at high metal concentrations and highly acidic pH. Comparisons at such conditions can expose new and efficient functional groups for Fe^{3+} separations, which could in turn allow replacement of current precipitation processes. Therefore, a study on the adsorption properties and preferences to Fe adsorption by resins with different functional groups is beneficial for a better resin selection at laboratory and industrial scale.

This chapter evaluates the adsorption capabilities and selectivity between Fe^{3+} and Ni^{2+} at high concentrations of the most common functional groups in commercial resins. In total, includes the analysis of 30 ion exchange-resins representing 15 of the different functional groups and a non-functionalized resin as illustrated in Figure 3.1. The functional groups selected are identified as the most commonly found in commercial resins; including (i) strong cationic exchangers, containing sulfonic acid groups; (ii) weak cationic exchangers, containing carboxylic acid groups; (iii) chelating resins, containing N-methylglucamine, amidoxime, iminodiacetic acid, bis-picolylamine, phosphinic, phosphoric, thiol, thiourea, isothiouronium, aminophosphonic acid, and combination of

sulfonic and phosphonic acid groups; and (iv) mixed bed resins, containing a combination of quaternary ammonium and sulfonic acid groups. Additionally, anion exchange resins containing quaternary ammonium groups and non-functionalized resins acted as control and blank experiment respectively. In order to address a Fe separation process beneficial for either type of Ni source (i.e., lateritic and sulfide Ni-bearing ores), experiments at similar Fe-Ni concentrations at 25 g/L were conducted. Among the resin tested, a group of seven best performer resins and non-functionalized resins underwent a series of systematic studies studied single factor optimization including: variation of metal concentration, ionic ratio, solution pH, temperature, and time.

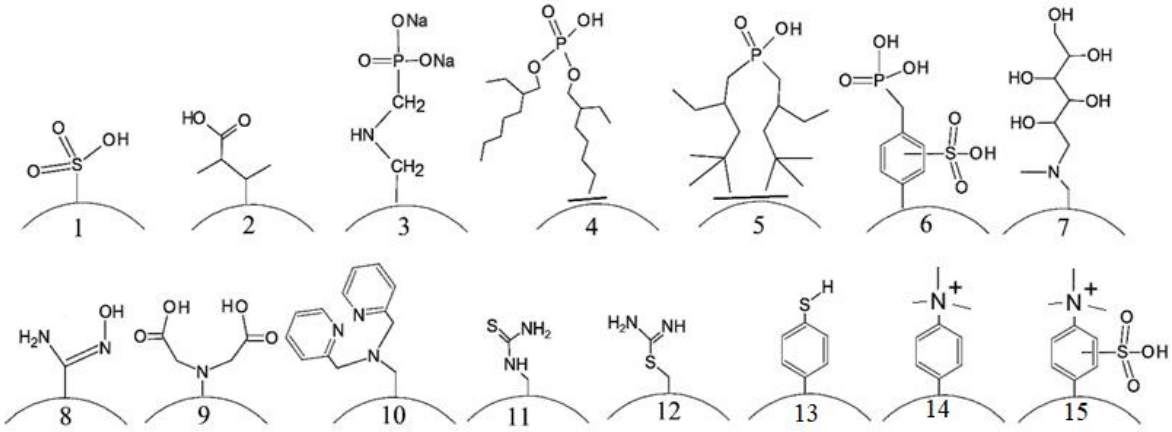

Figure 3.1: Collection of general diagrams of functional groups included in tested resins: 1) sulfonic groups, 2) carboxylic acid groups, 3) aminomethyl phosphonic groups, 4) phosphoric groups as in D2EHPA, 5) phosphinic groups as in bis-(2,4,4-trimethylpentyl-) phosphinate, 6) a combination of phosphonic and sulfonic groups, 7) methylglucamine groups, 8) amidoxime groups, 9) iminodiacetic acid groups, 10) bispicolylamine groups, 11) thiourea groups, 12) isothiouronium groups, 13) thiol groups, 14) quaternary ammonium, and 15) mixed bed resin. Modified from (Silva et al., 2019).

3.3 Materials and methods

3.3.1 Pre-conditioning

The separation of Fe^{3+} from Ni^{2+} was studied with resins detailed in Table 3.3. Resins underwent an initial pre-conditioning to reach homogeneous conditions during experiments. Pre-conditioning included a 24 h bath in a deionized water solution with pH corrected to 1.5 (1.5 DI) using HCl 30% (v/v). Resin concentration for the bath was set to 0.2 g of resin per mL and was agitated on a reciprocating platform shaker (Promax 2020, Heidolph Instruments GmbH&Co.KG) at 150 rpm. After, resins dried to constant weight at room temperature and negative pressure.

Table 3.3: Commercial resins used for Fe^{3+} and Ni^{2+} separation classified by functional group and specifications. Adapted from (Silva et al., 2019)

Functional group (ionic form)	**HSBA base classification**	**Resin brand**		**Producer**	**Particle size [mm]**	**Total exchange capacity**
Sulfonic (H^+)	Borderline[1]	1	IR120	Amberlite®	0.60–0.80	2 eq^2/L
		2	G-26	Dowex®	0.60–0.70	2 eq/L
Carboxylic acid (H^+)	Hard[1]	3	Mac-3	Dowex®	0.30–1.20	4 eq/L
		4	WACG-HP	Resintech	0.3–1.20	3.8 eq/L
Amino-phosphonic acid (Na^+)	Hard[1]	5	IRC747	Amberlite®	0.52–0.66	1.75 eq/L
		6	TP 260	Lewatit®	0.50–0.60	2.3 eq/L
		7	MTS9500 (S950)	Purolite®	0.60–0.85	24 gCa/L (1.2 eq/L)
		8	MTS9400 (S940)	Purolite®	0.42–0.85	20 gCa/L (1.0 eq/L)
		9	SIR-500	Resintech	0.30–1.18	1.4 eq/L
Phosphoric acid (D2EHPA / Di-2-ethylhexyl-phosphoric acid)	Hard[1]	10	VP OC 1026	Lewatit®	0.30–1.20	13 gZn/L (0.40 eq/L
Phosphinic acid (Bis-(2,4,4-trimethylpentyl-) phosphinic acid)	Hard[1]	11	TP272	Lewatit®	0.30–1.60	12.5 gZn/L (0.38 eq/L

Functional group (ionic form)	HSBA base classification	Resin brand		Producer	Particle size [mm]	Total exchange capacity
Phosphonic & Sulfonic (H^+)	Hard & borderline[1]	12	MTS9570 (S957)	Purolite®	0.55–0.75	18 g Fe/L (0.97 eq/L)
Iminodiacetic acid (Na^+)	Hard	13	IRC748	Amberlite®	0.50–0.65	1.35 eq/L
		14	TP 207	Lewatit®	0.40–1.25	2.2 eq/L
		15	TP208MDS	Lewatit®	0.30-0.40	2.8 eq/L
		16	TP208MP	Lewatit®	0.60-0.70	2.5 eq/L
		17	MTS9300 (S930)	Purolite®	0.60–0.85	30 gCu/L (0.94 eq/L)
Amidoxime	Borderline	18	MTS9100	Puromet®	0.30-1.20	40gCu/L (1.26 eq/L)
N-methylglucamine	Hard	19	S108	Purolite®	0.42-0.63	0.6 eq/L
Bis-pycolilamine	Soft[1]	20	M4195	DOWEX	0.30-0.85	35 gCu/L (1.10 eq/L)
		21	TP 220	Lewatit®	0.57–0.67	NR
Thiourea	Soft[1]	22	TP 214	Lewatit®	0.50-0.60	1.0 eq/L
		23	MTS9140	Puromet®	0.30-1.20	1.0 eq/L
Isothiouronium	Soft[1]	24	MTS9200	Puromet®	0.30-1.20	275 gHg/L (1.37 eq/L)
Thiol	Soft[1]	25	MTS9240	Puromet®	0.30-1.00	200 gHg/L (1.00eq/L)
Quaternary ammonium and sulfonic acid	Hard & Borderline[1]	26	IRN150	Amberlite	0.60-0.70	1.90/1.20[2]
		27	MDB-10	Resintech	0.30-1.20	0.6 eq/L
Quaternary ammonium	Hard	28	4400Cl^-	Amberjet	0.53-0.63	1.4 eq/L
		29	IRA440Cl^-	Amberlite	0.60-0.75	1.4 eq/L
Non-functionalized	None	30	XAD-7	Amberlite	0.56-0.71	None

[1](Silva et al., 2019); [2] eq stands for gram-equivalent

For each experiment, the required dosage of dry resins went through an initial swelling in 1.5 DI for 1 h. After swelling 1.5 DI was filtered and 20 mL of synthetic nickel leach liquor was added for adsorption test.

3.3.2 Synthetic leach liquor

Synthetic nickel leaching solutions contained 25 g/L of Fe^{3+} and 25 g/L of Ni^{2+} at a pH of 1.5. Equal metal concentrations were selected to approximate the average of Fe and Ni concentration commonly found in liquors after pressure leaching of Ni-bearing sulfide and laterite ores (Bhattacharjee et al., 2005; Dyson and Scott, 1976). The desired metal concentration was obtained by dissolving sulfate salts of analytical ACS reagent grade in the form of $Fe_2(SO_4)_3 \cdot 5H_2O$ and $NiSO_4 \cdot 6H_2O$ in deionized water.

3.3.3 Adsorption tests

Metal adsorption test at different resin dosage (i.e., 0.1, 0.2, 0.3, 0.4, and 0.5 g/mL) were conducted in 50 mL Erlenmeyer flasks in batch tests during 2h and agitated at 150 rpm on a reciprocating platform shaker at room temperature. The metal concentrations before and after the adsorption test were determined using wavelength dispersive X-ray fluorescence spectroscopy (XRF Supermini200, Rigaku Co.) and the difference in concentration used for the metal adsorption calculation following equation 3.1:

$$L(\%) = \left|\frac{(C_o - C_e)}{C_o}\right| \times 100 \qquad \text{Eq. (3.1)}$$

Where C_o and C_e are the initial and equilibrium concentrations of metals (g/L), respectively. The batch adsorption experiments were performed in triplicate. The reproducibility deviation of the measurements was within 5 %.

3.3.4 Systematic studies of single factor optimization

Resins determined as the best performers underwent a preconditioning in pH 1.5 deionized (1.5 DI) water (adjusted using 30% (v/v) HCl) and dried to constant weight during 72 hours at room temperature and negative atmosphere as described in Section 3.3.1. Table 3.4 includes a list of the best performer resin that underwent systematic studies.

Table 3.4: Commercial resins used for systematic studies for Fe^{3+} separations

Functional group (ionic form)	**Resin**		**Brand**
Aminophosphonic acid (Na^+)	1	SIR-500	Resintech
Phosphonic & Sulfonic (H^+)	2	MTS9570 (S957)	Purolite®
Iminodiacetic acid (Na^+)	3	MTS9300 (S930)	Purolite®
N-methylglucamine	4	S108	Purolite®
Carboxylic acid (H^+)	5	WACG-HP	Resintech
Quaternary ammonium	6	IRA440Cl^-	Amberlite
Amidoxime	7	MTS9100	Puromet®
Non-functionalized	8	XAD-7	Amberlite

For each experiment, resin dosage was adjusted using dry resin weight. The required amount of dry resin was placed in individual flasks in 1.5 DI water for 1 h to allow initial swelling. After swelling, remaining 1.5DI water was removed and replaced by 20 mL of synthetic leach solution. Adsorption tests were conducted at different metal concentrations and Fe:Ni concentration ratios. The metal concentrations selected for analyses were 5, 10, 15, 20, and 25 g/L of each metal and Fe:Ni concentration ratios of 3:1, 2:1, 1:1, 1:2, and 1:3.

Experiments at initial solution pH, temperature, and time were conducted between 0.8 and 2.3, 20°C to 80°C, and from 0 to 120 min, respectively. Unless otherwise stated

resin concentration remained at 0.2 g/mL with metal concentrations of 25 gFe/L, 25 gNi/L, pH 1.5, and 25 °C during 120 min. The metal concentrations before and after the adsorption test were determined using wavelength dispersive X-ray fluorescence spectroscopy and the difference in concentration used for the metal adsorption calculation following equation 3.1.

3.4 Results

3.4.1 Determination of best performer resins for iron adsorption

3.4.1.1 Resins with sulfonic groups

Both of the resins containing sulfonic groups tested (i.e., Amberlite IR120 and Dowex G-26) show high adsorption of Fe^{3+} and Ni^{2+}. As shown in Figure 3.2, the difference in ion adsorption was not enough to indicate Fe^{3+} selectivity. The highest resin dosage achieved the maximum total metal adsorption. Amberlite IR120 achieved the maximum Fe^{3+} adsorption at 78% and 65% of Ni^{2+}. On average, one gram of dry resin adsorbed 48 mg of Fe^{3+} and 39 mg of Ni^{2+}, respectively. The trends observed in Figure 3.2 suggest that resin dosages larger than 0.5 g/mL may achieve greater metal adsorption. However, the volume of larger resin dosages limits the resin-solute contact given the volume used in experiments (20 mL).

Based on the results obtained, resins with sulfonic groups are not recommended for Fe^{3+}:Ni^{2+} separation. Instead are an interesting alternative for the concentration and recovery of Fe^{3+} and Ni^{2+} from effluents at low metal concentration (Dizge et al., 2009; Maranon et al., 1999). Resins with sulfonic groups are one of the most common types of

strong cationic exchangers showing good performance in all types of cation adsorption. The high strength of the group allows adsorption with no apparent cation preference in solutions at high metal concentrations as confirmed in Figure 3.2.

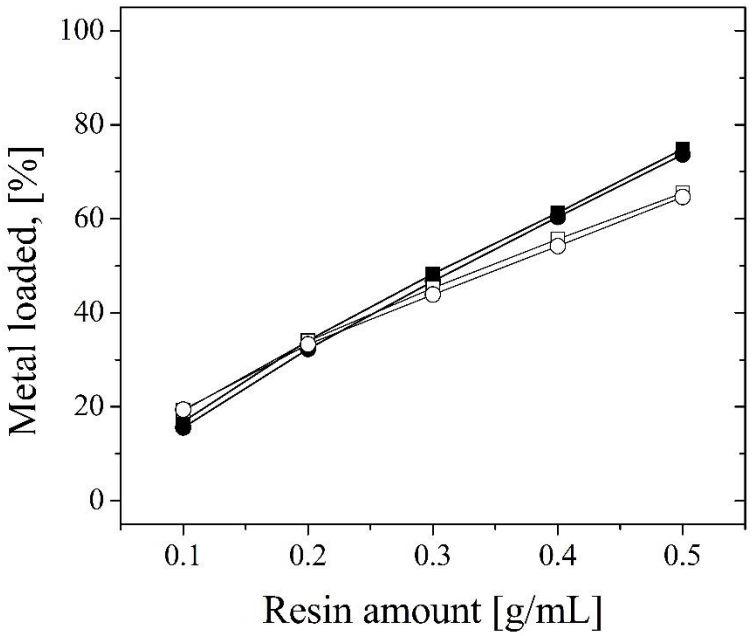

Figure 3.2: Percentage of metal adsorbed in resin containing sulfonic acid groups. (■) Fe and (□) Ni adsorbed on Amberlite IR 120 H^+ resin and (●) Fe and (○) Ni adsorbed on Dowex G-26

3.4.1.2 Resins with carboxylic acid groups

Dowex Mac-3 and Resintech WACG resins, containing carboxylic acid groups, showed similar adsorption trends (see Figure 3.3). Both resins showed a preference for Fe^{3+} adsorption over Ni^{2+}. Resintech WACG resins showed a higher metal adsorption for Fe^{3+} at 73% compared to 67% of Dowex Mac-3 at the highest resin dosage of 0.5 g/mL. The Fe^{3+} adsorption increased with resin dosage. Conversely, the Ni^{2+} co-adsorption was negligible for resin dosages lower than 0.3 g/mL, with a maximum Ni^{2+} co-adsorption of

8% at the largest resin dosage. Both resins showed similar Ni^{2+} adsorption capacities. The most efficient resin dosage was 0.3 g/mL as the Ni^{2+} co-adsorption remained close to 1%. On average, resins with carboxylic acid groups adsorbed 57 $mg/g_{dry\ resin}$ of Fe^{3+} and 3 $mg/g_{dry\ resin}$ of Ni^{2+}. The adsorption partiality is in accordance with the formation constant values for Fe^{3+} and Ni^{2+} carboxylate complexes. At ionic strength conditions of 0.1 M and 25 °C, the formation constant for Fe^{3+} and Ni^{2+} carboxylate complexes are 8.2 and 3.2, respectively (Smith and Martell, 1987).

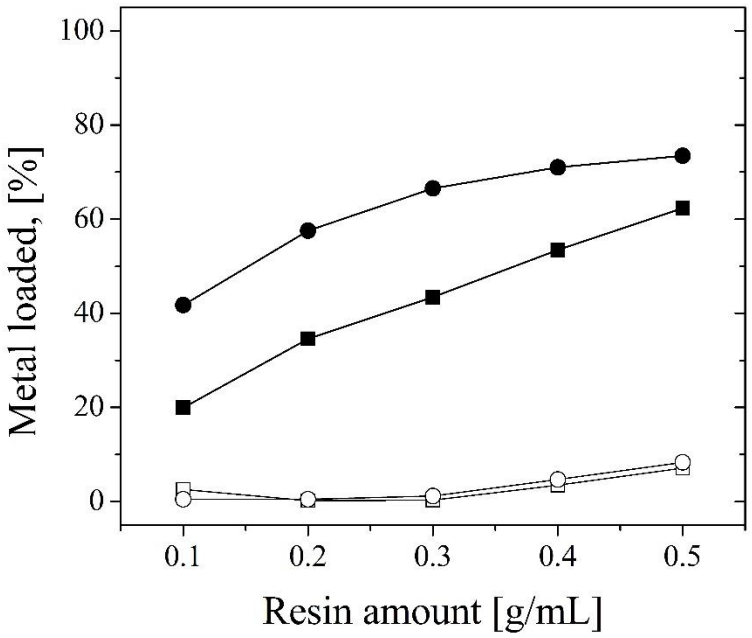

Figure 3.3: Percentage of metal adsorption in resin containing carboxylic acid group. (■) Fe and (□) Ni adsorbed on Dowex Mac-3 and (●) Fe and (○) Ni adsorbed on Resintech WACG

The increase in Ni^{2+} co-adsorption before a total depletion of Fe^{3+} may suggest a maximum adsorption of Fe^{3+} due higher availability of adsorption sites at higher resin

dosages. As Fe^{3+} depletes from solution a higher Ni:Fe concentration ratio allows higher Ni^{2+} co-adsorptions. This suggests that resin only adsorbs Ni^{2+} once Fe^{3+} is depleted. In Section 3.4.2 related to adsorption studies at different time, experimental evidence suggests that Fe^{3+} displaces the Ni^{2+} co-adsorbed. This is more likely due to higher complexing strength of Fe^{3+} compared to Ni^{2+}. Therefore, multiple stage adsorption with resin dosage under 0.3 g/ml could be a good approach to reduce Ni^{2+} co-adsorption and achieve higher Fe^{3+} removals.

Resins with carboxylic acid groups are the most common type of weak cationic exchangers. Despite their adsorption limitations at acidic conditions, these resins yielded good separation of Fe^{3+} and Ni^{2+}. The Fe^{3+} adsorption by resins with carboxylic acid groups was also reported by Riveros (2004) who concluded the potential use of these resins for metallurgical solutions purification with an added potential of iron sub production.

3.4.1.3 Resins with aminophosphonic acid groups

Five different types of resins containing aminophosphonic acid groups were tested. These were: Amberlite IRC747, Lewatit TP260, Puromet MTS9500 and MTS9400 (previously known as Purolite S950 and S940), and Resintech SIR-500 (see Table 3.3 for specifications). On average, these resins achieved Fe^{3+} adsorption greater than 85% at resin dosages of 0.5 g/mL. Resintech SIR-500 and Amberlite IRC 747 achieved the highest Fe^{3+} adsorption reaching over 90% at resin dosages of 0.3g/mL (See Figure 3.4). The most efficient separation was obtained by Resintech SIR-500 at resin dosages of 0.2 g/mL obtaining 94% of Fe^{3+} adsorption and 4.9% of Ni^{2+} co- adsorption. The Ni^{2+} co-adsorption

are almost negligible at dosages lower than 0.3 g/mL. Higher resin dosages increased Ni^{2+} co-adsorption considerably. On average, the maximum Ni^{2+} co-adsorption reached around 40% at resin dosage of 0.5 g/mL. Amberlite 747 achieved the highest amount of Ni^{2+} co-adsorption obtaining values close to 60% at 0.5 g/mL. The co-adsorption variations among resins with aminophosphonic acid groups relate to unknown structural/chemical specifics in the resins, such as synthesis process, structure length, and crosslinking degree.

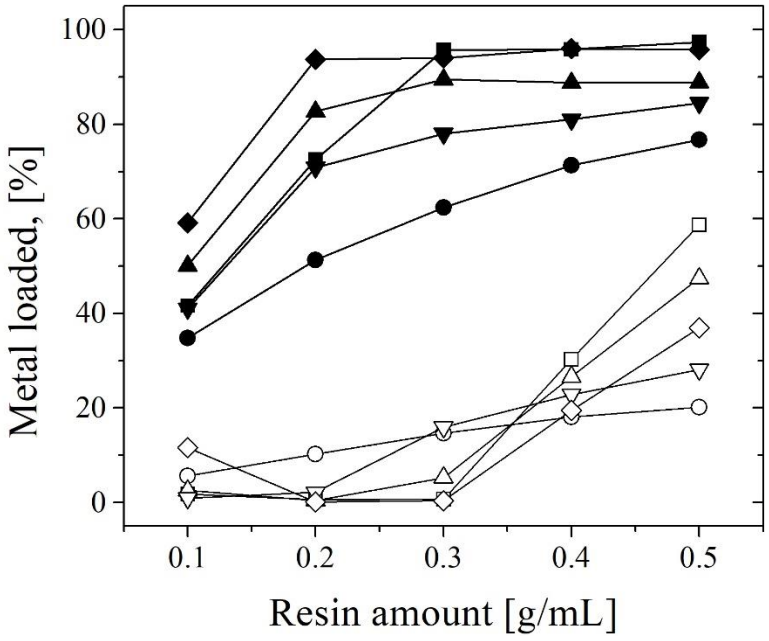

Figure 3.4: Percentage of metal adsorption in resin containing aminophosphonic acid groups (■) Fe and (□) Ni adsorbed on Amberlite IRC 747, (●) Fe and (○) Ni adsorbed on Lewatit TP260, (▲) Fe and (△) Ni adsorbed on Puromet MTS9400, (▼) Fe and (▽) Ni adsorbed on Puromet MTS9500, and (◆) Fe and (◇) Ni adsorbed on Resintech SIR-500

Increased Ni^{2+} co-adsorption in aminophosphonic acid groups occurred with stagnation of Fe^{3+} adsorption. This behaviour resembled the adsorption trend observed for resins with carboxylic acid groups. However, for resins with aminophosphonic acid groups,

the Ni^{2+} co-adsorption occurred at conditions with Fe^{3+} adsorption above 90%. This represent Fe^{3+} concentrations under 4 g/L at resin dosage of 0.3 g/mL. Therefore, the sharp increment in Ni^{2+} co-adsorptions may be related to Fe^{3+} depletion in the system. On average, Resintech SIR-500 and Amberlite IRC 747 obtained adsorption of 79 and 68 mg of Fe^{3+} and co-adsorption of 10 and 16 mg of Ni^{2+} per gram of dry resin, respectively. Puromet MTS9400 and MTS9500 achieved adsorption of 71 and 62 mg of Fe^{3+} and both had Ni^{2+} co-adsorption of 10 mg per gram of dry resin. Lewatit TP260 achieved 45 mg of Fe^{3+} and 10 mg of Ni^{2+} co-adsorption per gram of dry resin.

3.4.1.4 Resins with phosphoric groups

Resins with phosphoric groups favour Fe^{3+} over Ni^{2+} with increased metal adsorption at higher resin dosages. This type of resin adsorbed a maximum of 44% of Fe^{3+} at resin dosages of 0.5 g/mL. In contrast, adsorbed less than 3% of Ni^{2+} at all resin dosages tested (see Figure 3.5). On average, Lewatit VPOC 1026 achieved adsorption of 24 mg of Fe^{3+} and less than 1 mg of Ni^{2+} co-adsorption per gram of resin.

Resins with phosphoric groups are scarce. Commercial resins based on phosphoric groups are mainly Solvent Impregnated Resins (SIR) that emulate extractants already employed in solvent extraction processes. Lewatit VP OC 1026 is one such resin, which contains the extractant di-2-ethylhexyl-phosphoric acid (a.k.a., D2EHPA) used commercially for removal of Fe^{3+} from acidic solutions.

One observed characteristic of Lewatit VPOC 1026 was its low specific gravity (<1) in the Fe^{3+}:Ni^{2+} solution. At the agitation speed tested, the buoyant characteristic of

the resin made it difficult for the resin-solution contact. Greater agitation speed conditions improved the contact of resin and solution, thus increasing the metal adsorption by the resin (See Chapter 4).

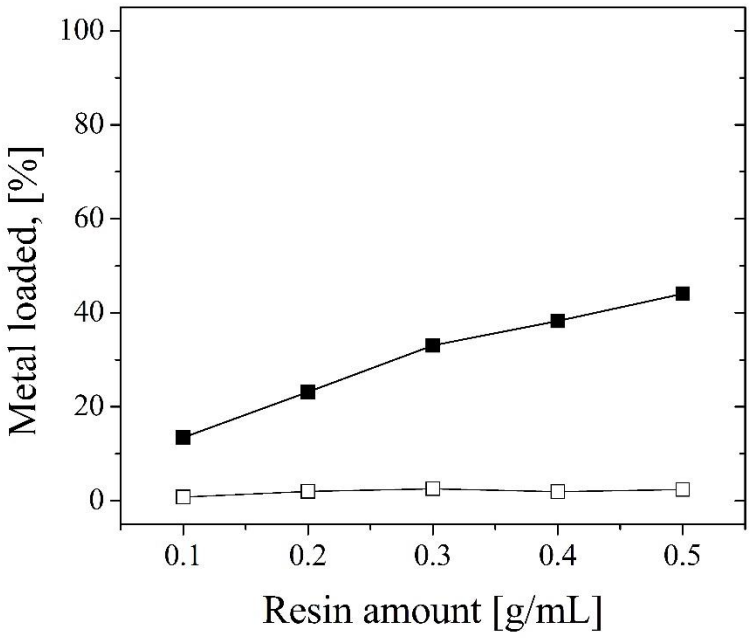

Figure 3.5: Percentage of metal adsorption in resin containing di-2-ethylhexyl-phosphoric acid (a.k.a., D2EHPA). (■) Fe and (□) Ni adsorbed on Lewatit VP OC 1026

3.4.1.5 Resins with phosphinic groups

Resins with phosphinic groups showed similar adsorption properties as resins with phosphoric groups, favouring Fe^{3+} adsorption over Ni^{2+} (See Figure 3.5 and Figure 3.6). The maximum Fe^{3+} adsorption for Lewatit TP 272 was 40%, obtained at the maximum resin dosage of 0.5 g/mL. This adsorption compares with the maximum adsorption of 44% by resins with phosphoric groups at similar conditions. In contrast, Lewatit TP 272 co-

adsorbed relatively higher amounts of Ni^{2+} achieving 11%. On average, this resin adsorbed 17 mg of Fe^{3+} and 4 mg of Ni^{2+}per gram of dry resin.

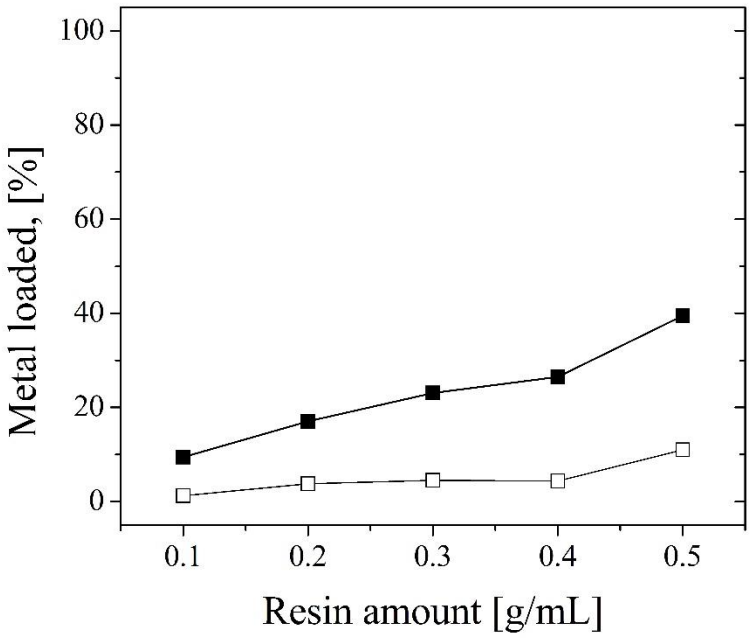

Figure 3.6: Percentage of metal adsorption in resin containing bis-(2,4,4-trimethylpentyl-) phosphinate groups. (■) Fe and (□) Ni adsorbed on Lewatit TP272

As with resins with phosphoric groups, commercial resin with phosphinic groups are scarce. The existing resins are SIR containing the extractant bis-(2,4,4-trimethylpentyl) phosphinic acid. This extractant is used in commercial solvent extraction processes for the removal of Fe^{3+} (Vaughan et al., 2016b). Likewise, Lewatit TP272 has a specific gravity lower than one affecting the resin-solution contact. High rates of agitation diminished the negative effects of buoyant characteristics (See Chapter 4).

3.4.1.6 Resins with mixed phosphonic and sulfonic groups

This resins favour the adsorption of Fe^{3+} over Ni^{2+}. Resin dosages as low as 0.2 g/mL achieved adsorption close to 90% of Fe^{3+} with Ni^{2+} co-adsorption under 10% (see Figure 3.7). The highest resin dosage achieved the highest Fe^{3+} adsorption, but increased only 4% with respect to a resin dosage of 0.2 g/mL. The maximum Fe^{3+} adsorption was 94%. The Ni^{2+} co-adsorption was almost negligible at resin dosages lower than 0.3 g/mL. However, increased considerably at resin dosages higher than 0.3 g/mL. The highest Ni^{2+} co-adsorption was 40% attained at resin dosage of 0.5 g/mL. On average, the adsorption obtained were 79 mg of Fe^{3+} and 8 mg of Ni^{2+} per gram of dry resin. The increment in Ni^{2+} co-adsorption with respect to resin dosage follows a stagnation of Fe^{3+} adsorption. This tendency was also observed in resins with carboxylic acid and aminophosphonic acid groups. Similar to resins with aminophosphonic acid, resins dosages higher than 0.2 g/mL depleted Fe^{3+} concentrations below 1.5 g/L in electrolyte allowing more opportunities for Ni^{2+} co-adsorption.

Unlike other phosphorous-based resins, the combination of sulfonic and phosphonic groups has a hydrophilic nature that eliminates the buoyancy issue. Higher hydrophilicity increases the contact between resin and electrolyte improving kinetics and metal uptake (Chiariza et al., 1997). These characteristics allowed high percentages of metal adsorption even at the agitation speed tested. Resin with combination of phosphonic and sulfonic groups are not common. Hence, the only resin tested was Puromet MTS9570 (Previously known as Purolite S957).

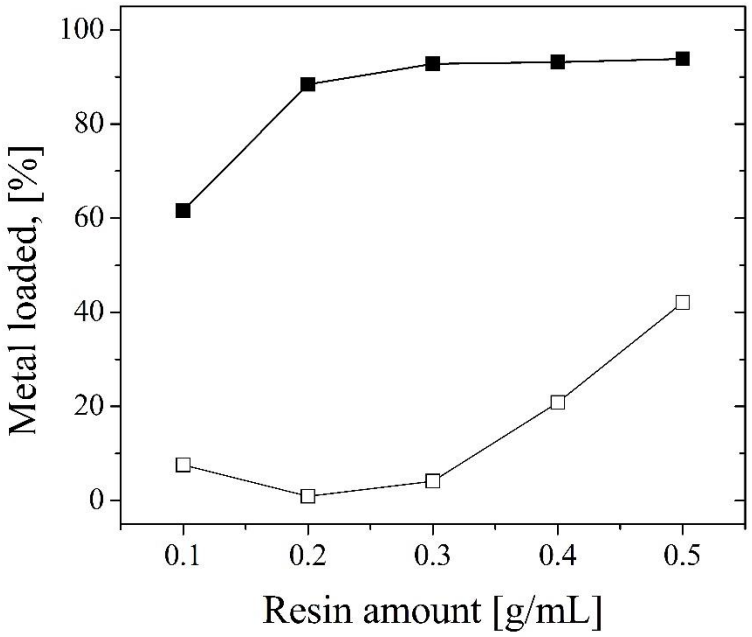

Figure 3.7: Percentage of metal adsorption in resin containing a combination of phosphonic and sulfonic groups. (■) Fe and (□) Ni adsorbed on Puromet MTS9570

3.4.1.7 Resins with iminodiacetic acid groups

The resins with iminodiacetic acid groups tested were Lewatit MP TP207, Lewatit MDS TP 208, Amberlite IRC748I, and Purolite S930E+ MR10 (Currently rebranded as Puromet MTS9300). Table 3.3 include details of these resins. Iminodiacetic acid groups favoured the Fe^{3+} adsorption with an increment of metal adsorption analog to the increase in resin dosage (see Figure 3.8). On average, the maximum Fe^{3+} adsorption reached 85% at 0.5 g/mL resin dosage. This condition also yielded the highest Ni^{2+} co-adsorption with an average of 30%. Lewatit MDS TP 208 and Purolite S930E+ (MR10) achieved the maximum metal adsorption at 90% of Fe^{3+} and 50% and 70% of Ni^{2+} co-adsorption, respectively. Lewatit MP TP207 and Amberlite IRC748I achieved maximum Fe^{3+}

adsorption of 75% and 81% with Ni^{2+} co-adsorption under 5%. Regardless of the resin brand, Ni^{2+} co-adsorption was negligible at resin dosage lower than 0.2 g/mL. On average, Lewatit MDS TP 208 and Purolite S930E+ (MR10) adsorbed 71 mg of Fe^{3+} and 9 mg and 15 mg of Ni^{2+} per gram dry resin, respectively. Lewatit MP TP207 and Amberlite IRC748I adsorbed 50 and 55 mg of Fe^{3+} and under 2 mg of Ni^{2+} per gram dry resin, in order. In general, resins with iminodiacetic acid groups were among the best performers for Fe^{3+}-Ni^{2+} separation of the nitrogen based groups tested.

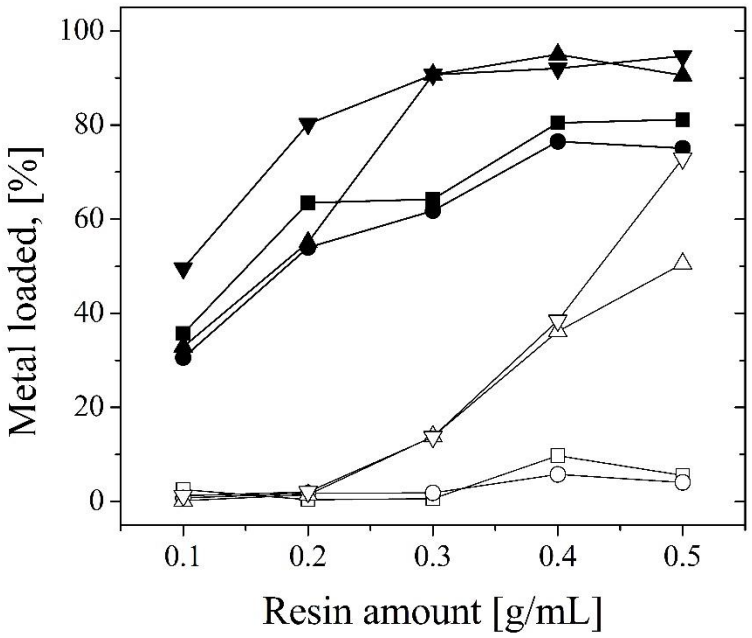

Figure 3.8: Percentage of metal adsorption in resins containing iminodiacetic acid groups. (■) Fe and (□) Ni adsorbed on Amberlite IRC 748i, (●) Fe and (○) Ni adsorbed on Lewatit TP207, (▲) Fe and (△) Ni adsorbed on Lewatit TP 208, and (▼) Fe and (▽) Ni adsorbed on Puromet MTS9300

The difference in iminodiacetic-metal formation constants between Fe^{3+} and Ni^{2+} further supports the high preference towards Fe^{3+}. At ionic strength conditions of 0.1 M

and 25 °C iminodiacetic acid has log K_1 values of 11.3 for Fe^{3+} and 8.2 for Ni^{2+} (Smith and Martell, 1987). Additionally, Fe^{3+} preference is reported in Table 3.3 as described by resin manufacturers (Silva et al., 2018).

3.4.1.8 Resins with amidoxime groups

Our results show that resin with amidoxime groups favour Fe^{3+} over Ni^{2+}. The Fe^{3+} adsorption reached a maximum of 59% at the highest resin dosage of 0.5 g/mL. However, this is only 1% higher than that at 0.4 g/mL (See Figure 3.9). As with other resins, there was a flattening of Fe^{3+} adsorption at high resin dosages accompanied an increase in Ni^{2+} adsorption (2% to 10%). Although Purolite MTS9100 underperformed in Fe^{3+} adsorption compared to other resins, there was a high Fe^{3+} selectivity over Ni^{2+}. The Ni^{2+} co-adsorption was among the lowest of all resins (adsorption around 2% at relatively high resin concentration of 0.4 g/mL). On average, the resin adsorbed 32 mg of Fe^{3+} against 1.8 mg of Ni^{2+} per gram of dry resin. These results are in accordance to the ones reported by Colella et al., (1980) that suggest higher Fe^{3+} uptake than Ni^{2+} at low mono metal concentration and pH < 2.

Resins with amidoxime groups are scarce. Purolite MTS9100 (previously known as Purolite S910) is among the few resins commercially available (Silva et al., 2018). The resin is commercialized for precious metal recovery and chromium III bath purification. It has a high preference towards Fe^{3+}. The strong Fe-amidoxime bonding also results in difficult elution process even at highly concentrated acids. The corrosive nature of strong acids negatively affects the physical integrity of the resin reducing the lifespan of the resins

(Hubicki, 1986). Therefore, the use for amidoxime groups for Fe^{3+} removal is not recommended. Hydroxy-oxime groups present good elution efficiencies at concentrations as low as 0.05 M H_2SO_4 allowing the removal of Fe (Zhang et al., 2016). Nonetheless, there is no hydroxyl-oxime resins available in Canadian market.

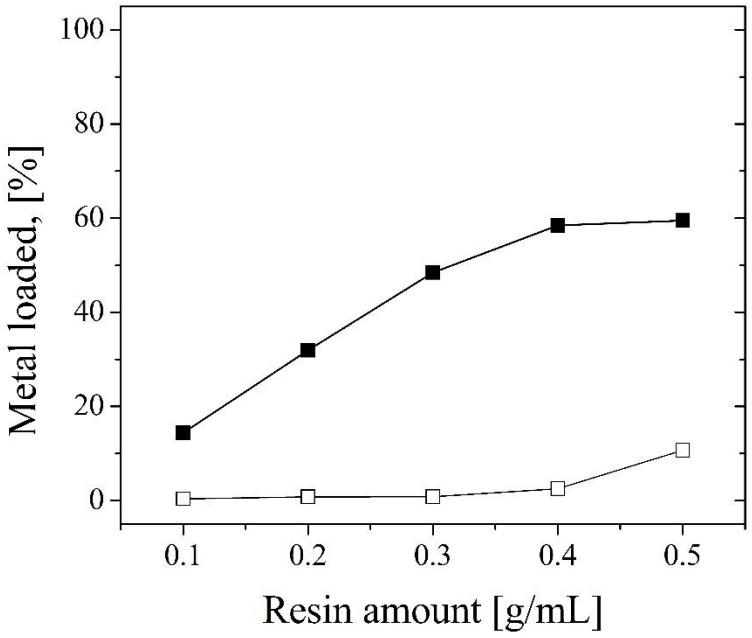

Figure 3.9: Percentage of metal adsorption in resin containing amidoxime groups. (■) Fe and (□) Ni adsorbed on Puromet MTS9100

3.4.1.9 Resins with Methylglucamine groups

Resins with methylglucamine groups as in Purolite S108 showed selective adsorption of Fe^{3+} over Ni^{2+}. Purolite S108 achieved Fe^{3+} adsorption higher than 90% with 18% of Ni^{2+} co-adsorption at the highest resin dosage (see Figure 3.10). Unlike other resins, resins with methylglucamine groups did not increase Ni^{2+} co-adsorption even with a

stagnation of Fe^{3+} adsorption at high resin dosages. At the lowest resin dosage, Fe^{3+} adsorption almost tripled that of Ni^{2+}. The Fe^{3+} preference observed in methylglucamine groups is higher than that observed by groups usually employed for Fe^{3+} removal like iminodiacetic acid and some aminophosphonic acid resins. One gram of dry resin adsorbed on average 51 mg of Fe^{3+} against 9 mg of Ni^{2+}. Results suggest that resins with methylglucamine groups are suitable for Fe^{3+} removal.

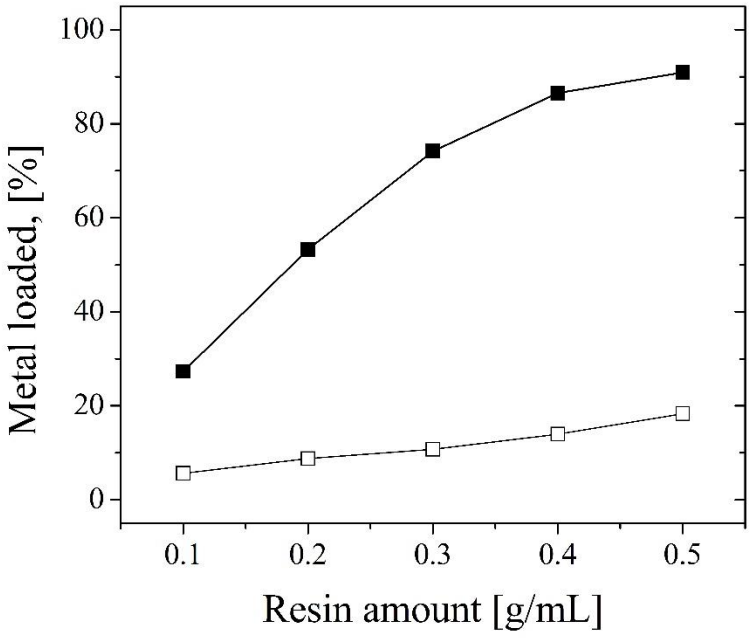

Figure 3.10: Percentage of metal adsorption in resin containing N-methylglucamine groups. (■) Fe and (□) Ni adsorbed on Purolite S108

Methylglucamine groups have amphoteric properties but weak anion exchanger characteristics prevail. Commercialized as N-methylglucamine groups, are commonly used to remove As, Ge, and B in their oxoacid forms (Kagaya et al., 2014). Also,

Methylglucamine groups are known to favour Hg^{2+} complexations over several base metal cations (Zhu and Alexandratos, 2005). The low complexation preferences by methylglucamine groups with base metals (in the bivalent state) were confirmed in our observations by the low adsorption yields obtained compared to the trivalent Fe.

Up to now, the Fe^{3+} adsorption mechanism is unknown. Given the acidic conditions of the system the cation exchange potential of the resin should be suppressed, therefore the interaction of Fe^{3+} with the resin is more likely due to coordination with the oxygen of the functional groups (see Figure 3.1) as suggested by Yoshimura et al. (1998).

3.4.1.10 Resins with bis-picolylamine groups

Unlike any other resin tested, resins containing bis-picolylamine groups (i.e., Dowex M4195 and Lewatit MDS TP 220) favoured Ni^{2+} adsorption over Fe^{3+}. The maximum Ni^{2+} adsorption reached approximately 60% at the highest resin dosage. For Fe^{3+}, the maximum adsorption was 44% by Lewatit TP220 and 37% by Dowex M4195 (see Figure 3.11). These results produced an average metal adsorption of 38 mg of Ni^{2+} and 25 mg of Fe^{3+} per gram of dry resin for Lewatit TP220, and 36 mg of Ni^{2+} and 21 mg of Fe^{3+} for Dowex M4195. The trends suggest that the higher the resin dosage the higher Ni adsorption. However, resin dosages higher than 0.5 g/mL could not be tested accurately due to mass transfer limitations (contact with resin and metal). Even if bis-pycolilamine resins can achieve Fe:Ni separations are not recommended for Fe^{3+} recovery.

Resin with bis-picolylamine are weak bases with soft characteristics according to HSAB theory (Wołowicz and Hubicki, 2012) and therefore, a better match for the

borderline acid characteristics of bivalent metals like Ni^{2+}, Co^{2+}, and Cu^{2+} (compared to the hard acid characteristics of the trivalent Fe^{3+}; (Pearson, 1963). In addition, bis-picolylamine offers selectivity among base metals. Therefore, it is currently used in industrial hydrometallurgy for Co-Ni separations (Van Deventer, 2011), and for Cu^{2+} recuperation due to strong Cu-picolylamine complex formation.

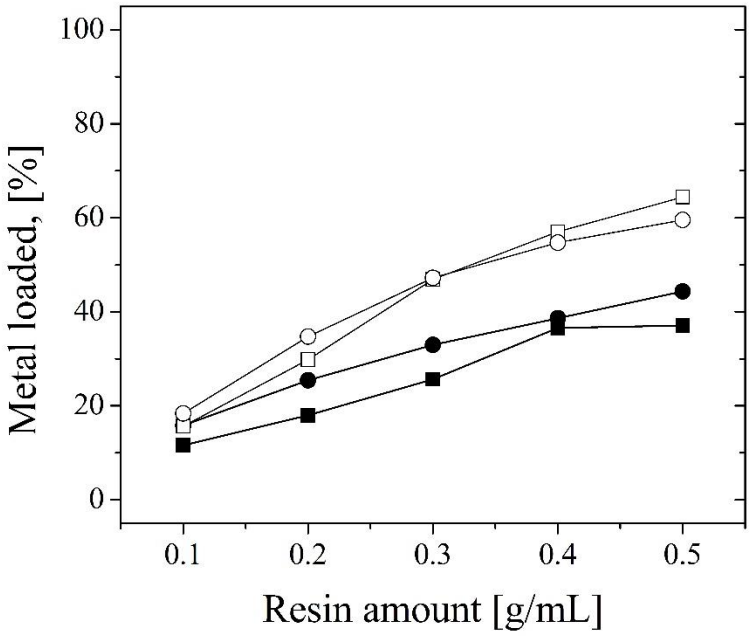

Figure 3.11: Percentage of metal adsorption in resins containing bis-picolylamine groups. (■) Fe and (□) Ni adsorbed on Dowex M4195 and (●) Fe and (○) Ni adsorbed on Lewatit TP220

3.4.1.11 Resins with thiourea and isothiouronium groups

Resin with thiourea (as in Lewatit MP TP214 and Puromet MTS9140) and its tautomeric form, isothiouronium (Puromet MTS9200), favoured Fe^{3+} adsorption over Ni^{2+}. Higher resin dosages resulted in higher metal adsorption with potential of higher metal

adsorption as resin dosages higher than 0.5g/mL. At the highest resin dosage (0.5 g/mL), the Fe^{3+} adsorption reached their maximum values being 53% for isothiouronium and 50% for thiourea groups (See Figure 3.12). The highest resin dosage resulted in the maximum Ni^{2+} co-adsorption reaching 24% with negligible difference among the tautomer configurations. On average, one gram of dry isothiouronium resin adsorbed 39 mg of Fe^{3+} and 12 mg of Ni^{2+} and thiourea adsorbed 29 mg of Fe^{3+} and 12 mg of Ni^{2+}. Although this group of resins favoured Fe^{3+} adsorption, the overall Fe^{3+} selectivity was far less than the ones observed with other functional groups.

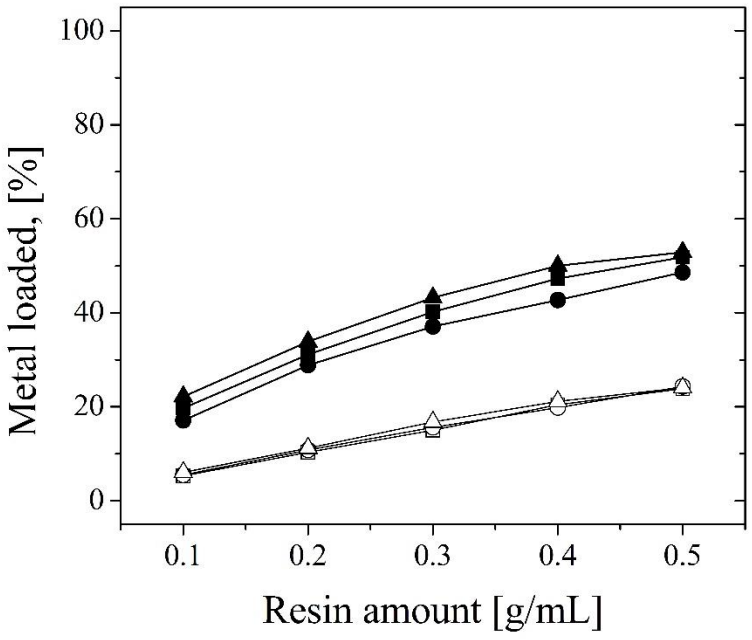

Figure 3.12: Percentage of metal adsorption in resins containing thiourea and isothiouronium groups. (■) Fe and (□) Ni adsorbed on Lewatit TP214 and (●) Fe and (○) Ni adsorbed on Puromet MTS9140 containing thiourea groups and (▲) Fe and (△) Ni adsorbed on Puromet MTS9200 with ishothiouronium

Resins containing thiourea and its tautomeric form isothiouronium coordinated complexes using S and N as electron donor atoms. Based on HSAB theory, both groups have soft base characteristics, and show preferential bonding with soft acid ions like Hg^{+}, Ag^{+}, Au^{+}, Cd^{2+}. In some instances, thiourea and isothiouronium favour bonding with borderline acids like Ni^{2+}, Cu^{2+}, and the bivalent Fe (Pearson, 1963). Less likely, coordinate with hard acids like Fe^{3+}. However, our results showed that even with soft base characteristics, thiourea/isothiouronium groups favoured the hard acid Fe^{3+} adsorption over the borderline Ni^{2+}. These results are in accordance to the bonding preference of bis-thiourea isomers reported by Fakhar et al., (2017). Based on both results, we speculate that the Fe^{3+} adsorption selectivity is due to the Ligand Field Stabilization Energy (LFSE) obtained among either group-metal complex as explained by Haas and Franz (2009).

3.4.1.12 Resins with thiol groups

Resins with thiol groups showed a minor adsorption preference of Fe^{3+} over Ni^{2+}. Thiol groups alongside resins with non-functionalized groups showed the lowest metal adsorption of all resin tested (see Figure 3.13). Thiol groups, as contained in Puromet MTS9240 (Previously Purolite S924) adsorbed 25% Fe^{3+} at the highest resin dosage with Ni^{2+} co-adsorption of 12%. The metal adsorption trends do not suggest substantial increments in metal adsorption at resin dosages higher than 0.5 g/mL. On average, thiol groups adsorbed 13 mg of Fe^{3+} and 5 mg of Ni^{2+} per gram of dry resin.

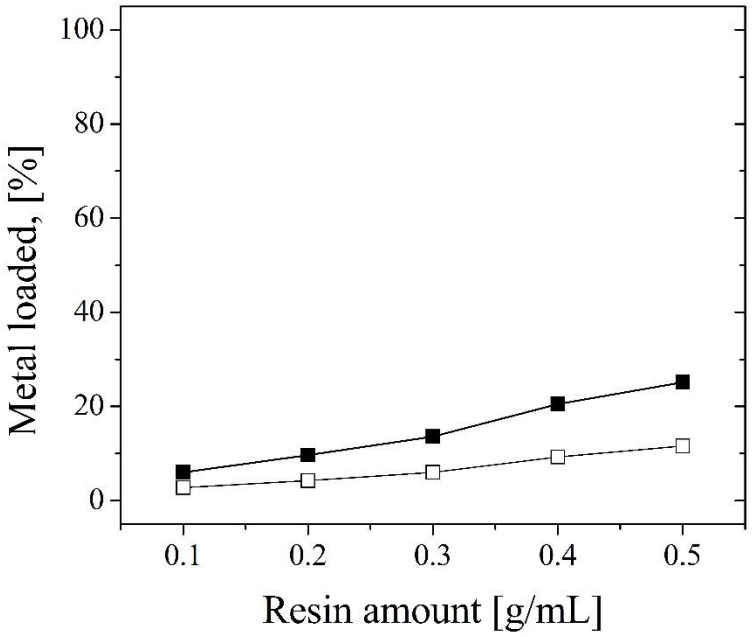

Figure 3.13: Percentage of metal adsorption in resin containing thiol groups. (■) Fe and (□) Ni adsorbed on Purometal MTS9240

Similar to thiourea, thiol groups have soft bases characteristics and therefore are more likely to form stable complexes with soft acid ions like Hg^{+}, Ag^{+}, Au^{+}, Cd^{2+} over hard acids like Fe^{3+}. Therefore, the use of thiol groups are not recommended for the recovery and separation of base metals and Fe^{3+}.

3.4.1.13 Resins with quaternary ammonium groups

Quaternary ammonium groups showed a very good selectivity for Fe^{3+} over Ni^{2+}. The Fe^{3+} adsorption increased with resin concentration, obtaining a maximum of 62% at the maximum resin dosage. The Fe^{3+} adsorption trend suggest a further increase in metal adsorption at resin dosages higher than 0.5 g/mL. Conversely, Ni^{2+} co-adsorption was

negligible at resin dosages lower than 0.3 g/mL (i.e., <1%) and only increased to a maximum of 7% at the highest resin dosage. On average, quaternary ammonium groups as in Amberlite 4400Cl^- adsorbed 41 mg of Fe^{3+} and 1.4 mg of Ni^{2+} per gram of dry resin.

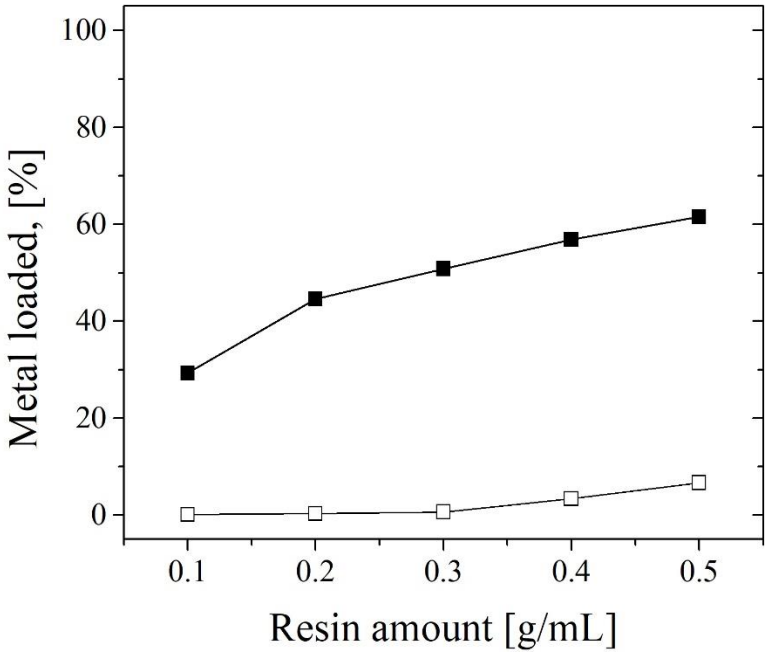

Figure 3.14: Percentage of metal adsorption in resins containing quaternary ammonium groups. (■) Fe and (□) Ni adsorbed on Amberlite 4400 Cl^-

Quaternary ammonium groups are strong anion exchangers and therefore not expected to obtain any adsorption of metals in cationic form. However, the group did achieve metal ion separation even at low resin dosage notwithstanding the positive charges of quaternary ammonium and Fe^{3+}. Up to now, it is unclear the mechanisms in which quaternary ammonium favoured Fe^{3+} adsorption. However, unpublished works suggest that the adsorption might be because of (i) Fe^{3+} interaction with other anion forms or (ii)

due to the surface modification of the resin by the anions. The former suggest that the anions in solution interact with Fe^{3+} producing species with an overall negative charge like $FeCl_4^-$ that then interact with quaternary ammonium (Harland, 1994). The latter, assumes that the anion SO_4^{2-} in solution bond with the resin matrix allowing a negative surface charge that in consequence allow Fe^{3+} bonding. Resins with quaternary ammonium groups are a good alternative for Fe^{3+} separation from Ni^{2+} solutions. However, no published literature was found implying its potential for Fe^{3+} removal.

3.4.1.14 Mixed bed resins with a mix of quaternary ammonium and sulfonic groups

Mixed bed resins (MBR) containing a combination of quaternary ammonium and sulfonic acid also showed Fe^{3+} adsorption preference over Ni^{2+}. Like resins containing only one of the groups, the metal adsorption increased as resin dosage increased. Similar to resin with sulfonic groups, the difference in ion adsorption was not enough to indicate Fe^{3+} selectivity. Figure 3.15 shows an almost liner relationship for metal adsorption and resin dosages. At the minimum resin dosage of 0.1 g/mL, the Fe^{3+} adsorption reached 25% while 14% for Ni^{2+}. At the maximum dosage of 0.5 g/mL, reached 69% of Fe^{3+} and 50% Ni^{2+}. On average, MBR as Resintech MDB adsorbed 49 mg of Fe^{3+} and 25 mg of Ni^{2+} per gram of dry resin.

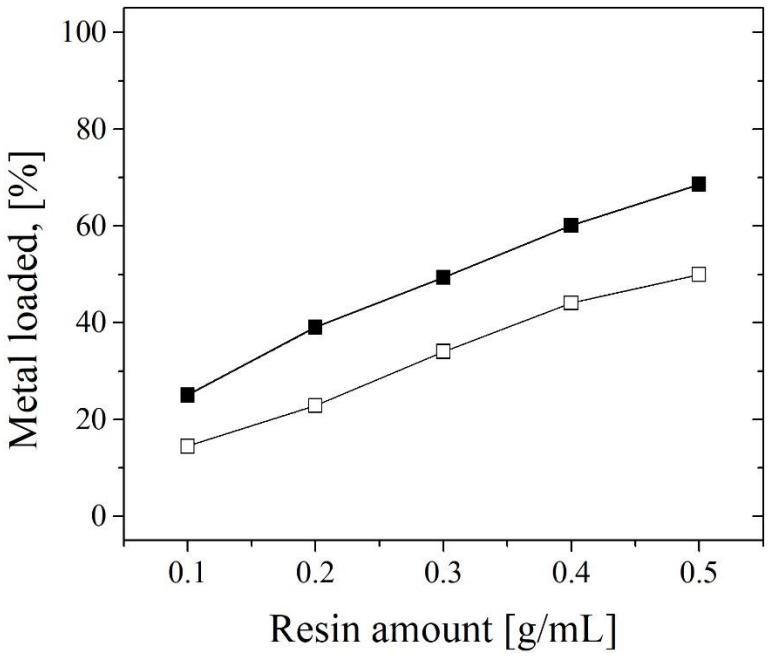

Figure 3.15: Percentage of metal adsorption in resins containing mixed quaternary ammonium and sulfonic groups. (■) Fe and (□) Ni adsorbed on Resintech MDB

With a high content of sulfonic groups, MBR showed particularly high adsorption of both metals as expected. However, there was no observed selectivity of Fe^{3+} with the quaternary ammonium groups. In general, it is possible to conclude that this type of resin showed average adsorption values between sulfonic and quaternary ammonium groups. These type of resins are not suggested for selective Fe^{3+} recovery from concentrated or diluted streams. Instead, resins with a combination of quaternary ammonium and sulfonic acid groups present opportunities for concentration and removal of wide variety of ionic species in water and wastewater treatments.

3.4.1.15 Non-functionalized resins

Non-functionalized resins (NFR) as Amberlite XAD-7 showed metal adsorption increase as the resin dosage increased (see Figure 3.16). The metal adsorption were among the lowest of the resin tested. At the lowest resin dosage of 0.1 g/mL a total of 17% of Fe^{3+} and 7% of Ni^{2+} were adsorbed. The highest resin dosage resulted in 44% and 24% of Fe^{3+} and Ni^{2+} adsorption respectively. On average, non-functionalized resins adsorbed 25 mg of Fe^{3+} and 13 mg of Ni^{2+} per gram of dry resin.

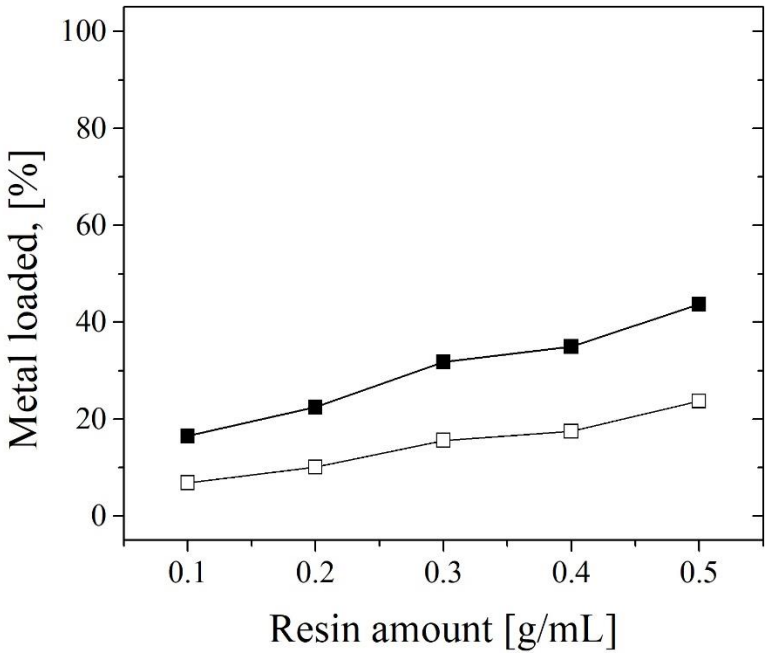

Figure 3.16: Percentage of metal adsorption in non-functionalized resins. (■) Fe and (□) Ni adsorbed on Amberlite XAD-7

Experiments using a NFR were conducted to rule out possible adsorption derived from ionic entrapment in the reticular body of the polymeric matrix of the resin. Any other

resin having metal adsorption higher than those in NFR indirectly suggest a type of functional group-metal ion interaction that enhance metal adsorption rather than any type of physical entrapment. Contrarily, if the extend of metal adsorption is lower than NFR, it suggest some type of repulsion from the resin matrix or from functional group. Therefore, any Fe^{3+} adsorption trends higher than NFR suggest a preferential Fe-adsorption due to Fe-functional group ion interaction. Conversely, any Ni^{2+} adsorption trend lower than that in NFR suggests that the resin could have repelled Ni^{2+}, unlike Fe^{3+}. NFR showed Fe^{3+} adsorption higher than thiol and bis-pycolilamine groups. However, showed Ni^{2+} adsorption higher than those groups showing preference for Fe^{3+} and only lower Ni^{2+} adsorption than sulfonic acid, MBR, and bis-pycolilamine.

3.4.2 Systematic studies for best performers

3.4.2.1 Variation of metal concentration

The impact of metal concentration on selectivity varied. Resins with aminophosphonic acid and a combination of sulfonic and phosphonic groups showed remarkable selectivity towards Fe^{3+} at high metal concentration and lower selectivity as the metal concentration decreased. This is particularly disadvantageous for continuous process where the depletion of Fe^{3+} in time could allow substantial Ni^{2+} co-adsorption. Resin with aminophosphonic acid groups (Figure 3.17 a1) showed an increased Ni^{2+} co-adsorption as the metal concentration decreased. The maximum Ni^{2+} co-adsorption was 55% at the lowest Fe:Ni concentration of 5 g/mL. This condition also produced the lowest Fe^{3+} adsorption at 67%. It is unclear the reasons behind the drop in Fe^{3+} adsorption. At low

metal concentration, there is a high availability of adsorption sites per metal ion in solution. Therefore, resins like aminophosphonic, capable of adsorption both ions should have high adsorption of both metals. This is the case of resins with a combination of sulfonic and phosphonic groups that show the highest adsorption of Fe^{3+} and Ni^{2+} at the lowest metal concentration (see Figure 3.17 a2) obtaining 94% Fe^{3+} and 83% Ni^{2+}.

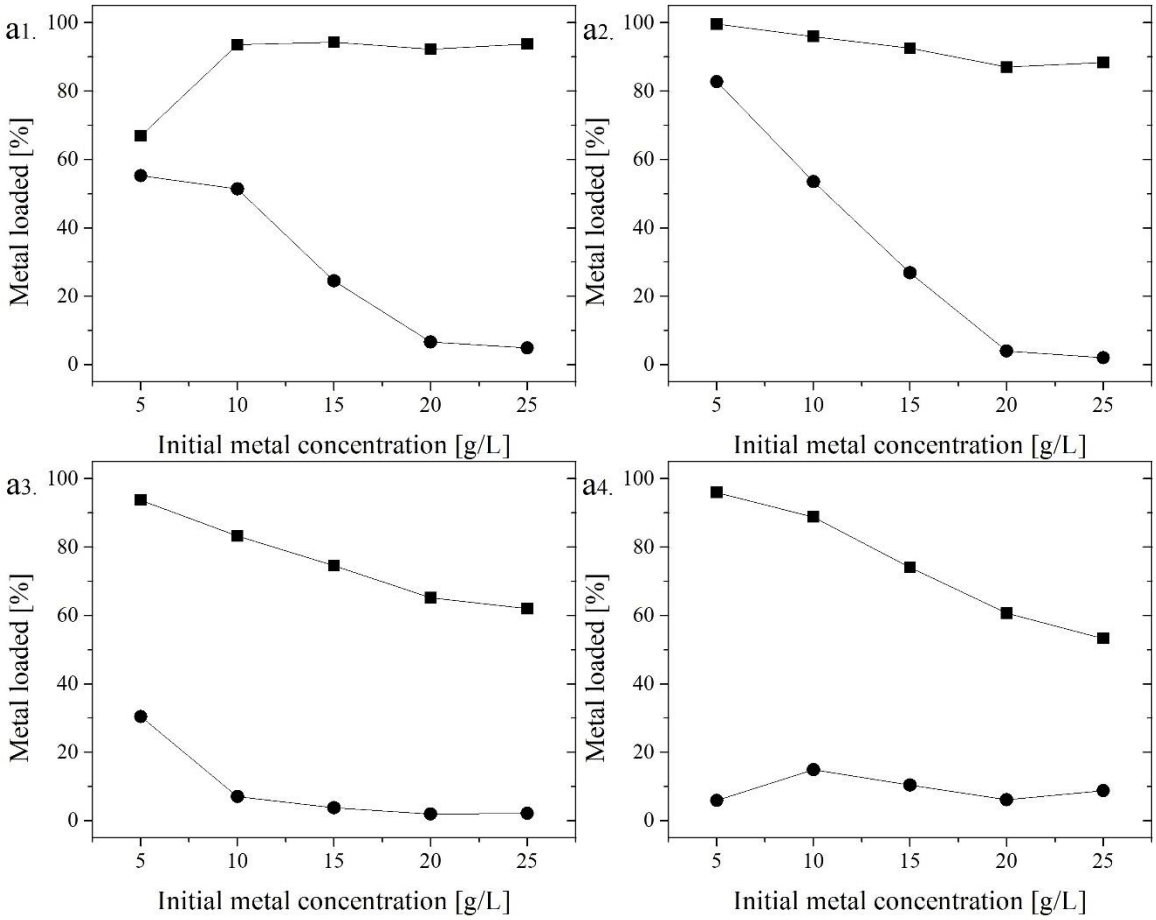

Figure 3.17a: Percentage of (■) Fe and (●) Ni adsorbed at different metal concentration in resins containing: a1) aminophosphonic acid groups, Resintech SIR-500; a2) a combination of phosphonic and sulfonic groups, Puromet MTS9570; a3) iminodiacetic acid groups, Puromet MTS9300; and a4) methylglucamine groups, Purolite S108

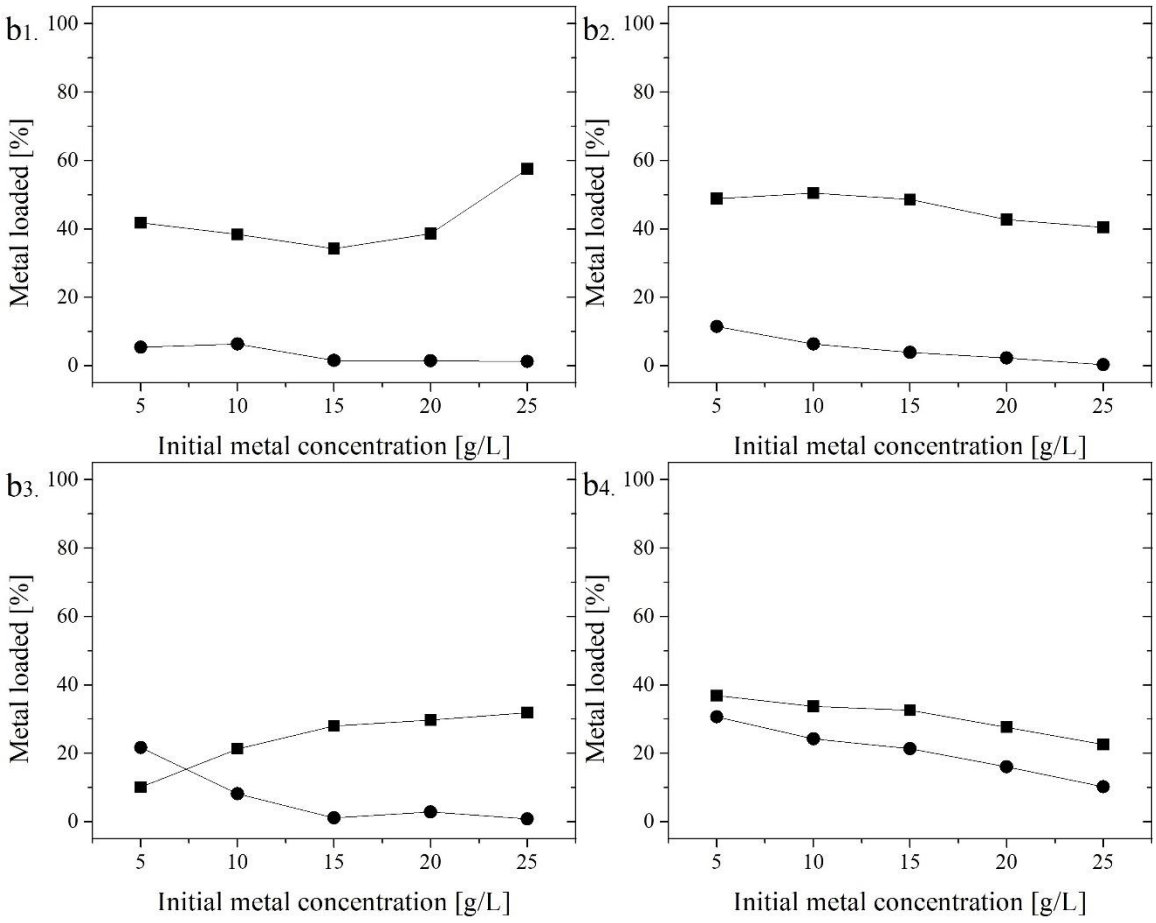

Figure 3.17b: Percentage of (■) Fe and (●) Ni adsorbed at different metal concentration in resins containing: b1) carboxylic acid groups, Resintech WACG; b2) quaternary ammonium groups, Amberlite IRA 440Cl; b3) Amidoxime groups, Puromet MTS9100; and a4) non-functionalized resins, Amberlite XAD-7

Resins with iminodiacetic acid and methylglucamine groups showed steep Fe^{3+} adsorption increases as metal concentration decreased (Figures 3.17 a3 and a4). iminodiacetic acid groups increased from 80% to 94% and methylglucamine from 53% to 94%. However, neither iminodiacetic acid nor methylglucamine showed increases in Ni co-adsorption as observed in the phosphorous containing resins. Ni co-adsorption in iminodiacetic acid resins remained under 7% in metal concentrations higher than 10 g/mL.

At the lowest metal concentration, Ni co-adsorption reached a maximum of 30%. Conversely, in methylglucamine resins Ni co-adsorption remained between 5%-15% through all metal concentrations analyzed suggesting stable selectivity even after Fe^{3+} depletion.

Resins with carboxylic acid (See Figure 3.17 b1) and quaternary ammonium groups (Figure 3.17 b2) showed relatively stable Fe^{3+} adsorption remaining between 35-57% and 43-51%, respectively regardless of metal concentrations. In addition, both groups showed stable Fe^{3+} selectivity, with Ni co-adsorption under 12% in quaternary ammonium groups, and under 7% in carboxylic acid groups throughout the concentrations tested. Resins containing amidoxime groups (Figure 3.17 b3) also showed stable Fe^{3+} and Ni^{2+} adsorption but only at metal concentrations of 15 g/L and higher. At metal concentrations under 15 g/L, amidoxime groups favoured Ni^{2+} adsorption as opposed to Fe^{3+}. The following section related to adsorption behaviours at different pH provides insight of this behaviour. Non-functionalized resin (Figure 3.17 b4) show parallel increases in percentage of metal adsorption as metal concentration decreased. However, it is possible that the amount of metal adsorbed remained the same for all conditions resulting on a higher percentage of removal at lower metal concentration.

Experiments at different Fe:Ni ratios show the effect of excess of either ion on the Fe^{3+} adsorption selectivity at relatively constant ionic strength. In general, the metal adsorption trends resemble those obtained at different metal concentration. Metal adsorption trends in resins with aminophosphonic acid groups showed a slight decline in Fe^{3+} adsorption in systems with excess Ni^{2+} (Figure 3.18 a1) resembling the lower Fe^{3+}

adsorption at low metal concentration (Figure 3.17 a1). However, Ni^{2+} co-adsorptions are significantly lower regardless of the increased Ni:Fe suggesting that elevated ionic strength is a contributing factor for selective Fe^{3+} adsorption. This observation was supported by the high Fe^{3+} adsorption obtained in Section 4.4.1 in a system with disproportionally low iron compared to the base metals in solution. High ionic strength does not enhance Fe^{3+} selectivity in resins with combination of phosphonic and sulfonic groups (Figure 3.18 a2). Regardless of high Fe^{3+} adsorption, Ni^{2+} co-adsorption increased as concentration of Ni increased. These observations also agree with results obtained in preceding sections. Resins with combination of phosphonic and sulfonic groups allowed increased Ni^{2+} co-adsorption as Fe^{3+} depleted from the system. Alternative, in a system with high availability of adsorption sites. This observation follow the low selectivity nature of resins containing exclusively sulfonic groups as observed in Section 3.4.1 and 4.4.1. Contrarily, resins with iminodiacetic acid and methylglucamine groups maintained the Fe^{3+} selectivity but the extent of adsorption decreased with increases in Fe^{3+} concentration in the system (Figure 3.18 a3 and a4). The decline in Fe^{3+} adsorption was dominant with high Fe:Ni in the system suggesting limited adsorption sites as the major contributing factor for declined adsorption. In other words, limited adsorption capacity of the resins (Silva et al., 2018).

Unlike resins in Figure 3.18a, resins in Figure 3.18b maintained selectivity regardless of the Fe:Ni in the system. Resins with carboxylic acid (Figure 3.18 b1), quaternary ammonium (Figure 3.18 b2), and amidoxime groups (Figure 3.18 b3) had Ni^{2+} co-adsorption under 5% throughout the variations of Fe:Ni. Although resins with carboxylic acid groups presented lower Fe^{3+} adsorption at low metal concentrations (Figure

3.17 b1), experiments at relatively constant ionic strength at high metal concentration maintained Fe^{3+} adsorption regardless of the excess of Ni^{2+} in the system. The Fe^{3+} selectivity was maintained in amidoxime resins unlike in low metal concentrations (Figure 3.17 b3). Resins with quaternary ammonium and amidoxime groups and iminodiacetic acid and methylglucamine groups showed a slight decline in Fe^{3+} adsorption attributed to limitations in adsorption capacity of the resin.

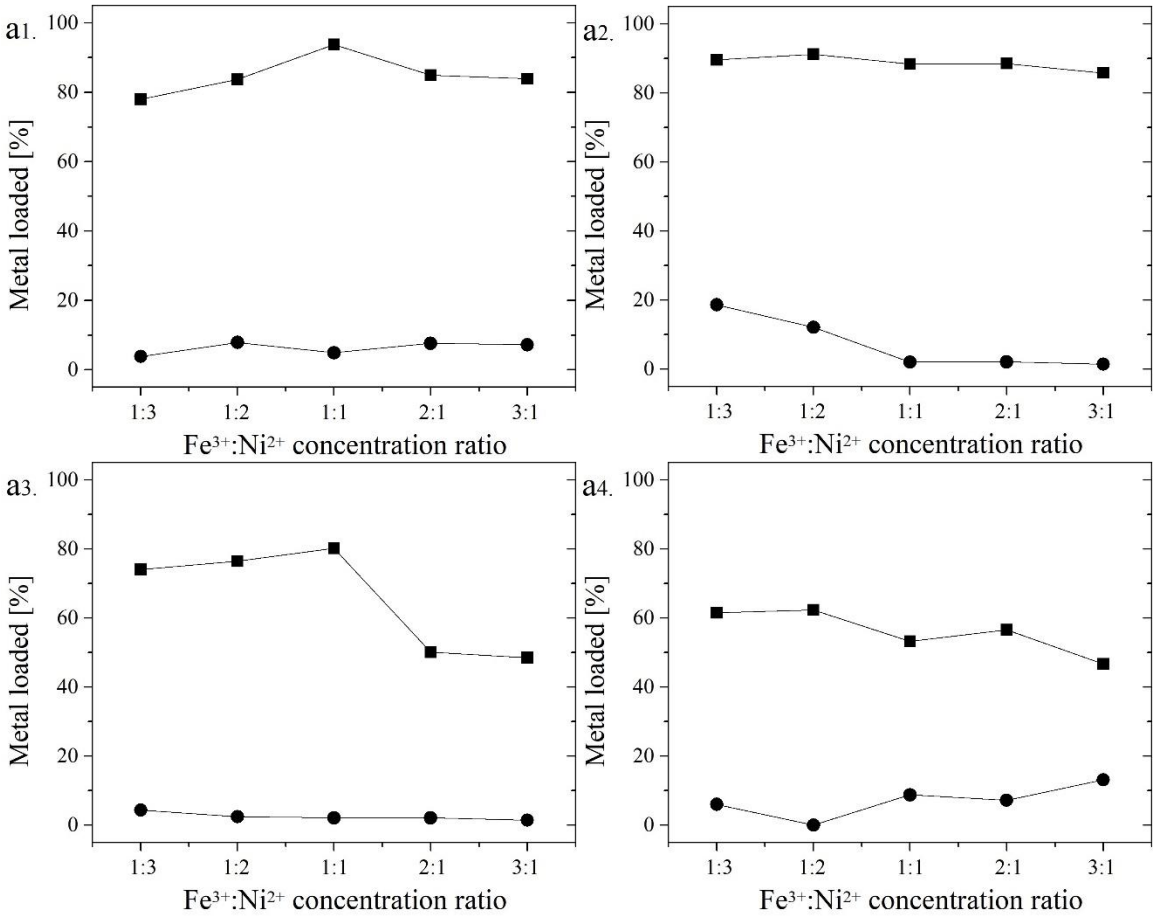

Figure 3.18a: Percentage of (■) Fe and (●) Ni adsorbed at different Fe:Ni concentration ratio in resins containing: a1) aminophosphonic acid groups, Resintech SIR-500; a2) a combination of phosphonic and sulfonic groups, Puromet MTS9570; a3) iminodiacetic acid groups, Puromet MTS9300; and a4) methylglucamine groups, Purolite S108

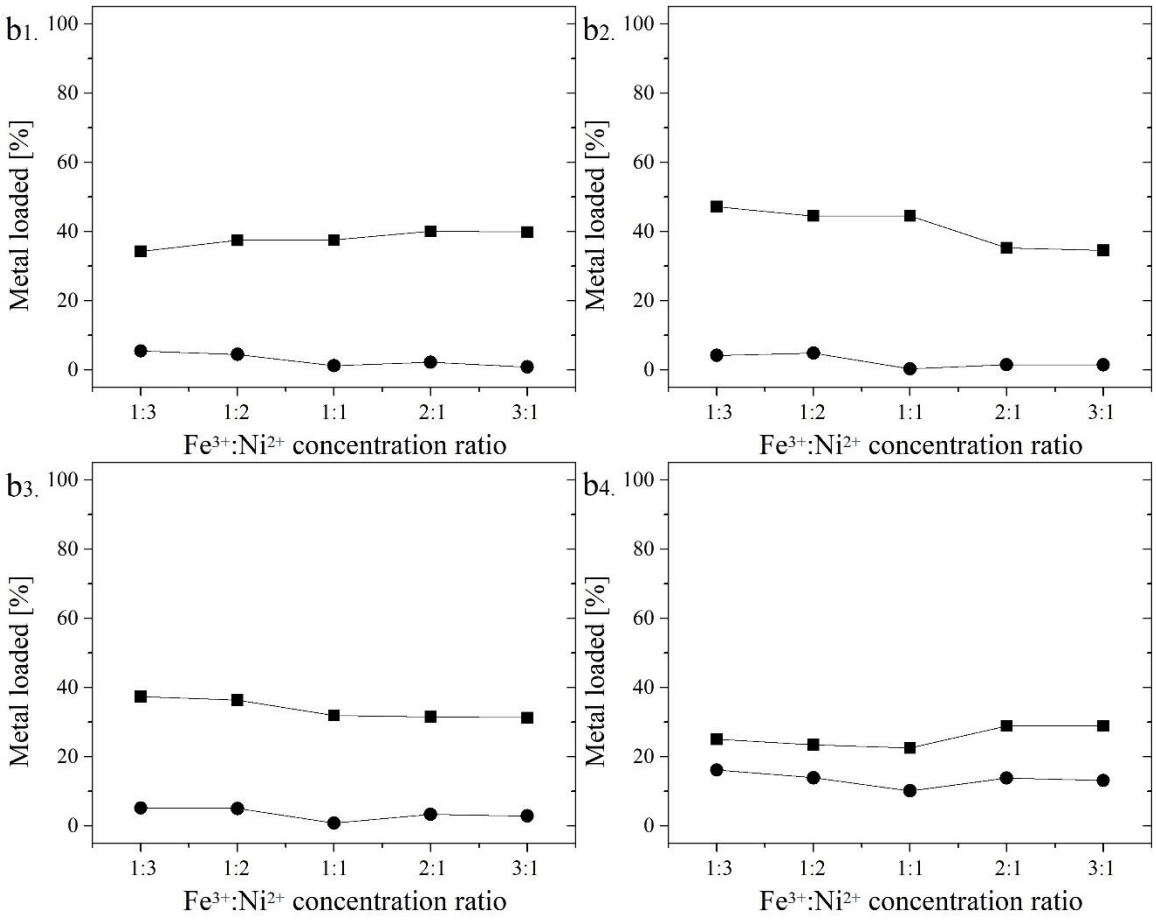

Figure 3.18b: Percentage of (■) Fe and (●) Ni adsorbed at different Fe:Ni concentration ratio in resins containing: b1) carboxylic acid groups, Resintech WACG; b2) quaternary ammonium groups, Amberlite IRA 440Cl; b3) Amidoxime groups, Puromet MTS9100; and a4) non-functionalized resins, Amberlite XAD-7

Non-functionalized resins representing blank experiments showed enhanced percentages of metal adsorption at low metal concentrations (Figure 3.17 b4) and maintained adsorption behaviour regardless of Fe:Ni ratios (Figure 3.18 b4). For all conditions, the amount of Fe^{3+} adsorbed by non-functionalized resins was under that of the rest of the resins tested. Conversely, the extent of Ni^{2+} co-adsorption was higher than the

majority of resin tested excepting for phosphorous groups (i.e., aminophosphonic acid and a combination of phosphonic and sulfonic groups) at low metal concentrations.

3.4.2.2 Variation of solution pH

The pH was studied at ranges below 2.3 to prevent Fe^{3+} precipitation. An Eh/pH (a.k.a., Pourbaix) diagram on a bimetallic system determined pH limits for soluble nickel and iron species at experimental conditions (see Figure 3.19). Simulations using OLI Studio 9.5 Analyzer software determined that $NiFe_2O_4$ precipitate forms at pH above 2.3 in systems at 25 g/L Fe^{3+}, 25 g/L Ni^{2+}, and 25°C. At pH higher than 3, Fe^{3+} commonly interacts with OH^- forming $Fe(OH)_n^{3-n}$ species and potentially precipitating as $Fe(OH)_3$. Up to know, it is unknown if a decreased charge of Fe^{3+} in the $Fe(OH)^{2+}$ and $Fe(OH)_2^+$ species affects the metal adsorption efficiency.

As a general trend, Fe^{3+} adsorption decreased as pH approached 2.3 (Figure 3.20a and 3.20b). Resins with phosphonic and sulfonic groups were the only functionalized group maintaining relatively high Fe^{3+} adsorption despite increments of pH to close to 2.3. Most resins also showed decreased Fe^{3+} adsorption as pH approached the lower limit of 1.0, excepting resins with aminophosphonic acid and a combination of phosphonic and sulfonic groups (Figure 3.20 a1 and 3.20 b2). Lack of precipitates in sample's vial suggested that the decrease in Fe^{3+} adsorption at pH close to 2.3 is not precipitate related, instead it relates to Fe^{3+} speciation to compounds that do not adsorb. Speciation may also be the cause for low Fe^{3+} adsorption at low pH. However, other factors such as low degree in

(de)protonation of resins might negatively affected Fe^{3+} adsorption, particularly for those following substitution reactions.

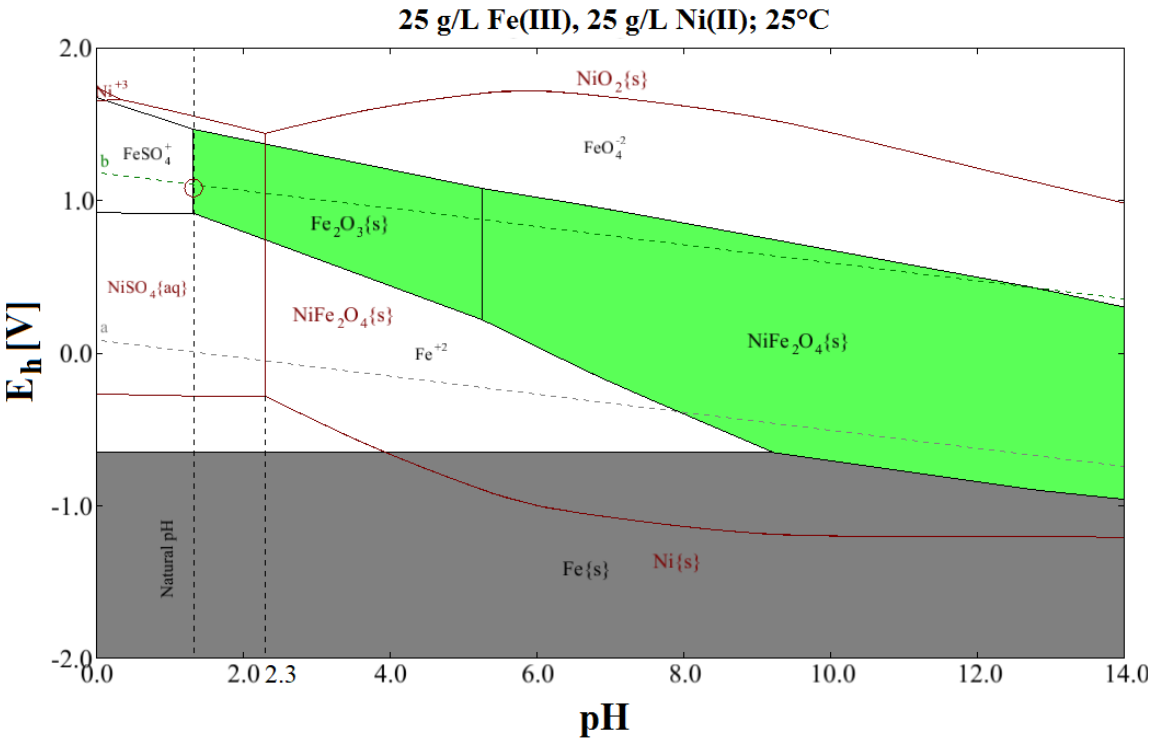

Figure 3.19: Eh-pH (a.k.a., Pourbaix) diagram of $Fe_2(SO_4)_3$ and $Ni(SO_4)$ in aqueous media at 25°C and equal concentration of 25 g/L of Fe and Ni calculated using OLI Studio 9.5 Analyzer software. The pH 2.3 shows a phase equilibrium boundary for the formation of $NiFe_2O_4$

Unlike Fe^{3+} adsorption, co-adsorptions of Ni^{2+} increased with pH showing the lowest co-adsorption value at 1.0. Resins with methylglucamine were the only group showing a slight decrease in Ni^{2+} co-adsorption as pH increased (Figure 3.20 a4). The maximum co-adsorption of Ni^{2+} was obtained by resins with aminophosphonic acid groups and a combination of phosphonic and sulfonic groups reaching above 20% as pH reaching 2.3. Conversely, co-adsorption by resin with amidoxime showed the least variation with

pH (Figure 3.20 b3). Non-functionalized resins showed Fe^{3+} and Ni^{2+} co-adsorption to be independent of pH (Figure 3.20 b4).

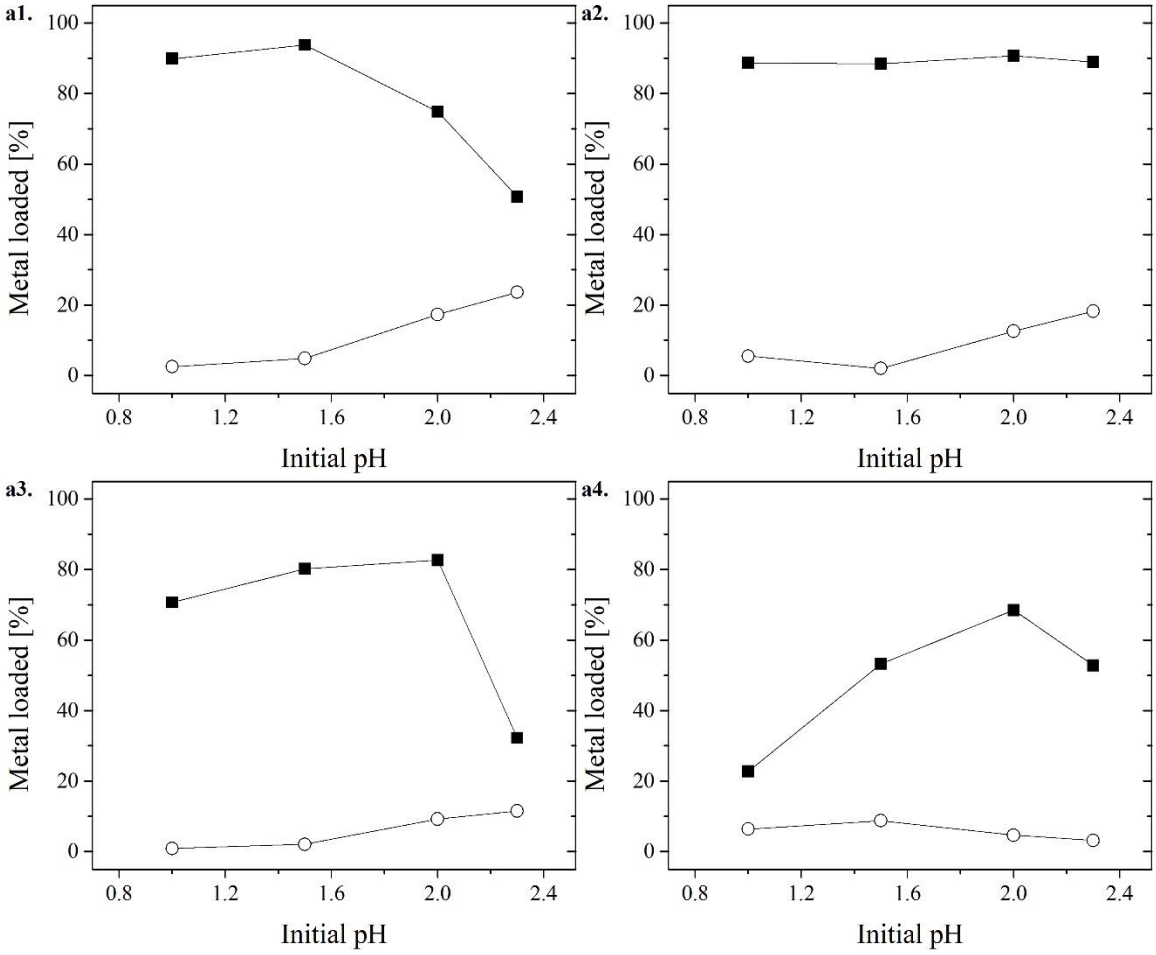

Figure 3.20a: Percentage of (■) Fe and (○) Ni adsorbed at different initial pH in resins containing: a1) aminophosphonic acid groups, Resintech SIR-500; a2) a combination of phosphonic and sulfonic groups, Puromet MTS9570; a3) iminodiacetic acid groups, Puromet MTS9300; and a4) methylglucamine groups, Purolite S108.

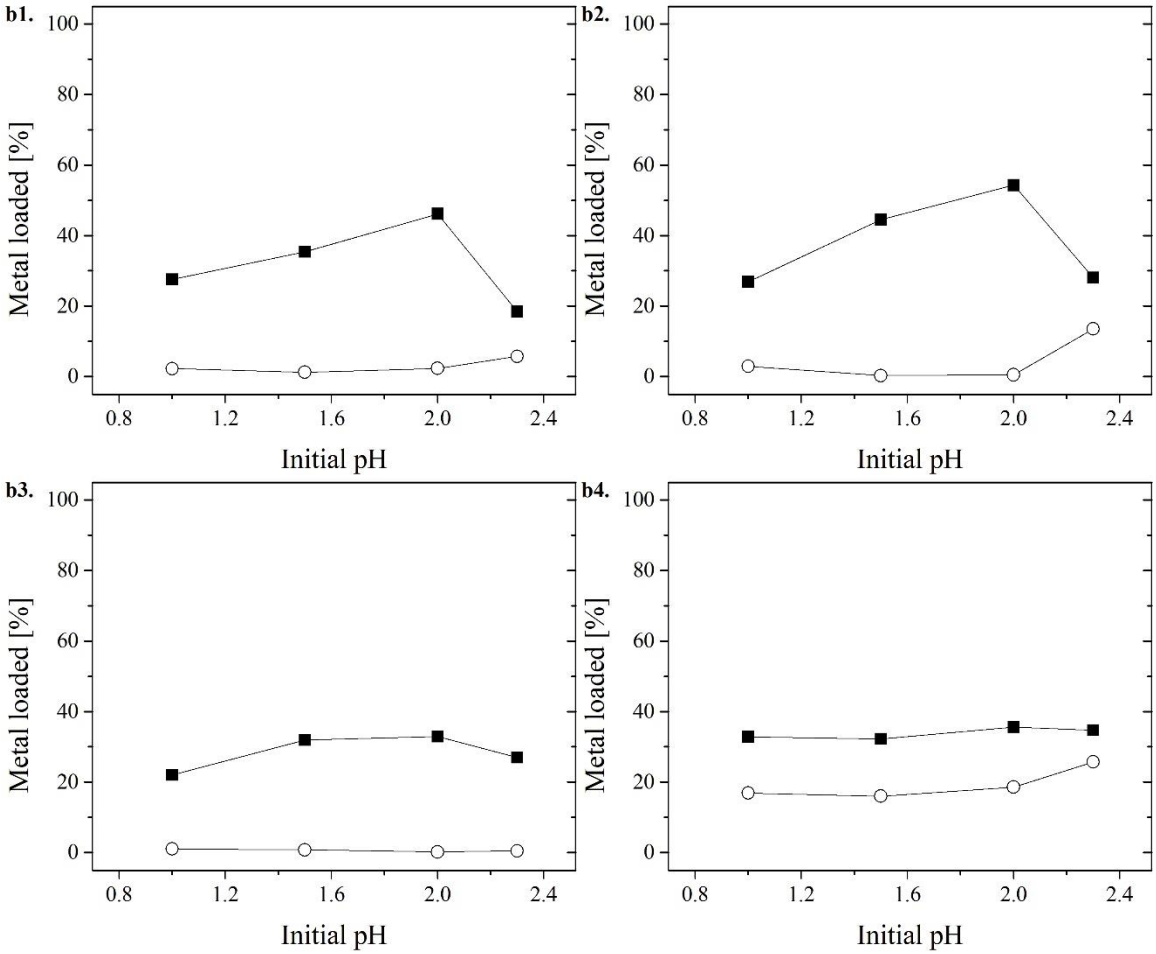

Figure 3.20b: Percentage of (■) Fe and (○) Ni adsorbed at different initial pH in resins containing: b1) carboxylic acid groups, Resintech WACG; b2) quaternary ammonium groups, Amberlite IRA 440Cl; b3) Amidoxime groups, Puromet MTS9100; and b4) non-functionalized resins, Amberlite XAD-7.

3.4.2.3 Variation of temperature

Overall temperature showed positive impacts on Fe^{3+} adsorption excepting for resins with aminophosphonic acid and iminodiacetic acid groups. Increases in temperature increased Fe^{3+} adsorption in the majority of resins (Figure 3.21a and 3.21b). Resins with aminophosphonic acid groups showed the biggest difference as temperature increased (Figure 5.5 a1). As temperature increased from 20 °C to 80 °C, Fe^{3+} adsorption for resins

with aminophosphonic acid groups decreased from 94% to 41% (Figure 3.21 a1) while resins with iminodiacetic acid groups showed a decrease in Fe^{3+} adsorption from 80 to 68% (Figure 3.21 a3).

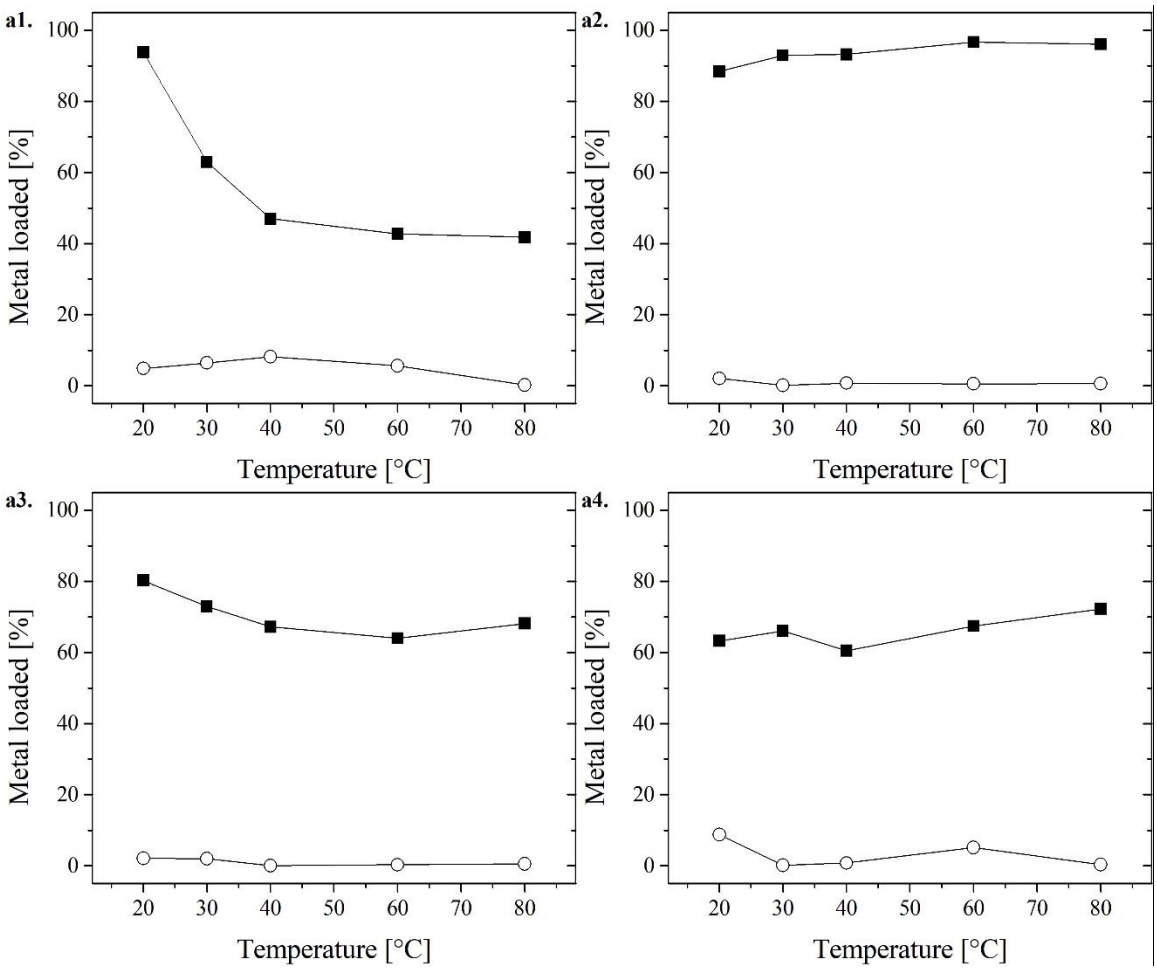

Figure 3.21a: Percentage of (■) Fe and (○) Ni adsorbed at different temperature in resins containing: a1) aminophosphonic acid groups, Resintech SIR-500; a2) a combination of phosphonic and sulfonic groups, Puromet MTS9570; a3) iminodiacetic acid groups, Puromet MTS9300; and a4) methylglucamine groups, Purolite S108.

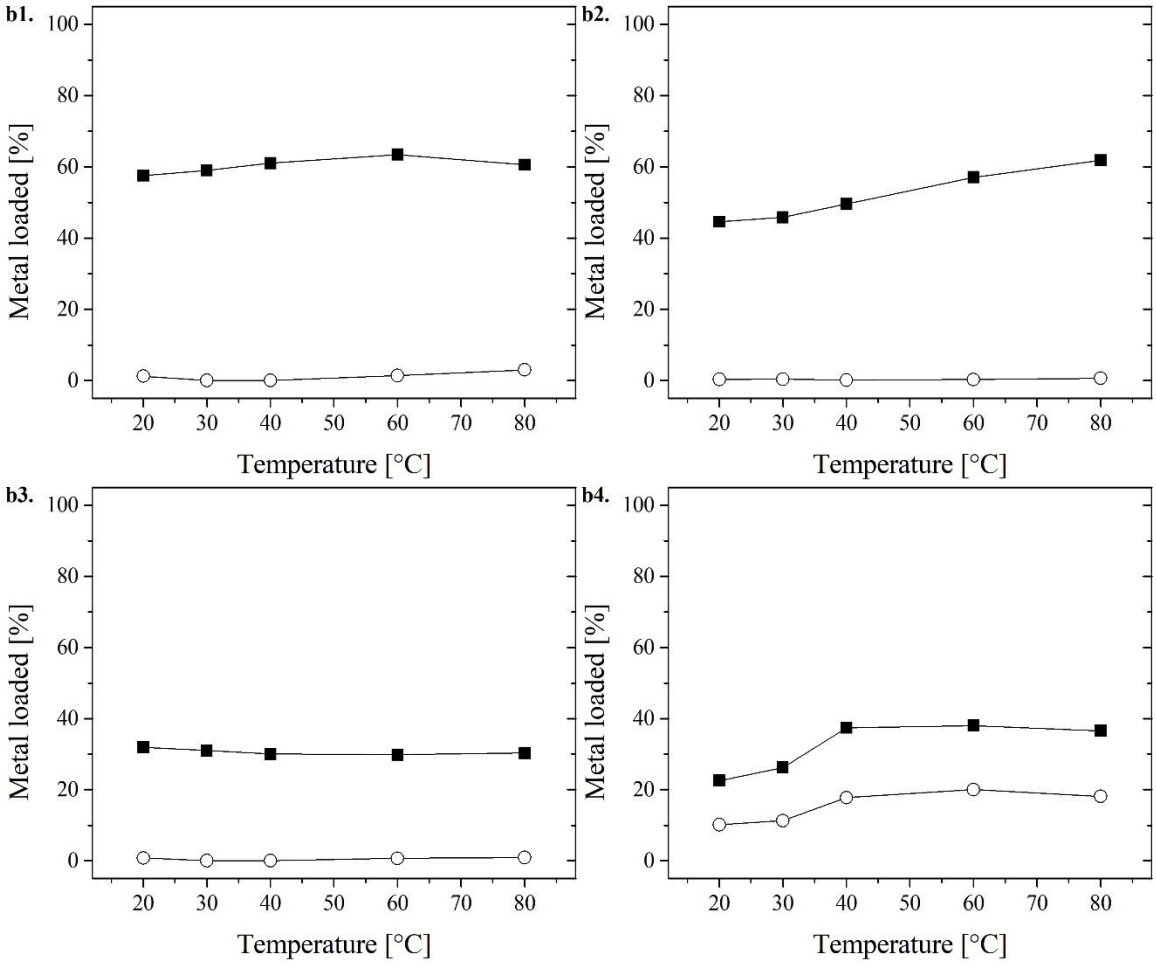

Figure 3.21b: Percentage of (■) Fe and (○) Ni adsorbed at different temperature in resins containing: b1) carboxylic acid groups, Resintech WACG; b2) quaternary ammonium groups, Amberlite IRA 440Cl; b3) Amidoxime groups, Puromet MTS9100; and b4) non-functionalized resins, Amberlite XAD-7.

In opposition, resins with a combination of phosphonic and sulfonic (Figure 3.21 a2), methylglucamine (Figure 3.21 a4), methylglucamine (Figure 3.21 a4), and quaternary ammonium (Figure 3.21 b2) showed increases in metal adsorption with increasing temperature. Among them, quaternary ammonium showed the highest increase. Resins with carboxylic acid (Figure 3.21 b1) and amidoxime groups (Figure 3.21 b3) showed almost negligible increases in Fe^{3+} with increasing temperature.

Temperature had a reduced effect in base metal co-adsorption. Co-adsorption of Ni^{2+}, remained relatively stable having variations under 10% over the temperatures studied. This was not the case for non-functionalized resins that increased Ni^{2+} and Fe^{3+} adsorptions in 10% and 20%, respectively. Temperatures of 80°C did not have negative effects on the physical integrity of the resin.

3.4.2.4 Variation of time

As a general trend, Fe^{3+} adsorption increased with time while Ni^{2+} co-adsorption decreased (Figures 3.22a and 3.22b). This was observed in all resins excepting in non-functionalized resins. The increments of Fe^{3+} adsorption were maintained through 120 min. Thereafter, the Fe^{3+} adsorption was negligible. The decrease in Ni^{2+} co-adsorption in time suggested an ionic substitution due adsorption preferences resulting in desorption of the least preferred metal. Metal desorption in time is reported elsewhere in literature (Aharoni and Tompkins, 1970; Tran et al., 2017). However, additional experiments with contact times up to 24 h showed increments in Ni^{2+} loading after 120 min (see Section 6.4.2).

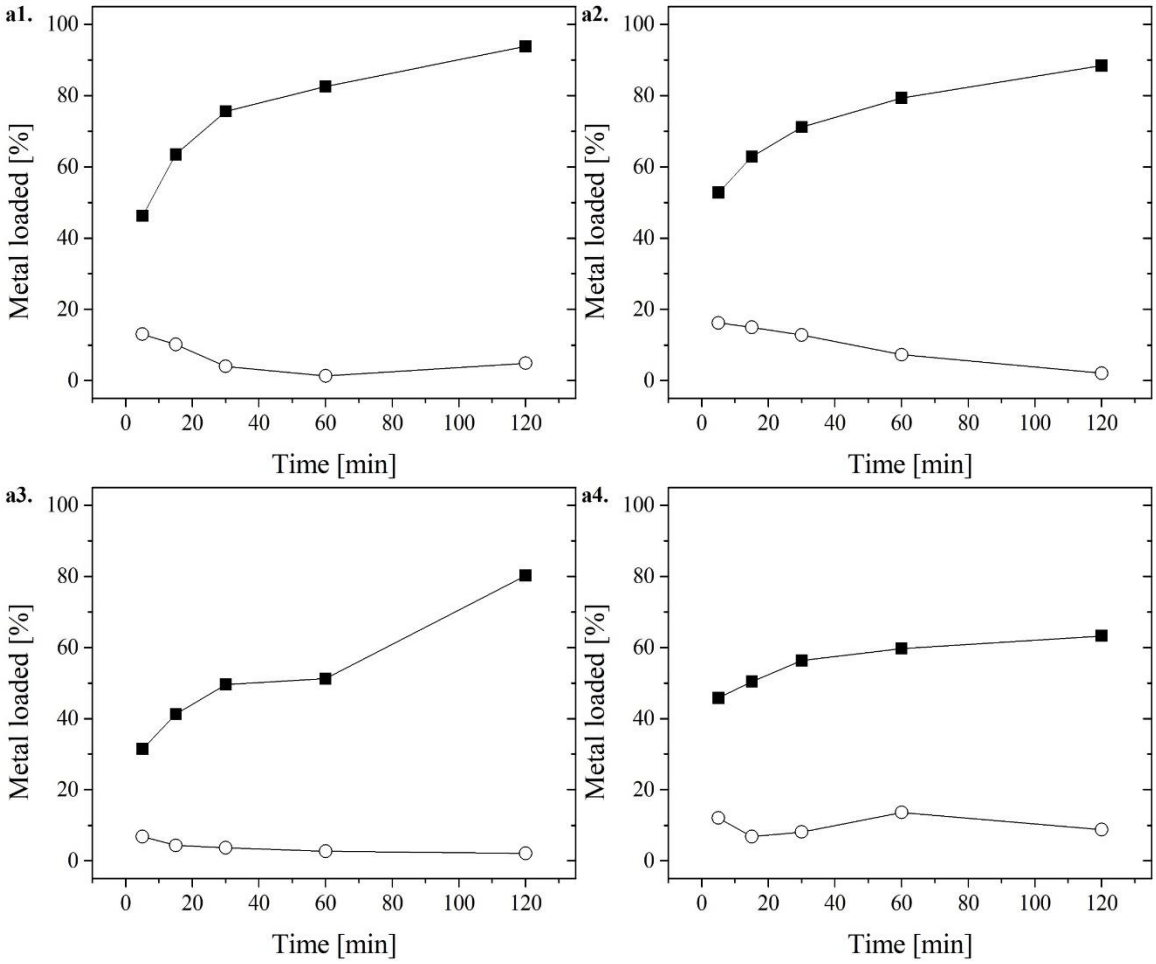

Figure 3.22a: Percentage of (■) Fe and (○) Ni adsorbed at different time in resins containing: a1) aminophosphonic acid groups, Resintech SIR-500; a2) a combination of phosphonic and sulfonic groups, Puromet MTS9570; a3) iminodiacetic acid groups, Puromet MTS9300; and a4) methylglucamine groups, Purolite S108.

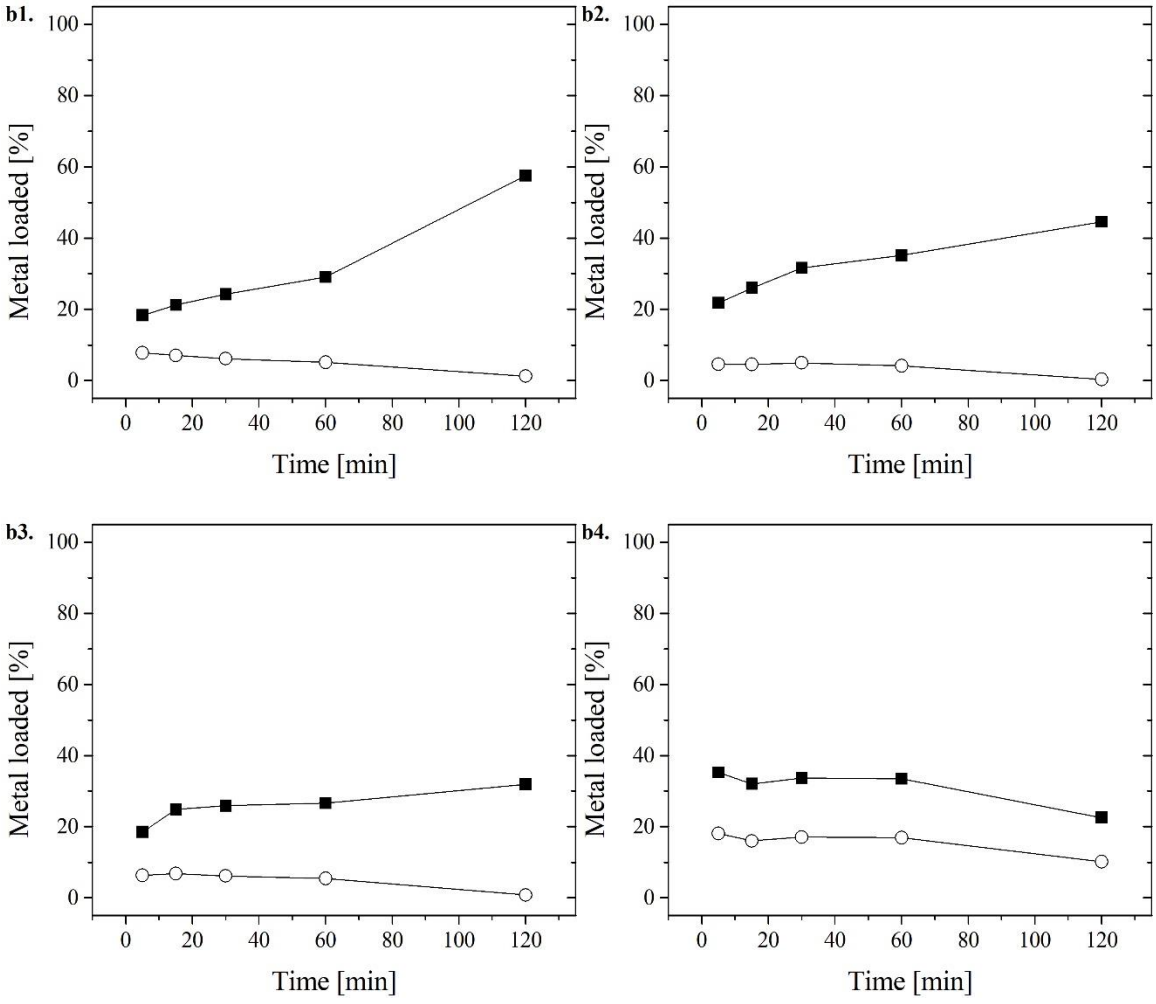

Figure 3.22b: Percentage of (■) Fe and (○) Ni adsorbed at different time in resins containing: b1) carboxylic acid groups, Resintech WACG; b2) quaternary ammonium groups, Amberlite IRA 440Cl; b3) Amidoxime groups, Puromet MTS9100; and b4) non-functionalized resins, Amberlite XAD-7.

3.5 Discussion

Almost all tested resins favoured Fe^{3+} adsorption over Ni^{2+} but only few showed notable selectivity. Theory states that higher ionic charge results in higher complex formation stabilities, thus higher adsorption (Harland, 1994; Helfferich, 1962). However, the results suggest that some ion exchange resins either favoured the complex formation of

the bivalent Ni (e.g., resins with bis-picolylamine groups) or do not show any preference for ion adsorption (e.g., resins with sulfonic groups). A general trend observed was that those resins containing groups cataloged as hard bases on HSAB theory strongly preferred the adsorption of the hard acid Fe^{3+}, those with borderline characteristics did not show preference for either metal ion, and those with soft characteristics either favoured the borderline acid Ni^{2+} or showed poor metal adsorption. The results are also in accordance to those currently available in literature, even though the metal separation were conducted at high metal concentration and acidic pH fixed at 1.5 (see Table 3.5). Theory suggest that we cannot expect similar metal adsorption trends going from low to high concentrations (Harland, 1994). However, studies of single factor optimization showed that any resin that provides successful separations at high metal concentrations performed accordingly at low metal concentration. In other words, if a resin proves satisfactory Fe adsorption in presence of high Ni concentration, low Ni concentration will not affect the overall Fe adsorption. However, high Fe adsorption obtained at low Ni concentration may differ at higher concentrations. Resins containing quaternary ammonium groups (i.e., strong anion exchanger groups) showed unusual behaviour for Fe^{3+} adsorption suggesting potential for efficient and selective adsorption.

Table 3.5: Summary of best performer resin among functional group, most efficient resin dosage, maximum metal adsorption, and average metal adsorption per gram of dry resin

	Functional group (Best performer resin)	Most efficient resin dosage	% Fe^{3+} adsorbed	% Ni^{2+} adsorbed	$\frac{mg Fe}{g_{resin}}$	$\frac{mg Ni}{g_{resin}}$
3.1	Sulfonic (Amberlite IR120)	0.5 g/mL	75%	65%	48	39
3.2	Carboxylic (Resintech WACG-HP)	0.3 g/mL	67%	0.9%	57	2.6
3.3	Amino-phosphonic (Resintech SIR-500)	0.2 g/mL	94%	4.9%	79	10
3.4	Phosphoric (Lewatit VPOC 1026)	0.5 g/mL	44%	2.4%	24	>1
3.5	Phosphinic (Lewatit TP272)	0.5 g/mL	40%	11%	17	3.9
3.6	Phosphonic & Sulfonic (Puromet MTS9570)	0.3 g/mL	93%	4.1%	79	8.5
3.7	Iminodiacetic (Lewatit TP 208)	0.3g/mL	92%	14%	71	8.8
3.8	Amidoxime (Puromet MTS9100)	0.4 g/mL	58%	2.5%	32	1.8
3.9	N-methylglucamine (Purolite S108)	0.5 g/mL	91%	18%	51	8.8
3.10	Bis-pycolilamine (Dowex M4195)	0.3g/mL	26%	47%	21	36
3.11	Thiourea and isothiouronium (Puromet MTS9200)	0.5 g/mL	52%	24%	39	12
3.12	Thiol (Puromet MTS9240)	0.5g/mL	25%	12%	13	5.2
3.13	Quaternary ammonium (Amberlite 4400 Cl^-)	0.5 g/mL	62%	6.7%	41	1.4
3.14	Quaternary ammonium and sulfonic (Resintech MDB-10)	0.5 g/mL	69%	50%	49	25
3.15	Non-functionalized (Amberlite XAD-7)	0.5 g/mL	44%	24%	25	13

Table 3.6: Comparison of Fe^{3+}/Ni^{2+} selectivity trends found in literature and obtained experimentally

	Functional group	Fe^{3+}/Ni^{2+} Selectivity in literature	Fe^{3+}/Ni^{2+} Selectivity obtained
3.1	Sulfonic	Not found	$Fe^{3+} \approx Ni^{2+}$
3.2	Carboxylic	Not found	$Fe^{3+} > Ni^{2+}$
3.3	Aminophosphonic	$Fe^{3+} > Ni^{2+}$	$Fe^{3+} > Ni^{2+}$
3.4	Phosphoric	$Fe^{3+} > Ni^{2+}$	$Fe^{3+} > Ni^{2+}$
3.5	Phosphinic	$Fe^{3+} > Ni^{2+}$	$Fe^{3+} > Ni^{2+}$
3.6	Phosphonic & Sulfonic	Not found	$Fe^{3+} > Ni^{2+}$
3.7	Iminodiacetic	$Fe^{3+} > Ni^{2+}$	$Fe^{3+} > Ni^{2+}$
3.8	Amidoxime	Not found	$Fe^{3+} > Ni^{2+}$
3.9	N-methylglucamine	Not found	$Fe^{3+} > Ni^{2+}$
3.10	Bis-pycolilamine	$Ni^{2+} > Fe^{3+}$	$Ni^{2+} > Fe^{3+}$
3.11	Thiourea and isothiouronium	Not found	$Fe^{3+} > Ni^{2+}$
3.12	Thiol	Not found	$Fe^{3+} > Ni^{2+}$
3.13	Quaternary ammonium	Not found	$Fe^{3+} > Ni^{2+}$
3.14	Quaternary ammonium and sulfonic	Not found	$Fe^{3+} > Ni^{2+}$
3.15	Non-functionalized resins	Not found	$Fe^{3+} > Ni^{2+}$

The best Fe^{3+} selectivity was obtained by resins with aminophosphonic acid groups (achieving adsorption of 98% Fe^{3+} and 1% Ni^{2+} at resin dosages of 0.2 g/mL) and resins with a combination of phosphonic and sulfonic groups (93% Fe^{3+} and 4% Ni^{2+} at 0.3g resin/mL). However, literature suggest that the stable Fe^{3+} complex produced by such groups may result in difficult elution process requiring strong complexing agents or large eluent volumes for successful recoveries (Chiariza et al., 1997; Zhang et al., 2016). Difficult elution is counterproductive for the overall process feasibility. Thus it is not recommended if the intention is to recover Fe^{3+}. Additionally, resins containing iminodiacetic acid groups (achieving adsorption of 91% Fe^{3+} and 14% Ni^{2+} at resin dosages of 0.3 g /mL) and resins with methylglucamine (91% Fe^{3+} and 18% Ni^{2+} at 0.5 g /mL) showed remarkable Fe^{3+} selectivity. Interestingly, resins with methylglucamine groups

have never been used for Fe^{3+} adsorption in hydrometallurgical operations. Other phosphorous-containing groups (i.e., phosphoric and phosphinic acid groups) showed preference for Fe^{3+} but did not achieve the expected adsorption as their buoyant characteristics prevented appropriated resin-liquid interaction in batch test systems. Our experimental conditions resulted in Fe^{3+} adsorption of 44% and 39% against 2% and 11% of Ni^{2+} for phosphoric and phosphinic acid groups, respectively. Resins containing carboxylic, amidoxime, and quaternary ammonium groups achieved low Fe^{3+} adsorption of 67%, 58%, and 62% respectively but Ni^{2+} co-adsorption under 10% even at the highest resin dosage. The low Ni^{2+} co-adsorption suggest a potential of further Fe^{3+} adsorption if several adsorption stages were available. However, the lack of Fe^{3+} elution studies is a major constraint for amidoxime groups (Hubicki, 1986).

Not surprisingly, variations in metal concentration, ionic ratio, pH, temperature, and time affected resins differently. Table 3.7 summarizes the best condition for Fe^{3+} adsorption and selectivity. Ion strength, and consequently overall concentration of metals in the electrolyte, significantly affect the resin's selectivity. Variations in metal concentration alter the speciation and phase equilibrium of ions in the system. This allows different complex formations and enables changes in ions' charge affecting overall selectivity. High metal concentrations reduce the water activity in the solution preventing full ionic solvation. It changes the ion-ion, ion-solvent interactions and relative ion-resin affinities (Free, 2013). In addition, high metal concentration in electrolyte affect the water equilibria in the solution-resin system preventing the resin's maximum swelling capacity. Low degree of swelling affects adsorption of large ions. As such, ionic strength alters the

"electroselectivity" of a resin, diminishing the pre-disposition to favour adsorption of the ion of the highest charge (Harland, 1994; Helfferich, 1962). At lower ionic strengths, the low metal concentrations in electrolyte enables the expansion of the resin's electrical double layer reducing resin-ions interactions. Low metal concentration solutions are also are prone to high variability in ionic strength, particularly for variations in the concentration of the ion with highest charge in the system. Reins with aminophosphonic acid (Figure 3.17 a1), a combination of phosphonic and sulfonic groups (Figure 3.17 a2), and iminodiacetic acid (Figure 3.17 a3) showed decreased metal adsorption selectivity as metal concentration decreased. In other words, Ni^{2+} co-adsorption increased as metal concentration decreased. Resins with N-methylglucamine (Figure 3.17 a4), carboxylic acid (Figure 3.17 b1), and quaternary ammonium groups (Figure 3.17 b2) maintained Fe^{3+} selectivity against Ni^{2+} but the extent of Fe^{3+} adsorption was different for each resin. Conditions of low metal concentration resembled those with high resin dosage given that both conditions had a relative low metal to available adsorption sites ratio. The main difference among these conditions was low ionic strength in systems with low metal concentration. The Fe^{3+} adsorptions at low metal concentration (Section 3.4.2.1) was similar to that obtained at conditions of high resin dosages (Section 3.4.1). Although, as metal concentration decreased, Ni^{2+} co-adsorption was higher compared to that obtained at high resin dosage. Resins with amidoxime groups obtained the highest Ni^{2+} co-adsorptions as metal concentration decreased allowing a shift in selectivity from Fe^{3+} to Ni^{2+} at metal concentrations under 10 g/L (Figure 3.17 b3).

Experiments at different Fe^{3+}:Ni^{2+} ratio maintained a relatively stable ionic strength and confirmed the relationship between reductions of ionic strength and increments in Ni^{2+} co-adsorption. While maintaining high metal concentration, high Fe to Ni ratio resulted in high Fe^{3+} adsorption with low Ni^{2+} co-adsorption. However, high Ni to Fe ratio also resulted in high Fe^{3+} adsorption with low Ni^{2+} co-adsorption. Interestingly, resins with amidoxime groups (Figure 5.2 b3) performed accordingly. Once metal concentration was kept constant, amidoxime groups maintained the selectivity for Fe^{3+} regardless of ionic ratio. Selectivity reductions with decrements in electrolyte concentration are particularly disadvantageous for a continuous process as it allows substantial Ni^{2+} co-adsorption once Fe^{3+} depletes. This type of behaviour shifts the separation from adsorption process to elution process requiring higher amounts of eluent solution for efficient separations.

Like ionic strength, pH is a fundamental parameter affecting the speciation and phase stability. Variations in pH may result in precipitation of metal species thereby fouling the resin. With precipitation, there is a decrease in the concentration of the precipitated species altering solution equilibriums and ionic strength. Solution pH influences complex formations enabling changes in ions' charge. All of these in affect the overall selectivity of the resin. Variations in pH also affect adsorption equilibrium altering the overall metal uptake. The functionality of a resin also depends on the dissociation or protonation of the functional groups contained. The dissociation of weak cation exchange resins (WCR) and protonation of weak anion exchange resins (WAR) are highly dependant on solution pH. The dissociation of WCR and protonation of WAR are fundamental steps to create charged sites for the adsorption of metal ions metal cations (Zagorodni, 2006).

Table 3.7: Most efficient conditions for selective Fe^{3+} adsorption from bimetallic systems

Functional group (ionic form)	**Conc. 5-25 g/L**	**Fe:Ni ratio 3:1-1:3**	**pH 0.5-2.3**	**Temp. 20-80°C**	**Time 5-120 min**
Amino-phosphonic acid (Na^+) - Resintech SIR 500	25 g/L 94% Fe^{3+} 5% Ni^{2+}	Indep.* 86% Fe^{3+} 6% Ni^{2+}	pH = 1.5 94% Fe^{3+} 5% Ni^{2+}	20 °C 94% Fe^{3+} 5% Ni^{2+}	120 min 94% Fe^{3+} 5% Ni^{2+}
Phosphonic & Sulfonic (H^+) - Puromet MTS9570	20-25 g/L 88% Fe^{3+} 3% Ni^{2+}	1:1 – 3:1 88% Fe^{3+} 2% Ni^{2+}	1-1.5 89% Fe^{3+} 4% Ni^{2+}	30 °C 93% Fe^{3+} 1% Ni^{2+}	120 min 88% Fe^{3+} 2% Ni^{2+}
Iminodiacetic acid (Na^+) - Puromet MTS9300	10-25 g/L 71% Fe^{3+} 3% Ni^{2+}	1:3 – 1:1 77% Fe^{3+} 3% Ni^{2+}	1.5 – 2.0 81% Fe^{3+} 6% Ni^{2+}	20 °C 80% Fe^{3+} 2% Ni^{2+}	120 min 80% Fe^{3+} 2% Ni^{2+}
N-methylglucamine - Purolite S108	5 – 10 g/L 92% Fe^{3+} 10% Ni^{2+}	1:3 – 1:1 59% Fe^{3+} 5% Ni^{2+}	1.5 – 2.0 61% Fe^{3+} 7% Ni^{2+}	80 °C 72% Fe^{3+} <1% Ni^{2+}	120 min 62% Fe^{3+} 9% Ni^{2+}
Carboxylic acid (H^+) - Resintech WACG-HP	25 g/L 58% Fe^{3+} 1% Ni^{2+}	Indep. 38% Fe^{3+} 3% Ni^{2+}	1.3 – 2.05 41% Fe^{3+} 2% Ni^{2+}	Indep. 60% Fe^{3+} 3% Ni^{2+}	120 min 58% Fe^{3+} 1% Ni^{2+}
Quaternary ammonium - Amberlite IRA440Cl	20 –25g/L 42% Fe^{3+} 1% Ni^{2+}	1:3 – 1:1 45% Fe^{3+} 3% Ni^{2+}	1.5 – 2.0 49% Fe^{3+} <1% Ni^{2+}	80 °C 62% Fe^{3+} <1% Ni^{2+}	120 min 45% Fe^{3+} <1% Ni^{2+}
Amidoxime - Puromet MTS9100	20-25 g/L 31% Fe^{3+} 2% Ni^{2+}	Indep. 34% Fe^{3+} 4% Ni^{2+}	1.3 – 2.05 32% Fe^{3+} <1% Ni^{2+}	Indep. 32% Fe^{3+} <1% Ni^{2+}	120 min 32% Fe^{3+} 1% Ni^{2+}

Indep.: Percentage of adsorption was independent of the variation of parameter conditions.

Variation of pH showed that Fe^{3+} adsorption significantly reduces as pH approaches 2.3. Also, most resins showed decreased Fe^{3+} adsorption as pH approached 1.0. At the lowest pH tested, the co-adsorption of Ni^{2+} was also the lowest. The low metal adsorption at low pH may be because of poor resin dissociation or complex metal formation with available anions in solution such as OH^- (Zhang et al., 2016). As pH increased to 2.2, there was enhanced Ni^{2+} co-adsorption analog to low Fe^{3+} adsorption. Reduction in Fe^{3+} adsorption is not likely due to Fe precipitation as this was absent in experimental vials. Equation 2.2 and 2.4 suggest that pH change as metal adsorption takes place. Therefore,

pH corrections during length of experiments are fundamental to maintain orders of selectivity. Preliminary experiments using resins with quaternary ammonium in OH^- form and N-methylglucamine without activation showed pH increments outside the Fe^{3+} solubility range highlighting the importance of proper resin activation.

Unlike pH and ionic strength, temperature plays a less prominent role in metal selectivity. There are few studies of the effects of temperature on metal adsorption and ion exchange. Temperature affects formation constants and impacts kinetics of adsorption reactions. Variations in temperature may increase the degree of deprotonation for resins with endothermic adsorptions and drive equilibriums towards an adsorbed metal in exothermic reactions. Therefore, result in overall increase in metal adsorption (Gode and Pehlivan, 2003). Manufacturers suggest that high process temperatures reduce the exchange capacity of resins due to functional group loses by volatility and compromises the physical integrity of the resins. Increases in temperature increased metal adsorption trends for most of the resins and maintained metal selectivity throughout the temperatures tested excepting for resins with aminophosphonic acid and iminodiacetic acid groups. Resins with aminophosphonic acid (Figure 7.21 a1) and resins with iminodiacetic acid groups (Figure 7.21 a3) showed decrease in Fe^{3+} adsorption with increases in temperature. Little variation in metal adsorption at different temperatures comes as an advantage of utilizing ion exchange resins for Fe^{3+} separations. Temperatures after pressure leaching process during base metal production fluctuates between environmental temperatures up to 100°C throughout the production.

As expected Fe^{3+} adsorption increased with time. However, the extent of Ni^{2+} co-adsorption decreased. This behaviour suggest an ion displacement favouring adsorption of the most preferred metal. Analysis of metal adsorption with time highlights Fe^{3+} adsorption preferences. Metal desorption from solid media is a common occurrence and gains importance as the adsorption reaction reaches equilibrium (Tran et al., 2017). Analysis conducted up to 24 h suggested that increases in Fe^{3+} adsorption after 2 h were negligible. Several resins showed good adsorption of Fe^{3+} prior 2 h.

In addition to selective Fe^{3+} adsorption, selective Fe^{3+} elution could achieve efficient Fe:Ni separation. With 75% Fe^{3+} adsorption and a vast body of research suggesting eluents capable of selective desorption, sulfonic acid groups present themselves as potential alternative. Similarly, a relatively simple Ni^{2+} elution from resins containing bis-picolylamine groups may result in successful recovery of Ni^{2+} from concentrated Fe^{3+} solutions.

Further studies including Fe^{3+} selectivity in a polymetallic system (Chapter 4), and elution potential (Chapter 5) would confirm the overall potential of the best performers for selective Fe^{3+} removal.

3.6 Conclusion

Ion exchange resins in batch systems at laboratory scale successfully separated Fe^{3+} from Ni^{2+} solutions at high metal concentrations conditions. After a direct comparison among 15 different types of ion exchange resins, the functional groups that most favoured Fe^{3+} adsorption over Ni^{2+} were aminophosphonic acid (94% Fe^{3+} vs 4.9% Ni^{2+}), a

combination of phosphonic and sulfonic groups (93% Fe^{3+} vs 4.1% Ni^{2+}), iminodiacetic acid (92% Fe^{3+} vs 14% Ni^{2+}), and methyl-glucamine groups (91% Fe^{3+} vs 18% Ni^{2+}). Resins with carboxylic acid (67% Fe^{3+} vs 0.9% Ni^{2+}), quaternary ammonium (62% Fe^{3+} vs 6.7% Ni^{2+}), and amidoxime groups (58% Fe^{3+} vs 2.5% Ni^{2+}) also showed the potential for selective Fe^{3+} removal but the extent of metal adsorption is substantially lower than the best performers. Based on the trends obtained, all best performers suggest a potential for higher Fe^{3+} adsorption after subsequent adsorption batches or higher number of adsorption stages.

Metal concentration and solution pH were dominant solution factors affecting the adsorption trends in the best performer resins tested. Low metal concentration negatively impacted the selectivity of the resin. At metal concentrations under 10 g/L, resins co-adsorbed high amounts of Ni^{2+}. If metal concentration remained over 20 g/L, resins obtained low base metal co-adsorptions despite low Fe to Ni ratio. Adsorption of Fe^{3+} decreased significantly as solution pH approached 2.3. However, adsorption of Fe^{3+} was also affected as pH reached the lower limit of 1.0. In opposition, co-adsorption of Ni^{2+} increased with pH.

Variations in temperature had little effect on the metal adsorption trends maintaining a close to constant metal selectivity on all best performers but resins with aminophosphonic acid and iminodiacetic acid. This is an advantage of utilizing ion exchange resins in hydrometallurgy as temperature fluctuate throughout the process. Rendering resins operable throughout all the hydrometallurgy steps. Adsorption time helped to increase adsorption of Fe^{3+} while decreasing the extent of metal co-adsorption.

This observation suggest a base metal displacement by Fe^{3+} confirming its adsorption selectivity. Further kinetic studies are included in Chapter 5.

The high Fe^{3+} adsorption at Ni^{2+} concentrations of 25 g/L, confirm ion exchange as a viable alternative to iron removal. This suggest ion exchange as a potential alternative to iron precipitation in nickel purification processes. Given the results obtained at the given experimental conditions, ion exchange could be applicable to process beneficiating Ni from either sulfide or laterite type ores. However, further experimentations among the best performers is essential to conclude potential of high purity iron sub-production. Likewise, further economic studies are required to determine the cost benefit of increased operative cost by ion exchange compared to reduced environmental footprint and reduction of solid handling in Fe^{3+} removal by precipitation.

Chapter 4 Adsorption selectivity in Fe-Ni-Co-Cu polymetallic system

This chapter includes information based on the unpublished manuscripts:

1. R.A. Silva, Y. Zhang, K. Hawboldt, & L.A. James. (Pending submission). Selective Fe(III) loading from base metals using non-traditional ion exchange resins at low pH and high sulfate concentration conditions. having the following roles:

Rene A. Silva designed experimental conditions, conducted adsorption experiments, and wrote the manuscript. Dr. Yahui Zhang supervised the design of the experiment, reviewed and edited the final version of the manuscript. Dr. Kelly Hawboldt and Dr. Lesley James reviewed and edited the final version of the manuscript.

2. R.A. Silva, Y. Zhang, K. Hawboldt, & L.A. James. (Pending submission). Use of resins with a combination of phosphonic and sulfonic acid for Fe^{3+} adsorption at low pH and high base metal concentration conditions

Rene A. Silva designed experimental conditions, conducted adsorption experiments, and wrote the manuscript. Dr. Yahui Zhang supervised the design of the experiment, reviewed and edited the final version of the manuscript. Dr. Kelly Hawboldt and Dr. Lesley James reviewed and edited the final version of the manuscript.

4.1 Abstract

This chapter builds on the fundamental work from Chapter 3 where a synthetic leach liquor was simulated to observe the effects of competing base metals on the selective adsorption of Fe^{3+}. For this chapter, the synthetic leach liquor was made up of 2.5 g/L Fe^{3+}, 100 g/L Ni^{2+}, 3 g/L Co^{2+}, and 5.5 g/L Cu^{2+}. The metal ion concentrations selected were to simulate the post pressure leaching systems in a hydrometallurgy plants using Ni-bearing sulfide ore for Ni processing. The extent of Fe^{3+} adsorption and selectivity was studied in 14 different functional groups represented in 27 ion exchange resins. Results suggest an overall Fe^{3+} adsorption selectivity over Ni^{2+}. However, the co-adsorption of Cu^{2+} became significant for several resins; meanwhile the adsorption of Co^{2+} was the lowest among all base metals.

The best Fe^{3+} adsorption performance followed the order of phosphoric acid > aminophosphonic acid > phosphinic > N-methylglucamine > mixed phosphonic and sulfonic > carboxylic acid > iminodiacetic acid > amidoxime > quaternary ammonium > mixed bed > sulfonic > bis-picolylamine > thiourea/isothiouronium > thiol. The last four in the list obtained higher Ni^{2+} adsorption than Fe^{3+}. While resins with thiourea/isothiouronium and thiol showed Ni^{2+} adsorption higher than 50% of that obtained for Fe^{3+}. Noteworthy co-adsorption of Cu^{2+} appeared with an increase in resin dosage in resins with aminophosphonic, iminodiacetic, and N-methylglucamine groups. In resins with aminophosphonic, high resin dosages obtained similar Cu^{2+} and Fe^{3+} adsorptions. Resins with N-methylglucamine groups obtained Cu^{2+} co-adsorption close to 75% of Fe^{3+} while resins with iminodiacetic acid groups obtained Cu^{2+} co-adsorption higher than Fe^{3+}

through all resin dosage tested. No preference for Co^{2+} was observed among the resins tested. Despite the introduction of Co^{2+} and Cu^{2+}in the system, ion exchange maintains its potential as an alternative for successful Fe^{3+} removal in nickel solution purification processes.

This Chapter also includes a systematic study of single factor optimization to assess impact of process conditions on the adsorption preference of Fe^{3+} on the best performer resins. The process conditions analyzed were solution pH, temperature and time. The best performer resins were aminophosphonic acid, a combination of phosphonic and sulfonic groups, iminodiacetic, N-methylglucamine, carboxylic acid, quaternary ammonium, amidoxime, and phosphoric acid. Results show the most efficient conditions for selective adsorption was a pH range of 1.0-2.2 while temperature had little effect on the metal adsorption trends maintaining metal selectivity throughout the temperatures tested. As a general trend, Fe^{3+} adsorption increased with time while base metal adsorptions decreased suggesting a possible displacement by preferred Fe^{3+} adsorption.

4.2 Introduction

Primary nickel production worldwide reaches over two million tonnes per year. Nickel is the fifth most common element on earth occurring naturally in Ni-bearing sulfide and lateritic ore forms. Common uses of Nickel in industry include the production of stainless steel, Cu-Ni alloys and other chromatic alloys, plating, and more recently, rechargeable batteries (Nickel Institute, 2018). Although global Ni deposits are estimated to be 70% laterite-type ore and 30% in sulfide ore, some suggest that about 60% of the

worldwide production is obtained from Ni-bearing sulfide ores while the remaining 40% is obtained from nickeliferous lateritic ores (Agatzini-Leonardou et al., 2009; Mudd, 2010). The preference for the production of Ni from sulfide ores is due to the comparatively simple production of high grade Ni-concentrates through physical separations (e.g., gravity concentration and froth flotation) that it is not possible with laterite ores. In addition, the relatively high cost of Ni production from laterite ores makes this route a less favourable alternative (Silva et al., 2018).

Globally, Indonesia, Philippines, Russia, New Caledonia, and Canada are the top producers of primary nickel. Canada contributed with 180 thousands of tons of primary Nickel in 2018, representing 7.7% of the world's production. Alberta, Manitoba, Ontario, and Newfoundland and Labrador are the Canadian provinces actively mining nickel, where the latter contributes to 29% of the country production (National Resources Canada, 2020). The Voisey's Bay project in the Nain region in Newfoundland and Labrador, holds one of the most renowned nickel deposits worldwide with ores containing 2.96% Ni, 1.89% Cu, 0.16% Co, 59% Fe, and 34% S. It is described as [sic] "one of the most substantial mineral discoveries in Canada in the past 40 years" and contributes to the total nickel production of the province (INCO, 2006). The ore is dominantly composed of pyrrhotite (iron sulfide) with minor amounts of pentlandite (nickel-iron sulfide) and millerite (nickel sulfide) as nickel sources (INCO, 2006; Kerr, 2008). After extraction and mineral processing, sulfide ores undergo a Ni concentration process based in flotation circuits obtaining concentrates up to 25% Ni, 3.5% Cu, and 1.25% Co. Base metals are then dissolved through PL

processes enabling further concentration through hydrometallurgy (Whittington and Muir, 2000).

As earlier described, the fundamental process for Fe^{3+} removal in base metal primary production is precipitation thorough goethite, hematite, and jarosite type minerals formation. However, several complications occur depending on the precipitation process selected. Each precipitation pathway has its own inherent difficulties but all share the major drawbacks of production of large amounts of solid waste with high concentrations of heavy metals, operation cost related to solids management, and the co-precipitation of nickel (i.e., 5-20% nickel loss) with the iron precipitates (Wang et al., 2011). Chapter 3 presents the use ion exchange resins for Fe:Ni separations in synthetic leach liquors containing metal concentration of approximately 25 g/L. However, as explained in this introduction, Ni-bearing sulfide ores commonly occur together with considerable concentrations of Co^{2+} and Cu^{2+}. These conditions differ the equilibria in the bimetallic electrolyte-ion exchange resins systems presented in Chapter 3. Therefore, selectivity in systems containing Fe^{3+}, Ni^{2+}, Co^{2+}, and Cu^{2+} are required to further study.

This chapter evaluates the adsorption capabilities and selectivity of ion exchange resins for Fe^{3+} adsorption in solutions containing Ni^{2+}, Co^{2+}, and Cu^{2+}. Metal concentrations are approximates to post PL in hydrometallurgy plants of Ni beneficiation. In total, 14 main functional groups studied the metal adsorption selectivity accounted in 27 different ion exchange-resins. The ion exchange resins studied span a sample of the most commonly found functional groups in commercial resins containing sulfonic acid, carboxylic acid, N-methylglucamine, amidoxime, iminodiacetic acid, bis-picolylamine,

phosphinic, phosphoric, thiol, thiourea, isothiouronium, aminophosphonic acid, and combination of sulfonic and phosphonic acid groups. Likewise mixed bed resins containing a combination of quaternary ammonium and sulfonic acid groups and anion exchange resins containing quaternary ammonium groups were included. Among the resin tested, a group of eight best performer resins underwent a series of systematic studies studied single factor optimization including: solution pH, temperature, and time.

4.3 Materials and methods

4.3.1 Pre-conditioning

Preconditioning followed the procedures stated in Section 3.3.1. Pre-conditioning included a 24 h bath of 0.2 g of resin per mL of a pH 1.5 solution of deionized water (1.5 DI) in HCl (adjusted using 30% (v/v) HCl) on a reciprocating platform shaker (Promax 2020, Heidolph Instruments GmbH&Co.KG) at 150 rpm. After, resins dried to constant weight at room temperature and negative atmosphere. Table 4.1 includes A detail of the resins analyzed in polymetallic systems. Resins' specifications are detailed in Table 3.3

For each experiment, the required amount of dry resins went through an initial swelling in 1.5 DI during 1 h. After swelling 1.5 DI was filtered and 20 mL of synthetic nickel leach liquor was added for adsorption test.

Table 4.1: Commercial resins used for Fe^{3+} separations from solutions containing Ni^{2+} , Co^{2+}, and Cu^{2+} classified by functional

Functional group (ionic form)	**Resin brand**		**Producer**
Sulfonic (H^+)	1	IR120	Amberlite®
	2	G-26	Dowex®
Carboxylic acid (H^+)	3	Mac-3	Dowex®
	4	WACG-HP	Resintech
Aminophosphonic acid (Na^+)	5	IRC747	Amberlite®
	6	TP 260	Lewatit®
	7	MTS9500 (S950)	Purolite®
	8	MTS9400 (S940)	Purolite®
	9	SIR-500	Resintech
Phosphoric acid (D2EHPA /Di-2-ethylhexyl-phosphoric acid)	10	VP OC 1026	Lewatit®
Phosphinic acid (Bis-(2,4,4-trimethylpentyl-) phosphinic acid)	11	TP272	Lewatit®
Phosphonic & Sulfonic (H^+)	12	MTS9570 (S957)	Purolite®
Iminodiacetic acid (Na^+)	13	IRC748	Amberlite®
	14	TP 207	Lewatit®
	15	TP208MDS	Lewatit®
	16	MTS9300 (S930)	Purolite®
Amidoxime	17	MTS9100	Puromet®
N-methylglucamine	18	S108	Purolite®
Bis-pycolilamine	19	TP 220	Lewatit®
Thiourea	20	TP 214	Lewatit®
	21	MTS9140	Puromet®
Isothiouronium	22	MTS9200	Puromet®
Thiol	23	MTS9240	Puromet®
Quaternary ammonium and sulfonic acid	24	IRN150	Amberlite
	25	MDB-10	Resintech
Quaternary ammonium	26	$4400Cl^-$	Amberjet
	27	$IRA440Cl^-$	Amberlite

4.3.2 Synthetic leach liquor

Synthetic nickel leaching solutions for Fe^{3+} removal in presence of Ni^{2+}, Co^{2+}, and Cu^{2+} emulated metal concentration after pressure leaching systems in a hydrometallurgy plant using Ni-bearing sulfide minerals. Solution sample contained ionic concentrations of

2.5 g/L Fe^{3+}, 100 g/L Ni^{2+}, 3 g/L Co^{2+}, and 5.5 g/L Cu^{2+} in 11 g/L of free acid. All metal ions were obtained from their respective hydrated sulfate salts of analytical ACS reagent grade in the form of $Ni(SO_4)\cdot 6H_2O$, $Co(SO_4)\cdot 7H_2O$, $Cu(SO_4)\cdot 5H_2O$, and $Fe_2(SO_4)_3\cdot 5H_2O$.

4.3.3 Adsorption test

Metal adsorption test at different resin dosages (i.e., 0.1, 0.2, 0.3, 0.4, and 0.5 g/mL) were conducted in 50 mL Erlenmeyer flasks in batch tests during 2h and agitated at 150 rpm on a reciprocating platform shaker at 90 °C. Before each experiment, 125 mL of metal solution was heated up to 90 °C in a separate flask. After reaching required temperature, volume was corrected to 125 mL by either evaporation or adjustment with 90 °C distilled water at pH 1.5 with sulfuric acid. Aliquots of 20 mL were placed in 5 flasks containing pre-conditioned and swelled resins at different dosages. The remaining solution (25 mL) used as a control experiment and for initial metal concentration analyzes. All 6 flasks were placed on stirred hot plates at around 300 rpm to maintain temperature above 90 °C during 2 h. Volume was corrected every 10 min using heated distilled water at pH 1.5 with sulfuric acid. The metal concentrations before and after the adsorption test were determined using wavelength dispersive X-ray fluorescence spectroscopy (XRF Supermini200, Rigaku Co.) and the difference in concentration used for the metal adsorption calculation following Equation 3.1. The batch adsorption experiments were performed in triplicate. The reproducibility deviation of the measurements was within 5 %.

4.3.4 Systematic studies of single factor optimization

Resins determined as the best performers underwent a preconditioning in pH 1.5 deionized (1.5 DI) water (adjusted using 30% (v/v) HCl) and dried to constant weight during 72 hours at room temperature and negative atmosphere as described in previous chapters. Table 4.2 includes a detail of the best performer resin that underwent systematic studies.

Table 4.2: Commercial resins used for systematic studies for Fe^{3+} separations

Functional group (ionic form)	**Resin**		**Brand**
Aminophosphonic acid (Na^+)	1	TP 260	Lewatit®
Phosphonic & Sulfonic (H^+)	2	MTS9570 (S957)	Purolite®
Iminodiacetic acid (Na^+)	3	MTS9300 (S930)	Purolite®
N-methylglucamine	4	S108	Purolite®
Carboxylic acid (H^+)	5	WACG-HP	Resintech
Quaternary ammonium	6	IRA440Cl^-	Amberlite
Amidoxime	7	MTS9100	Puromet®
Phosphoric acid (D2EHPA /Di-2-ethylhexyl-phosphoric acid)	8	VP OC 1026	Lewatit®

For each experiment, resin dosage was adjusted using dry resin weight. The required amount of dry resin was placed in individual flasks in 1.5 DI water for 1 h to allow initial swelling. After swelling, remaining 1.5DI water was removed and replaced with 20 mL of synthetic leach solution. Unless otherwise stated, adsorption tests were conducted at 0.2 g/mL resin at 90 °C during 120 min as standard parameter having 100 g/L of Ni^{2+}, 3 g/L of Co^{2+}, 5.5 g/L of Cu^{2+}, and 2.5 g/L Fe^{3+} in 11 g/L of free acid. The metal concentrations before and after the adsorption test were determined using wavelength dispersive X-ray fluorescence spectroscopy (XRF Supermini200, Rigaku Co.) and the

difference in concentration used for the metal adsorption calculation following Equation 3.1.

4.4 Results

4.4.1 Determination of best performer resin for iron adsorption

4.4.1.1 Resins with sulfonic groups

Resins with sulfonic groups showed similar adsorption trends of Ni^{2+}, Cu^{2+}, and Co^{2+} notwithstanding the high Ni^{2+} concentration in the system (see Figure 4.1). Unlike in the Fe^{3+}:Ni^{2+} binary system, the Fe^{3+} adsorption achieved only half of that of the bivalent cations. On average, resin containing sulfonic groups (Amberlite IR120 and Dowex G-26) achieved adsorption of 21% of Fe^{3+} and co-adsorption of 37% of Cu^{2+}, 41% of Co^{2+}, and 45% of Ni^{2+}. The small difference among the base metal adsorption makes it difficult to stablish a metal preference trend, confirming the low selectivity of the resin. Each gram of dry resin adsorbed 97 mg of Ni^{2+}, 2.0 mg of Co^{2+}, 3.2 mg of Cu^{2+}, and 0.70 mg of Fe^{3+} further disproving the resin's capabilities of selectively removing Fe^{3+}.

Results confirm that sulfonic groups can be used for a general removal/recovery of metals from water streams but are not recommended when specific adsorption is required. Both trends suggest possibilities of high metal removals once enough resin is available.

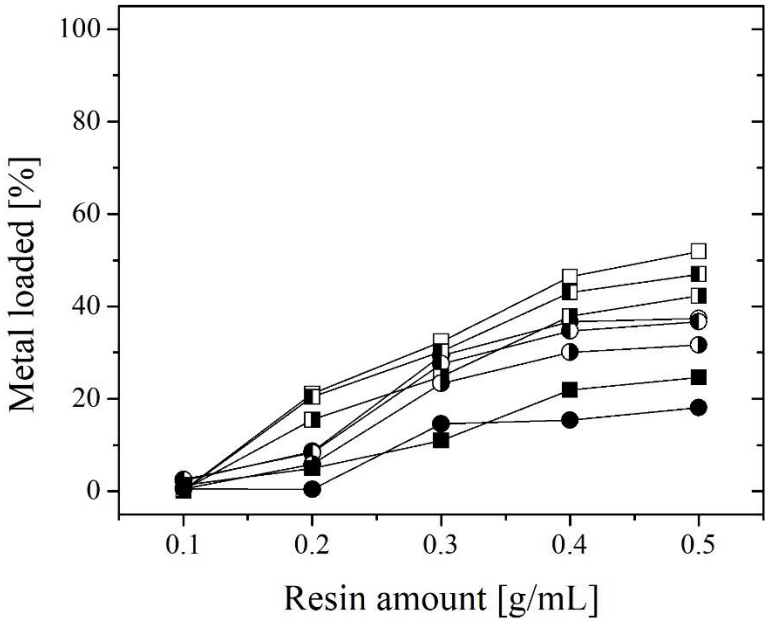

Figure 4.1: Percentage of metal adsorption in resin containing sulfonic acid groups in polymetallic system. (■) Fe, (□) Ni, (◧) Co, and (◨) Cu adsorbed on Amberlite IR 120 H^+ resin and (●) Fe, (○) Ni, (◐) Co, and (◑) Cu adsorbed on Dowex G-26

4.4.1.2 Resins with carboxylic acid groups

Resins with carboxylic acid groups favoured the adsorption of Fe^{3+} compared to that of the rest of base metals. Carboxylic acid groups achieved High Fe^{3+} adsorption even with the higher concentration of other metals in the system. For both resins used (Dowex Mac-3 and Resintech WACG), Fe^{3+} adsorption increased as resin dosage increased but reached a relatively stable adsorption after resin dosage of 0.3 g/mL. The increase in resin dosage did not seem to affect base metal co-adsorption excepting the highest resin dosage using Dowex Mac-3 resin. The highest resin dosage achieved the highest metal adsorption of 6.8% Ni^{2+}, 6.9 % Co^{2+}, 7.6% Cu^{2+}, and 79% Fe^{3+}. On average, each gram of resin adsorbed 7.0 mg of Ni^{2+}, 0.2 mg of Co^{2+}, 0.4 mg of Cu^{2+}, and 6.1 mg of Fe^{3+}.

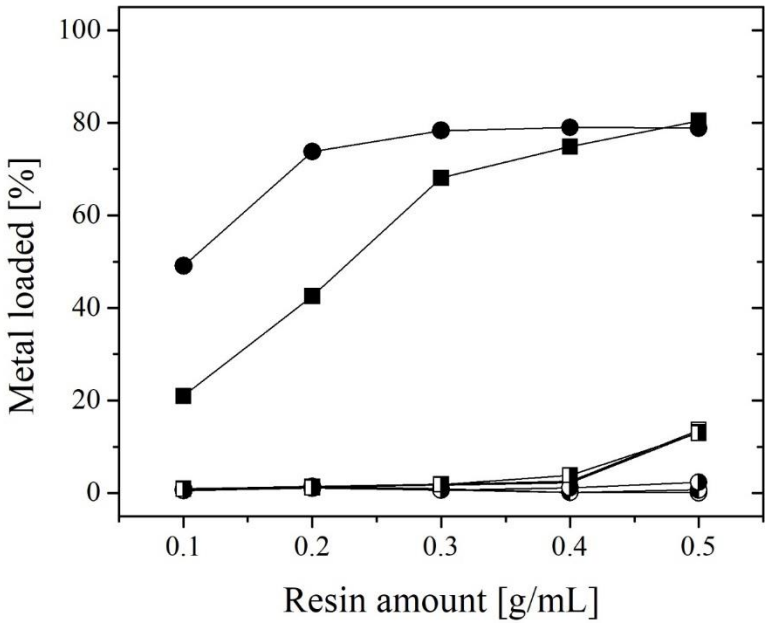

Figure 4.2: Percentage of metal adsorption in resin containing carboxylic acid groups in polymetallic system. (■) Fe, (□) Ni, (◧) Co, and (◨) Cu adsorbed on Dowex Mac-3 resin and (●) Fe, (○) Ni, (◐) Co, and (◑) Cu adsorbed on Resintech WACG

Even though the amount of Ni^{2+} adsorbed by the resin was higher than that of Fe^{3+}, it should be noted the concentration of Ni^{2+} in the polymetallic system is almost 50 times more than that of Fe^{3+}. Similarly, bimetallic systems (see Section 3.4.2) showed that equivalent concentrations of Fe^{3+} and Ni^{2+} in solution resulted in higher Fe^{3+} adsorption (e.g., 57 mg of Fe^{3+} per gram resin against 3 mg of Ni^{2+}). This suggest the higher Ni^{2+} adsorbed is mainly due to its excess in the system rather than a selectivity over Co^{2+} and Cu^{2+} by the resin. Thus, confirming the selective Fe^{3+} adsorption over the base metals Ni^{2+}, Co^{2+}, and Cu^{2+} by carboxylic acid resins.

4.4.1.3 Resins with aminophosphonic acid groups

Resin with aminophosphonic acid groups favoured the adsorption of Fe^{3+} over Ni^{2+} in presence of Co^{2+} and Cu^{2+} (see Figure 4.3). However, at high resin dosage, the Cu^{2+} co-adsorption reached values close to 90% in all resins tested (Amberlite IRC747, Lewatit TP260, Puromet MTS9500 and MTS9400). Aminophosphonic acid maintained adsorption behaviour regardless of the type and manufacturer brand. Similarly, Cu^{2+}, Co^{2+} and Ni^{2+} show increasing adsorption at high resin dosage suggesting reduced selectivity of Fe^{3+} as the amount of resin increases (e.g., process with consecutive adsorption steps) or higher number of adsorption sites with respect of Fe^{3+}. At the lowest resin dosage, resins containing aminophosphonic acid groups adsorbed on average 85% Fe^{3+} with Cu^{2+} co-adsorption of 13% and Ni^{2+} and Co^{2+} under 2%. Instead, at the highest resin dosage the adsorption of Fe^{3+} and Cu^{2+} reached 92% and 91%, and co-adsorption of Ni^{2+} and Co^{2+} of 24% and 34%, respectively. This results in average adsorption of 9.6 mg of Fe^{3+} and 12, 1.2, and 36 mg of Cu^{2+}, Co^{2+}, and Ni^{2+} per gram of resin. The high adsorption of Cu^{2+} by resins containing aminophosphonic acid groups challenge the potentials of the resins for selective Fe^{3+} removals.

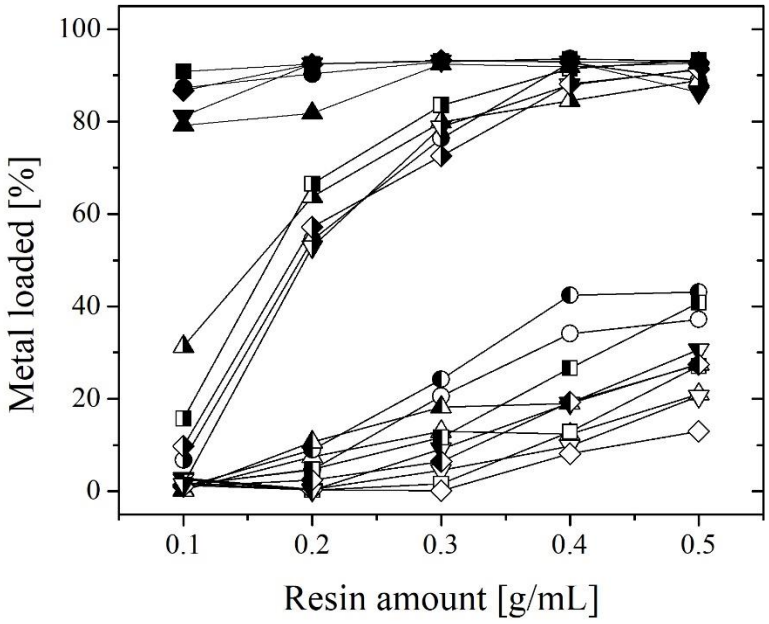

Figure 4.3: Percentage of metal adsorption in resin containing aminophosphonic acid groups in polymetallic system. (■) Fe, (□) Ni, (◧) Co, and (◨) Cu adsorbed in Amberlite IRC747, (●) Fe, (○) Ni, (◐) Co, and (◑) Cu adsorbed in Lewatit TP260, (▲) Fe, (△) Ni, (◭) Co, and (◮) Cu adsorbed in Puromet MTS9400, (▼) Fe, (▽) Ni, (▾) Co, and (▿) Cu adsorbed in Puromet MTS9500, and (◆) Fe, (◇) Ni, (◈) Co, and (⬗) Cu adsorbed in Resintech SIR-500.

Resins with aminophosphonic acid groups, are used in industry for copper and nickel sulfate purification process and separation of copper and zinc from cobalt electrolytes (Van Deventer, 2011). This explains the sharp increase in Cu^{2+} adsorption after Fe^{3+} removal from the system. Section 3.3 related to bimetallic systems suggest increases in Ni^{2+} co-adsorption once Fe^{3+} removals reached above 90%. Similarly, in polymetallic systems co-adsorption of Cu^{2+} occurred as Fe^{3+} adsorption reached close to 90% while Ni^{2+} and Co^{2+} co-adsorption increased as Cu^{2+} was depleted. Although aminophosphonic acid groups strongly bond with Fe^{3+}, the selectivity is low at low Fe^{3+} concentration and in presence of Cu^{2+} in the system

4.4.1.4 Resins with phosphoric groups

Resins with D2EHPA (phosphoric acid groups) favoured Fe^{3+} over the base metals (see Figure 4.4). At resin dosages of 0.3 mg/L, Fe^{3+} reached adsorption of 92%. While the maximum Fe^{3+} adsorption was 93% at 0.5 mg/L. Despite the high Fe^{3+} adsorption at low resin dosage, there was no increase in base metal co-adsorption at high resin dosages. Co-adsorption of base metals remained under 2% even at 0.5 mg/L. On average, one gram of dry resin adsorbed 8.0 mg of Fe^{3+}, 6.6 mg of Ni^{2+}, 0.1 mg of Co^{2+}, and 0.2 mg of Cu^{2+}.

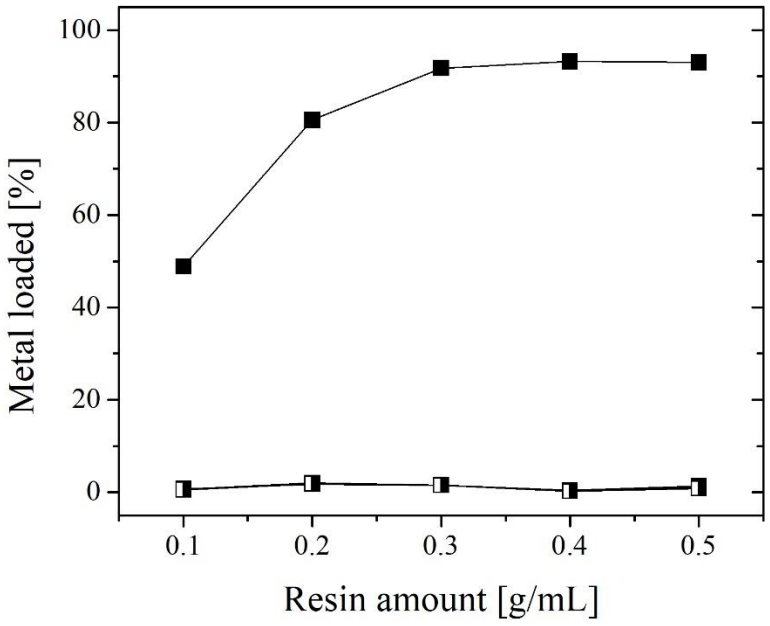

Figure 4.4: Percentage of metal adsorption in resin containing di-2-ethylhexyl-phosphoric acid (a.k.a., D2EHPA) in polymetallic system. (■) Fe, (□) Ni, (◧) Co, and (◨) Cu adsorbed in Lewatit VP OC 1026

In bimetallic systems, these resins reached a maximum Fe^{3+} adsorption of 44% at 0.5 g/mL resin (Section 3.4.1) whereas in polymetallic systems dosages of 0.1 g/mL

produced 48% of Fe^{3+} adsorption. The difference in performance is due to enhancement of resin-electrolyte contact during the experiment. Phosphoric acid groups favour the selective adsorption of Fe^{3+} from multi-metal electrolytes at low pH (Sole et al., 2018). In addition, phosphoric groups are widely used in solvent extraction technology for Fe^{3+} removal. Chapter 5 includes further analysis of metal adsorption with phosphoric groups. Given the results obtained, resin with phosphoric groups are recommended for selective Fe^{3+} removal from base metal electrolytes once proper resin-electrolyte contact is allowed.

4.4.1.5 Resins with phosphinic groups

Resin with phosphinic group in phosphinate form show similar metal adsorption trends as phosphoric groups in polymetallic and bimetallic systems. As with resin with phosphoric groups, resins with phosphinic groups favoured the Fe^{3+} adsorption over base metals. Resin dosages of 0.2 g/mL and higher reached Fe^{3+} adsorption ranging from 79 to 84% (see Figure 4:5). Nonetheless, the co-adsorption of base metals remained under 3%. The highest resin dosage produced the maximum co-adsorption reaching values of 3.2% Ni^{2+}, 2.9% Co^{2+}, and 2.7% Cu^{2+}. On average each gram of dry resin adsorbed 8.9 mg of Ni^{2+}, 0.2 mg of Co^{2+}, 0.3 mg of Cu^{2+}, and 7.4 mg of Fe^{3+}.

The improvement of resin-electrolyte contact increased the maximum Fe^{3+} adsorption from 40% in bimetallic systems to 81% in polymetallic systems. Both phosphinic and phosphoric groups are traditionally employed in industry for electrolyte purifications. Although phosphinic groups obtained good Fe^{3+} adsorption, phosphoric groups showed higher percentage of adsorption from the Fe:Ni:Co:Cu system.

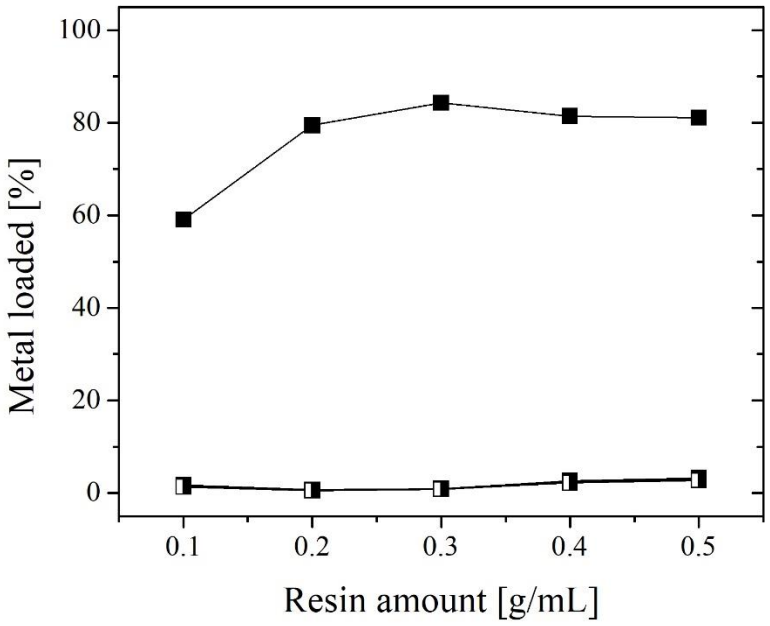

Figure 4.5: Percentage of metal adsorption in resin containing bis-(2,4,4-trimethylpentyl-) phosphinate groups in polymetallic system. (■) Fe, (□) Ni, (◧) Co, and (◨) Cu adsorbed in Lewatit TP272

4.4.1.6 Resins with mixed phosphonic and sulfonic groups

Resins with a combination of sulfonic and phosphonic groups favoured the adsorption of Fe^{3+} over the base metals studied. Up to 83% of Fe^{3+} adsorption was reached at the lowest resin dosage and increased up to 92% at the highest of 0.5 g/mL. Like resin with sulfonic groups, the extent of base metal co-adsorption increased as resin dosage increased but maintained selectivity to Fe^{3+} over base metals. Cu^{2+} showed the highest co-adsorption among base metals; however, the adsorption was under 40% at the highest resin dosage. The highest resin dosage studied gave the maximum base metal co-adsorption of

24% Ni^{2+}, 26% Co^{2+}, and 34% Cu^{2+}. The average metal adsorption per gram of dry resin reached 33 mg of Ni^{2+}, 0.8 mg of Co^{2+}, 2.5 mg of Cu^{2+}, and 8.9 mg of Fe^{3+}.

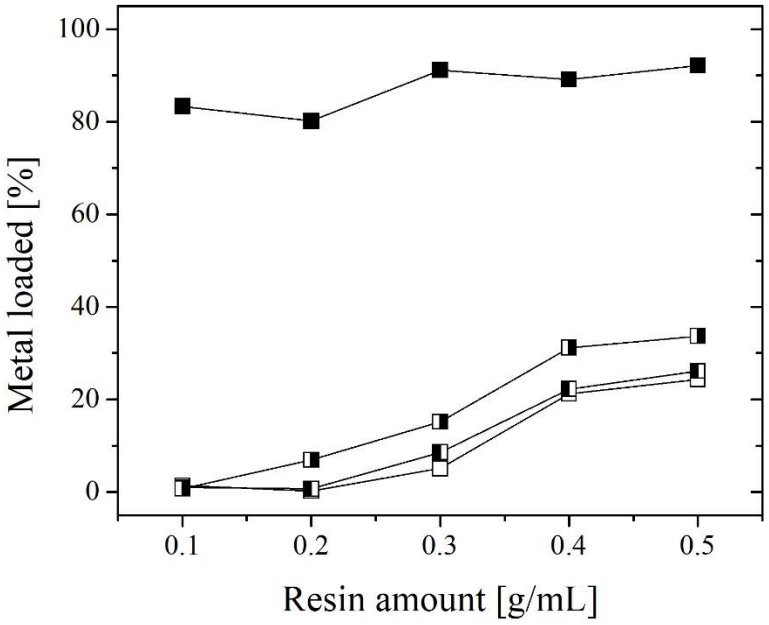

Figure 4.6: Percentage of metal adsorption in resin containing a combination of phosphonic and sulfonic groups in polymetallic system. (■) Fe, (□) Ni, (◧) Co, and (◨) Cu adsorbed in Puromet MTS9570

Industrial applications of resins containing a combinations of phosphonic and sulfonic groups are the control Fe in electrolytes for copper electrowinning (Chiariza et al., 1997; Sole et al., 2018). The Fe^{3+} adsorption behavior in bimetallic systems (Section 3.4.1.6) show a rapid Ni^{2+} uptake once Fe^{3+} is depleted from solution. Similarly, co-adsorption of base metals in polymetallic systems increase at low Fe^{3+} concentration. The similar increments of base metal co-adsorption at low Fe^{3+} concentration suggest non base

metal selectivity by resin. Given the rapid Fe^{3+} depletion, iron-adsorption preference was confirmed.

4.4.1.7 Resins with iminodiacetic acid groups

Resin with iminodiacetic acid groups favoured Cu^{2+} over Fe^{3+} and the other base metals studied. All resins regardless of manufacturer and brand followed this trend (see Figure 4.7). Increases in resin dosage increased the Fe^{3+} and Cu^{2+} adsorption but the co-adsorption of $Ni^{2+}$and Co^{2+} only reached ~10% at resin dosages higher than 0.3 g/mL. The maximum resin dosage resulted in maximum metal adsorption at 91% Cu^{2+}, 73% Fe^{3+}, 30% Ni^{2+}, and 18% Co^{2+}. Amberlite IR748i showed the lowest co-adsorption of Ni^{2+} and Co^{2+}. On average, resin containing iminodiacetic acid groups achieved adsorption of 48 mg of Ni^{2+}, 0.6 mg of Co^{2+}, 16 mg of Cu^{2+}, and 5.1 mg of Fe^{3+} per gram of dry resin.

Resins with iminodiacetic acid groups are used commercially for the purification of Co^{2+} electrolyte solutions prior to electrowining (Sole et al., 2018) and the recovery of Cu^{2+} from heap leaching solutions (Jurrius et al., 2014). High preference for Fe^{3+} and Cu^{2+} is reported by resin manufacturers (Silva et al., 2018). Our results resembled preference observed in both applications obtaining high Fe^{3+} and Cu^{2+} adsorptions with low Co^{2+} co-adsorption. The complex formation/stability constant of iminodiacetic acid groups and metal ions support the observations. At ionic strength conditions of 0.1 M and 25 °C iminodiacetic acid has complexing log k_1 value of 11.3 and 10.6 for Fe^{3+} and Cu^{2+}, respectively. In comparison log k_1 values for Ni^{2+} are 8.2 and 7.0 for Co^{2+} (Smith and

Martell, 1987). Resins with iminodiacetic acid groups are effective for Fe^{3+} removal. However, the Fe^{3+} adsorption is not selective in presence of Cu^{2+}.

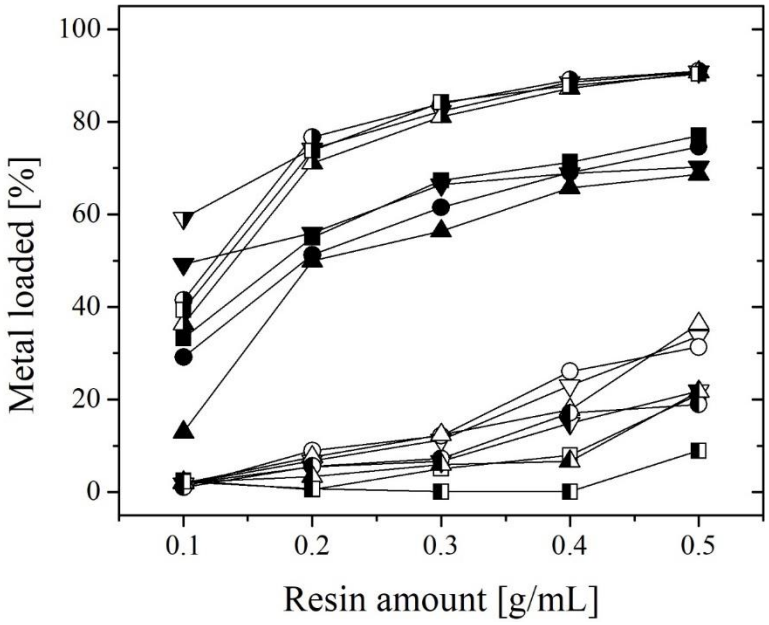

Figure 4.7: Percentage of metal adsorption in resin containing iminodiacetic acid groups in polymetallic system. (■) Fe, (□) Ni, (◧) Co, and (◨) Cu adsorbed in Amberlite IR748i, (●) Fe (○) Ni, (◐) Co, and (◑) Cu adsorbed in Lewatit TP207, (▲) Fe, (△) Ni, (◭) Co, and (◮) Cu adsorbed in Lewatit TP208, and (▼) Fe, (▽) Ni, (▾) Co, and (▿) Cu adsorbed in Puromet MTS9300

4.4.1.8 Resins with amidoxime groups

Resins with amidoxime groups showed selective adsorption of Cu^{2+} and Fe^{3+} depending on the resin dosage (See Figure 4.8). At resin dosages lower than 0.2 g/mL, amidoxime groups favoured Cu^{2+} adsorption. Resin dosages of 0.3 g/mL and higher, favoured Fe^{3+} adsorption. The Cu^{2+} adsorption remained relatively stable at all resin dosages, between 16 and 30%. Contrarily, Fe^{3+} adsorption increased with resin dosage

going from adsorption of 5% at 0.1 g/mL to 66% at 0.5 g/mL. Along with the increase in Fe^{3+} adsorption, the co-adsorption of Ni^{2+} and Co^{2+} increased with resin dosage reaching a maximum of 14% and 12% respectively. The average metal adsorption per gram of dry resin reached values of 42 mg of Ni^{2+}, 0.9 mg of Co^{2+}, 0.5 mg of Cu^{2+}, and 1.4 mg of Fe^{3+}.

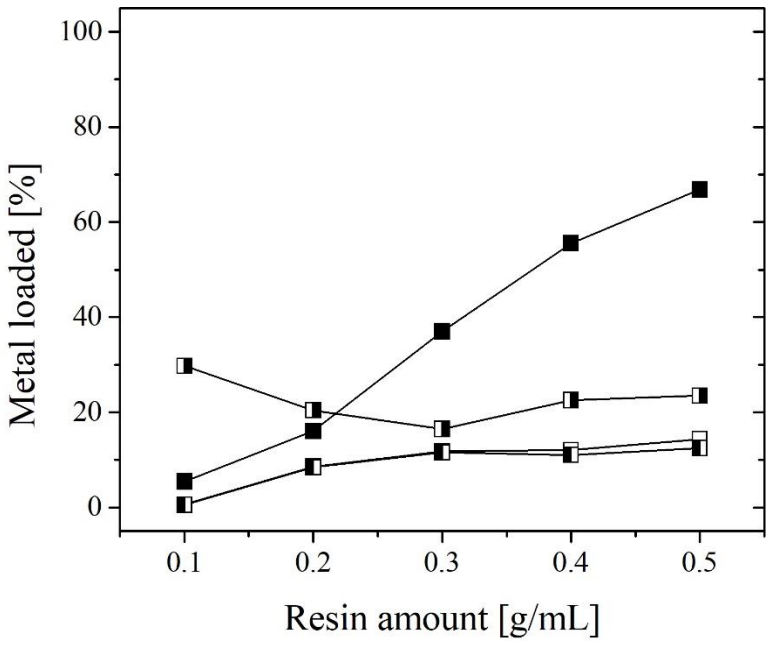

Figure 4.8: Percentage of metal adsorption in resin containing amidoxime groups in polymetallic system. (■) Fe, (□) Ni, (◧) Co, and (◨) Cu adsorbed in Puromet MTS9100

Amidoxime groups are known to have high stability with Fe^{3+} and Cu^{2+} in sulfate systems (Hubicki, 1986). Several experimental runs confirmed the adsorption behaviour and the trends observed for other metals studied (Figure 4.8). The trends observed suggest preferential Cu^{2+} adsorption at low resin dosage but preferential Fe^{3+} and high resin dosage. Up to now it is unclear the reasons for different metal preference depending on resin dosage. However, Section 3.4.2.2 and 4.4.2.1 related to metal adsorption at different

solution pH obtained similar adsorption trends. Unpublished works by our research team showed that electrolytes at high metal concentration containing similar amounts of Cu^{2+}/Fe^{3+} favoured Fe^{3+} adsorption over Cu^{2+} throughout the resin dosage tested. No experiments at different Cu^{2+}/Fe^{3+} concentration in polymetallic systems were conducted to confirm this behaviour. Even so, literature suggest that the high stability of amidoxime groups with Fe^{3+} and Cu^{2+} makes the elution process difficult, requiring highly acidic solutions (e.g., 1M H_2SO_4) which impacts the physical integrity of the resin.

4.4.1.9 Resins with methylglucamine groups

Resins with methylglucamine groups favoured Fe^{3+} over the base metals studied (see Figure 4.9). Among the base metals, Cu^{2+} showed the highest co-adsorption. The metal adsorption increased as resin dosage increased but showed negligible base metal co-adsorption at resin dosages of 0.2 g/mL and lower. At dosages of 0.2 g/mL the amount of Fe^{3+} adsorption reached approximately 49%. The highest resin dosage achieved 94% of Fe^{3+} adsorption but showed a substantial Cu^{2+} co-adsorption that reached 75%. Co-adsorption of Ni^{2+} and Co^{2+} reached 15% and 16% at the highest concentration of resins, respectively. On average each gram of dry resin adsorbed 27 mg of Ni^{2+}, 0.6 mg of Co^{2+}, 4.5 mg of Cu^{2+}, and 5.0 mg of Fe^{3+}.

Although resins with methylglucamine groups are not common in hydrometallurgy, the extent of Fe^{3+} selectivity over the rest of base metals is equivalent to those traditionally employed for the task. The high co-adsorption of Cu^{2+} resemble those of aminophosphonic acid and iminodiacetic acid groups suggesting itself as an alternative. Particularly after

obtaining lower Ni^{2+} co-adsorption than the aforementioned groups. The high amount of Ni^{2+} adsorbed per gram of dry resin is attributed to the excess of the ion in the system rather than a preferred adsorption. This suggest that in presence of more Fe^{3+} the amount of Ni^{2+} adsorbed may decrease as observed in Section 3.4.1.9.

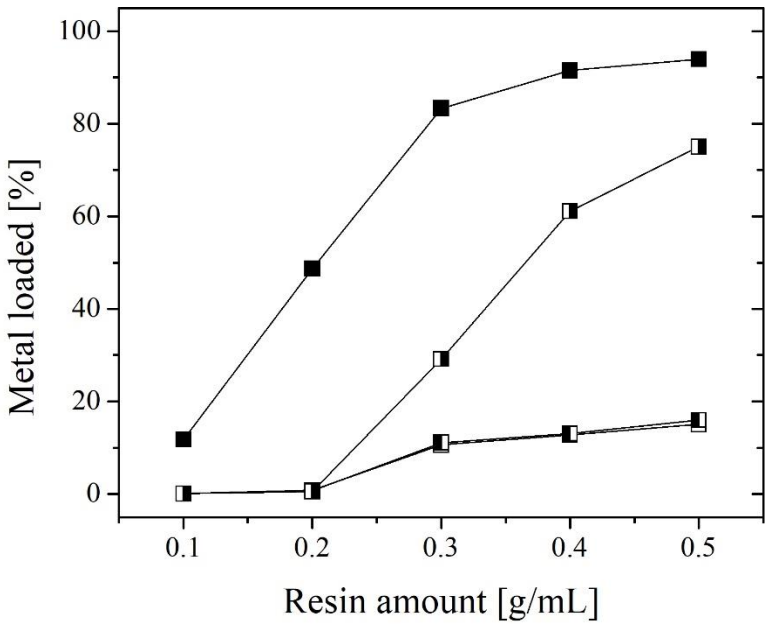

Figure 4.9: Percentage of metal adsorption in resin containing N-methylglucamine groups in polymetallic system. (■) Fe, (□) Ni, (◧) Co, and (◨) Cu adsorbed in Purolite S108

4.4.1.10 Resins with bis-picolylamine groups

Resins with bis-picolylamine groups, along with iminodiacetic acid groups favoured the adsorption of Cu^{2+} over other metals. However, unlike iminodiacetic acid the adsorption of other studied metals remained low even at the highest resin dosage (see Figure 4.10). At the lowest resin dosage, the Cu^{2+} adsorption preference was clear. The adsorption of Cu^{2+} reached 43% meanwhile the other metals showed adsorption under 1%.

Resin dosages of 0.4 g/mL obtained the highest Cu^{2+} adsorption at 93%. Little to no increase in Cu^{2+} adsorption was obtained thereafter. The highest resin dosage resulted in highest co-adsorption of Ni^{2+}, Fe^{3+}, and Co^{2+} at 23%, 14%, and 9.3%. The average adsorptions of metals per gram of dry resin reached 31 mg of Ni^{2+}, 0.2 mg of Co^{2+}, 17 mg of Cu^{2+}, and 0.5 mg of Fe^{3+}.

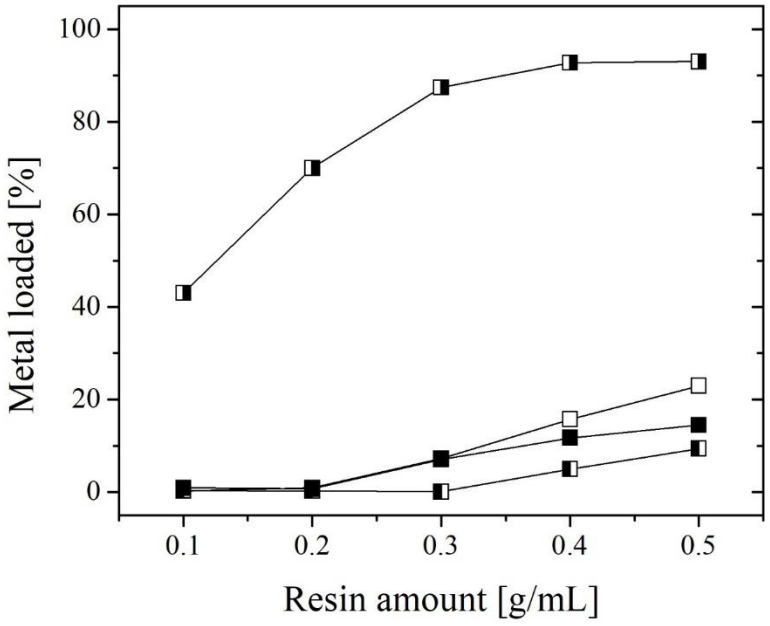

Figure 4.10: Percentage of metal adsorption in resin containing bis-picolylamine groups in polymetallic system. (■) Fe, (□) Ni, (◧) Co, and (◨) Cu adsorbed in Lewatit TP220

Bis-picolylamine resin find its use in industry in the separation of Cu from Co and Ni solutions (Van Deventer, 2011) and other Cu recovery processes (Kagaya et al., 2014). Particularly, bis-picolylamine is used due to its strong bonding with Cu^{2+} and Ni^{2+} among other metals. Our results confirmed the Cu^{2+} selectivity of the group. However, it showed minimum preference for Ni^{2+} adsorption in presence of Fe^{3+} and Cu^{2+} as seen in

polymetallic and bimetallic systems. Resins with bis-pycolilamine are not suitable for selective Fe^{3+} recovery or the purification of Fe^{3+} solutions from base metals.

4.4.1.11 Resins with thiourea and isothiouronium groups

Commercial resins containing thiourea and its tautomeric isothiouronium were among the resins favouring Cu^{2+} adsorption over other metals tested. Both tautomeric configurations reached similar adsorption of Cu^{2+} at the highest resin dosage obtaining a maximum of 94% (see Figure 4.11). However, thiourea configurations reached higher adsorption at resin dosages of 0.1 g/mL reaching an average of 66% while isothiouronium reached 16%. Aside the Cu^{2+} adsorption trends, the rest of the metals followed similar co-adsorption trends depending on the type of the resin employed. Negligible co-adsorption at low resin dosages and maximum average adsorption values of 20% Ni^{2+}, 18% Co^{2+}, and 19% Fe^{3+} at the highest resin dosage. Interestingly, each resin showed similar adsorption trends of Fe^{3+}, Co^{2+}, and Ni^{2+} depending on the brand and type of resin suggesting non-selective co-adsorption. On average, each gram of dry resin adsorbed 38 mg of Ni^{2+}, 0.8 mg of Co^{2+}, 19 mg of Cu^{2+}, and 0.7 mg of Fe^{3+}.

Unlike the bimetallic systems, the adsorption of Fe^{3+} decreased from 50% to 20% once Cu^{2+} was introduced in polymetallic systems. Nonetheless, Ni^{2+} co-adsorption remained relatively constant obtaining adsorption between 20 to 24% not withstanding the metal concentration differences between bimetallic and polymetallic systems. Poor selectivity towards Fe^{3+} in polymetallic systems and a compromised Fe^{3+} selectivity in

bimetallic systems disprove thiourea/isothiouronium resins' capabilities of selectively removals.

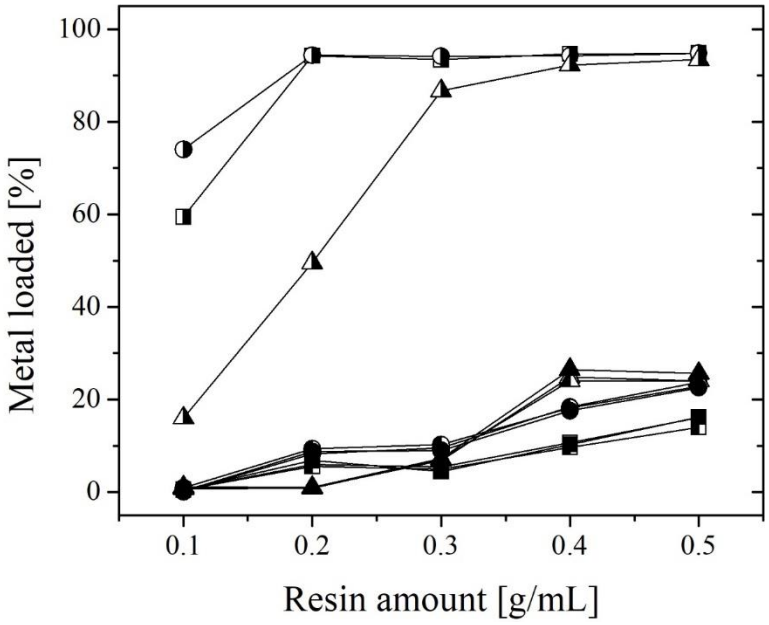

Figure 4.11: Percentage of metal adsorption in resin containing containing thiourea and isothiouronium groups in polymetallic system. Containing thiourea groups (■) Fe, (□) Ni, (◧) Co, and (◨) Cu adsorbed in Lewatit TP214 and (●) Fe (○) Ni, (◐) Co, and (◑) Cu adsorbed in Puromet S9140. Containing ishothiouronium groups (▲) Fe, (△) Ni, (◭) Co, and (◮) Cu adsorbed in Puromet S9200

4.4.1.12 Resins with thiol groups

As with resins with thiourea groups, thiol resins show good selectivity towards Cu^{2+} adsorption (See Figure 4.12). Interestingly, thiol groups show the maximum Cu^{2+} adsorption at resin dosages of 0.2 and 0.3 g/mL achieving approximately 91%. At these resin dosages, the adsorption of Fe^{3+}, Ni^{2+}, and Co^{2+} were under 10%. Higher resin dosages decreased the extent of Cu^{2+} adsorption but increased the adsorption of the rest of the

metals. At the highest resin dosage, thiol groups adsorbed 75% of Cu^{2+}, 19% of Ni^{2+}, 18% of Fe^{3+}, and 17% of Co^{2+}. The average metal adsorption per gram of dry resin reached 30 mg of Ni^{2+}, 0.6 mg of Co^{2+}, 18 mg of Cu^{2+}, and 0.5 mg of Fe^{3+}.

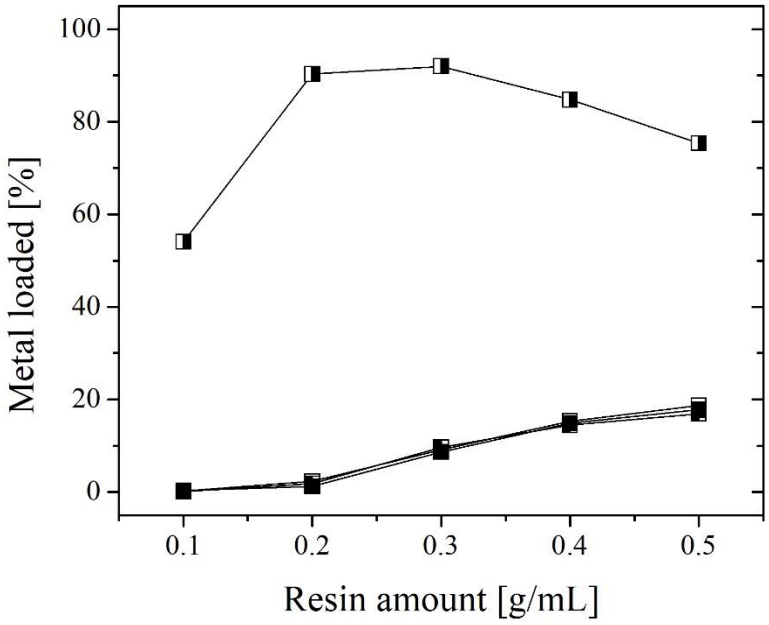

Figure 4.12: Percentage of metal adsorption in resin containing thiol groups in polymetallic system. (■) Fe, (□) Ni, (◧) Co, and (◨) Cu adsorbed in Puromet MTS9240

The poor performance in bimetallic systems was also present in polymetallic systems, indicating resins with thiol groups are not suitable for selective Fe^{3+} adsorption. Resins with thiol groups showed equivalent adsorption of Fe^{3+} in bimetallic and polymetallic system. In contrast, the higher Ni^{2+} concentration in polymetallic system increased adsorption from 12% to 19%. However, this increase is not comparable to the Cu^{2+} adsorption by the resin.

4.4.1.13 Resins with quaternary ammonium groups

Resins containing quaternary ammonium groups show preference towards Fe^{3+} adsorption over the resin dosage analyzed (see Figure 4.13). At resin dosages of 0.1 g/mL the Fe^{3+} adsorption reached 38% while the co-adsorption of the rest of the base metals remained under 5%. The Fe^{3+} adsorption increased with resin dosage, reaching a maximum of 49% a the highest resin dosage. Along with the increases in Fe^{3+} adsorption, the base metal co-loadgins increased reaching a maximum of 14% of Co^{2+} and an equal 11% of Ni^{2+} and Cu^{2+}. Similar co-adsorption trends suggest non-selectivity of base metals and this is regardless of metal concentration. On average one of dry resin adsorbed 25 mg of Ni^{2+}, 0.7 mg of Co^{2+}, 1.1 mg of Cu^{2+}, and 4.9 mg of Fe^{3+}.

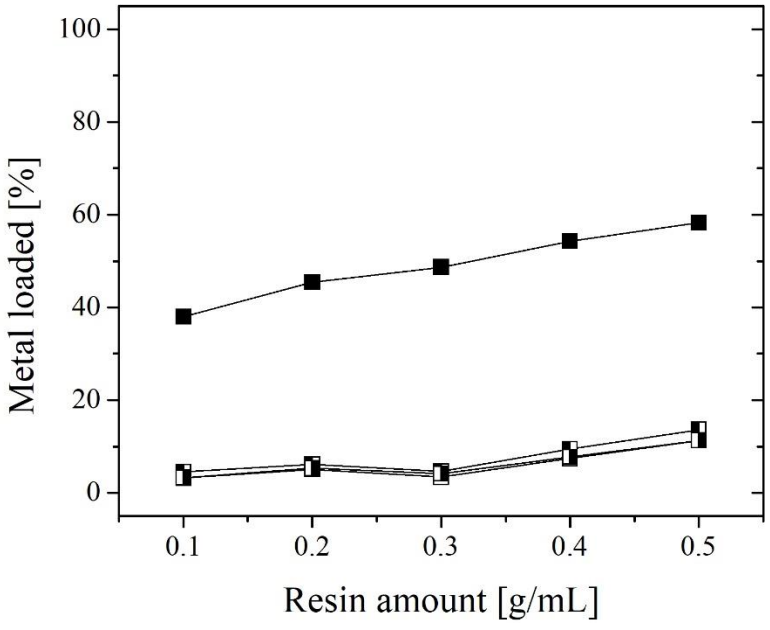

Figure 4.13: Percentage of metal adsorption in resin containing quaternary ammonium groups in polymetallic system. (■) Fe, (□) Ni, (◧) Co, and (◨) Cu adsorbed in Amberlite IRA 440 Cl^-

Quaternary ammonium groups maintained the Fe^{3+} selectivity observed in bimetallic systems. Similarly, the base metal co-adsorption remained close to 10% even at Fe^{3+} concentrations significantly lower than in bimetallic systems and in Ni^{2+} excess. Up to now, there is no applications for quaternary ammonium groups in industry. Based on the selectivity observed and the nature of the group, these type of resins are a potential candidate for Fe^{3+} separation processes at an industrial scale. Chapter 5 discusses further Fe^{3+} removals under different system parameters.

4.4.1.14 Resins with mixed quaternary ammonium and sulfonic groups

Resins with a combination of quaternary ammonium and sulfonic groups favoured Fe^{3+} adsorption over the other metals tested (see Figure 4.14). Substantial increases in Fe^{3+} adsorption occurred between resin dosages of 0.1 and 0.2 g/mL and continued to increase with dosage. Approximately 35% of Fe^{3+} adsorption was obtained at 0.2 g/mL and a maximum of 48% at the maximum resin dosage. As with resins with only quaternary ammonium groups, the base metal co-adsorption remained under 15% reaching maximum adsorption of 13% of Ni^{2+}, 12% of Co^{2+}, and 11% of Cu^{2+} at the maximum resin dosage. Besides Fe^{3+} selectivity, there was no selective base metal adsorption. The average metal adsorption per gram of dry resin reached 20 mg of Ni^{2+}, 0.4 mg of Co^{2+}, 0.8 mg of Cu^{2+}, and 2.5 mg of Fe^{3+}.

Regardless of the MBR characteristics of these resins, the behaviour of a combination of quaternary ammonium and sulfonic acid groups resembled that of quaternary ammonium groups in polymetallic systems. Unlike in bimetallic systems that

showed average adsorption between the independent groups, there was very little if any base metal adsorption in polymetallic systems. As with quaternary ammonium groups, base metal co-adsorption trends suggest Fe^{3+} selectivity. Up to now, the adsorption mechanism is unclear. Based on the results of bimetallic systems these type of resins fail to obtain selective Fe^{3+} removals. Thus, focused efforts should be given to studies employing resins containing exclusively quaternary ammonium groups.

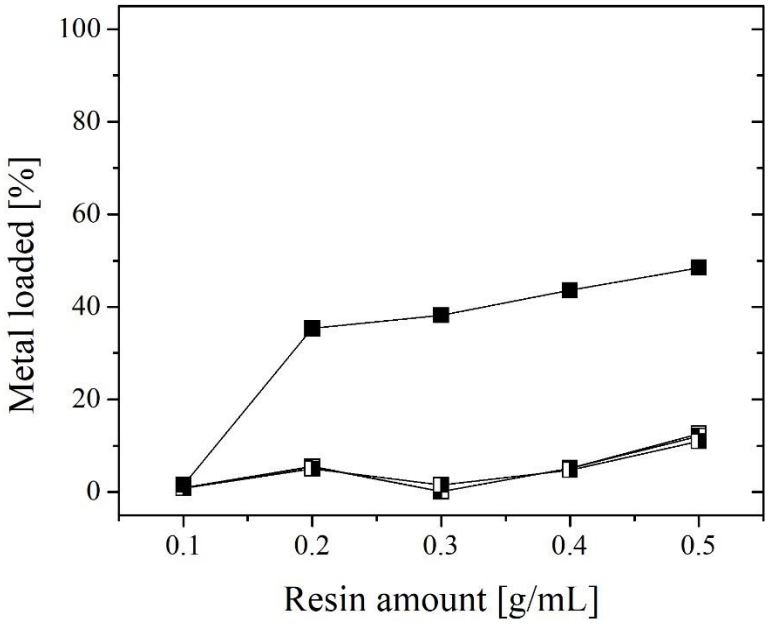

Figure 4.14: Percentage of metal adsorption in resin containing a combination of quaternary ammonium and sulfonic acid groups in polymetallic system. (■) Fe, (□) Ni, (◧) Co, and (◨) Cu adsorbed in Resintech MBD-15

4.4.2 Systematic studies for best performers

4.4.2.1 Variation of solution pH

Simulations of phase equilibrium boundaries for systems with 2.5 g/L Fe^{3+}, 100 g/L Ni^{2+}, 3 g/L Co^{2+}, and 5.5 g/L Cu^{2+} in 11 g/L of free acid did not identified other pH boundary limits than that presented in Section 3.4.2.2. Like in bi-metallic systems, OLI Studio 9.5 only identified potential precipitation at pH higher than 2.3 (See Figure 3.19). No Pourbaix diagram for Fe-Ni-Co-Cu systems is included due to its complexity.

Similar to bi-metallic systems, Fe^{3+} adsorption decreased as pH approached 2.3 (Figure 4.15a and 4.15b). Most resins showed decreased Fe^{3+} adsorption as pH approached the lower limit of 1.0. The adsorption trend obtained suggest a narrow pH range for maximum Fe^{3+} adsorption between 1.0 and 2.2. No precipitates were found in sample's vial. Interestingly, the lowest and highest pH values obtained the lowest Fe^{3+} adsorption among all parameters analyzed (different metal concentration, Fe:Ni ratio, time, and temperature) confirming the narrow pH for optimum operations.

Base metal co-adsorptions were dependant on the resin's functional group. The Cu^{2+} co-adsorption dominated and varied with pH. Resins with aminophosphonic acid groups showed that as the percentage of Fe^{3+} adsorbed decreased with pH, co-adsorption of Cu^{2+}, Co^{2+}, and Ni^{2+} increased (Figure 4.15 a1). The increase in base metal co-adsorption as pH increased was not apparent in resins containing a combination of phosphonic and sulfonic groups except for Ni^{2+} co-adsorption in bimetallic systems (Figure 4.15 a2). Although resins with phosphonic and sulfonic groups were the only functionalized group maintaining high Fe^{3+} adsorption at pH close to 2.3 in bimetallic systems, in polymetallic

systems showed the most abrupt decline in Fe^{3+} adsorption. The Cu^{2+} co-adsorption with iminodiacetic acid group resins was favoured and enhanced as solution pH approached 2.3 (Figure 4.15 a3). At these conditions, Cu^{2+} adsorption by iminodiacetic acid groups were among highest of the best performing resins while Fe^{3+} adsorption was the lowest. Co-adsorption of Ni^{2+} and Co^{2+} were low for iminodiacetic acid resins. Resins with methylglucamine groups showed Fe^{3+} selectivity at pH lower than 1.7 but allowed Cu^{2+} co-adsorption above this pH (Figure 4.15 a4). The maximum Fe^{3+} adsorption on this resins occurred at pH values between 1.5 and 2.2 corresponding to the increase in Cu^{2+} adsorption. Methylglucamine groups also show significant Cu^{2+} co-adsorption as resin dosage increases in polymetallic systems.

Resins with carboxylic acid and quaternary ammonium showed similar adsorption trends as pH increased (Figure 4.15 b1 and b2). Both showed moderate Fe^{3+} adsorption but the lowest base metal co-adsorption with no signs of preference for Cu^{2+} or Ni^{2+}. Resin with carboxylic acid groups produced the highest Fe^{3+} adsorption between pH of 2.0-2.2 while resins with quaternary ammonium between 1.5 and 2.0. Most likely, this is the results of poor deprotonation of carboxylic acid groups at acidic pH and different Fe^{3+} speciation in quaternary ammonium as it reaches the 2.3 threshold.

As with the adsorption trends in amidoxime resins at different resin dosage (Section 4.4.1.8) initial pH also shifted the Fe:Cu preference. At low pH, amidoxime groups adsorbed exclusively Cu^{2+} (Figure 4.15 b3) which decreased as pH increased. With the decrease in Cu^{2+} adsorption, Fe^{3+} adsorption increased up to a maximum between a pH of 1.7 – 2.2. Thereafter, Fe^{3+} adsorption decreased but Cu^{3+} adsorption continued declining.

The Fe:Cu preference trend observed at different pH matches the observations obtained at low resin concentrations suggesting the solution's pH is changing due to the adsorption of resin. Resin with phosphoric groups (Figure 4.15 b4) showed Fe^{3+} adsorption throughout the pH range tested and the highest Fe^{3+} adsorption at the highest pH in the study. The highest pH also showed the highest Cu^{2+} co-adsorption of all resins.

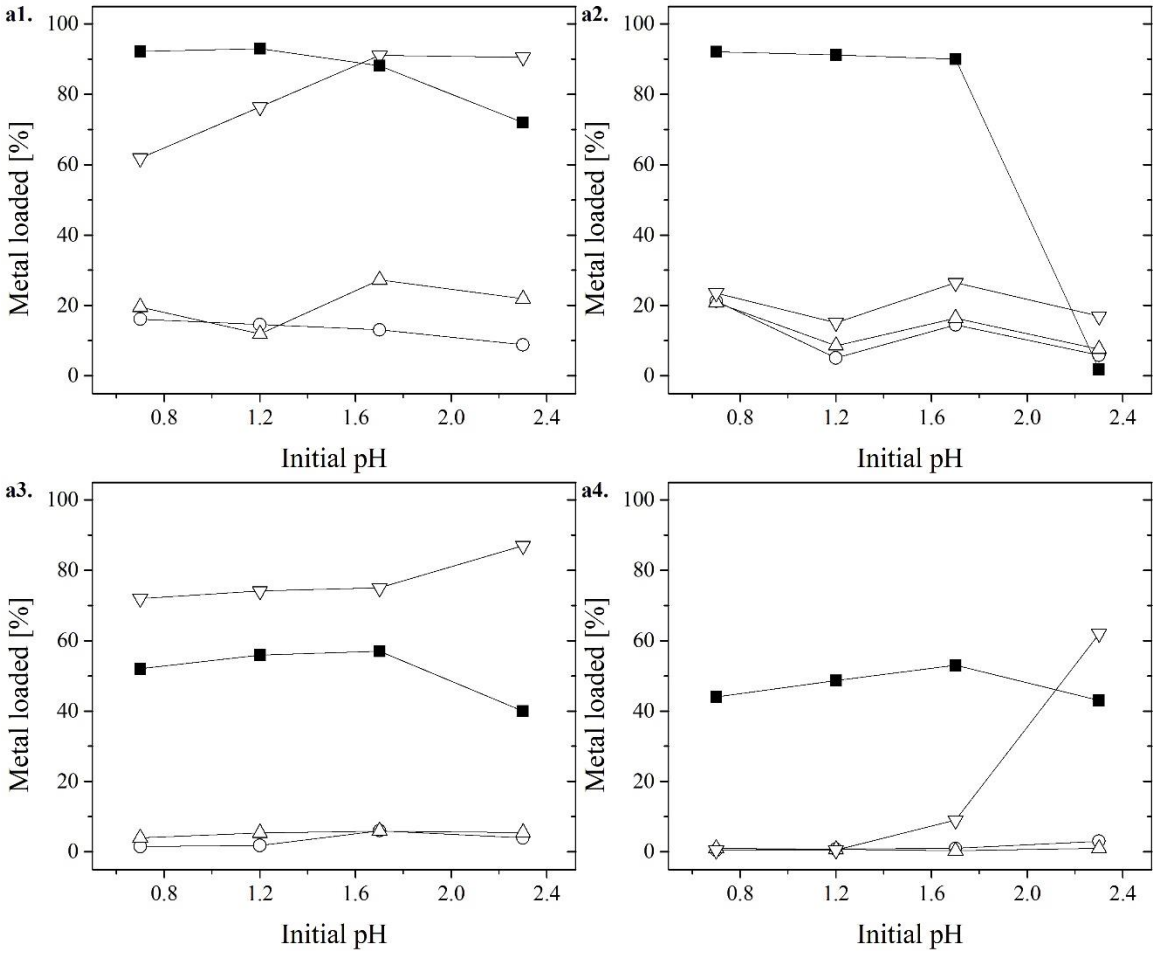

Figure 4.15a: Percentage (■) Fe, (○) Ni, (△) Co, and (▽) Cu adsorbed at different initial pH in resins containing: a1) aminophosphonic acid groups, Lewatit TP260; a2) a combination of phosphonic and sulfonic groups, Puromet MTS9570; a3) iminodiacetic acid groups, Puromet MTS9300; and a4) methylglucamine groups, Purolite S108.

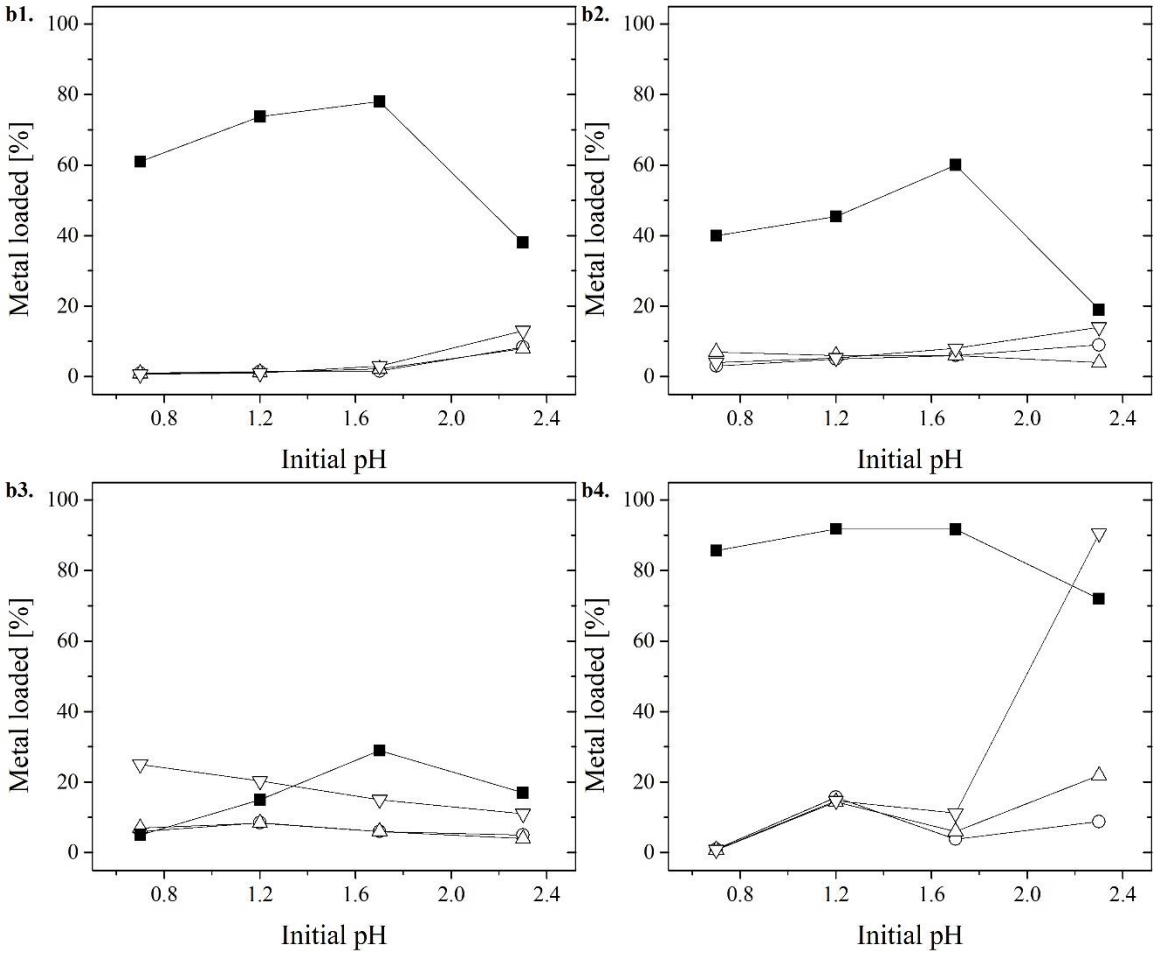

Figure 4.15b: Percentage of (■) Fe, (○) Ni, (△) Co, and (▽) Cu adsorbed at different initial pH in resins containing: b1) carboxylic acid groups, Resintech WACG; b2) quaternary ammonium groups, Amberlite IRA 440Cl; b3) Amidoxime groups, Puromet MTS9100; and a4) phosphoric acid resins, Lewatit VP OC 1026.

4.4.2.2 Variation of temperature

Temperature affected differently on Fe^{3+} adsorption depending on the functional groups (see Figure 4.16a and 4.16b). Adsorption of Fe^{3+} increased with temperature in resins containing iminodiacetic acid (Figure 4.16 a3), methylglucamine (Figure 4.16 a4), quaternary ammonium (Figure 4.16 b2), and phosphoric acid (Figure 4.16 b4). The rest of resins, aminophosphonic acid (Figure 4.16 a1), a combination of phosphonic and sulfonic

(Figure 4.16 a2), carboxylic acid (Figure 4.16 b1), and amidoxime groups (Figure 4.16 b3), showed little to no increment with temperature. The results suggest that, relatively speaking, temperature has higher impact in bimetallic systems (Section 3.4.2.3) systems than in polymetallic. This is particularly true for resins with aminophosphonic acid and iminodiacetic acid groups that showed the biggest difference as temperature increased in bimetallic systems (Figure 3.21a) but did not change in polymetallic systems (Figure 4.16a).

The relatively stable Fe^{3+} adsorption in polymetallic systems is likely due to low Fe^{3+} concentration compared to that of based metals in solution allowing maximum adsorption independently of the effects of temperature on the resin. Conversely, any adverse effect on a resin's adsorption capacity due temperature may only become apparent at high Fe^{3+} concentrations as observed in bimetallic systems.

Temperature had a reduced effect in base metal co-adsorption with Cu^{2+} the most impacted. Adsorption of Cu^{2+} was representative in resins with iminodiacetic, aminophosphonic, methylglucamine, and amidoxime, in order. These group of resins showed co-adsorptions trends of Cu^{2+} similar to the adsorption trends of Fe^{3+}. This means resins with aminophosphonic acid groups showed a slight decrease in Cu^{2+} adsorption with increasing temperature while methylglucamine and iminodiacetic acid resins showed an increase in Cu^{2+} adsorption. Resins with amidoxime appeared to have adsorptions of Fe^{3+} and Cu^{2+} independent of temperature. Resins with iminodiacetic acid was the only group among best performers that obtained the Cu^{2+} adsorptions larger than that of Fe^{3+}.

Adsorption of Ni^{2+}, and Co^{2+} remained relatively stable ranging from negligible to 10% over the temperatures studied.

Under the 2 h lasting experiments of this study, temperatures approaching 90°C did not affect the physical integrity of the resin as suggested by manufacturers. However, longer experimental times are required to validate the observations.

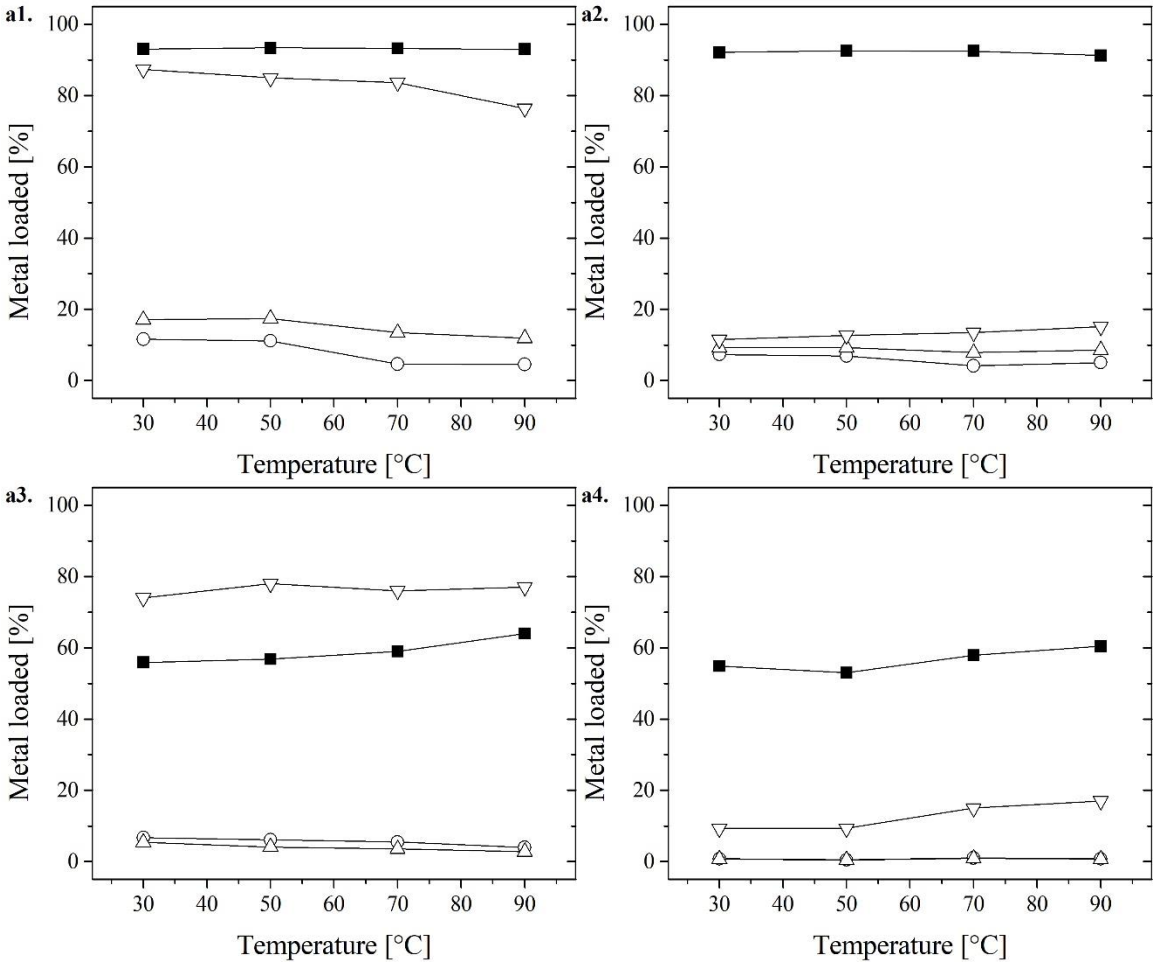

Figure 4.16a: Percentage of (■) Fe, (○) Ni, (△) Co, and (▽) Cu adsorbed at different temperature in resins containing: a1) aminophosphonic acid groups, Lewatit TP260; a2) a combination of phosphonic and sulfonic groups, Puromet MTS9570; a3) iminodiacetic acid groups, Puromet MTS9300; and a4) methylglucamine groups, Purolite S108.

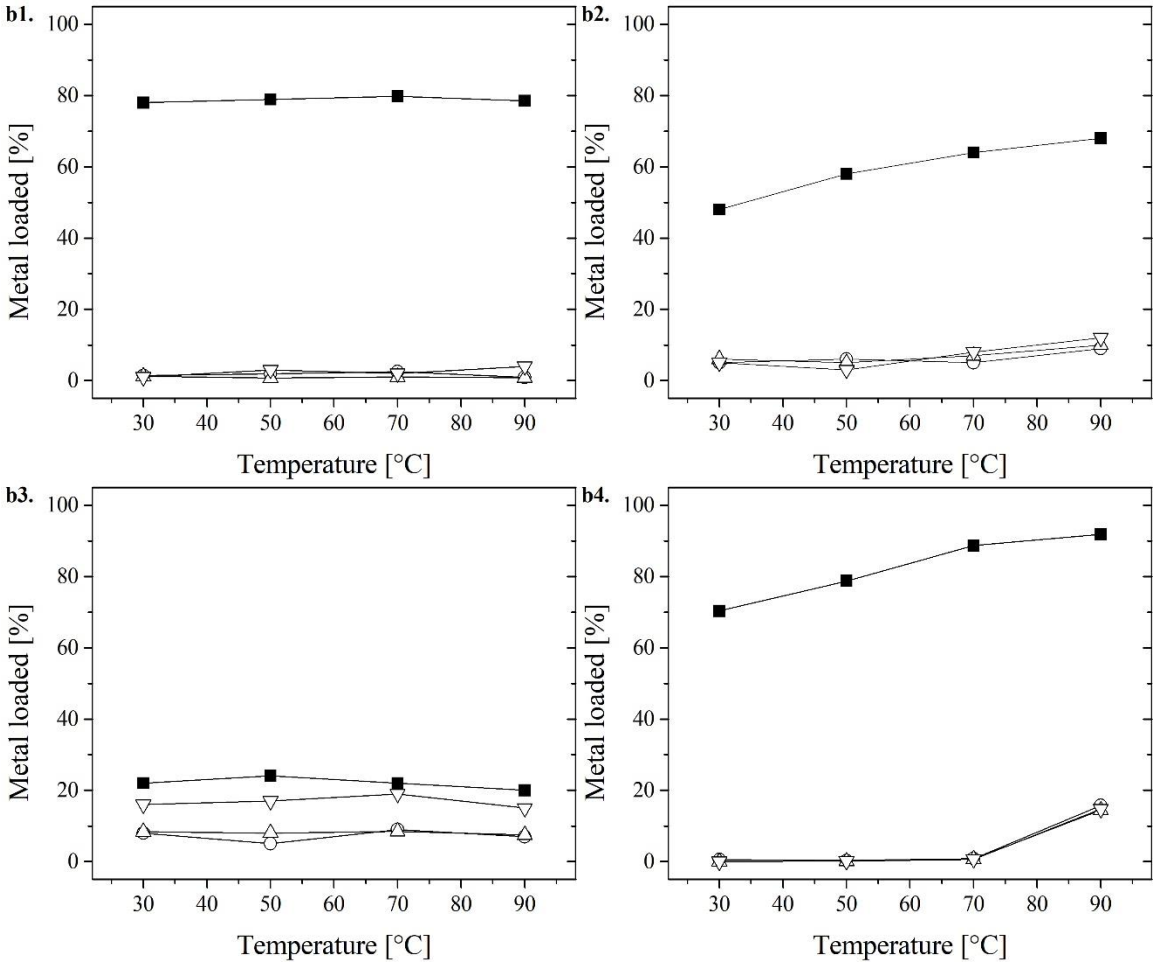

Figure 4.16b: Percentage of (■) Fe, (○) Ni, (△) Co, and (▽) Cu adsorbed at different temperature in resins containing: b1) carboxylic acid groups, Resintech WACG; b2) quaternary ammonium groups, Amberlite IRA 440Cl; b3) Amidoxime groups, Puromet MTS9100; and a4) phosphoric acid resins, Lewatit VP OC 1026.

4.4.2.3 Variation of time

As a general trend, Fe^{3+} adsorption increased with time while base metal adsorption decreased (Figures 4.17a and 4.17b). This trend was also observed in bimetallic systems (See Section 3.4.2.4. A decline in base metal adsorption with time, analog to increases in Fe^{3+} adsorption, suggested an ionic substitution due adsorption preferences. Resins showing representative Cu^{2+} co-adsorption such as aminophosphonic acid (Figure 4.17 a1)

and iminodiacetic acid (Figure 4.17 a3) showed Cu^{2+} increases mirroring Fe^{3+} trends while Co^{2+} and Ni^{2+} decreased.

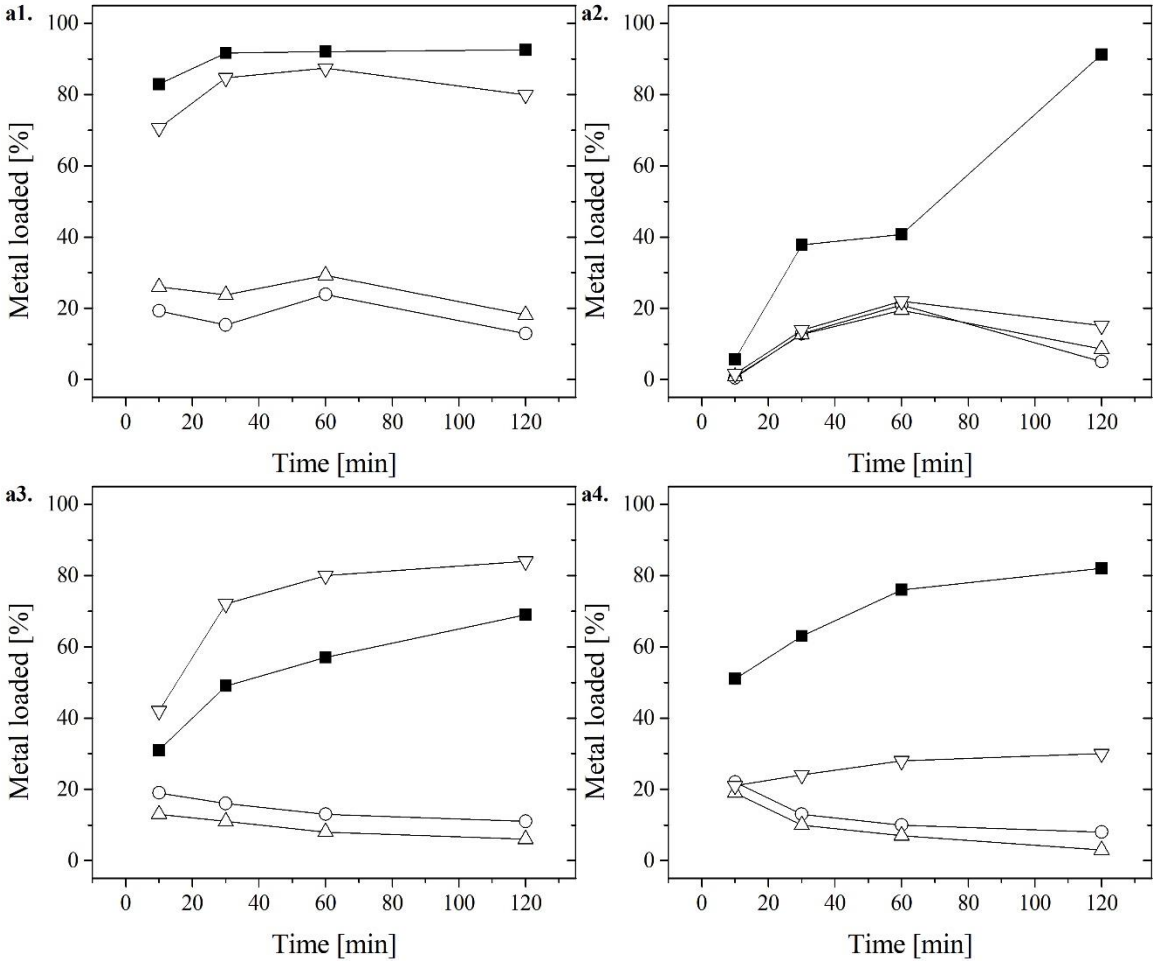

Figure 4.17a: Percentage of (■) Fe, (○) Ni, (△) Co, and (▽) Cu adsorbed at different time in resins containing: a1) aminophosphonic acid groups, Lewatit TP260; a2) a combination of phosphonic and sulfonic groups, Puromet MTS9570; a3) iminodiacetic acid groups, Puromet MTS9300; and a4) methylglucamine groups, Purolite S108.

Resins with phosphoric acid groups (Figure 4.17 b4) showed the best Fe^{3+} separation among best performers. However, several resins appear to reach maximum Fe^{3+} adsorptions before 120 min. Resins such as aminophosphonic acid (Figure 4.17 a1),

amidoxime (Figure 4.17 b3), and phosphoric groups (Figure 4.17 b4) appear to reach maximum Fe^{3+} adsorption before 30 min.

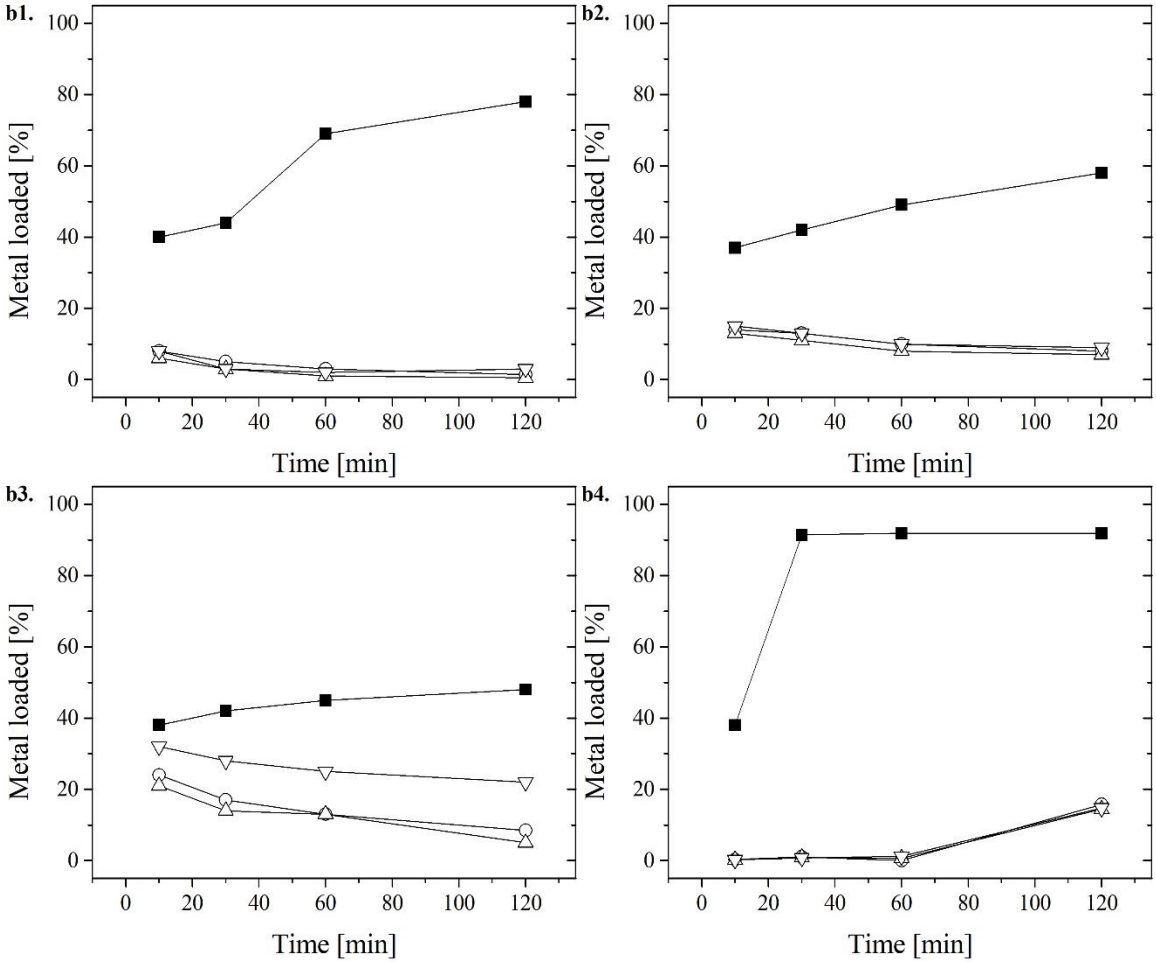

Figure 4.17b: Percentage of (■) Fe, (○) Ni, (△) Co, and (▽) Cu adsorbed at different time in resins containing: b1) carboxylic acid groups, Resintech WACG; b2) quaternary ammonium groups, Amberlite IRA 440Cl; b3) Amidoxime groups, Puromet MTS9100; and a4) phosphoric acid resins, Lewatit VP OC 1026.

4.5 Discussion

Results show that most of the resin favour Fe^{3+} adsorption over Ni^{2+}, Co^{2+}, and Cu^{2+} regardless the disproportion of ionic concentration in the system (see Table 4.2). Even though Ni^{2+} concentration was 70X more than Fe^{3+} and close to 25X more than Cu^{2+}, only resins containing sulfonic acid groups showed higher Ni^{2+} adsorption over the rest of metals obtaining 52% Ni^{2+}, 47% Co^{2+}, 42% Cu^{2+}, and 25% Fe^{3+} (see Table 4.3). Although sulfonic acid groups adsorbed more Ni^{2+} than the rest of metals, it is not possible to conclude preferential adsorption given nickel excess in the system compared to the rest of the metals. Bimetallic system suggest the potential of sulfonic groups for Fe^{3+} removal only if selective elution process is available. However, sulfonic groups lacked adsorption preferences in polymetallic systems suggesting a rather complicated selective elution. Although, the rest of the resins show low percentage of Ni^{2+} adsorption, the amount of Ni^{2+} adsorbed per gram of dry resin was the highest among base metals (Table 4.4). Given the excess of Ni^{2+} in the system, high amounts of Ni^{2+} adsorbed per gram of resin were expected. However, higher adsorption of any given metal coexisting at low concentration with Ni^{2+} in excess suggest a degree of selectivity towards the scarce metal. Any resin proving satisfactory adsorption of a given metal in presence of another metal at high concentration, will obtain a similar or enhanced adsorption at low concentrations of associated metal (Harland, 1994). Similarly, previous studies suggest that a metal ion having preferential adsorption by a resin displaces any counter ion previously adsorbed once the resin is exposed to more of the preferred metal (Silva et al., 2018).

Table 4.3: Comparison of selectivity trends among Fe^{3+}, Ni^{2+}, Co^{2+}, and Cu^{2+} found in literature and obtained experimentally

	Functional group	$Fe^{3+}/Ni^{2+}/Co^{2+}/Cu^{2+}$ Selectivity in literature	Selectivity based on percentage adsorbed
4.1	Sulfonic	Not found	$Ni^{2+} \approx Co^{2+} > Cu^{2+} > Fe^{3+}$
4.2	Carboxylic	Not found	$Fe^{3+} >> Ni^{2+} = Cu^{2+} = Co^{2+}$
4.3	Amino-phosphonic	$Fe^{3+} > Cu^{2+} > Ni^{2+} > Co^{2+}$	$Fe^{3+} >> Cu^{2+} > Co^{2+} \approx Ni^{2+}$
4.4	Phosphoric	$Fe^{3+} > Cu^{2+} > Co^{2+} > Ni^{2+}$	$Fe^{3+} >> Ni^{2+} = Cu^{2+} = Co^{2+}$
4.5	Phosphinic	$Fe^{3+} > Cu^{2+} > Co^{2+} > Ni^{2+}$	$Fe^{3+} >> Ni^{2+} = Cu^{2+} = Co^{2+}$
4.6	Phosphonic & Sulfonic	Not found	$Fe^{3+} >> Cu^{2+} > Co^{2+} = Ni^{2+}$
4.7	Iminodiacetic	$Fe^{3+} > Cu^{2+} > Ni^{2+} > Co^{2+}$	$Cu^{2+} > Fe^{3+} >> Ni^{2+} > Co^{2+}$
4.8	Amidoxime	Not found	$Fe^{3+} >> Cu^{2+} > Ni^{2+} \approx Co^{2+}$
4.9	N-methylglucamine	Not found	$Fe^{3+} > Cu^{2+} >> Co^{2+} \approx Ni^{2+}$
4.10	Bis-pycolilamine	$Cu^{2+} > Ni^{2+} > Fe^{3+} > Co^{2+}$	$Cu^{2+} >> Ni^{2+} > Fe^{3+} > Co^{2+}$
4.11	Thiourea and isothiouronium	$Cu^{2+} > Ni^{2+}$	$Cu^{2+} >> Fe^{3+} = Ni^{2+} = Co^{2+}$
4.12	Thiol	Not found	$Cu^{2+} >> Fe^{3+} = Ni^{2+} = Co^{2+}$
4.13	Quaternary ammonium	Not found	$Fe^{3+} >> Co^{2+} \approx Ni^{2+} = Cu^{2+}$
4.14	Quaternary ammonium and sulfonic	Not found	$Fe^{3+} >> Ni^{2+} = Co^{2+} \approx Cu^{2+}$

The occurrence of Cu^{2+} in polymetallic systems eliminated Fe^{3+} selectivity in several resins. As compared with Chapter 3 resins containing iminodiacetic acid, thiourea, isothiouronium, and thiol groups favoured Cu^{2+} adsorption instead of Fe^{3+}. Iminodiacetic acid groups maintained Fe^{3+} preference over nickel as in bimetallic systems (see Figure 3.8, Section 3.4.1.7) but decreased the extent of Fe^{3+} adsorption from 92% to 67% in polymetallic systems. This difference between Fe^{3+} adsorption in bimetallic and polymetallic systems was attributed to a preferred Cu^{2+} adsorption that reached 84%. As resin yielded high Cu^{2+} adsorption, there were limited adsorption sites free for Fe^{3+} adsorption. Neither of the Ni^{2+} nor Co^{2+} adsorption were remarkable enough to suggest alterations in the adsorption trends. On the other hand, resins with thiourea, isothiouronium, and thiol groups lost any Fe^{3+} preference over Ni^{2+} presented in bimetallic systems. Instead presented a forthright Cu^{2+} preference at early resin dosages and

maintained throughout all resin dosages analyzed. At resin dosages of 0.2 g/mL, thiourea and isothiouronium groups obtained Cu^{2+} adsorption of 94% while maintained Ni^{2+}, Fe^{3+}, and Co^{2+} adsorption under 7%. Likewise, resins with thiol groups obtained adsorption up to 90% of Cu^{2+} with maintained Ni^{2+}, Fe^{3+}, and Co^{2+} adsorption under 3%.

Resins with aminophosphonic acid and methylglucamine favoured Fe^{3+} adsorption but also adsorbed Cu^{2+}. As the resin dosage increased, resins with aminophosphonic acid groups reached almost equal adsorption of Fe^{3+} and Cu^{2+}, up to 92%. Likewise, resins with aminophosphonic acid groups showed increased Ni^{2+} and Co^{2+} co-adsorption as resin dosage increased. Methylglucamine groups maintained Fe^{3+} selectivity but Cu^{2+} adsorption increased from being 46% of that of Fe^{3+} at resin dosages of 0.3 g/mL to 81% at 0.5 g/mL. Although, the co-adsorption of Ni^{2+} and Co^{2+} remained around 15% even at the highest resin dosage. The high Cu^{2+} adsorption by these resins challenge the Fe^{3+} selectivity observed in bimetallic systems. Further studies related to the parameters influencing Cu^{2+} absorption could bring back the potential of this resin for Fe^{3+} removal. Likewise, selective elution may achieve efficient Fe removals in aminophosphonic acid resins or allow Fe:Cu separation in methylglucamine resins.

Resins containing phosphoric and phosphinic groups achieved the best Fe^{3+} selectivity in polymetallic systems with negligible base metal co-adsorption throughout the resins dosages analyzed. Both resins obtained satisfactory Fe^{3+} adsorption at resin dosages of 0.3 g/mL with little to no increase at higher concentrations. Phosphoric groups achieved 92% of Fe^{3+} adsorption with base metal co-adsorption under 2%. Phosphinic groups achieved Fe^{3+} adsorption of 84% with co-adsorption under 1%. The difference in Fe^{3+}

adsorption between bimetallic and polymetallic systems is due to the greater agitation speed conditions in polymetallic systems

Table 4.4: Summary of best performer resin among functional groups tested, most efficient resin amount, and maximum metal adsorption at most efficient resin dosages

	Functional group (Best performer resin)	**Most efficient resin amount**	**% Fe^{3+}**	**% Ni^{2+}**	**% Co^{2+}**	**% Cu^{2+}**
4.1	Sulfonic acid (Amberlite IR120)	0.5 g/mL	25%	52%	47%	42%
4.2	Carboxylic acid (Resintech WACG-HP)	0.3 g/mL	78%	0.9%	0.7%	0.6%
4.3	Aminophosphonic acid (Lewatit TP 260)	0.1 g/mL	87%	1.3%	1.0%	6.7%
4.4	Phosphoric (Lewatit VPOC 1026)	0.3 g/mL	92%	1.6%	1.4%	1.5%
4.5	Phosphinic (Lewatit TP272)	0.3 g/mL	84%	0.9%	0.8%	0.8%
4.6	Phosphonic & Sulfonic (Puromet MTS9570)	0.2 g/mL	80%	0.2%	0.6%	6.9%
4.7	Iminodiacetic acid (Amberlite IR748i)	0.3 g/mL	67%	5.0%	0.0%	84%
4.8	Amidoxime (Puromet MTS9100)	0.5 g/mL	67%	14%	12%	23%
4.9	N-methylglucamine (Purolite S108)	0.3 g/mL	83%	11%	11%	61%
4.10	Bis-pycolilamine (Lewatit TP220)	0.5 g/mL	14%	23%	9.3%	93%
4.11	Thiourea and isothiouronium (Lewatit TP214)	0.2 g/mL	6.8%	5.9%	5.6%	94%
4.12	Thiol (Puromet MTS9240)	0.2 g/mL	2.3%	1.8%	0.1%	90%
4.13	Quaternary ammonium (Amberlite IRA440Cl^-)	0.5 g/mL	48%	11%	13%	11%
4.14	Quaternary ammonium and sulfonic acid (Resintech MDB-10)	0.4 g/mL	44%	5.2%	5.1%	4.7%

High agitation speed improved resin-electrolyte contact enhancing metal recoveries for resins with densities lower than the electrolyte. Adsorption of metals in resins with

densities higher than electrolyte was independent to agitation speed. Resins containing a combination of phosphonic and sulfonic acid groups also obtained satisfactory separations of Fe^{3+} (i.e., 92%) but also yielded considerable base metal co-adsorption as the resin dosage increased reaching maximums of 24% Ni^{2+}, 26% Co^{2+}, and 34% Cu^{2+}. Following, resins containing carboxylic acid and quaternary ammonium groups obtaining 88% and 48% Fe^{3+} adsorptions. However, resin containing carboxylic acid obtained negligible co-adsorption of base metals while quaternary ammonium groups obtained close to 10% (see Table 4.3). Lastly, MBR containing a combination of quaternary ammonium and sulfonic groups also showed satisfactory Fe^{3+} adsorption and its behaviour resembled that of quaternary ammonium groups in polymetallic systems regardless of the mixed bed characteristics.

Table 4.5: Average metal adsorption per gram of dry resin

	Functional group	Average mgFe/g $_{resin}$	Average mgNi/g $_{resin}$	Average mgCo/g $_{resin}$	Average mgCu/g $_{resin}$
4.1	Sulfonic acid	<1	97	2.0	3.2
4.2	Carboxylic acid	6.1	7.0	<1	<1
4.3	Aminophosphonic acid	9.6	36	1.2	12
4.4	Phosphoric acid	8.0	6.6	<1	<1
4.5	Phosphinic	7.4	8.9	<1	<1
4.6	Phosphonic & Sulfonic	8.9	33	<1	2.5
4.7	Iminodiacetic acid	5.1	48	<1	16
4.8	Amidoxime	1.4	42	<1	<1
4.9	N-methylglucamine	5.0	27	<1	4.5
4.10	Bis-pycolilamine	<1	31	<1	17
4.11	Thiourea and isothiouronium	<1	38	<1	19
4.12	Thiol	<1	30	<1	18
4.13	Quaternary ammonium	4.9	25	<1	1.1
4.14	Quaternary ammonium and sulfonic	2.5	20	<1	<1

Resins with amidoxime groups showed an inconsistent behaviour, favouring Cu^{2+} a low resin dosage and Fe^{3+} as the resin dosages increased. However, resin dosages of 0.5 g/mL obtained satisfactory separations with Fe^{3+} adsorptions close to 70% while maintaining base metal co-adsorption between 15% and 20% (see Table 4.3).

Further analysis of the parameters affecting the Cu:Fe preference is required to confirm resins potential for selective Fe^{3+} removals. Lastly, resins with bis-picolylamine groups showed a forthright Cu^{2+} preference and like in bimetallic system, allowed higher Ni^{2+} than Fe^{3+} adsorption.

Variations in the process conditions affected resins differently. However, Fe^{3+} and Ni^{2+} adsorption trends remained similar between bimetallic (See Section 3.4.2) and polymetallic systems excepting for lower Fe^{3+} adsorption in presence of Cu^{2+}. Table 4.6 summarizes the best condition for Fe^{3+} adsorption and selectivity in polymetallic systems. Variation of pH showed that ion exchange resins have a narrow range of selectivity for Fe^{3+}, between 1.0 and 2.2 among all resin tested. At these conditions, the co-adsorption of base metal were also among the lowest excepting in resins with iminodiacetic acid groups that showed a increased Cu^{2+} adsorption with pH. Overall, results showed a decreased trend of metal adsorption at pH lower than 1.5. Similar to bimetallic systems, the low metal adsorption by resins at low pH may be because of poor resin dissociation or complex metal formations such as $M^{x+}(OH^{-})_{x-n}$(Zhang et al., 2016)(Zhang et al., 2016). Similarly, reduction in Fe^{3+} adsorption at pH higher than 2.2 was not likely due to Fe precipitation as this was absent from experimental flasks. The narrow range for optimal Fe^{3+} loading and selectivity observed on all best performer resins highlights the need of pH corrections

during adsorption processes. The correction of pH counteracts any pH variations derived from the adsorption reactions in Equation 2.2 and 2.4.

Increases in temperature increased metal adsorption trends for most of the resins and maintained metal selectivity throughout the temperatures tested. Increases in temperature increased Fe^{3+} adsorption in resins in the order of quaternary ammonium (Figure 4.16 b2) > phosphoric acid (Figure 4.16 b4) > N-methylglucamine (Figure 4.16 a4) > iminodiacetic acid groups (Figure 4.16 a3). Resins with aminophosphonic acid (Figure 4.16 a1), combination of phosphonic and sulfonic groups (Figure 4.16 a2), carboxylic acid (Figure 4.16 b1) and amidoxime groups (Figure 4.16 b3) showed almost negligible changes in Fe^{3+} adsorption with changes in temperature. Therefore, confirms the technical viability for using ion exchange resins for high process temperatures during base metal production.

As expected Fe^{3+} adsorption increased with time. However, the extent of base metal co-adsorption decreased. Some resins showed different behaviour between bimetallic and polymetallic systems. Aminophosphonic acid groups showed a steady increase in Fe^{3+} adsorption during the first 2h in bimetallic systems. In polymetallic systems, reached stable adsorption after 30 min. For resins with a combination of phosphonic and sulfonic groups, maximum Fe^{3+} adsorption in bimetallic systems was achieved at a faster rate than polymetallic. Aside resins showing high Cu^{2+} adsorptions, the highest co-adsorption of base metals occurred under 5 min. However, as time increased the co-adsorption of base metals decreased analog to increments in Fe^{3+} adsorption. This behaviour further suggest ion displacement discussed in bimetallic systems.

Table 4.6: Most efficient conditions for selective Fe^{3+} adsorption from polymetallic systems

Functional group (ionic form)	**pH 0.7-2.3**	**Temp. 30-90°C**	**Time 5-120 min**
Aminophosphonic acid (Na^+)	0.7 - 1.2	Indep.	30
- Lewatit TP 260	93% Fe^{3+}	93% Fe^{3+}	92% Fe^{3+}
	15% Ni^{2+}	11% Ni^{2+}	15% Ni^{2+}
	12% Co^{2+}	17% Co^{2+}	24% Co^{2+}
	76% Cu^{2+}	85% Cu^{2+}	85% Cu^{2+}
Phosphonic & Sulfonic (H^+)	0.7 – 1.7	Indep.	120
- Puromet MTS9570	92% Fe^{3+}	93% Fe^{3+}	91% Fe^{3+}
	21% Ni^{2+}	7% Ni^{2+}	5% Ni^{2+}
	21% Co^{2+}	9% Co^{2+}	9% Co^{2+}
	24% Cu^{2+}	13% Cu^{2+}	15% Cu^{2+}
Iminodiacetic acid (Na^+)	1.2 - 1.7	90	120
- Puromet MTS9300	57% Fe^{3+}	64% Fe^{3+}	69% Fe^{3+}
	6% Ni^{2+}	4% Ni^{2+}	11% Ni^{2+}
	6% Co^{2+}	3% Co^{2+}	6% Co^{2+}
	75% Cu^{2+}	77% Cu^{2+}	84% Cu^{2+}
N-methylglucamine	1.7	90	120
- Purolite S108	53% Fe^{3+}	60% Fe^{3+}	82% Fe^{3+}
	1% Ni^{2+}	1% Ni^{2+}	8% Ni^{2+}
	>1% Co^{2+}	1% Co^{2+}	3% Co^{2+}
	9% Cu^{2+}	17% Cu^{2+}	30% Cu^{2+}
Carboxylic acid (H^+)	1.2 – 1.7	Indep.	120 min
- Resintech WACG-HP	78% Fe^{3+}	80% Fe^{3+}	78% Fe^{3+}
	2% Ni^{2+}	2% Ni^{2+}	1% Ni^{2+}
	2% Co^{2+}	1% Co^{2+}	<1% Co^{2+}
	3% Cu^{2+}	2% Cu^{2+}	3% Cu^{2+}
Quaternary ammonium	1.7	90	120 min
- Amberlite IRA440Cl	60% Fe^{3+}	68% Fe^{3+}	58% Fe^{3+}
	6% Ni^{2+}	9% Ni^{2+}	8% Ni^{2+}
	6% Co^{2+}	10% Co^{2+}	7% Co^{2+}
	8% Cu^{2+}	12% Cu^{2+}	9% Cu^{2+}
Amidoxime	1.7	Indep.	60 min
- Puromet MTS9100	29% Fe^{3+}	24% Fe^{3+}	45% Fe^{3+}
	6% Ni^{2+}	5% Ni^{2+}	13% Ni^{2+}
	6% Co^{2+}	8% Co^{2+}	13% Co^{2+}
	15% Cu^{2+}	17% Cu^{2+}	25% Cu^{2+}
Phosphoric acid	1.2 – 1.7	90	20
(D2EHPA)	92% Fe^{3+}	92% Fe^{3+}	91% Fe^{3+}
- Lewatit VP OC 1026	16% Ni^{2+}	16% Ni^{2+}	1% Ni^{2+}
	14% Co^{2+}	14% Co^{2+}	1% Co^{2+}
	15% Cu^{2+}	15% Cu^{2+}	1% Cu^{2+}

4.6 Conclusion

Ion exchange resins successfully separated Fe^{3+} from an electrolyte containing 70X excess of Ni^{2+}, close to 25X of Cu^{2+}, and equal Co^{2+} concentrations. Among the 15 functional groups analyzed, resins containing phosphoric groups and phosphinic groups achieved the best Fe^{3+} selectivity obtaining Fe^{3+} adsorption of 92% and 84% with base metal co-adsorption under 2%. Following, resins with a combination of phosphonic and sulfonic groups obtained Fe^{3+} adsorption of 92% with base metal co-adsorption around 24-34%. Resin with carboxylic acid and quaternary ammonium groups obtained selective Fe^{3+} adsorption at 88% and 48% with negligible base metal co-adsorption for carboxylic acid groups and around 10% in quaternary ammonium groups. Lastly, resins containing a combination of quaternary ammonium and sulfonic groups followed the behaviour of their SAR groups obtaining metal adsorption resembling resins with exclusively quaternary ammonium groups.

The presence of Cu^{2+} in the system altered the Fe^{3+} selectivity in resins containing aminophosphonic acid and methylglucamine groups as showed in bimetallic systems. Although both groups reached Fe^{3+} adsorption above 90% also yielded considerable base metal co-adsorption. Resins with aminophosphonic acid reached base metal co-adsorption of 91% Cu^{2+}, 23% Ni^{2+}, and 33% Co^{2+} while resins with methylglucamine reached 75% Cu^{2+}, 15% Ni^{2+}, and 16% Co^{2+} at the highest resin dosage. It is unclear metal ion preference for resins with amidoxime groups as it show different preference at different resin dosage. However, the Fe^{3+} preference obtained at the highest resin dosage suggest some potential for selective removal. The potential for using resins with aminophosphonic,

methylglucamine, and amidoxime for selective Fe^{3+} separations may increase in favourable elution processes. Likewise, resins with iminodiacetic acid groups become a potential alternative with selective elution given the Cu^{2+} preference observed. However, further experimentation for efficient elution processes is still required.

Similar to bimetallic systems, polymetallic systems show metal concentration and solution pH as dominant solution factors affecting the adsorption trends in the best performer resins tested. Adsorption of Fe^{3+} decreased significantly as solution pH approached 2.3. However, adsorption of Fe^{3+} was also affected as pH decreased under 1.0. In opposition, base metal co-adsorption increased with pH. Solution pH ranging between 1.0 and 2.2 showed the best Fe^{3+} selectivity. This range was ideal among all best performer resin tested. At these conditions, Fe^{3+} adsorption was the highest while the co-adsorptions of base metals were among the lowest.

Variations in temperature had little effect on the metal adsorption trends showing little to none increments in Fe^{3+} and base metal adsorptions on all best performers. However, temperatures under 50°C should be preferred to satisfy temperature specifications according to manufacturers to extend operational life of resins. As expected, adsorption time also helped to increase adsorption of Fe^{3+} while decreasing the extent of metal co-adsorption in polymetallic systems. Further kinetic studies are included in Chapter 5.

Successful separation of Fe^{3+} from base metal electrolytes at concentration commonly found after PL in hydrometallurgy plants confirm the potential of ion exchange to substitute current iron precipitation processes. However, further experimentations

among the best performers is essential to conclude potential of high purity iron sub-production. Likewise, further economic studies are required to determine the cost benefit of the technology.

Chapter 5 Semi-continuous process and elution exploration

This chapter includes information based on the unpublished manuscripts:

1. R.A. Silva, Y. Zhang, K. Hawboldt, & L.A. James. (Pending submission). Selective Fe(III) loading from base metals using non-traditional ion exchange resins at low pH and high sulfate concentration conditions. having the following roles:

Rene A. Silva designed experimental conditions, conducted adsorption experiments, and wrote the manuscript. Dr. Yahui Zhang supervised the design of the experiment, reviewed and edited the final version of the manuscript. Dr. Kelly Hawboldt and Dr. Lesley James reviewed and edited the final version of the manuscript.

2. R.A. Silva, Y. Zhang, K. Hawboldt, & L.A. James. (Pending submission). Use of resins with a combination of phosphonic and sulfonic acid for Fe^{3+} adsorption at low pH and high base metal concentration conditions

Rene A. Silva designed experimental conditions, conducted adsorption experiments, and wrote the manuscript. Dr. Yahui Zhang supervised the design of the experiment, reviewed and edited the final version of the manuscript. Dr. Kelly Hawboldt and Dr. Lesley James reviewed and edited the final version of the manuscript.

5.1 Abstract

Use of ion exchange resins for metal separation at industrial scale requires a continuous process to be technically and economically viable. Continuous process deal with a decreasing concentration of the target metal in solution and co-adsorption of undesired metals which impact the selectivity of the process. In this chapter, a semi-continuous process with consecutive adsorption steps was used to further study the Fe^{3+} adsorption behaviour along with co-adsorption of Ni^{2+} in the best performer resins identified in previous chapters. The tested resins included a combination of phosphonic and sulfonic groups; aminophosphonic acid; carboxylic acid; iminodiacetic; phosphoric acid; quaternary ammonium; and N-methylglucamine. A series of experiments were also performed on adsorbed resins to identify the best conditions for selective elution. A selective elution process has two different stages, i.e., primary and secondary elution. Primary elution included the study of selective Ni^{2+} elution using H_2SO_4 and HCl as eluents and analyzing the best concentration and volume. The resin with the most selective Ni^{2+} elution characteristics underwent a series of studies to determine most efficient conditions for secondary elution. The study of secondary elution used high concentration of H_2SO_4 and HCl and different concentration of complexing agents as eluents. The complexing agents were oxalic acid, citric acid, and Ethylenediaminetetraacetic acid (EDTA). The best elution time and temperature for primary and secondary elution were identified.

Results showed that resins with a combination of phosphonic and sulfonic groups obtained the best adsorption properties among the resins tested and the most selective stripping of Ni^{2+} during primary elution. At low eluent volumes (equivalent 2 bed volumes)

and low concentration (0.5% v/v) of H_2SO_4 or HCl the extent of Ni^{2+} stripped reached close to 80% while less than 8% of Fe^{3+}. Oxalic acid (10% w/w) and EDTA (5% w/w) stripped Fe^{3+} during secondary elution. However, the instability of Fe-EDTA complex formation at our experimental conditions resulted in precipitation. Further studies with oxalic acid suggested that selective recovery of Ni^{2+} during primary elution and Fe^{3+} in secondary elution were time and temperature dependent. Room temperatures and periods of 30 min favoured selectivity of Ni^{2+} stripping in primary elution. Meanwhile, high temperatures and periods between 60 and 120 min favoured Fe^{3+} stripping in secondary elution. The use of these conditions for elution processes in with quaternary ammonium, phosphoric acid, and aminophosphonic acid groups was unsuccessful. Further studies employing different eluent may improve selectivity for elution in such resins.

5.2 Introduction

Ion exchange processes occur in either batch or continuous processes. Continuous process employ fixed bed column reactors at industrial scale, pilot plants, and research laboratories (Wachinski, 2016). Once the column is saturated, it undergoes a desorption/elution stage. To operate continuously, column reactors are operated in parallel to allow for adsorption/desorption (See Figure 5.1). Alternatively, some process use resins in stirred tank reactors which are operated semi-continuously allowing ample reaction time (Zagorodni, 2006). The resin-solution separation process is more complex than in column reactors. Not withstanding the disadvantages, these type of reactors have found applications in mining industry. Known as Resins-in-Pulp (RIP) process, the use of resins

is an alternative for the widely employed activated carbon separation used in gold beneficiation, copper purification, and the zinc industry (Kotze et al., 2005). Figure 5.2 includes an example of copper purification in RIP process.

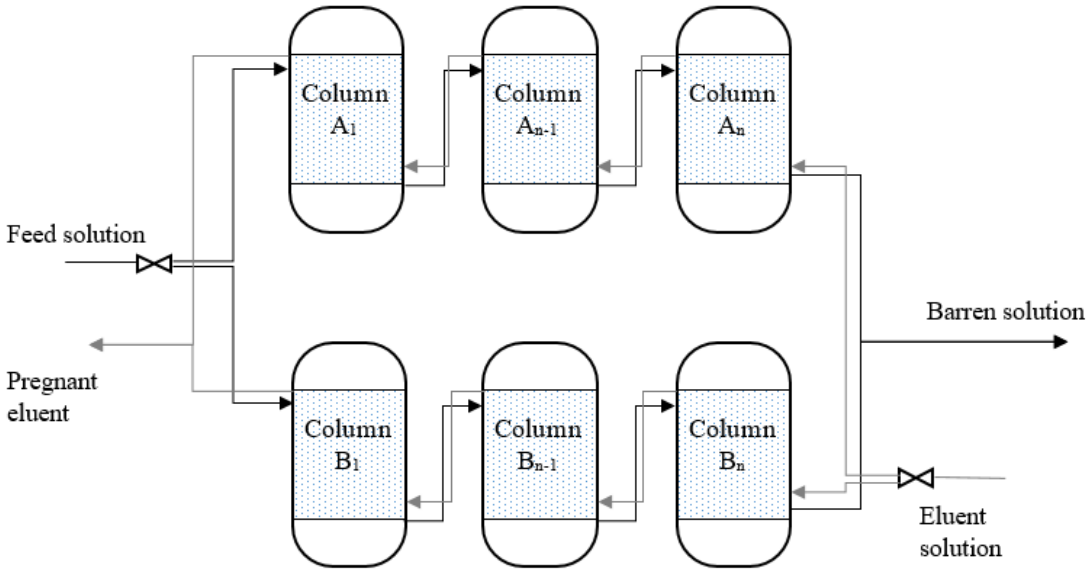

Figure 5.1: A series of column reactors in parallel to satisfy adsorption/desorption continuity

One of the main advantages of RIP systems is the option for pH correction during adsorption. In Chapter 2, Equation 2.2 and 2.4 outline the variation in pH during ion exchange adsorption. Correction of pH is virtually impossible in column reactors. Correction of pH is important as some resins require specific pH conditions and metal solubility/complex formation is strongly pH dependant. Correction of pH mid process enhances the metal adsorption capabilities and selectivity of resins in RIP. An example is

the enhancement of Fe^{3+} adsorption after pH correction in batch process when compared with column reactors using carboxylic acid resins (Riveros, 2004).

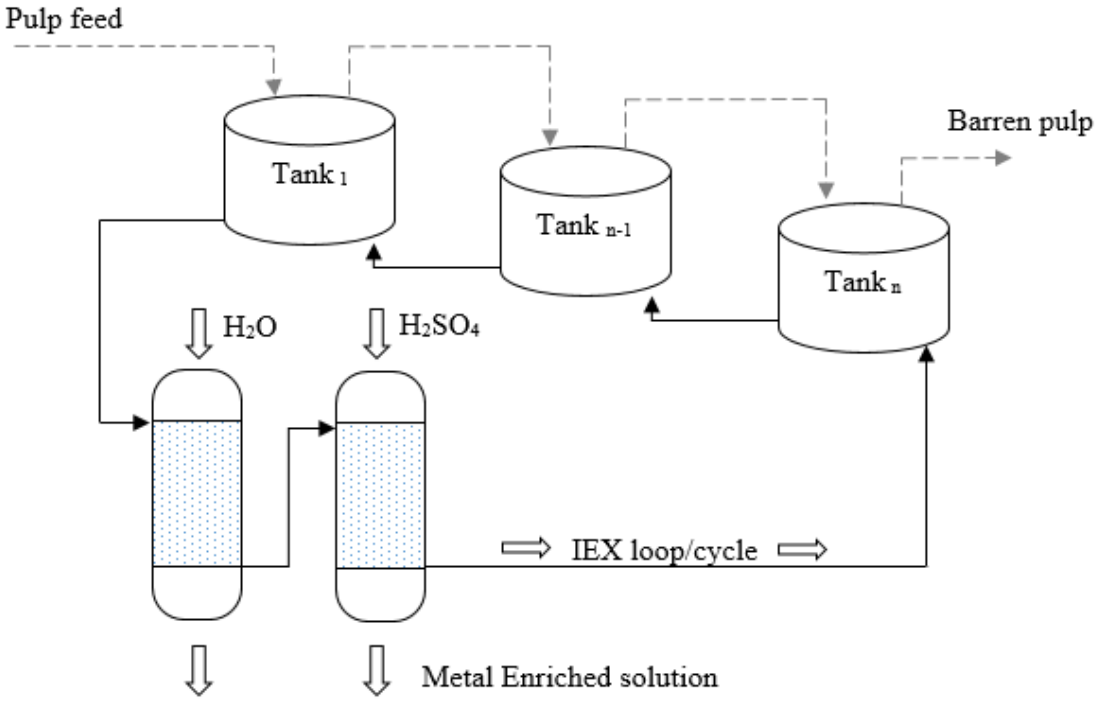

Figure 5.2: Resin in Pulp (RIP) diagram for metal beneficiation (Laxness advertisement material)

Metal co-adsorption is unwanted and it is controlled to an extent by limiting reaction time. Section 3.4.2.4 and Section 4.4.2.2 show that co-adsorption increases with time, as the concentration of the target metal depletes from electrolyte solution (See section 3.4.2.1). The co-adsorbed metals usually have different bonding strength with the resin compared to the target metal. The lower the selectivity of a particular metal on a resin, the lower the bonding strength (see Section 4.4.1.7). Low volumes of mildly acidic eluents can break any weak bonding between co-adsorbed metals and resin. The use of low acid

concentration to elute selectively co-adsorbed metals is the primary elution process. The eluate of primary elution often has a rich concentration of the metal with the weaker bonding strength. For example, Figure 5.3 outlining the removal and purification of Fe^{3+} from a Cu^{2+} electrolyte solution, the eluate of primary elution will be rich in Cu^{2+}. The eluate from primary elution is sent back to the leaching solution for further Fe^{3+} recovery. Once the resin is free of co-adsorbed metals, it undergoes a secondary elution to recover the target metals from the resin. Eluents for secondary elution have more acidic characteristics than the primary elution and in some cases include complexing agents to enhance metal elution. The eluate of the secondary elution has a high purity of the target metal ready for further processing. Once resin is free from the adsorbed metals is ready for a regeneration process to start a new adsorption/elution cycle.

Elution process is the reverse of adsorption. However, the variables affecting elution performance are far more complex than that of adsorption. Unlike the limited options of functional groups in resins, there is a wider range of complexing agents that can impact efficiencies in elution. The type, amount, and concentration of eluent, along with contact time and temperature are some of the variables affecting recoveries and selectivity (Zagorodni, 2006). In some cases, metal elution from resin requires the use of catalytic materials for improved elution and the use of complexing agents to strip metals from resins (Lv et al., 2019; Zhang et al., 2016). Auxiliary redox reactions are also used in the removal of metals. For example, the patented method for Fe^{3+} elution from resins containing a combination of phosphonic and sulfonic resin using the cuprous sulfate pathway (McKevitt and Dreisinger, 2009).

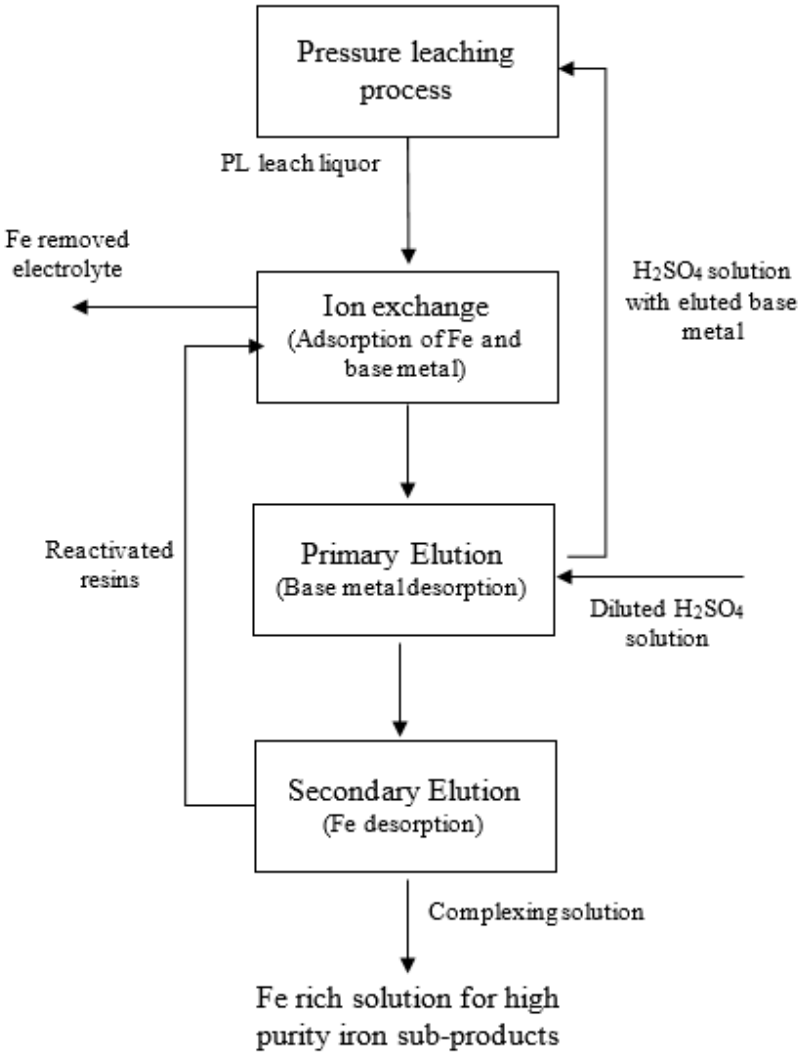

Figure 5.3: Separation of iron from base metals leach solution in a closed circuit process, adapted from Zhang et al., (2016)

This chapter analyzes the adsorption potential of the best performing resins in a semi-continuous process. Chapters 2–4 identified resins with a combination of phosphonic and phosphoric, aminophosphonic acid, carboxylic acid, iminodiacetic acid, phosphoric, quaternary ammonium, and N-methylglucamine as best performers for Fe^{3+} adsorption.

The different options for primary and secondary elution for the selective removal of Ni^{2+} and Fe^{3+} from the adsorbed resins are also analyzed in this chapter. The eluents used for Ni^{2+} and Fe^{3+} stripping are among the most common eluents in hydrometallurgy. Analysis of primary elution included the extent of metal eluted using H_2SO_4 and HCl as eluents, varying volume of solution, and acid concentration. The resin with the best performing primary elution characteristics underwent a secondary elution study using high concentrations of H_2SO_4 and HCl and varying concentrations of oxalic acid, citric acid, and Ethylenediaminetetraacetic acid (EDTA) as complexing agents. The study included determination of optimum elution time and temperature for primary and secondary elution. Several experimental runs were conducted to assess repeatability of experimental procedures.

5.3 Materials and methods

5.3.1 Metal adsorption in Consecutive Process Steps

A series of consecutive adsorption tests (multiple steps) were conducted on the best performer resins after single factor optimization (Chapter 3 and 4). Tests, lasting 60 min per step were conducted at resin amounts of 0.5 g/mL in synthetic leach solutions of 25 g/L of Fe^{3+} and 25 g/L of Ni^{2+} at pH of 1.5 and room temperature following bimetallic systems of Chapter 3. Table 5.1 includes a list of resins analyzed in consecutive adsorption experiments. After each step, resin was separated from synthetic leach solution using a borosilicate Buchner funnel with fritted disc. After separation, 4 mL of solution were used for metal analyses and fresh resin was added to remaining leach sample to satisfy

requirements of resin amount tested. Metal analyses were determined using wavelength dispersive X-ray fluorescence spectroscopy (XRF Supermini200, Rigaku Co.) and the difference in concentration before and after adsorption used for the metal adsorption calculation following Equation 3.1.

Table 5.1: Commercial resins used in Fe^{3+} separations at consecutive adsorption test

Functional group (ionic form)	**Resin brand**		**Producer**
Phosphonic & Sulfonic (H^+)	1	MTS9570 (S957)	Purolite®
N-methylglucamine	2	S108	Purolite®
Carboxylic acid (H^+)	3	WACG-HP	Resintech
Quaternary ammonium	4	IRA440Cl^-	Amberlite
Phosphoric acid (D2EHPA /di-2-ethylhexyl-phosphoric acid)	5	VP OC 1026	Lewatit®

5.3.2 Metal Elution in Consecutive Process Steps

A series of consecutive elution tests (multiple steps) were conducted during 60 min per step in eluents of different acid concentrations. Initially, best performer resins were tested for elution with H_2SO_4 at concentrations of 1.0, 5.0, and 10% v/v. If elution with H_2SO_4 was determined satisfactory, further evaluation was conducted at concentrations of 0.2 and 0.5% along with additional analysis with HCl at 0.2, 0.5, and 1.0% v/v, respectively. Before elution, a preliminary adsorption experiment was conducted at conditions to maximize metal adsorption with enough resin sample to satisfy homogeneity in elution tests. Preliminary adsorption experiment was conducted in solution containing 25 g/L of Fe^{3+} and 25 g/L of Ni^{2+} in sulfate media at resin dosages of 0.2 g/mL. After adsorption, resin was placed in eluent solution and agitated during one hour per step. After

each step, resin was separated from eluent using a borosilicate Buchner funnel with fritted disc and new acid solution placed for subsequent step. Pregnant solution of each step was diluted as required for Inductively Couple Plasma Optical Emission Spectroscopy (ICP-OES; Perkin-Elmer 5300 DV) analysis.

Each elution step of 20 mL had eluent volume equivalent to two bed volumes calculated by swollen bulk density of resin. Table 5.2 includes information pertinent to the bulk density of dry and swollen resins. Bulk density of resins was calculated by measuring the occupied volume of approximately 1 g of dry resin on a 10 mL graduated cylinder. Subsequently, 5 mL of 1.5DI were added to the graduated cylinder and the resin's volume after 2 h recorded for swollen resin' bulk density calculations.

Table 5.2: Resin employed for first stage elution with respective bulk densities

Functional group (ionic form)	**Resin brand**		**Producer**	**Volume of 1 g resin**	
				Dry [mL]	**Swollen [mL]**
Phosphonic & Sulfonic (H^+)	1	MTS9570 (S957)	Puromet®	1.392	2.883
Aminophosphonic acid	2	SIR-500	Resintech	1.727	2.687
Carboxylic acid(H^+)	3	WACG-HP	Resintech	1.002	1.821
Iminodiacetic acid	4	MTS9300 (S930)	Puromet®	1.786	3.175
D2EHPA	5	VP OC 1026	Lewatit®	0.919	0.995
Quaternary ammonium	6	IRA440Cl^-	Amberlite®	1.414	2.168
N-methylglucamine	7	S108	Purolite®	2.393	3.490

The extent of metal eluted was calculated using Equation 5.1:

$$E(\%) = \left| \frac{\left({}^{X_l}/_{w_E} \right)}{x_R} \right| \times 100 \qquad \text{Eq. (5.1)}$$

Where X_l is the total amount of metal eluted in elution experiment (i.e., final concentration times sample volume), w_E the amount of resin employed in elution experiments, and x_R the average metal adsorption per gram of resin obtained by Equation 5.2:

$$x_R = \frac{(C_o - C_E)}{w_R} * v_L \qquad \text{Eq. (5.2)}$$

Where v_L corresponds to the volume of sample in adsorption experiments and w_R the amount of resin used in adsorption experiments.

5.3.3 Secondary Elution with Complexing Agents

A secondary elution stage was conducted using oxalic acid, citric acid, and EDTA as complexing agents at concentrations of 1.0, 2.5, 5.0, and 10% w/v. All complexing agents were forms of carboxylic acids having two, three, and four carboxyl groups, respectively (See Figure 5.4). For comparison, a secondary elution was conducted in H_2SO_4 and HCl solutions with concentrations of 30 and 50% v/v. Secondary elution was conducted in one-step lasting 4 h with eluent volume equivalent to eight bed volumes calculated by swollen bulk density of resin presented in Table 5.2. At the end of experiment, resin was separated from eluent using a borosilicate Buchner funnel with fritted disc. Pregnant solution was diluted as required for Inductively Couple Plasma Optical Emission Spectroscopy (ICP-OES; Perkin-Elmer 5300 DV) analysis. The secondary elution was conducted with Puromet MTS9570 (S957), which presented the most efficient adsorption and elution on primary stage.

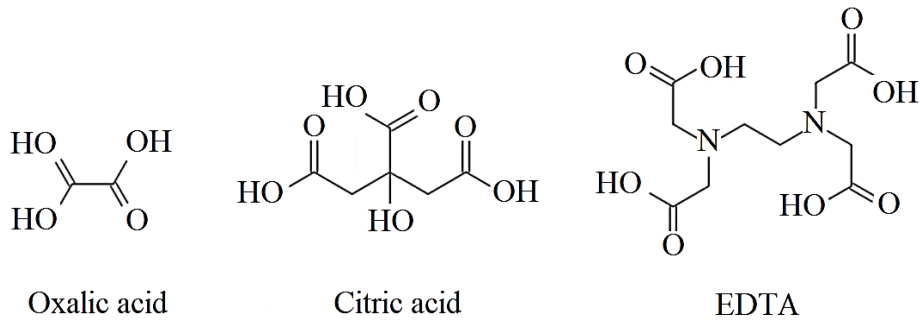

Figure 5.4: General diagrams of complexing agents employed in secondary elution

A preliminary adsorption experiment was conducted at conditions to maximize metal adsorption with enough resin sample to satisfy homogeneity in elution tests. Preliminary adsorption experiment was conducted in solution containing 25 g/L of Fe^{3+} and 25 g/L of Ni^{2+} in sulfate media at resin dosages of 0.4 g/L. Afterwards, a primary elution was conducted using a H_2SO_4 at 0.5% v/v as eluent on single step for all resin sample to maintain homogeneity on secondary elution. First stage elution lasted 4h with solution equivalent to eight bed volumes.

The extent of metal eluted in secondary stage elution was calculated by modifying Equation 5.1 to include specifications of secondary elution stage as follows:

$$E_2(\%) = \left| \frac{\left({}^{X_{l2}}/_{w_{E2}} \right)}{x_R} \right| \times 100 \qquad \text{Eq. (5.3)}$$

where X_{l2} is the amount of metal eluted in second stage, w_{E2} the amount of resin employed in secondary elution experiments, and x_R the average metal adsorption per gram of resin

obtained by Equation 5.2. The addition of Equation 5.1 and 5.3 obtains the overall metal elution resulting in Equation 6.4:

$$E_O(\%) = \left| \frac{\left({}^{X_l}/_{w_E}\right) + \left({}^{X_{l2}}/_{w_{E2}}\right)}{x_R} \right| \times 100 \qquad \text{Eq. (5.4)}$$

5.3.4 Time and Temperature Dependency

The effect of time (5-1440 min) and temperature (20, 30, 40, 60, 80 °C) on primary and secondary elution was studied to determine the most efficient conditions. Concentrations of 0.5% H_2SO_4 and 10% oxalic acid were used as primary and secondary eluents, respectively. Elution experiments followed experimental procedures of Section 5.3.3 using the equivalent volume of 8 BV by swollen bulk density.

5.3.5 Elution Repeatability

After the determination of the best conditions for primary and secondary elution, a set of triplicated experiments were conducted to confirm repeatability of the adsorption and elution at most efficient experimental conditions. Results were compared with data obtained in other chapters. Adsorption experiments were conducted on synthetic leach of 25 g/L Fe^{3+} and 25 g/L Ni^{2+} during 2 h at resin concentration of 0.2 g/mL. Primary and secondary elution in 1-step processes had the equivalent of 8 B.V. lasting 4 h. To compare the extent of elution obtained with resins containing a mixture of sulfonic and phosphonic resins, a primary and secondary elution was analyzed with other resins following experimental procedures detailed in Section 5.3.3.

5.4 Results

5.4.1 Metal Adsorption in Consecutive Process steps

Consecutive process steps increased the Fe^{3+} adsorption (See Figure 5.5). Resins containing N-methylglucamine and a combination of sulfonic and phosphonic groups achieved Fe^{3+} adsorption of 99% as early as the first step. However, as the number of step increased, so did the percentage of Ni^{2+} co-adsorption. By the third step, both resins had Ni^{2+} co-adsorption above 97%, and reached a maximum of 99% at the fourth and last stage. The other resins analysed showed preference for Fe^{3+} adsorption and maintained an adsorption increase with the increase in process steps. The Ni^{2+} co-adsorption increased with the number of steps but remained lower than that of Fe^{3+}. Resins with phosphoric groups, D2EHPA, reached a maximum Fe^{3+} adsorption of 96% by the fifth adsorption step with 59% of Ni^{2+} co-adsorption. Resins with carboxylic acid and quaternary ammonium groups outperformed phosphoric groups at the first adsorption step. However, by the fifth step both showed lower Fe^{3+} adsorption than phosphoric groups at 85% and 82%, respectively. Resins with phosphoric groups maintained lower Ni^{2+} co-adsorption throughout the experiment. Both, carboxylic acid and quaternary ammonium groups reached maximum Ni^{2+} co-adsorption of 68% and 67% respectively.

All resins selected had satisfactory Fe^{3+} adsorption reaching values above 80% by the last step. However, Ni^{2+}co-adsorption also increased significantly with the number of process steps. These tendencies followed the trends from Section 3.4.1 and 4.4.1 showing increments in metal co-adsorption as resin dosages increases. This is counterproductive for efficient Fe^{3+}/Ni^{2+} separations and requires highly efficient and selective elution process to

maintain process viability. High efficient elution process have high separation selectivity requiring only low eluent volumes of mild acidic characteristics. Confirmation of the viability of efficient Fe^{3+}/Ni^{2+} separations using ion exchange resins was studied in the subsequent sections related to the study of elution properties for the best performer resins

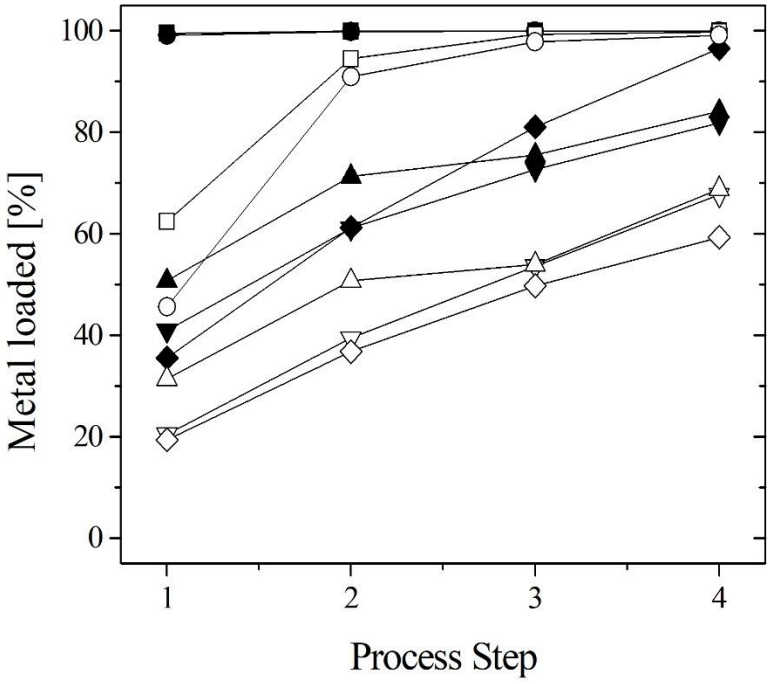

Figure 5.5: Percentage of metal adsorption at consecutive process steps with 0.5 g/mL. (■) Fe and (□) Ni adsorbed on Puroment MTS9570, (●) Fe and (○) Ni adsorbed on Purolite S108, (▲) Fe and (△) Ni adsorbed on Resintech WACG, (▼) Fe and (▽) Ni adsorbed on Amberlite IRA440 Cl, and (◆) Fe and (◇) Ni adsorbed on Lewatit VPOC 1026

5.4.2 Metal Eluted in Consecutive Process Steps

A series of elution experiments using H_2SO_4 and HCl at different concentrations were used to identify the resins presenting the most efficient elution. An efficient eluent solution requires the stripping of Ni^{2+} while conserving Fe^{3+} on resin. At the acid

concentrations tested, resins with a combination of phosphonic and sulfonic groups, aminophosphonic, and phosphoric acid, showed higher percentages of Ni^{2+} elution than Fe^{3+}. Resin with carboxylic acid and iminodiacetic acid groups showed preferential elution of Ni^{2+} or Fe^{3+} depending on the acid concentration. Resins with quaternary ammonium groups showed higher Fe^{3+} elution than Ni^{2+} and resins with N-methylglucamine did not confirmed any selectivity.

5.4.2.1 Primary elution of resin containing phosphonic and sulfonic groups

Resins containing phosphonic and sulfonic groups, favoured Ni^{2+} elution over Fe^{3+} in H_2SO_4 and HCl. The extent of metal eluted was dependent on the concentration of H_2SO_4 but did not vary with the concentration of HCl (see Figure 5.6). Concentration of 0.5% v/v H_2SO_4 reached maximum Ni^{2+} elution of approximately 74%. High H_2SO_4 concentration enhanced Fe^{3+} elution up to a maximum of 28% at 10% v/v H_2SO_4. Fe^{3+} elution by HCl was independent of the concentration achieving an average of 4% after the fourth elution step.

Both acid showed good results for selective metal elution. Figure 5.6 shows that most of the Ni^{2+} eluted occurred at early stages of the elution process inferring the low volume requirements of eluent. Given that resins with a combination of phosphonic and sulfonic groups adsorbed low quantities of Ni^{2+}, the Ni^{2+} not eluted from the resin is considered low compared to that of Fe^{3+}. Unlike other phosphorous containing resins, Fe^{3+} elutes relatively simple from resin containing a combination of phosphonic and sulfonic

groups (Lv et al., 2019). This allow possibilities of high Fe^{3+} stripping for high purity iron beneficiation.

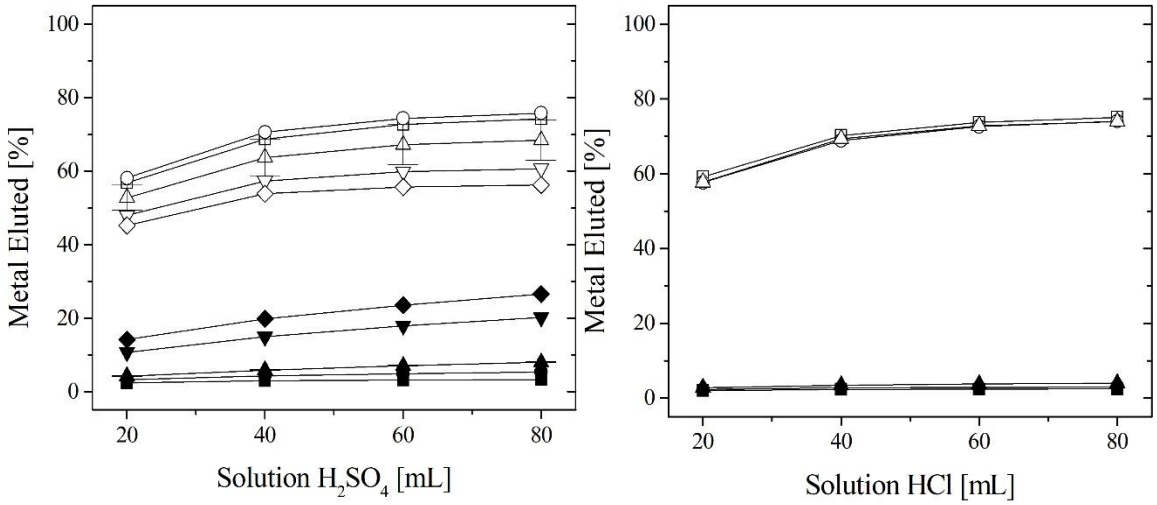

Figure 5.6: Elution of Resin S957 with combination of phosphonic and sulfonic groups at different acid concentration. (■) Fe and (□) Ni eluted in 0.2% acid, (●) Fe and (○) Ni eluted in 0.5% acid, (▲) Fe and (△) Ni eluted in 1.0% acid, (▼) Fe and (▽) Ni eluted in 5.0% acid, and (◆) Fe and (◇) Ni eluted in 10% acid. Acid concentration in v/v%

5.4.2.2 Primary elution of resin containing aminophosphonic acid groups

Resins with aminophosphonic acid groups favoured Ni^{2+} elution over Fe^{3+}. However, significant amounts of Fe^{3+} eluted along with Ni^{2+} (see Figure 5.7). Both acids showed increased metal elution as acid concentration increased. H_2SO_4 achieved the highest Ni^{2+} elution of 86% at acid concentration of 10% v/v. At the lowest acid concentration of 0.2% v/v, reached 63% Ni^{2+}. At the highest and lowest acid concentration, H_2SO_4 eluted 51 and 34% of Fe^{3+}, respectively. Metal elution with HCl was less dependant on acid concentration. Elution of Fe^{3+} averaged 36% with a deviation of less than 4% for

all HCl concentration. The maximum Ni^{2+} elution reached 69% with deviation of +6% from the average elution.

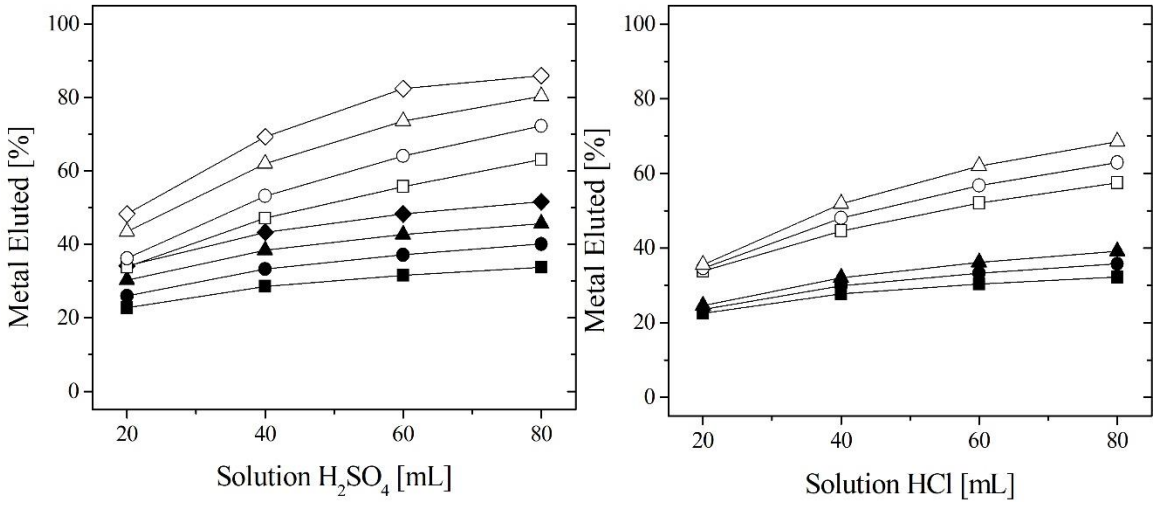

Figure 5.7: Elution of Resin SIR-500 with aminophosphonic acid groups at different acid concentration. (■) Fe and (□) Ni eluted in 0.2% acid, (●) Fe and (○) Ni eluted in 0.5% acid, (▲) Fe and (△) Ni eluted in 1.0% acid, and (◆) Fe and (◇) Ni eluted in 10% acid. Acid concentration in v/v%

Sulfuric acid solutions eluted higher amounts of metal than HCl. However, in general resins with aminophosphonic acid groups showed a lower elution selectivity at the acid concentrations tested. The elution trends obtained suggested that increases in acid concentration might increase Ni^{2+} elution. However, further elution of Fe^{3+} is less likely. Scholars have identified the difficulties in eluting Fe^{3+} and regeneration of aminophosphonic acid resins (Arroyo-Torralvo et al., 2017; Lv et al., 2019). Concentrations of H_2SO_4 higher than 10% damaged the physical integrity of the resin (see Section 5.4.3). Likewise, concentrations up to 6 M HCl (50% v/v) with the addition of

complexing agents like 0.2 M of Na_2SO_3 or 3M H_3PO_4 were not enough to significantly remove Fe^{3+} from aminophosphonic acid resins (Lv et al., 2019).

5.4.2.3 Primary elution of resin containing carboxylic acid groups

Elution trends from resins containing carboxylic acid groups differed depending on the type of acid employed (See Figure 5.8) and elution trends with H_2SO_4 were heavily dependent on acid concentration. As acid concentration increased, elution of Fe^{3+} increased. High acid concentrations favoured Fe^{3+} over Ni^{2+} reaching a maximum of 71% and 23%, respectively. Low H_2SO_4 concentrations (<1% v/v) favoured Ni^{2+} elution. At concentration lower than 0.5% v/v, elution of Fe^{3+} showed little improvements as the number of process step increased. Meanwhile, elution of Ni^{2+} remained stable throughout all H_2SO_4 and HCl concentrations. In H_2SO_4, Ni^{2+} elution reached a maximum of 26% while in HCl 27%. Little improvement on Ni^{2+} elution was observed as number of elution steps increased.

Resins with carboxylic acid groups show selective elution depending on acid concentration and eluent volume. However, the extent of metal eluted was lower than that obtained with other type of resins. Low acid concentration may result in selective Ni^{2+} elution. However, given the limited increase in metal eluted as process step increased, it is unlikely that results are due to acid stripping by ion exchange. Instead, are simple carried out by drag into solution. Further experiments using water to prewash carboxylic acid resins before elution could confirm this observation. Other studies reported that

concentrations of 1.5M H_2SO_4 (8% v/v) had selective elution of base metals from a carboxylic acid resin adsorbed with Fe^{3+} (Riveros, 2004).

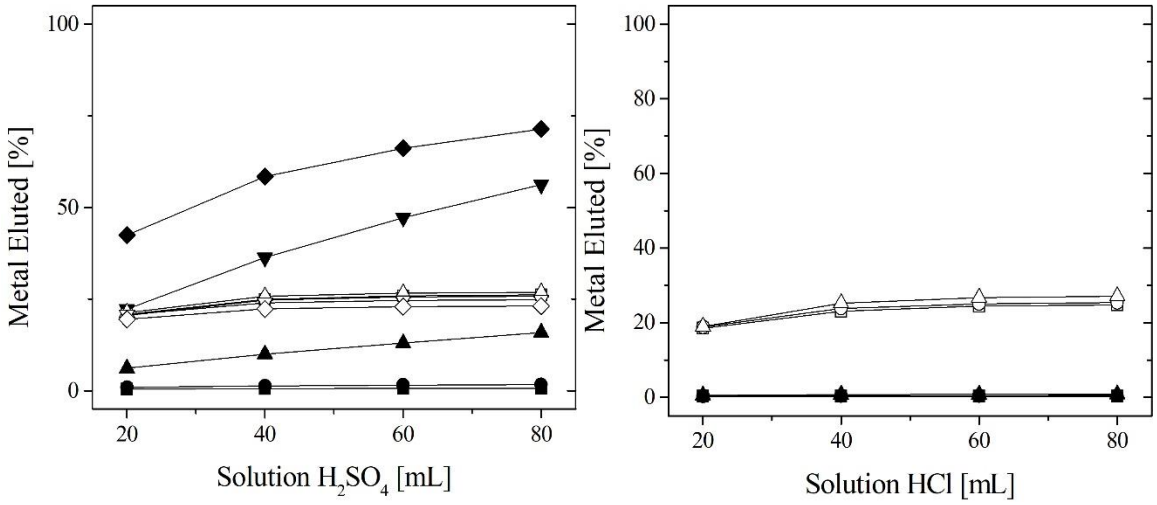

Figure 5.8: Elution of Resin WACG with carboxylic acid groups at different acid concentration. (■) Fe and (□) Ni eluted in 0.2% acid, (●) Fe and (○) Ni eluted in 0.5% acid, (▲) Fe and (△) Ni eluted in 1.0% acid, (▼) Fe and (▽) Ni eluted in 5.0% acid, and (◆) Fe and (◇) Ni eluted in 10% acid. Acid concentration in v/v%

5.4.2.4 Primary elution of resin containing iminodiacetic acid groups

Elution trends obtained with resins with iminodiacetic acid resemble those obtained with carboxylic acid groups (Section 5.4.2.3). Iminodiacetic acid share some of the functionalities with carboxylic acid groups given the double carboxylate formation (Figure 3.1). Similar to carboxylic acid, the elution of Ni^{2+} was independent of acid concentration with similar trends for both acids reaching approximately 50% by the end of the fourth elution step (See Figure 5.9). Elution of Fe^{3+} was highly dependant on H_2SO_4 concentration but less dependant on HCl. Low sulfuric acid concentration resulted in Fe^{3+} elution under that of Ni^{2+}. At concentrations of 1.0% H_2SO_4, the elution of Fe^{3+} surpassed that of Ni^{2+}

reaching a maximum of 61% against 51%, respectively. At concentration of 10% v/v Fe^{3+} elution reached 69% while 55% of Ni^{2+}.

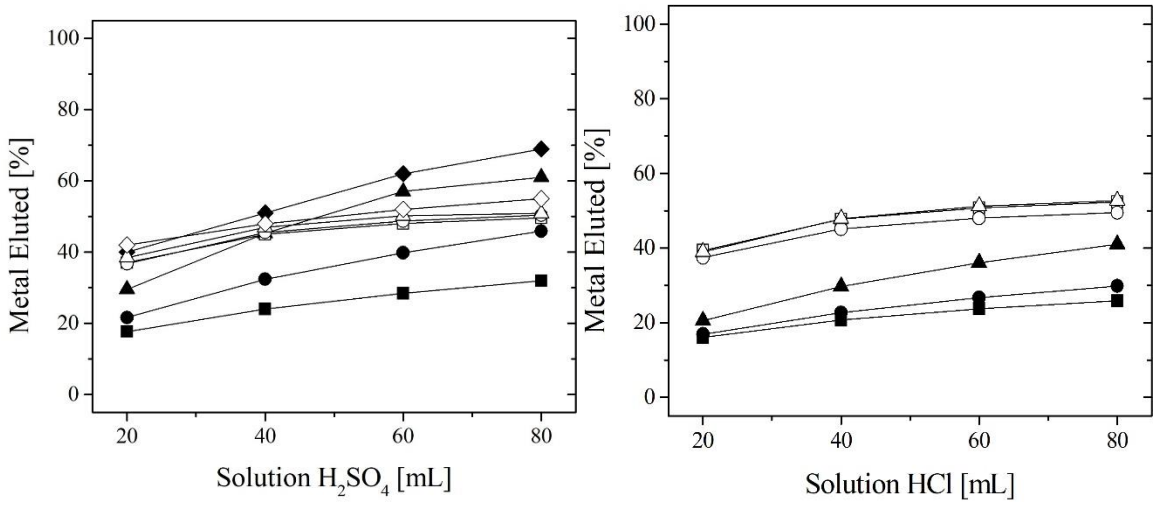

Figure 5.9: Elution of Resin S930 with iminodiacetic acid groups at different acid concentration. (■) Fe and (□) Ni eluted in 0.2% acid, (●) Fe and (○) Ni eluted in 0.5% acid, (▲) Fe and (△) Ni eluted in 1.0% acid, and (◆) Fe and (◇) Ni eluted in 10% acid. Acid concentration in v/v%

None of the concentrations of acid tested showed satisfactory results. The differences in elution were minimum at the conditions studied. Results show that the maximum difference in elution among metals occurs at low eluent volumes. Therefore, it is plausible that time might be an affecting factor to selectively elute Fe^{+3} or Ni^{2+} from resins with iminodiacetic. Given the low performance of the resin, no further studies were conducted. Although literature suggest a combination of ammonium sulfate with divalent salts (i.e., magnesium sulfate) and hydrogen peroxide as suitable eluent for base metals and multivalent elements from iminodiacetic acid resins (Littlejohn and Vaughan, 2014; YABUTANI et al., 2012).

5.4.2.5 Primary elution of resin containing D2EHPA groups

Resins containing phosphoric acid groups in the D2EHPA form favoured elution of Ni^{2+} over Fe^{3+}, and this regardless of the acid concentration (See Figure 5.10). Although, almost all metal eluted at the first elution step with little to no increases further after. The maximum Ni^{2+} eluted reached up to 48% while Fe^{3+} reached 16%. Resins with D2EHPA should undergo an initial pre-washing to confirm that the elution obtained was by reverse ion exchange and dismiss any metal released by a physical drag ("washing") into solution. As VPOC 1026 resins are SIR having weekly bonding with the organic solvent extractant, exposure with aqueous solution of mild alkaline pH or water may result in the leaching of D2EHPA. This results in the chemical degradation of the resin requiring D2EHPA reimpregnation with C272-ethanol-water mixture (Vaughan et al., 2016b).

There are little studies regarding the elution and regeneration of resins containing phosphoric groups as in Lewatit VPOC 1026. The studies found stated that elution of this resin with H_2SO_4 at concentrations of 100 g/L (≈5% v/v) accomplished total elution of Ni^{2+} and Co^{2+} in experiments lasting 48h (Vaughan et al., 2016a). Most of the studies for metal stripping of D2EPHA focus on solvent extractions obtaining results of 80% using HCl at concentration higher than 160 g/L or 10% v/v (Sahu and Das, 2000).

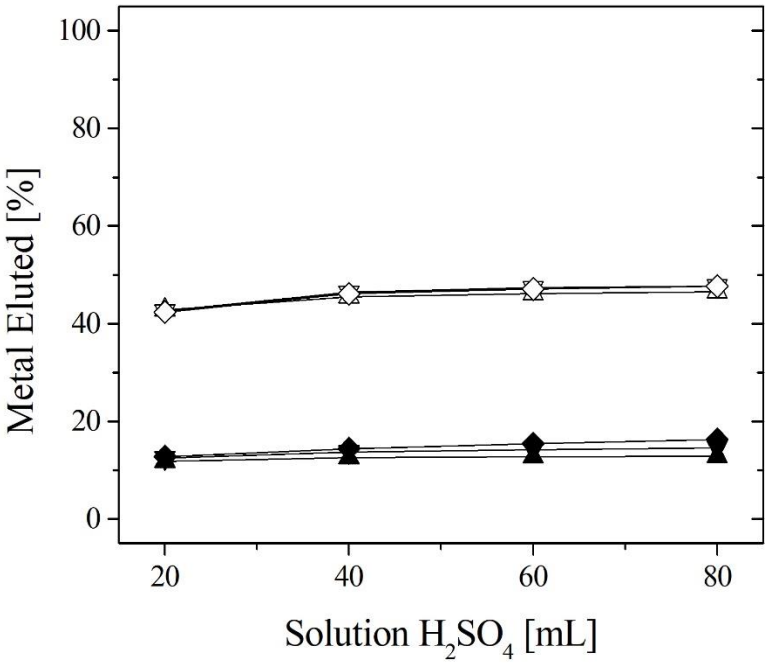

Figure 5.10: Elution of Resin VPOC 1026 with phosphoric acid groups at different acid concentration. (▲) Fe and (△) Ni eluted in 1.0% acid, (▼) Fe and (▽) Ni eluted in 5.0% acid, and (◆) Fe and (◇) Ni eluted in 10% acid. Acid concentration in v/v%

5.4.2.6 Primary elution of resin containing quaternary ammonium groups

Resin containing quaternary ammonium groups were the only group favouring Fe^{3+} elution over Ni^{2+}. Acid concentration had little effect on metal elution (See Figure 5.11). The elution of Fe^{3+} increased as bed volume increased going from 41% at the initial step to 53% at the last. The elution of Ni^{2+} remained similar through all the bed volumes reaching between 16% and 19% for the first and last step, respectively. Even with selective Fe^{3+} elution, quaternary ammonium resins had unsatisfactory performance. Therefore, not considered for further experimentation.

There is no information related to the elution potential of Fe^{3+} from quaternary ammonium resin. However, studies pertinent to solvent extraction suggest the use of

NaH_2PO_4 as complexing agent for Fe^{3+} stripping from a commercially available quaternary ammonium salt (Aliquat 336) employed in solvent extraction (Zhang et al., 2021). Other studies suggest that H_2SO_4 at concentrations of 1.0 M (5% v/v) and 2.0 M of HCl (5% v/v) stripped up to 99% of Ni^{2+} adsorbed on Aliquat 336 previously adsorbed in a Co-Ni solution (Nayl, 2010).

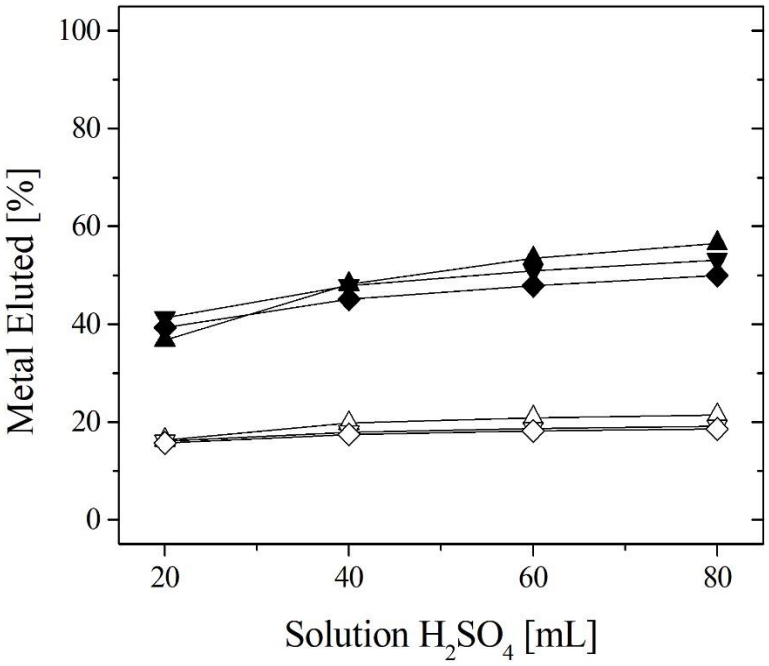

Figure 5.11: Elution of Resin IRA 440 with quaternary ammonium groups at different acid concentration. (▲) Fe and (△) Ni eluted in 1.0% acid, (▼) Fe and (▽) Ni eluted in 5.0% acid, and (◆) Fe and (◇) Ni eluted in 10% acid. Acid concentration in v/v%

5.4.2.7 Primary elution of resin containing N-methylglucamine groups

Elution of N-methylglucamine resin had similar Fe^{3+} and Ni^{2+} trends (see Figure 5.12). The extent of elution was similar regardless of H_2SO_4 concentration. Acid concentrations of 10% v/v obtained a maximum Fe^{3+} elution of 87% and 75% of Ni^{2+}. The

lowest acid concentration of 1% had elution of 79% Fe^{3+} and 69% of Ni^{2+}. Elution from N-methylglucamine resin achieved among the highest percentages of elution of all the resin tested but did not achieve selectivity. Therefore, not considered for further experimentation.

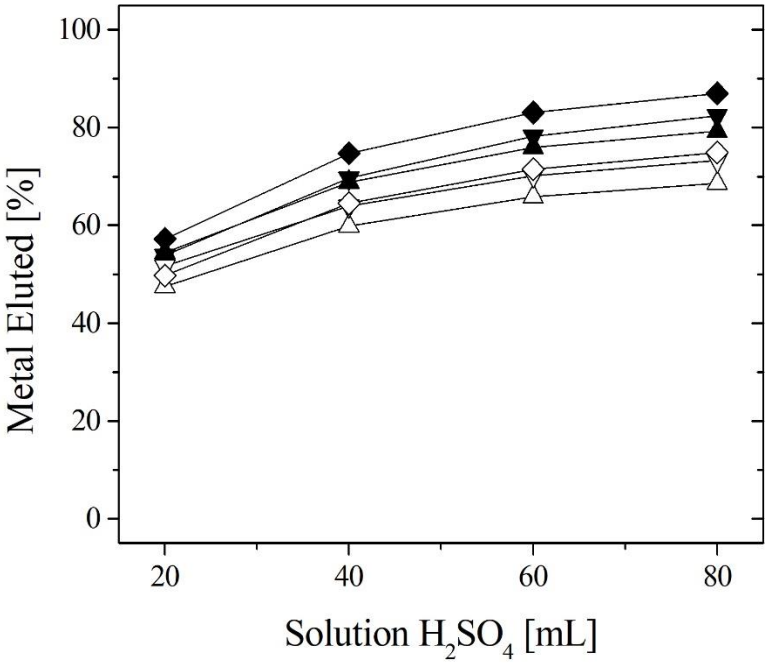

Figure 5.12: Elution of Resin S108 with N-methylglucamine groups at different acid concentration. (▲) Fe and (△) Ni eluted in 1.0% acid, (▼) Fe and (▽) Ni eluted in 5.0% acid, and (◆) Fe and (◇) Ni eluted in 10% acid. Acid concentration in v/v%

Resin with methylglucamine are anion exchangers, which ease the elution of any metal adsorbed. Manufacturer of S108 recommend the use of acidic solution to strip any adsorption but also recommend the reconversion of the resin to a free base using caustic soda solution. As stated in earlier sections, there are no studies related to Fe^{3+} removal using N-methylglucamine or its subsequent elution.

5.4.3 Secondary elution with complexing agents

Exploratory experiments on secondary elution used the resin showing the best characteristics for primary elution at the most efficient acid concentration. The resin showing the best results was Puromet MTS9570 (previously Purolite S957) at H_2SO_4 concentrations of 0.5%. Primary elution of Puromet MTS9570 resulted in high elution percentages of Ni^{2+} while maintaining significant amount Fe^{3+} adsorbed onto the resin. Secondary elution aims to strip as much of the Fe^{3+} remaining on the resin as possible. Experiments at high concentration of H_2SO_4 and HCl confirmed the need of complexing agents after a preliminary acid elution. The complexing agents employed are traditionally used for the removal of Fe^{3+} from resins given their strong complexing potential with Fe^{3+} (Zhang et al., 2016).

5.4.3.1 Secondary elution using acids at high concentration

Increases in acid concentration in secondary elution further increased the amount of metal eluted from resin. Elution of Fe^{3+} at high concentrations of H_2SO_4 increased on average a 14% when compared to that obtained at concentrations of 0.5% v/v H_2SO_4 in primary elution. The extent of Ni^{2+} removed in secondary elution was between 20 and 30% compared to the 70% removed in primary elution. The extent of Ni^{2+} removed by primary and secondary elution reached above 95% (See Figure 5.13).

While secondary elution further increased the percentage of Fe^{3+} eluted, the increase in H_2SO_4 concentration from 30% to 50% v/v was not beneficial. The maximum Fe^{3+} eluted was still too low to allow an effective resin regeneration. Furthermore, acid

concentration of 30% v/v showed early signs of physical damage to the resin while concentrations of 50% had negative effects on the physical integrity of the resin.

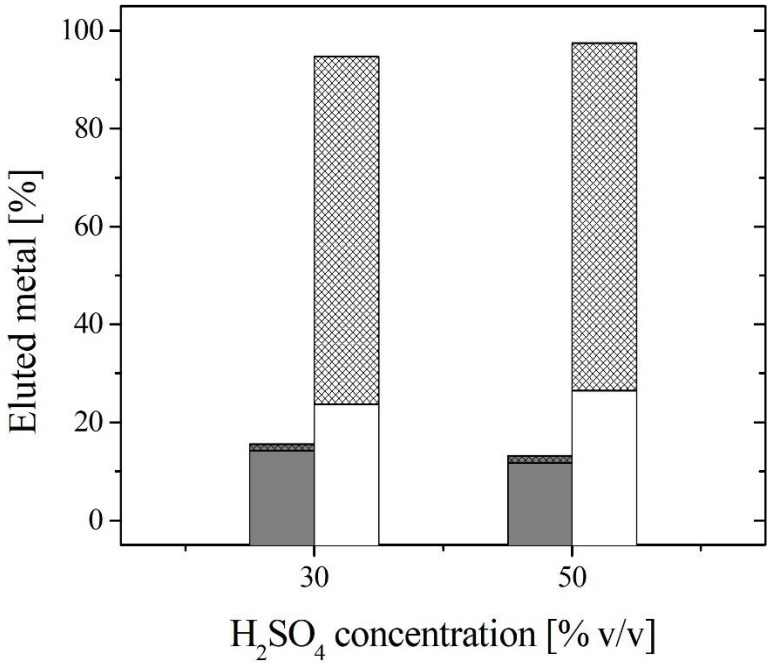

Figure 5.13: Percentage of Fe^{3+} (grey bars) and Ni^{2+} (white) eluted in secondary elution using H_2SO_4 at different concentration. Solid bars – Percentage of metal eluted in secondary elution. Grill pattern bars – Cumulative percentage eluted in secondary plus primary elution.

Overall, HCl showed higher Fe^{3+} elution than H_2SO_4. At HCl concentration of 30% v/v, the elution of Fe^{3+} reached above 30%. At acid concentrations of 50% v/v, elution of Fe^{3+} reached above 60% (See Figure 5.14). However, the total Fe^{3+} eluted (i.e., Fe^{3+} eluted by primary and secondary elution) remained under 65% even at the highest acid concentration. Secondary elution with HCl completed the elution of Ni^{2+} regardless of its concentration. HCl showed less damage on resins, although no microscopic analysis was conducted to confirm these observations.

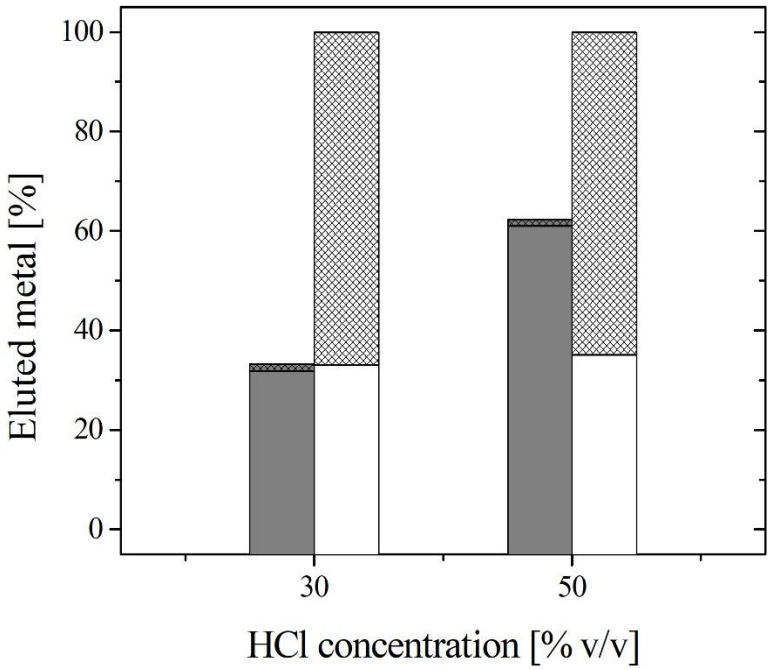

Figure 5.14: Percentage of Fe^{3+} (grey bars) and Ni^{2+} (white) eluted in secondary elution using HCl at different concentration. Grill pattern bars – Cumulative percentage eluted in secondary plus primary elution.

Neither H_2SO_4 nor HCl showed satisfactory results for Fe^{3+} elution. This suggest the need of complexing agents for the complete elution of Fe^{3+}. Complete elution of metals is required to achieve complete regeneration of resin. Without this, the efficiency of the resin decreases considerably disabling its application in subsequent adsorption/elution cycles.

5.4.3.2 Secondary elution using complexing agents

After a primary elution employing 0.5% v/v H_2SO_4, resin underwent a secondary elution using different concentrations of oxalic acid, citric acid, and EDTA acting as

complexing agents. The complexing agents employed for secondary elution correspond to those highlighted by Zhang et. al 2016 for the elution of Fe^{3+} (Zhang et al., 2016).

Oxalic acid and EDTA showed significant elution of Fe^{3+} with corresponding increases as concentration of complexing agent increased (See Figure 5.15 and 5.16, respectively). At concentrations of 1.0% w/w, oxalic acid and EDTA eluted more Fe^{3+} than H_2SO_4 at concentration of 50% v/v. At concentrations of 2.5% w/w, oxalic acid and EDTA reached similar Fe^{3+} elution than that obtained in 50% v/v HCl. Unlike the high concentration of acids, the studied concentrations of complexing agent did not caused apparent damage to the physical integrity of the resin. The extent of Fe^{3+} elution followed the order EDTA>oxalic acid. Unlike Fe^{3+} elution, the extent of Ni^{2+} elution was less dependant on complexing agent concentration. Elution of Ni^{2+} by EDTA was comparable with that obtained with HCl reaching values between 25-32% but was significantly lower with oxalic acid reaching values under 10%. Elution of Fe^{3+} by citric acid was negligible with minimum increases as acid concentration increased (Figure 5.17). Elution of Ni^{2+} by citric acid was also low and reached maximum elution under 20%.

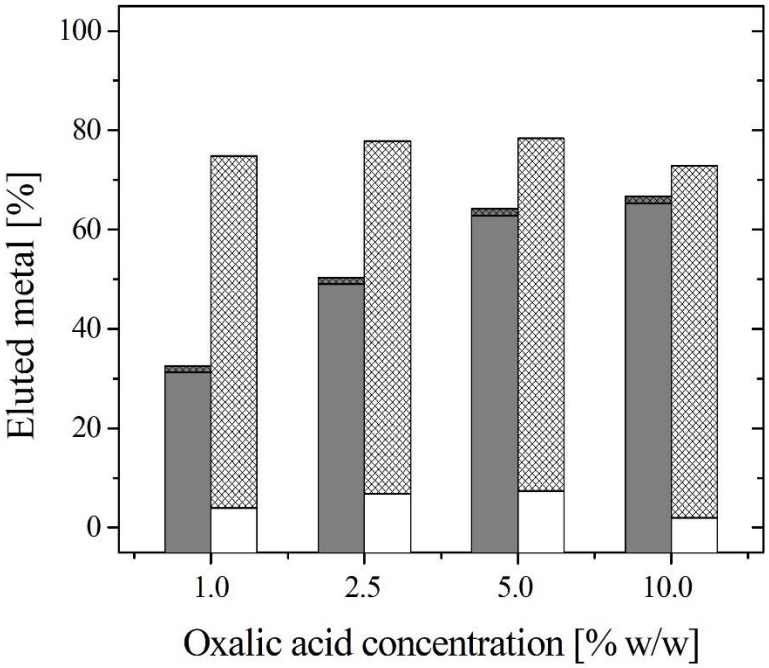

Figure 5.15: Percentage of Fe^{3+} (grey bars) and Ni^{2+} (white) eluted in secondary elution using Oxalic Acid at different concentration. Grill pattern bars – Cumulative percentage eluted in secondary plus primary elution.

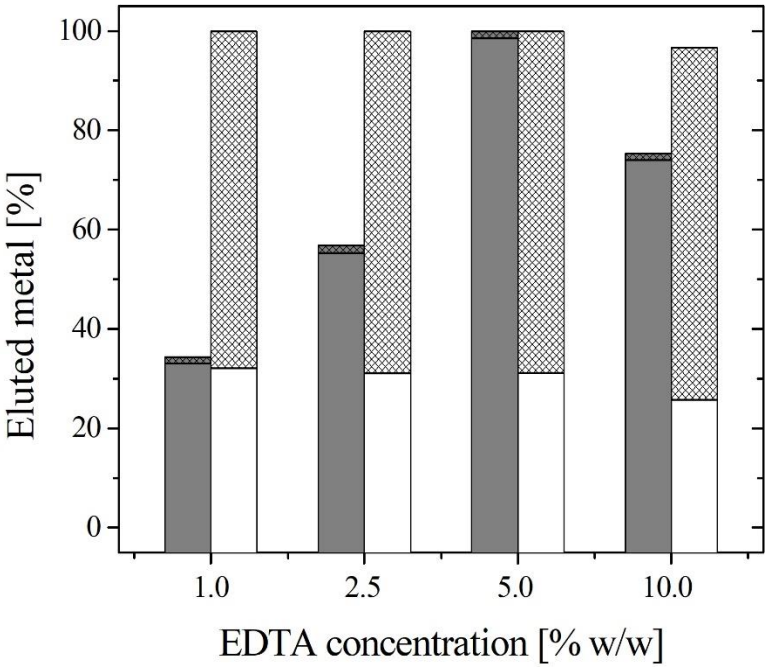

Figure 5.16: Percentage of Fe^{3+} (grey bars) and Ni^{2+} (white) eluted in secondary elution using EDTA at different concentration. Grill pattern bars – Cumulative percentage eluted in secondary plus primary elution.

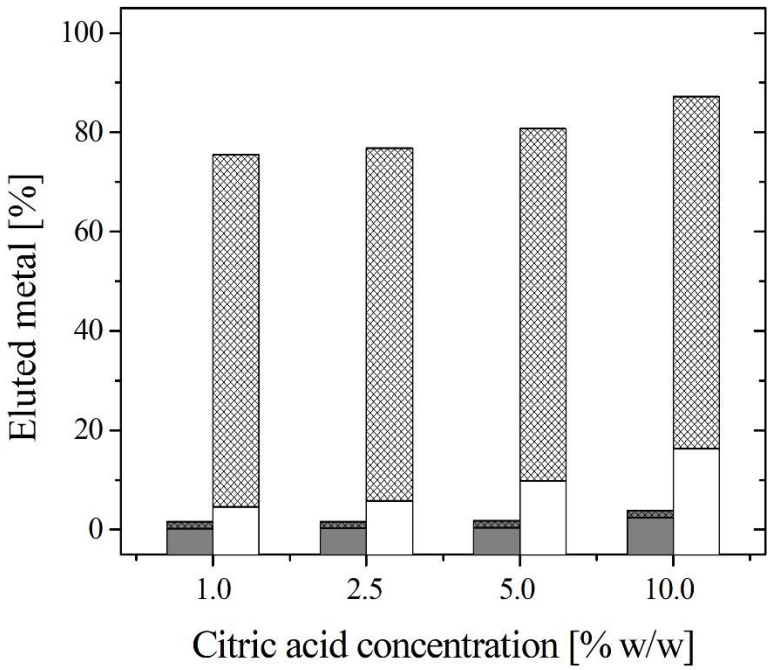

Figure 5.17: Percentage of Fe^{3+} (grey bars) and Ni^{2+} (white) eluted in secondary elution using Citric Acid at different concentration. Grill pattern bars – Cumulative percentage eluted in secondary plus primary elution.

Although all complexing agents eluted higher amounts of Fe^{3+} compared to that of primary elution, only oxalic acid and EDTA showed adequate Fe^{3+} stripping properties. Among them, EDTA reached the most satisfactory metal elution with potential for resin regeneration. When combined primary and secondary elution, EDTA at concentration of 5% w/w eluted 99.99% of the Fe^{3+} and Ni^{2+}. Concentration of 10% w/w of EDTA formed important amounts of a white-yellow precipitate, presumable Ferric-EDTA complex. The formation of precipitates was responsible for the decreased elution values at 10% w/w EDTA presented in Figure 5.16. No precipitate formation appeared in EDTA concentrations of 5% w/w. Nevertheless, precipitates appeared on sample containing 5%

w/w EDTA overnight. Oxalic acid at 10% w/w as secondary elution achieved a combined 67% of Fe^{3+} with 76% of Ni^{2+} and there was no signs of precipitation.

Even though the combination of 0.5 v/v H_2SO_4 and 5% w/w EDTA removed all the metal adsorbed by the resin, the use of EDTA may result in difficulties of downstream Fe^{3+} beneficiation process. Especially if Fe^{3+} beneficiation is intended for the production of electrolytic iron powder or the electrodeposition of electrolytic iron (Izaki, 2010; Zhang et al., 2016). Although, novel research suggest the fabrication of Fe^{3+} nanoparticles capped with EDTA can be employed for important applications such as the treatment of tumor tissues, contrast agents in magnetic resonance imaging, targeted drug delivery, adsorbents, energy conversion and storage, and others (Aghazadeh et al., 2017).

5.4.4 Effect of time and temperature in elution experiments

The study on metal elution in time suggest that H_2SO_4 as primary eluent achieved the highest Ni^{2+} removal by the first 30 min of reaction (See Figure 5.18). Thereafter, the extent of elution of Ni^{2+} maintained a relatively stable decrease up to the 24 h of analysis. Meanwhile, the maximum elution of Fe^{3+} appeared after 1 h and remaining stable afterwards. As time goes by the selectivity of primary elution decreases, suggesting that elution with 0.5% H_2SO_4 should not last over 30 min.

Secondary elution with 10% oxalic acid showed little to none increase in Ni^{2+} elution throughout the 24 h of the study. However, the maximum Fe^{3+} eluted was obtained between 60 and 120 min. As time goes by, the concentration of Fe^{3+} in eluate decreased suggesting re-adsorption by the resin.

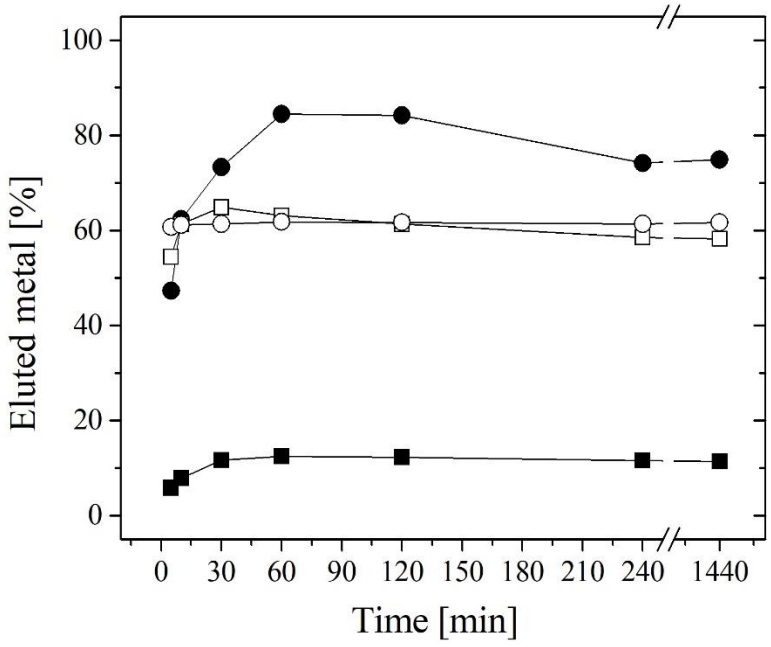

Figure 5.18: Metal elution in time. (■) Fe and (□) Ni eluted in primary elution, total (●) Fe and (○) Ni eluted in primary and secondary elution

Elution of Fe^{3+} was not dependant on temperature in primary elution. Contrarily, the elution of Ni^{2+} decreased as temperature increased (Figure 5.19). A decrease in the extent elution as temperature increases suggest the exothermic properties of Ni^{2+} elution. Alternatively, the endothermic properties of Ni^{2+}-resin adsorption increased the adsorption temperature as explained in Section 4.4.2.2. An exothermic elution reaction will have difficulties eluting at high temperatures (See Chapter 6). The use of oxalic acid at temperatures between 20°C and 80°C in secondary elution did not affect the percentage of Ni^{2+} elution. However, high temperatures increased the extent of Fe^{3+} elution suggesting that for best results secondary elution should be conducted at high temperatures. Further studies are required to describe this phenomenon.

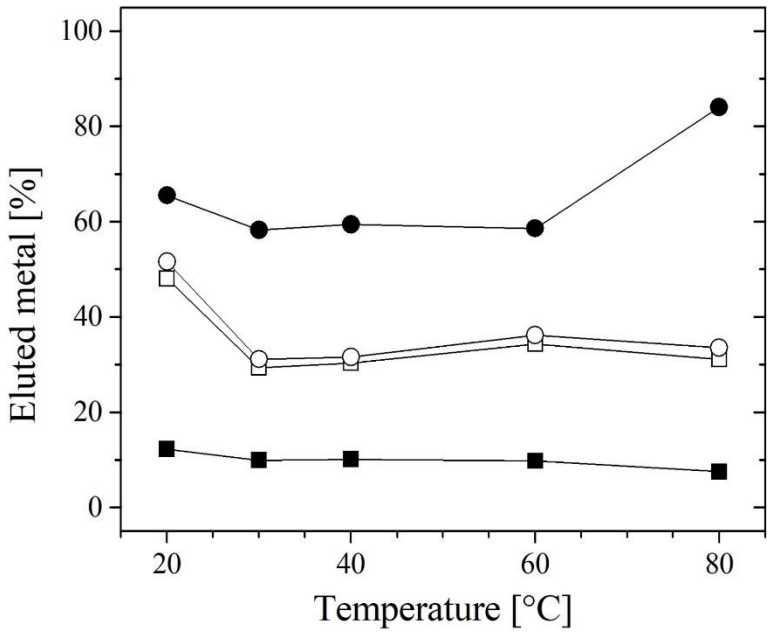

Figure 5.19: Metal elution with temperature. (■) Fe and (□) Ni eluted in primary elution, total (●) Fe and (○) Ni eluted in primary and secondary elution

5.4.5 Replicability of adsorption/elution of metals

Fivefold experiments studied the replicability of the most efficient conditions for adsorption and elution of mixed phosphonic and sulfonic resins (Figure 5.20). In general, all processes remained under 12% standard deviation confirming the replicability presented throughout the manuscript. This included, preferential Fe^{3+} adsorption over Ni^{2+}, preferential Ni^{2+} elution by H_2SO_4 0.5% v/v, and preferential Fe^{3+} elution by oxalic acid at 10% w/w and EDTA at 5% w/w, respectively. Therefore, confirmed the EDTA best metal elution properties compared to that of oxalic acid.

Although EDTA eluted more metal than oxalic acid, oxalic acid produced Fe^{3+} electrolyte of higher purity given the lower amounts of Ni^{2+} eluted. Satisfactory Fe^{3+} elution with 10% w/w oxalic acid after the purification of Cu^{2+} electrolyte solution was

reported by Zhang et.al, 2016. The removal of Fe^{3+} by oxalic acid route favour the formation of iron oxalates, which could be later employed for the production of iron powder allowing the recycling of oxalic acid. Figure 5.21 shows a representation of the coloration of the different stages in the Fe:Ni separation process having Figure 5.22 as a reference for the coloration of pure solution of Fe^{3+} and Ni^{2+} at 25g/L and the combination of them having 25g/L each.

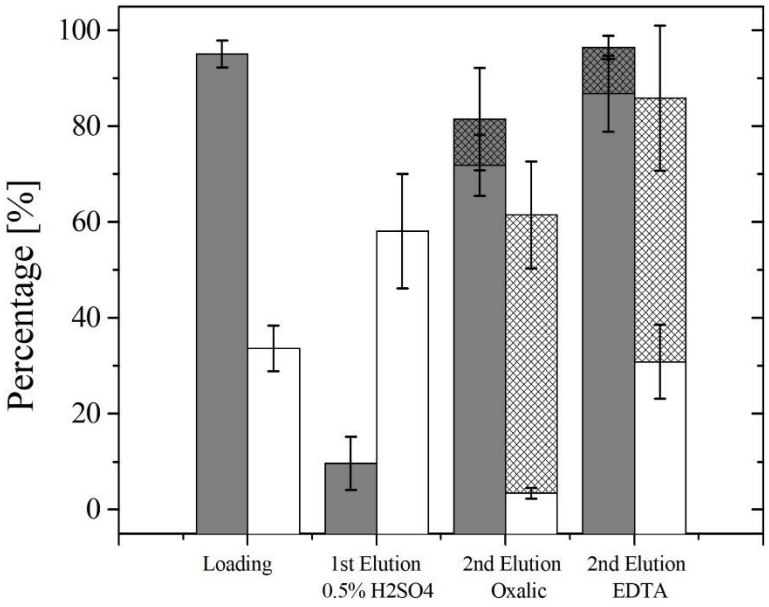

Figure 5.20: Percentage of Fe^{3+} (grey bars) and Ni^{2+} (white) and respective error for each step in separation process. Grill pattern bars – Cumulative percentage eluted in primary plus secondary elution

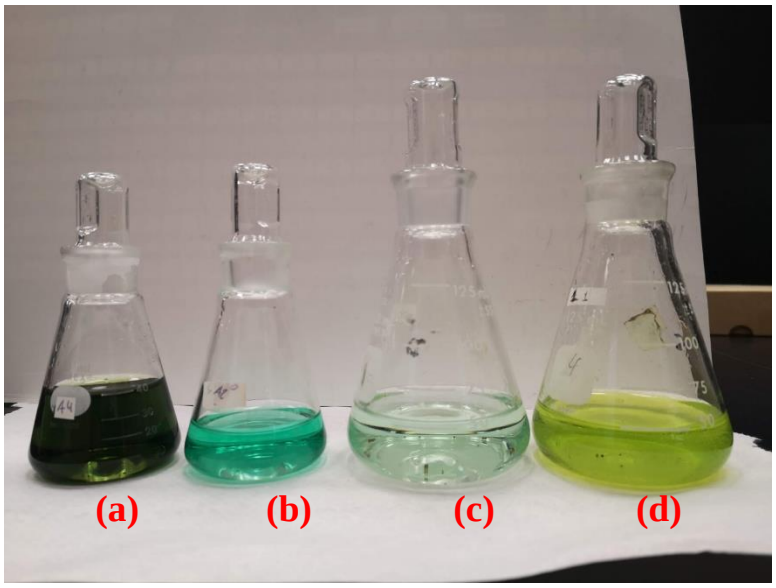

Figure 5.21: (a) synthetic solution of 25 g/L Fe^{3+} and 25 g/L Ni^{2+}; (b) synthetic solution after adsorption experiments on resins with combination of phosphonic and sulfonic groups; (c) solution after primary elution with H_2SO_4 0.5% v/v; (d) solution after secondary elution with 10% w/w of oxalic acid

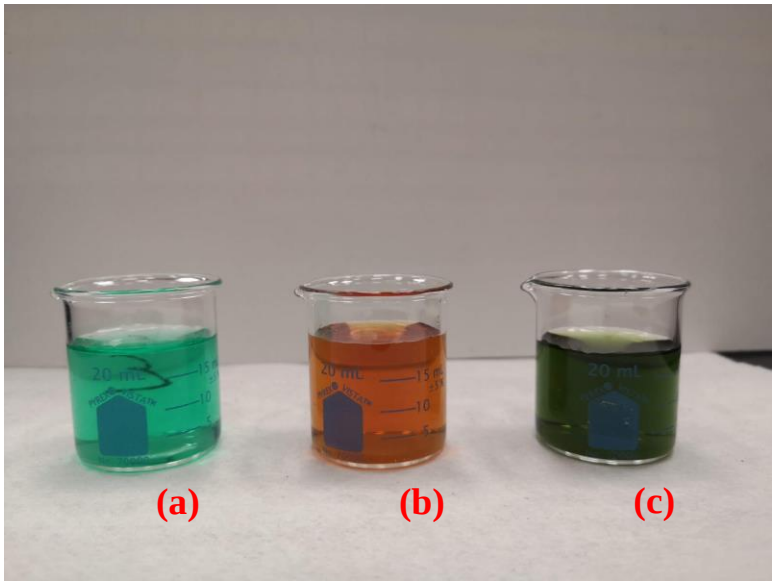

Figure 5.22: (a) Synthetic solution of 25 g/L Ni^{2+}; (b) synthetic solution of 25 g/L Fe^{3+}; (c) synthetic solution of 25 g/L Fe^{3+} and 25 g/L Ni^{2+};

Analyses of a complete separation process in resins containing quaternary ammonium, phosphoric acid, and aminophosphonic acid groups served as reference for results obtained with resins containing a combination of phosphonic and sulfonic groups. Error for metal adsorption in these resins also remained under the 10% in triplicated experiments (see Figure 5.23) but the extent of error in elution with 0.5% H_2SO_4 increased considerably (see Figure 5.24).

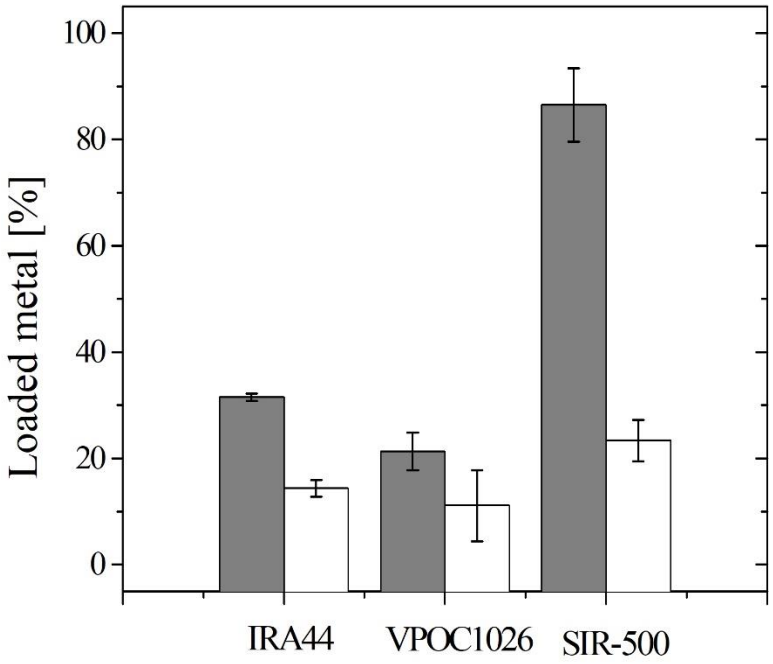

Figure 5.23: Percentage of Fe^{3+} (grey bars) and Ni^{2+} (white) adsorbed on different ion exchange resins

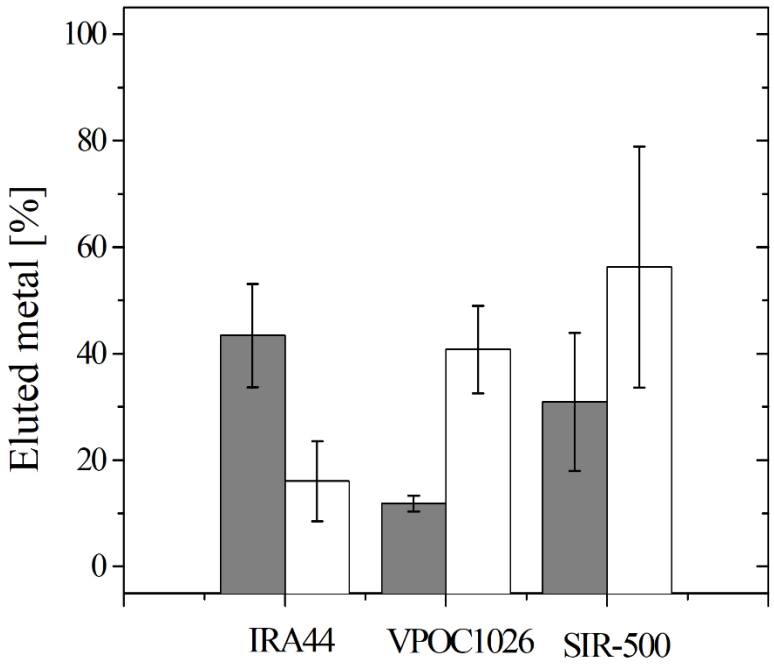

Figure 5.24: Percentage of Fe^{3+} (grey bars) and Ni^{2+} (white) eluted in 0.5% v/v H_2SO_4 as primary elution

Based on the error observed in Figure 5.24, only resins with phosphoric acid and quaternary ammonium groups showed a selective elution towards Ni^{2+} using 0.5% H_2SO_4. The error obtained in experiments with aminophosphonic acid groups do not suggest a selective elution for either metal. Secondary elution using oxalic acid did not improve elution of metals in quaternary ammonium or aminophosphonic acid groups. However, oxalic acid showed remarkable properties for Fe^{3+} elution from phosphoric acid resins with low percentages of Ni^{2+} elution (See Figure 5.24). The use of 10% w/w of oxalic acid damaged considerable the structure of the resin containing phosphoric groups rendering it inoperable for subsequent adsorption-elution steps. Based on the results obtained, oxalic

acid is not recommended as complexing agent for the secondary elution of quaternary ammonium, aminophosphonic, or phosphoric acid resins.

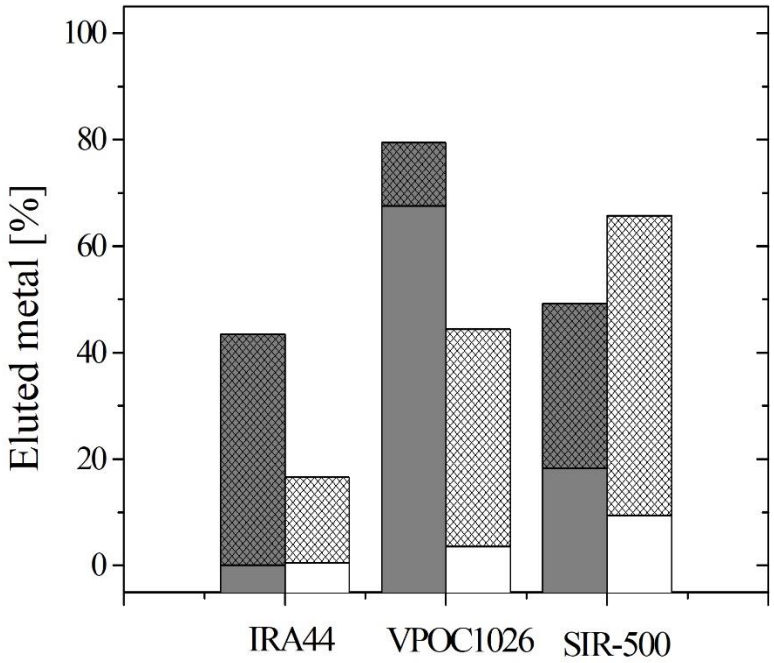

Figure 5.25: Percentage of Fe^{3+} (grey bars) and Ni^{2+} (white) eluted in secondary elution with 10% oxalic acid. Grill pattern bars – Cumulative percentage eluted in secondary elution plus primary elution in 0.5% v/v H_2SO_4.

5.5 Discussion

Results showed that adsorption in process steps increased considerably the adsorption of Fe^{3+} compared to single batch experiments (see Figure 5.5). Similar to the results obtained in Sections 3.4.1 and 4.4.1, in excess of resin to metal and once iron started depleting from the solution, the co-adsorption of Ni^{2+} increases considerably. All resins tested reached over 80% Fe^{3+} adsorption proving process steps beneficial for efficient removals. With the high co-adsorptions of Ni^{2+} observed the goal of efficient metal

separation moves down in the process relying on efficient elution processes. Efficient elution processes have two different elution stages named primary and secondary elution.

As shown in Figure 5.3, the objective of primary elution is to remove any base metal co-adsorbed during adsorption process. Ideally, low volumes of mildly acidic characteristics constitute the ideal eluent of primary elution. From initial experiments using sulfuric acid at concentrations 1.0-10% only resins with iminodiacetic, carboxylic acid, aminophosphonic acid and a combination of phosphonic and sulfonic acid showed promising elution. Therefore, these resins underwent further exploration at lower acid concentration 0.2-0.5% v/v H_2SO_4 and 0.2-1.0% HCl. The overall results showed that resins with phosphorous groups eluted more Ni^{2+} than Fe^{3+} However, resins with a mixture of phosphonic and sulfonic resins (Figure 5.6) outperformed the elution obtained from phosphoric acid groups (Figure 5.10) and this regardless of the type and concentration of eluent. Although phosphoric groups eluted more Ni^{2+} than Fe^{3+}, the extent of Ni^{2+} elution achieved was not promising. The other phosphorus containing resins, aminophosphonic acid groups (Figure 5.7), obtained representative elution of Ni^{2+} but eluted significant amount of Fe^{3+} as concentration of HCl and H_2SO_4 increased. Elution of Ni^{2+} from resins containing carboxyl groups differed depending on the type of eluent and concentration. HCl selectively eluted Ni^{2+} from carboxylic acid (Figure 5.8) and iminodiacetic acid resins (Figure 5.9) regardless of acid concentration. Conversely, H_2SO_4 only achieved selective elution of Ni^{2+} from carboxylic acid (Figure 5.8) and iminodiacetic acid resins (Figure 5.9) at concentrations under 1% v/v. The selectivity observed from iminodiacetic acid resins declined as volume of eluent increased. Resins with quaternary ammonium groups (Figure

5.11) showed selective Fe^{3+} elution but the extent of elution was not promising for further experiments. Resins with N-methylglucamine (Figure 5.12) obtained high elution of metals without apparent selectivity resulting in unsuccessful primary elution.

Both HCl and H_2SO_4 selectively eluted Ni^{2+} from resin containing a combination of phosphonic and sulfonic groups. HCl was more selective than H_2SO_4. Figure 5.3 shows that the pregnant solution of primary elution returns to pressure leaching process. Leach liquors are rich in SO_4^{2-} and therefore the use of H_2SO_4 for primary elution would be preferred despite the higher elution obtained with HCl. The introduction of Cl^- in leach liquors at high electrolyte concentration could favour anionic complex formations, thus modifying the overall chemistry in the hydrometallurgy. Introduction of Cl^- in leach liquors may enable the formation of metal insoluble species, or formation of $FeCl_3$ and $FeCl_4^-$ not ideal at early base metal production processes (Harland, 1994; Helfferich, 1962). If the intention is a direct electroplating of base metals after primary elution then HCl is the best option. The most efficient H_2SO_4 concentration for selective Ni^{2+} elution was 0.5% v/v.

Once Ni^{2+} eluted from resins with a combination of phosphonic and sulfonic groups, a secondary elution process studied the feasibility of Fe^{3+} elution. Exploration for secondary elution started using high concentration of the same acids employed in primary elution. First to confirm a maximum Ni^{2+} elution, and second to study its potential for removing Fe^{3+}. The results disproved the effectiveness of H_2SO_4 and HCl for Fe^{3+} elution at high concentrations. Moreover, high acid concentration resulted in negative effects to the physical integrity of the resin. The poor performance of concentrated acids as eluent solution highlighted the need of complexing agents to aid in the elution of Fe^{3+}. The

complexing agents employed in secondary elution were oxalic acid, citric acid, and EDTA. All complexing agents were forms of carboxylic acids having two, three, and four carboxyl groups, respectively. EDTA includes further ligand potential having two amino groups for coordination (See Figure 5.4). Among the complexing agents, EDTA (Figure 5.16) and oxalic acid (Figure 5.15) showed the best Fe^{3+} elution, in order. Secondary elution with EDTA eluted 100% of Fe^{3+} at concentrations of 5% w/w. However, EDTA concentration of 10%w/w presented precipitates at the end of the experiment in the form of Fe^{3+}-EDTA complex. Precipitate formation hampers metal concentration analysis suggesting that elution with EDTA at 10% w/w might have reached higher elution values than those obtained by metal analysis. Due to precipitation, Fe^{3+} concentration in solution decreases. Duplication of EDTA experiments at 10% w/w (Figure 5.20) confirmed these observations. Results obtained with oxalic did not produced precipitates, but the maximum Fe^{3+} elution reached under 70% at the highest concentration. Secondary elution with citric acid (Figure 5.17) had unsatisfactory results even at the highest concentration, Fe^{3+} elution reached under 10%. Although EDTA outperformed oxalic acid, the formation of precipitates hindered the appropriate assessment of the extent of Fe^{3+} elution. Thus, further studies analysing the potential of Fe^{3+} elution were conducted with oxalic acid.

Elution experiments studying the effect of time and temperature employed H_2SO_4 at 0.5% v/v as primary eluent and oxalic acid at 10% w/w as secondary eluent. The selection of sulfuric acid solution at 0.5% v/v for primary elution relied on the high performance obtained in Section 5.4.2. Meanwhile the selection of oxalic acid at 10% w/w for secondary elution relied on the solubility and stability of oxalate forms at the

experimental conditions. Similar to adsorption results obtained at different temperature (Section 4.4.2.2), co-elution of Fe^{3+} at primary elution was not dependant on temperature. Nonetheless, secondary Fe^{3+} elution increased with temperature. Conversely, the elution of Ni^{2+} in primary elution decreased as temperature increased but remained stable during secondary elution (Figure 5.19). These results suggest that low temperatures should be preferred for primary elution as the release of Ni^{2+} is at its highest. Inversely, high temperatures should be preferred to enhance recovery of Fe^{3+} in secondary elution and prevent precipitation. Similarly, temperature, different elution time enhanced selectivity between Fe^{3+} and Ni^{2+}. In primary elution, Ni^{2+} elution reached its maximum at 30 min. Periods longer than that promoted elution of Fe^{3+} reaching maximum elution after 60 min. In secondary elution, the maximum Fe^{3+} removal appeared between 60 and 120 min while Ni^{2+} elution was negligible throughout the 24 h analysis.

Replicability studies for adsorption and elution of resins containing a combination of phosphonic and sulfonic acid suggested a 12% error among all the values obtained. Although a large error, the results confirmed the selectivity trends for adsorption and elution. Thus, confirmed Purolite MTS 9570 with a combination of phosphonic and sulfonic groups as the best performer for Fe:Ni separation among resins containing quaternary ammonium, phosphoric acid, and aminophosphonic acid groups. Further exploration for more efficient eluents is highly recommended.

5.6 Conclusion

Semi continuous process at consecutive steps enhanced the amount of Fe^{3+} adsorbed by ion exchange resins. Resins containing a combination of phosphonic and sulfonic groups and N-methylglucamine displayed the best properties for Fe adsorption among resins containing carboxylic acid, phosphoric acid, and quaternary ammonium groups. However, as the adsorption of Fe^{3+} increased with each consecutive step so did the co-adsorption of Ni^{2+} reaching values close to the maximum obtained for Fe^{3+}. The high co-adsorption of Ni^{2+} required efficient selectivity during elution process for effective Fe:Ni separation. A two-step elution process divided into primary and secondary elution assessed the viability of selective metal elution after Ni^{2+} co-adsorption.

A series of exploratory experiments using H_2SO_4 and HCl at different concentration intended to asses the selective removal of Ni^{2+} during primary elution. Resins with a combination of phosphonic and sulfonic groups showed the best Ni^{2+} elution properties. The rest of the resins had relative selectivity for Ni^{2+} or Fe^{3+} elution but underperformed. Conversely, resins containing N-methylglucamine had high percentages of metal elution but no selectivity. Resins containing a combination of phosphonic and sulfonic groups required low acid concentrations of 0.5% v/v of either eluent to remove satisfactory amounts of Ni^{2+}. Likewise, achieved high percentages of Ni^{2+} elution requiring only low volumes of eluent equivalent to 2BV.

Secondary elution tested the viability of Fe^{3+} elution from resins containing phosphonic and sulfonic groups. Eluents containing high concentrations of H_2SO_4 and HCl did not obtained suitable results for Fe^{3+} elution. Instead, the high acid concentration

damaged the physical integrity of the resin. The use of complexing agents of carboxyl nature enhanced the Fe^{3+} elution. Eluents composed of EDTA at concentrations higher than 5% w/w achieved close to 99% removals of iron. Eluents composed of oxalic acid achieved reasonable Fe^{3+} removals at 67% but the extent of elution was lower than that obtained with EDTA at 5%w/w. Citric acid did not obtain favourable results for Fe^{3+} elution. Although EDTA outperformed oxalic acid, a compromised Fe-EDTA stability resulted in precipitation at the experimental conditions. Therefore, oxalic acid was selected for further studies.

Studies related to the effects of time and temperature highlighted parameters to enhance further the selectivity of elution processes. Selective recovery of Ni^{2+} during primary elution showed to be time and temperature dependent favoring selectivity at temperatures of 20° C in periods of 30 min. Meanwhile, Fe^{3+} selectivity in secondary elution resulted from temperatures close to 80°C in periods between 60 and 120 min. Elution studies employing resins with quaternary ammonium, phosphoric acid, and aminophosphonic acid groups were unsuccessful using the eluents selected for combination of phosphonic and sulfonic groups. Further studies employing different eluent may obtain satisfactory selective elution.

Chapter 6 Thermodynamic and kinetic analysis

This chapter includes information based on the unpublished manuscripts:

1.. R.A. Silva, Y. Zhang, K. Hawboldt, & L.A. James. (Pending submission). Use of resins with a combination of phosphonic and sulfonic acid for Fe^{3+} adsorption at low pH and high base metal concentration conditions

Rene A. Silva designed experimental conditions, conducted adsorption experiments, and wrote the manuscript. Dr. Yahui Zhang supervised the design of the experiment, reviewed and edited the final version of the manuscript. Dr. Kelly Hawboldt and Dr. Lesley James reviewed and edited the final version of the manuscript.

6.1 Abstract

The thermodynamic and kinetic characteristics of Fe^{3+} and Ni^{2+} adsorption on ion exchange resins with a combination of phosphonic and sulfonic groups were determined in monometallic ($Fe_{Ø}$ and $Ni_{Ø}$) and bimetallic (Fe_{Ni} and Ni_{Fe}) systems at high concentrations. Due to the complexity of systems at high concentrations, the determination of thermodynamic characteristics resulted from the calculation of the distribution constant requiring the calculation of ionic activity coefficients. The approximations of Debye-Huckel and Davis equations aided to estimate the activity coefficients at high concentrations and the results compared with the limit conditions an ideal solution. The Pseudo First and Second Order (PFO and PSO), Elovich, and Intra Particle Diffusion (IDP) equations models were compared to determine the adsorption rate. The results indicated favourable Fe^{3+} adsorption having exothermic and exergonic properties and were independent of the presence of Ni in the system. In contrast, Ni^{2+} adsorption was favourable only in $Ni_{Ø}$ systems. In Ni_{Fe} systems, the adsorption of Ni^{2+} showed a negative entropy and positive Gibbs energy, suggesting Fe^{3+} in solution resulted unfavourable adsorption for Ni^{2+}. This observation was confirmed by the low Ni^{2+} adsorption compared to that of Fe^{3+} in this chapter and previous chapters studying the Ni:Fe separation by resins with a combination of phosphonic and sulfonic groups. The PSO best described the Fe^{3+} adsorption kinetics with a R^2 correlation > 0.999. However, non-linear PSO showed a decreased R^2 suggesting that the rate of reaction may also be dependent on transport phenomena not described by PSO equations. The poor correlation of Elovich equation confirmed that chemisorption did not governed the adsorption of Fe^{3+} and Ni^{2+}. According

to the plot obtained by an Intra Particle Diffusion model, more than one type of diffusion might rule the adsorption rate of Fe^{3+} and Ni^{2+} on ion exchange.

6.2 Introduction

Mostly all research of equilibria and selectivity of ion exchange resins focuses on systems of diluted media where reaction rates, equilibrium constants, diffusion coefficients, thermodynamic, and numerical models discussing adsorption behaviors occur in aqueous concentrations below 1.0 M (Harland, 1994). Given the low concentrations, common adsorption isotherms originally developed to describe gas adsorption onto activated carbon were adequate in describing adsorption in aqueous systems.

Each isotherm model has specific assumptions inherent to the type of adsorption phenomena. As an example, the Langmuir isotherm describes the reversible adsorption equilibrium assuming limited adsorption sites on a monolayer manner (Hawari and Mulligan, 2006). Other models include potential of a multilayered structure (Vasiliu et al., 2011), whether the nature of the adsorption mechanism is by physical sorption or chemisorption (Bayramoglu et al., 2016), interactions between adsorbent-adsorbate (Vasiliu et al., 2011), affinity of binding sites, interaction between adsorbed species, and effect of surface coverage on adsorption, and others (Bayramoglu et al., 2016; Liu, 2009).

Adsorption isotherms are typically used to assess the adsorption mechanism as mono or multilayer or to determine if adsorption is physical sorption or chemisorption. One of the main outcomes of isotherms is the determination of thermodynamic equilibrium constant used to calculate the Gibbs energy ($\Delta G°$), heat of reaction at constant pressure

(ΔH°), an change in entropy (ΔS°). These values give important insights of the nature of adsorption reaction. A negative ΔG° values indicates spontaneous adsorption suggesting higher probability of occurrence. The magnitude of ΔG° indirectly suggest preferable reaction conditions and may predict adsorption preferences among different types of adsorbates (e.g., metal ions like Fe^{2+} and Ni^{2+}). The values of ΔH° and ΔS° indicate adsorption preference (Bayramoglu et al., 2016; Kiefer and Höll, 2001).

The general equilibrium reaction used in adsorption isotherm modeling is:

$$\text{Pol-Fg}_{(res)} + \text{M}^{\pm}_{(aq)} \leftrightarrow \text{Pol-Fg M}_{(res)} \qquad \text{Eq. (6.1)}$$

Where Pol-Fg represents the vacant sites of an unloaded resin, $M^{\pm}$ the metal ions in the bulk solution, and Pol-FgM the metal adsorbed on the resin, or in other terms, the occupied sites. Following Equation 6.1, the general thermodynamic equilibrium constant (K_a) becomes the relationship of activities (a) of each of the species as follows:

$$K_a = \frac{a_{Pol-Fg\,M}}{(a_{Pol-Fg})(a_{M^{\pm}})} \qquad \text{Eq. (6.2)}$$

Given that the activity coefficient of the vacant and occupied sites on a resin are considered equivalent (Liu, 2009), Equation 6.2 becomes:

$$K_a = \frac{\theta_E}{(1-\theta_E)(\gamma_{M^{\pm}} \cdot c_{M^{\pm}})} \qquad \text{Eq. (6.3)}$$

In which θ_E is the fraction of occupied adsorption sites defined by Equation 6.4, $\gamma_{M^{\pm}}$ the activity coefficient of the metal in solution, and $C_{M^{\pm}}$ the metal ion molar concentration.

$$\theta_E = \frac{q_e}{q_{max}}$$ Eq. (6.4)

Where q_E and q_{max} are the adsorption capacity of adsorbent at equilibrium and at its maximum value.

Langmuir isotherm (Equation 6.5) assumes a monolayer adsorption on its model at equilibrium

$$q_e = q_{max}\frac{C_e K_L}{C_e K_L + 1}$$ Eq. (6.5)

Therefore, it is possible to employ Equation 6.4 to readjust Equation 6.5 and substituting C_e for $C_M^{\pm}$, results in:

$$K_L = \frac{\theta_E}{(1-\theta_E)(C_{M^{\pm}})}$$ Eq. (6.6)

Comparing Langmuir equilibrium constant K_L (Equation 6.6) with the thermodynamic equilibrium constant (Equation 6.3) results in the following relationship:

$$K_a = \frac{K_L}{\gamma_{M^{\pm}}}$$ Eq. (6.6)

Other isotherm models have similar relationship with the thermodynamic equilibrium constant presented in Equation 6.2 (Liu, 2009). However, in systems at low concentration, the activity coefficient of the metal species approaches the unity suggesting equivalences between the thermodynamic equilibrium constant and the equilibrium constant obtained with isotherm models (See Equation 6.6 for Langmuir reference). This is not the case for concentrated solutions. For concentrated solutions, the determination of activity coefficients becomes mandatory. Pitzer equations and Monte Carlo simulations

enable the calculation of activity coefficients of electrolyte concentrations as high as 6.0 M. This allow close approximations of thermodynamic equilibrium constant of adsorption reactions at high electrolyte concentrations. However, both approximation require extensive experimental data, fitting parameters, and substantial computational resources to obtain reliable calculations (Abbas and Ahlberg, 2019).

To simplify the exploration of thermodynamic parameters at high electrolyte concentration, the thermodynamic equilibrium constant can be related to the distribution constant (K_D) of the adsorption (Gode and Pehlivan, 2003; Liu, 2009; Salvestrini et al., 2014). The adsorption potential of the adsorbent is assumed much higher than the amount of adsorbate to be removed. In other words, the activity coefficient of the resin is assumed equal to that of a pure solid simplifying Equation 6.2 into:

$$K_D \approx \frac{[Pol{-}Fg\ M]}{(\gamma_{M\pm} \cdot C_{M\pm})} \qquad \text{Eq. (6.7)}$$

This assumption however is an oversimplification, and the thermodynamic results obtained can only be used to determine relative values of ΔG°, ΔH°, and ΔS° (positive or negative implying spontaneity), exo(endo)thermic reaction, and comparing values to determine if one system is favourable over another. Simple analytical equations like Debye-Huckel and Davies equations can provide reliable approximation of activity coefficients avoiding exhaustive experimental exploration.

Once K_D is defined with experimental data, ΔG° is calculated as follows:

$$\Delta G° = -RT \ln K_D \approx -RT \ln \frac{[Pol{-}Fg\ M]}{(\gamma_{M\pm} \cdot C_{M\pm})} \qquad \text{Eq. (6.8)}$$

Using adsorption data at different temperatures, it is possible to determine ΔH° and ΔS° of the system following the relationship:

$$\Delta G° = \Delta H° - T \cdot \Delta S° \quad \text{Eq. (6.9)}$$

Combining Eq. 6.8 and 6.9 results in the Van't Hoff equation:

$$\Delta G° = -RT \ln K_D = \Delta H° - T \cdot \Delta S° \quad \text{Eq. (6.10)}$$

or

$$\ln K_D = -\frac{\Delta H°}{RT} + \frac{\Delta S°}{R} \quad \text{Eq. (6.11)}$$

The slope and the intercept are equivalent to ΔH° and ΔS° related to the ideal gas constant R (8.315 J/mol·K), respectively. However, these approximations are only reliable to determine whether ΔG°, ΔH°, and ΔS° are higher or lower than zero.

Analysis of the kinetics of the adsorption reaction of Fe^{3+} and Ni^{2+} is required for scale up and design of the process. As Section 5.4.4 shows, resins adsorbed Ni^{2+} early in the experiment but the adsorbed percentage decreased with time. In contrast, the adsorption of Fe increased continuously suggesting a displacement of Fe^{3+} by Ni^{2+}. Attempts to predict the adsorption behavior of each of the metals can help to design processes with increased recoveries of the desired metal. Several authors have concluded that the adsorption of metals is quite fast regardless of the type of adsorbent as long as it is in non-porous media (Guo et al., 2015; Müller et al., 2012; Tran et al., 2016). Percentages of adsorption greater

than 80% in less than 10 min are common in for metal ions (Tran et al., 2017). Similarly, several studies of reaction kinetics have identified desorption phenomenon before or after equilibrium suggesting that long contact times are not necessarily beneficial for high adsorption rates (Halder et al., 2016; Sharma et al., 1990; Tran et al., 2017). This suggest the existence of an ideal period to achieve greatest separation yields between adsorbates.

Mathematical models describing reaction kinetics use the relationship between the amounts of adsorbate per unit mass of the adsorbent or adsorption capacity (q_t) at any given time. Examples of equations using this relationship are the Pseudo First and Second Order reactions (PFO and PSO, respectively) and other models such as the Elovich or Roginskye-Zeldovich model, and the Intra-Particle Diffusion model (IPD). The latter two are used when the former do not describe the behavior observed experimentally (Tran et al., 2017). For example, the use of PFO (a.k.a, Lagergren's first-order rate equation) can appropriate describe only the first 20-30 min of contact time (Ho and McKay, 1998; Lagergren, 1898). Likewise, tends to fail with improper selection of the equilibrium data (q_E). This is particularly true if desorption occurs before reaching equilibrium conditions resulting in $q_t > q_E$. In these cases, there are implicit restrictions of the mathematical model that would require obtaining logarithms of negative numbers due to the mathematical relationship:

$$ln(q_e - q_t) = -k_1 t + ln(q_e) \qquad \text{Eq. (6.12)}$$

Where q_t and q_E are a function of the amount of adsorbate in the adsorbent in mg / g, t in min, and the reaction constant k_1 in 1/min. To avoid an inaccurate q_E, is recommended to use the non-linear regression form as follows:

$$q_t = q_e(1 - e^{-k_1 t})$$ Eq. (6.13)

PFO describes reaction behaviors similar to first order equations. First order equations describe the behavior of reactions with one of the reactants in excess or maintaining a close to constant concentration despite the depletion of the other. Therefore, the rate of the reaction depends solely on the concentration of the limiting reagent. For short times, the adsorption of Equation 6.1 maintains a close to constant adsorption sites with respect to the change in metal concentration in solution. However, this assumption is no longer valid at high adsorbate concentrations or as time approaches equilibrium conditions. When equation 6.1 tends to equilibrium, most of the adsorption sites are occupied and the reaction behavior is no longer described by first order equations. Thus, at equilibrium conditions is safe to assume that the reaction rate of Equation 6.1 is bounded by the remaining adsorbate in solution and the available adsorption sites on the resin. This suggest that reaction kinetics follows the behavior of a second order in function of the concentration of both species. Adsorption reactions on ion exchange resins are more complex than a simple second order reaction, thus the dependency on the concentration of both species follows the behavior of a PSO. PSOs were developed to describe heavy metal removal using archaic forms of ion exchange media (Blanchard et al., 1984; Tran et al., 2017) following the linear form:

$$\frac{t}{q_t} = \left(\frac{1}{q_e}\right) t + \frac{1}{k_2 q_e^2}$$ Eq. (6.14)

And the integrated non-linear expression:

$$q_t = \frac{q_e^2 k_2 t}{1 + k_2 q_e t} \quad \text{Eq. (6.15)}$$

Where k_2 (mg/g·min) is the PSO second order reaction constant.

Several authors assume chemisorption processes if PSO adequately describe the adsorption processes. However, high degrees of correlation between PSO and experimental data only express the dependency of the reaction rate with the concentration of the species and do not provide specifics on the adsorption mechanism (Rengaraj et al., 2007).

This chapter focuses on the thermodynamic properties and kinetic behavior of the adsorption of Fe^{3+} and Ni^{2+} for resins with a combination of phosphonic and sulfonic groups. Both monometallic ($Fe_{Ø}$ and $Ni_{Ø}$) and bimetallic (Fe_{Ni} and Ni_{Fe}) systems were studied at concentrations of 25 g/L each. Due to the complexity of systems at high concentrations, values of activity coefficients at experimental conditions were approximated to obtain the change in adsorption heat, change in entropy, and Gibbs energy. As such, the results of thermodynamic analysis only allowed qualitative analysis of the thermodynamic properties. The reaction kinetics were compared with PFO and PSO models in an attempt to describe the behavior of Fe:Ni separation. The Elovich and IPD equations were used to identify the influence of any phenomena affecting reaction kinetics that are not taken into consideration by PFO and PSO.

6.3 Materials and methods

6.3.1 Thermodynamics

Ion exchange resins containing a combination of phosphonic and sulfonic groups underwent preconditioning as detailed in earlier sections (See Section 3.3.1). Adsorption experiments were conducted during 2 h using synthetic leach liquor containing 25 g/L of Fe^{3+} and 25 g/L of Ni^{2+} and individual solutions of each metal at 25 g/L with pH corrected to 1.5. The temperatures studied ranged from 20°C to 80°C following common temperatures found after pressure leaching process in hydrometallurgy of Ni^{2+} purification. The metal concentrations before and after the adsorption test were determined using Inductively Couple Plasma Optical Emission Spectroscopy (ICP-OES; Perkin-Elmer 5300 DV) analysis and the difference in concentration used for the metal adsorption calculation following Equation 3.1.

The activity coefficient for each metal ion was theoretically estimated using Debye-Huckel limiting law (DHLL; Equation 6.16), Extended Debye-Huckel (EDH; Equation 6.17), and Davies equations (Equation 6.18) as presented in Table 6.1.

Table 6.1: Specifics of approximation equations for activity coefficient determination methods with respective limit conditions for application

Activity coefficient approximation method			**Ionic strength limit conditions**
DHLL	$\log \gamma_{M^{\pm}} = -Az^2 \cdot \sqrt{I}$	Eq. (6.16)	0.01M
EDH	$\log \gamma_{M^{\pm}} = -Az^2 \cdot \frac{\sqrt{I}}{1 + Bd\sqrt{I}}$	Eq. (6.17)	0.1 M
Davies	$\log \gamma_{M^{\pm}} = -Az^2 \cdot \left(\frac{\sqrt{I}}{1+\sqrt{I}} - 0.2I\right)$	Eq. (6.18)	0.5 M

Where A and B are Debye-Huckel constants as a function of temperature included in Table 6.2, *z* the integer charge of the ions present in the electrolyte, *I* the ionic strength obtained by Equation 6.19, and *d* the effective hydrated diameter. The values employed as Fe^{3+} and Ni^{2+} effective hydrated diameter were 0.9 nm and 0.6 nm, respectively (Kielland, 1937)

$$I = \frac{1}{2}\sum Z_i^2 \cdot C_{M^{\pm}} \qquad \text{Eq. (6.19)}$$

Table 6.2: Values of the constants in the Debye-Huckel equation for activity coefficient determination at different temperatures as published in Manov et al. (1943)

Temperature [°C]	Temperature [K]	A	B [nm^{-1}]
20	293.15	0.5046	0.3276
30	303.15	0.5141	0.3297
40	313.15	0.5241	0.3318
60	333.15	0.5471	0.3366
80	353.15	0.5739	0.342

Thereafter, the thermodynamic values obtained using the activity coefficient were compared with those assuming the unity for activity coefficients.

6.3.2 Kinetics

After preconditioning (See Section 3.3.1), adsorption experiments were conducted using synthetic leach liquor containing a mixed solution of 25 g/L of Fe^{3+} and 25 g/L of Ni^{2+} defined as Fe_{ni} and Ni_{Fe} system and individual solutions of each metal (defined as $Fe_{Ø}$ and $Ni_{Ø}$ systems) at 25 g/L with pH corrected to 1.5. The experimental volume for kinetic studies was large enough to assume minimum alterations to the system after sampling for metal analysis concentration. Correction to sample volume and resin concentration were

considered for mass balance determination. Time dependency analysis ranged from 6s to 24 h of resin – solution contact time. Adsorption experiments were conducted at constant temperature of 20°C. The metal concentrations before and after the adsorption test were determined using ICP-OES. The difference in concentration before and after adsorption was used for the metal adsorption calculation following Equation 3.1. OriginPro 9.0 was used for analytical linear and non-linear curve fittings.

6.4 Results and Discussion

6.4.1 Thermodynamic analysis

The distribution constant of Equation 6.7 determined the thermodynamic characteristics of the adsorption reaction of Fe^{3+} and Ni^{2+} on ion exchange resins in systems containing Fe^{3+} ($Fe_{Ø}$), Ni^{2+} ($Ni_{Ø}$), and the mixture of Fe:Ni (Fe_{Ni} and $Ni_{Fe)}$. To do so, DHLL, EDH, and Davies equations aided to obtain activity coefficient values corrected to the concentration and temperature at which the adsorption took place. However, given that these approximation models are limited to concentration conditions, the results only reflect qualitative thermodynamic characteristics but not the real thermodynamic values. As electrolyte concentration increase, the activity coefficient decrease. Therefore, calculations assuming activity coefficient equal to the unity served as the limit conditions for thermodynamic values.

Activity coefficients values fluctuated significantly depending on the approximation model employed (see Table 6.3 and Table 6.4). This is not surprising given that each model has independent limits for ion strength conditions. Activity coefficients

using DHLL ranged between 10^{-6} and 10^{-8} for both Fe^{3+} systems (i.e., $Fe_{Ø}$ and Fe_{Ni}). Meanwhile remained between 10^{-3} and 10^{-4} for $Ni_{Ø}$ and Ni_{Fe}. These values are in accordance with the literature showing underestimated activity coefficients by DHLL as ion strength of the electrolyte increases above the limit of 0.01M (Skoog et al., 2014). This limit is due the fact that the only adjustable parameter in DHLL is ionic strength, neglecting ion size, short-range interactions, and ion-ion correlations (Abbas and Ahlberg, 2019). With a correction for hydrated ion size and ionic interactions, activity coefficients with EDH remained on the range of 10^{-2} for $Fe_{Ø}$ and Fe_{Ni} systems and 10^{-1} for $Ni_{Ø}$ and Ni_{Fe}. Literature suggest that activity coefficient values decrease as electrolyte concentration increases supporting the values obtained with EDH. However, the system's ion strength was well above the maximum EDH limit of 0.1 M. Activity coefficient approximation method by the Davies equation, has a maximum ion strength limit of 0.5 M, and gave activities in the 10^{-2} range for $Fe_{Ø}$ and 10^{-1} for Fe_{Ni}. The Davies equation showed activity coefficients on the 10^{-1} for $Ni_{Ø}$ and Ni_{Fe} but achieved the maximum of all approximation models reaching values above 0.8 (See Table 6.3 and 6.4). The limits for Davies equation are still under the average ion strength in the experiments in this work (1.9 M). There was lack of input data to use the Pitzer and Monte Carlo simulations for determination of activity coefficient for $Fe_{Ø}$, $Fe_{Ni,}$ $Ni_{Ø}$, Ni_{Fe} systems.

Table 6.3: Activity coefficients for monometal systems ($Fe_{Ø}$ and $Ni_{Ø}$)

	Debye-Huckel Limiting Law (DBLL)		Extended Debye-Huckel (EDB)		Davies	
T [°C]	**$\gamma Fe_{Ø}$ [x10^{-6}]**	**$\gamma Ni_{Ø}$ [x10^{-3}]**	**$\gamma Fe_{Ø}$**	**$\gamma Ni_{Ø}$**	**$\gamma Fe_{Ø}$**	**$\gamma Ni_{Ø}$**
20	2.70	5.15	0.062	0.196	0.073	0.280
30	1.97	4.70	0.060	0.191	0.071	0.272
40	1.99	4.52	0.058	0.188	0.063	0.262
60	0.989	3.52	0.053	0.177	0.057	0.247
80	0.598	3.05	0.048	0.168	0.048	0.224

Table 6.4: Activity coefficient for bimetal systems (Fe_{Ni} and Ni_{Fe})

	Debye-Huckel Limiting Law (DBLL)		Extended Debye-Huckel (EDB)		Davies	
T [°C]	**γFe_{Ni} [x10^{-8}]**	**γNi_{Fe} [x10^{-4}]**	**γFe_{Ni} [x10^{-2}]**	**γNi_{Fe}**	**γFe_{Ni}**	**γNi_{Fe}**
20	1.32	3.15	5.15	0.161	0.712	0.860
30	0.670	2.33	4.90	0.156	0.858	0.934
40	0.407	1.87	4.68	0.151	0.923	0.965
60	0.249	1.50	4.29	0.143	0.750	0.880
80	0.129	1.12	3.88	0.134	0.620	0.809

Distribution constants depends on activity of the species in the reaction (See Equation 6.7). As the values of activity coefficients decrease so does the activity in the liquid fraction resulting in greater distribution constant. Greater distribution constants increase the slope and the intercept in the Van't Hoff plot (see Figures 6.1 – 6.3). For comparison, distribution constants calculated from activity coefficients of ideal systems are outlined in Figure 6.4. Although each figure had different values, some adsorption trends were common. Negative slopes with positive intercepts were common for Fe^{3+} adsorption in $Fe_{Ø}$ and Fe_{Ni} systems and for Ni^{2+} in $Ni_{Ø}$ systems but the values were lower than those of Fe^{3+}. Adsorption of Ni^{2+} in Ni_{Fe} systems showed positive slopes with negative intercepts for all but the DHLL model. As defined by Van't Hoff, the slope of the ln K_D vs

1/T relationship represent ΔH while the intercept ΔS. A negative slope results in negative ΔH values suggesting adsorption is exothermic. Positive ΔH suggest endothermic. Adsorption reactions like Equation 6.1 which are exothermic can shift the equilibrium to the left side of the equation at high temperatures. This means, high temperatures have the potential to decrease the overall metal adsorption by the resin. Conversely, at high temperatures endothermic reactions shift the equilibrium to the right side of Equation 6.1 allowing higher adsorption. However, the likelihood of an enhanced adsorption reaction by changes in temperature is also dependant on the change in entropy of the system. By the second law of thermodynamics, reactions resulting in systems with greater entropy are more likely to occur, thus favour adsorption. According to all Van't Hoff plots obtained, the ΔS for the adsorption of Fe^{3+} was higher than that of Ni^{2+}. The ΔS of adsorption of Fe^{3+} onto the resin was expected to be larger than Ni^{2+} given its higher valence. Each Fe^{3+} atom adsorbed on the resin losses some of its associated water molecules and exchanges three H^+ ions from the resin. In the adsorption of Ni^{2+} only two H^+ ion are involved. Equation 6.20 and 6.21 provide an oversimplified adsorption reaction of Fe^{3+} and Ni^{2+} assuming each metal adsorbs into adjacent sulfonic and phosphonic groups as show in Figure 3.1. The adsorption of Fe^{3+} (Equation 6.20) results in formation of more chemical species on the right side of the equation than in the adsorption of Ni^{2+} (Equation 6.21). The formation of a higher number of chemical species is entropically favoured.

$$Pol\text{-}SO_3H\text{-}PO_3H_2 + [Fe(H_2O)_6]^{3+} \leftrightarrow Pol\text{-}SO_3^{-}\text{-}PO_3^{2-}\cdot Fe^{3+} nH_2O + 3H_3O^{+}\cdot mH_2O \quad \text{Eq. (6.20)}$$

$$Pol\text{-}SO_3H\text{-}PO_3H_2 + [Ni(H_2O)_6]^{2+} \leftrightarrow Pol\text{-}SO_3H\text{-}PO_3^{2-}\cdot Ni^{2+} nH_2O + 2H_3O^{+}\cdot mH_2O \quad \text{Eq. (6.21)}$$

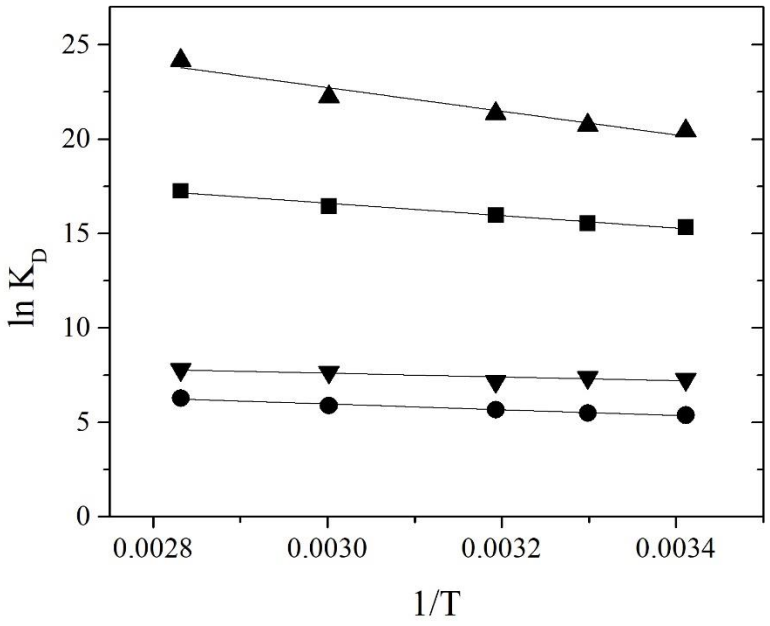

Figure 6.1: Vant Hoff linearization using Debye-Huckel Limit Law (DHLL) for determination of K_D values. (■) ln K_D of $Fe_{Ø}$ systems, (●) ln K_D of $Ni_{Ø}$ systems, (▲) ln K_D of Fe_{Ni} systems, and (▼) ln K_D of Ni_{Fe} systems

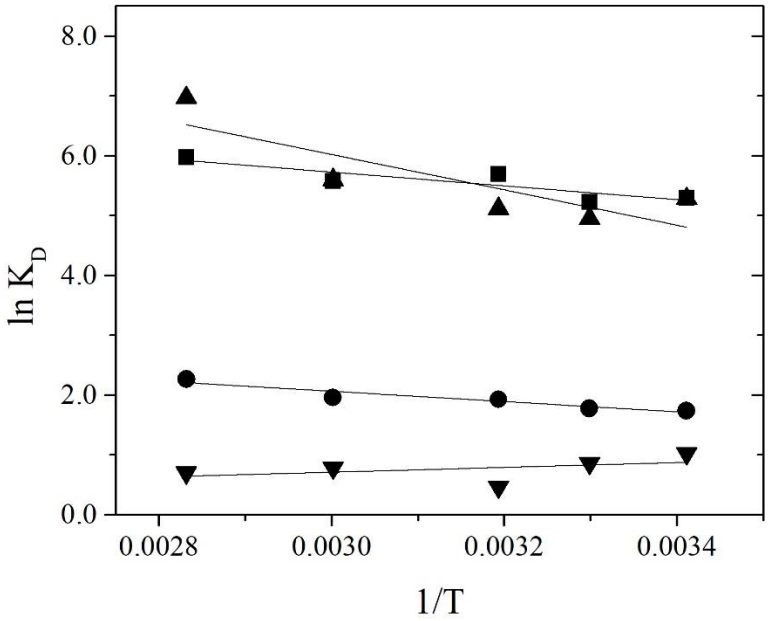

Figure 6.2: Vant Hoff linearization using Extended Debye-Huckel equation (EDH) for determination of K_D values. (■) ln K_D of $Fe_{Ø}$ systems, (●) ln K_D of $Ni_{Ø}$ systems, (▲) ln K_D of Fe_{Ni} systems, and (▼) ln K_D of Ni_{Fe} systems

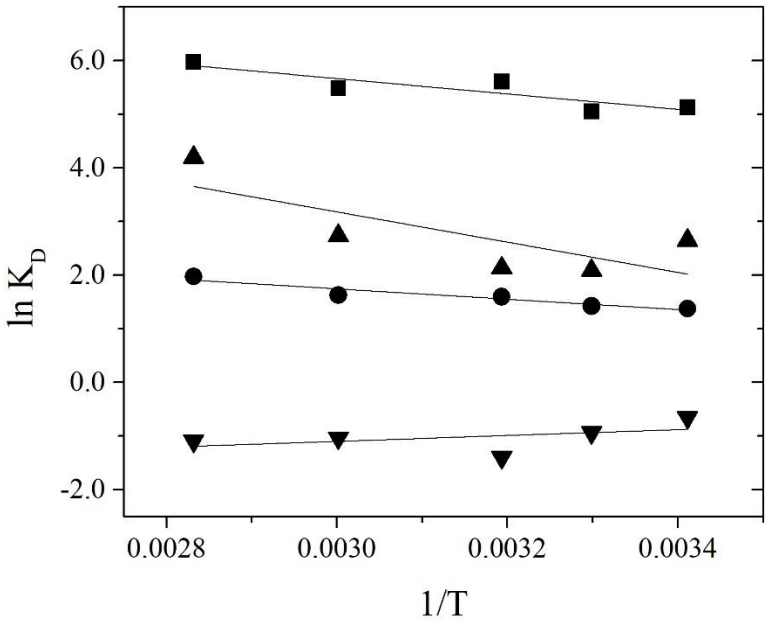

Figure 6.3: Vant Hoff linearization using Davies equation for determination of K_D values. (■) ln K_D of $Fe_{Ø}$ systems, (●) ln K_D of $Ni_{Ø}$ systems, (▲) ln K_D of Fe_{Ni} systems, and (▼) ln K_D of Ni_{Fe} systems

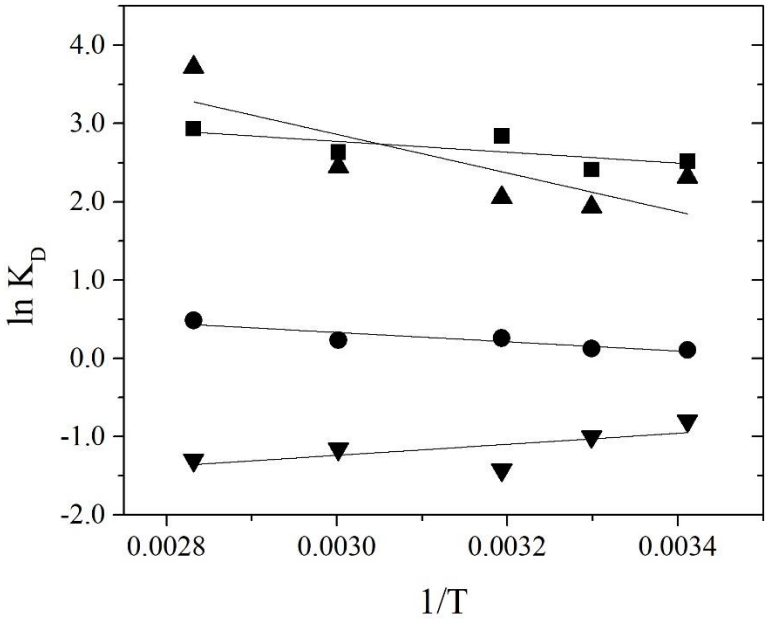

Figure 6.4: Vant Hoff linearization assuming activity coefficients of an ideal solution for determination of K_D values. (■) ln K_D of $Fe_{Ø}$ systems, (●) ln K_D of $Ni_{Ø}$ systems, (▲) ln K_D of Fe_{Ni} systems, and (▼) ln K_D of Ni_{Fe} systems

Figure 6.5 and 6.6 include the variation of the enthalpy and entropy derived from the calculation of activity coefficients by each approximation model. Calculation derived from DHLL showed the smallest values of ΔH while the largest ΔS. The lowest and largest values of ΔH and ΔS obtained by DHLL came as a result of the underestimation of activity coefficients for solutions of high ionic strength. In opposition, the assumption of and ideal solution with activity coefficients equal to the unity showed the largest values of ΔH and smallest of ΔS. It is safe to assume that the real values of enthalpy and entropy for adsorption should fall between the underestimation of DHLL and those obtained by an ideal solution. Given that EDB and Davies' equation are far from the ideality of electrolytes at low concentration, their approximations should fall closer to the actual thermodynamic values of the system. Therefore, the real thermodynamic values should fall between EDB, Davie's, and ideal solution. Regardless, all models indicate that the adsorption of Fe^{3+} in $Fe_{Ø}$ and Fe_{Ni} systems has a greater change in enthalpy than the adsorption of Ni^{2+}. The models also show that Fe^{3+} adsorption is more exothermic than that of Ni^{2+}. Interestingly, Ni^{2+} adsorption in Ni_{Fe} show borderline endothermic properties. This do not imply that Ni^{2+} adsorption changes between exothermic and endothermic properties once iron exists in the system but rather the ΔS for Fe^{3+} adsorption in bimetal systems is far greater than that of Ni^{2+} rendering the adsorption of the later unfavourable (see Figure 6.6).

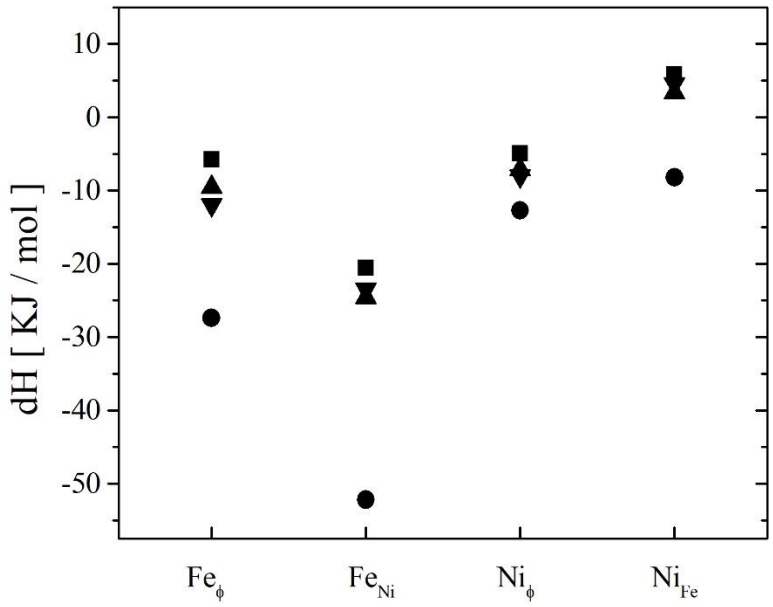

Figure 6.5: Variation of change of enthalpy in Fe$_{Ø}$, Ni$_{Ø}$, Fe$_{Ni}$, and Ni$_{Fe}$ systems (■) assuming activity coefficients of an ideal solution, (●) DHLL, (▲) EDH, and (▼) Davies equations

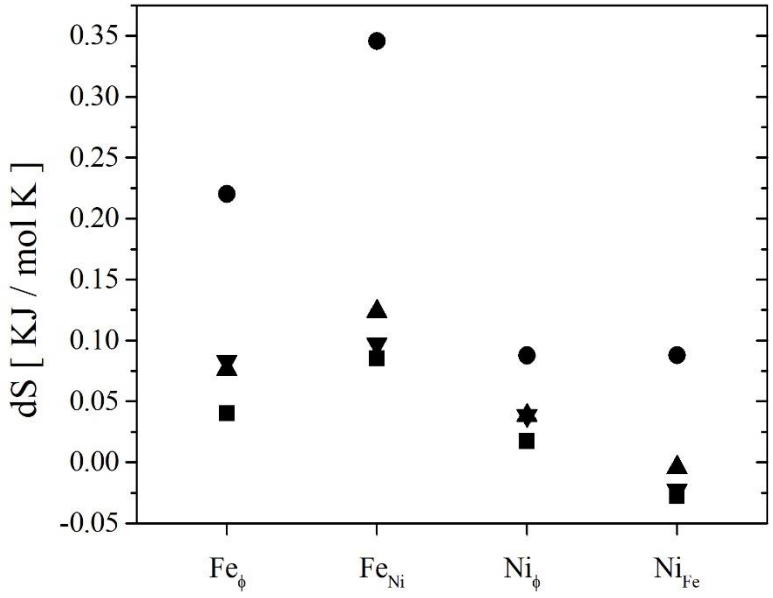

Figure 6.6: Variation of change of entropy in Fe$_{Ø}$, Ni$_{Ø}$, Fe$_{Ni}$, and Ni$_{Fe}$ systems (■) assuming activity coefficients of an ideal solution, (●) DHLL, (▲) EDH, and (▼) Davies equations

The Gibbs energy is used to determine the likelihood for a reaction to occur (See Equation 6.10). Figure 6.7 includes the ΔG values from distribution constant obtained with different activity coefficient models. Our results suggest that only Fe^{3+} showed significant decreases in ΔG as temperature increased. Exergonic reactions having ΔG values lower than zero express that a reaction is spontaneous. Figure 6.7 shows that the adsorption of Fe^{3+} is more likely to occur at higher temperatures, despite showing exothermic characteristics. As described previously, the actual values of Gibbs energy should fall between the predictions using the DHLL model and the assumption of activity coefficient equal to unity and approach the values obtained with Davies and EDH. Figure 6.7 also shows adsorption is borderline spontaneous in Ni_{Fe} and $Ni_{Ø}$ systems for all but DHLL approximations. Based on Van't Hoff plots, ΔS for the adsorption of Ni^{2+} approached zero in $Ni_{Ø}$ systems and had negative values in Ni_{Fe} systems (See Figure 6.6). These observations confirm that Ni^{2+} adsorption reactions are less favourable than Fe^{3+}. Thus, confirming preference of iron adsorption on resins containing a combination of phosphonic and sulfonic groups despite increases in temperature as observed in Figure 3.21 a2 showing the effects of temperature on Fe:Ni adsorption.

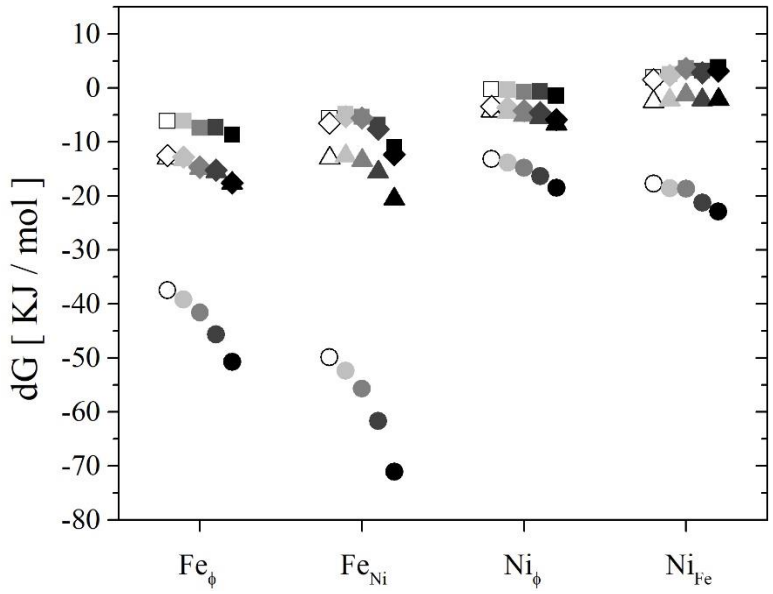

Figure 6.7: Distribution of Gibbs energy obtained by assuming activity coefficients of an ideal solution (squares), DHLL (circles), EDH (triangles), and Davies (diamonds) for $Fe_{Ø}$, $Ni_{Ø}$, Fe_{Ni} and Ni_{Fe} systems. The changes in color from white to black correspond to increases in temperature ranging from 20°C to 80°C, respectively

6.4.2 Kinetic analysis

The highest yield of metal separations with ion exchange resins do not necessarily occur at equilibrium. Instead, it can occur at any time before equilibrium. An analysis of the ratio of Fe^{3+} and Ni^{2+} adsorbed per gram of resin (See Figure 6.8) shows that in monometallic systems ($Fe_{Ø}$ and $Ni_{Ø}$) the resin adsorbs both metals rapidly. However, in bimetallic systems (Fe_{Ni} and Ni_{Fe}) the amount of Ni^{2+} adsorbed decreases significantly in presence of Fe^{3+} while the Fe^{3+} adsorption is less affected by Ni^{2+}. In both systems (mono and bimetallic), the adsorption of Ni^{2+} reaches an apparent equilibrium after 30 min, while the adsorption of Fe^{3+} continues to increase until approximately 60 min. However, in bimetallic system Ni^{2+} adsorption start to increase once Fe^{3+} adsorption stabilizes after 120

min. This confirms that the time to achieve high selectivity depends not only on the adsorption rate of each of the adsorbates but also some interaction between them. Therefore, this suggests that long contact periods are not necessarily beneficial for higher selectivity highlighting the importance of the kinetic studies.

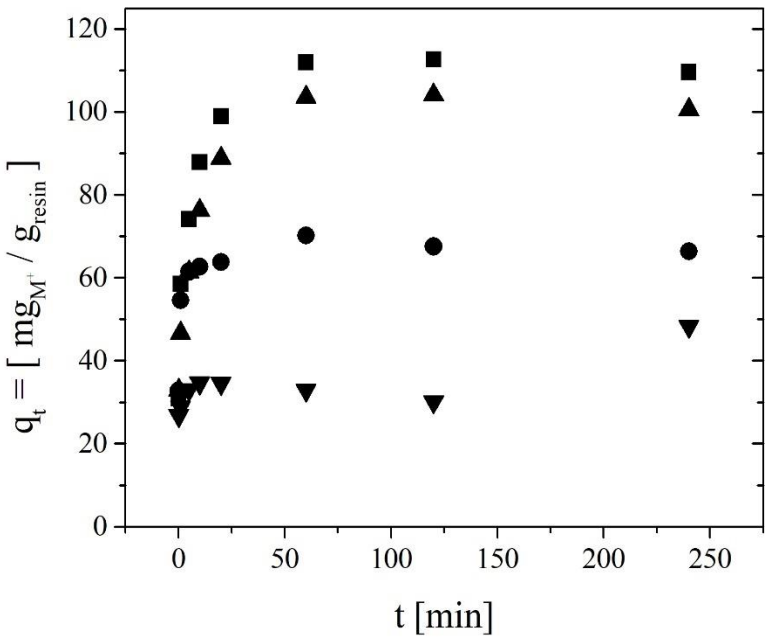

Figure 6.8: Metal adsorption capacity with respect of time. Adsorption of: (■) Fe^{3+} in $Fe_{Ø}$ systems, (●) Ni^{2+} in $Ni_{Ø}$ systems (▲) Fe^{3+} in Fe_{Ni} systems, and (▼) Ni^{2+} in Ni_{Fe} systems

Although kinetic experiments were over 24 h, the PFO generally is limited in representing adsorption where experimental times exceed 30 min and/or in concentrated solutions (Tran et al., 2017). Figure 6.9 shows the linear fit of the PFO using Equation 6.12. A nonlinear regression was also done using the linear model parameters as a basis. Table 6.5 compiles the calculated data for k_1, q_E, and the R^2 correlations for the linear and nonlinear fit for the PFO. The PFO obtained approximated q_E with respect to the

experimental data however; the R^2 was lower than 0.82 with a difference between linear and non-linear kinetic constant of three to four orders of magnitude. The calculation of chi-square (χ^2) values for non-linear PFO confirm significant difference between the values obtained by the model and the experimental data. Given the poor estimation of k_1 values, low R^2, and high χ^2, PFO fails to describe the adsorption kinetics at the given experimental conditions.

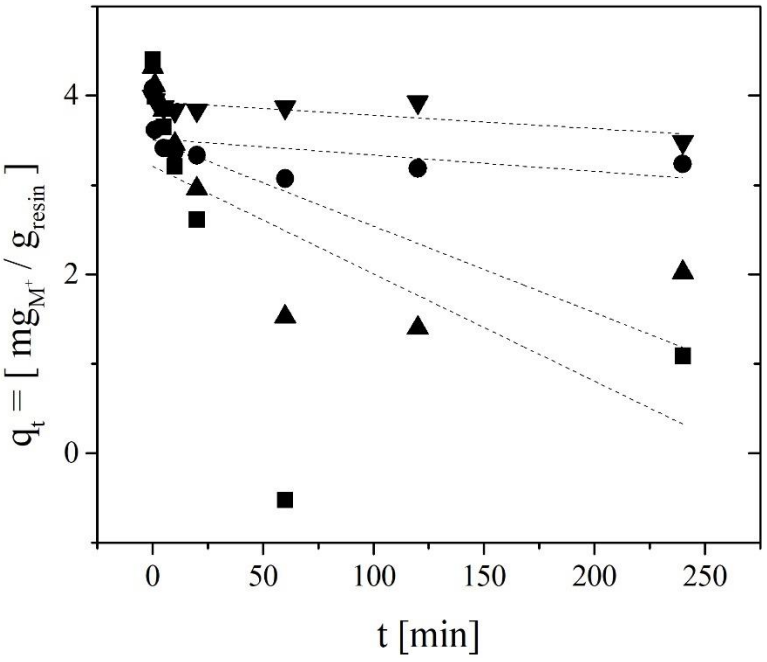

Figure 6.9: Pseudo First Order (a.k.a, Lagergren's first order rate expression) plot for (■) Fe^{3+} in $Fe_{Ø}$ systems, (●) Ni^{2+} in $Ni_{Ø}$ systems (▲) Fe^{3+} in Fe_{Ni} systems, and (▼) Ni^{2+} in Ni_{Fe} systems

Calculation of PSO obtained q_E values were close to those observed experimentally (See Table 6.6). Figure 6.10 shows the linear regression of PSO using Equation 6.14. Overall, R^2 values of PSO were higher than those on PFO for all systems but Ni_{Fe}.

Similarly, PSO maintained consistency among the calculation of kinetic constant for all but Ni_{Fe}. Lastly, χ^2 values resulted half of those with PFO for all but Ni_{Fe}. The low correlation for Ni_{Fe} systems with PFO and PSO infers a complex metal-metal and metal-resin interactions, which complicates the kinetics making these simplified models impractical.

Table 6.5: Comparison of kinetic parameters for metal adsorption using linear and non-linear forms of PFO

System	$q_{e\text{ - exp}}$ [mg/g]	Linear Pseudo first order			Non-linear Pseudo first order			
		q_{e-calc} [mg/g]	k_1 [min^{-1}]	R^2	q_{e-calc} [mg/g]	k_1 [min^{-1}]	R^2	χ^2
$Fe_{Ø}$	112.59	24.78	0.012	0.2225	99.49	0.946	0.6817	275.222
$Ni_{Ø}$	91.83	33.74	0.002	0.1172	63.83	7.144	0.8215	25.466
Fe_{Ni}	108.17	33.44	0.010	0.4055	96.58	0.256	0.5662	324.913
Ni_{Fe}	80.90	51.01	0.002	0.6062	34.60	14.847	0.0425	41.029

Table 6.6: Comparison of kinetic parameters for metal adsorption using linear and non-linear forms of PSO

System	$q_{e\text{ - exp}}$ [mg/g]	Linear Pseudo second order			Non-linear Pseudo second order			
		q_{e-calc} [mg/g]	k_2 [mg/g·min^{-1}]	R^2	q_{e-calc} [mg/g]	k_2 [mg/g·min^{-1}]	R^2	χ^2
$Fe_{Ø}$	112.59	110.99	0.008	0.9995	105.71	0.010	0.8291	147.80
$Ni_{Ø}$	91.83	66.67	0.104	0.9997	65.33	0.138	0.9257	10.61
Fe_{Ni}	108.17	102.15	0.007	0.9992	98.77	0.006	0.7384	195.96
Ni_{Fe}	80.90	44.68	0.002	0.9228	34.96	0.810	0.0914	38.93

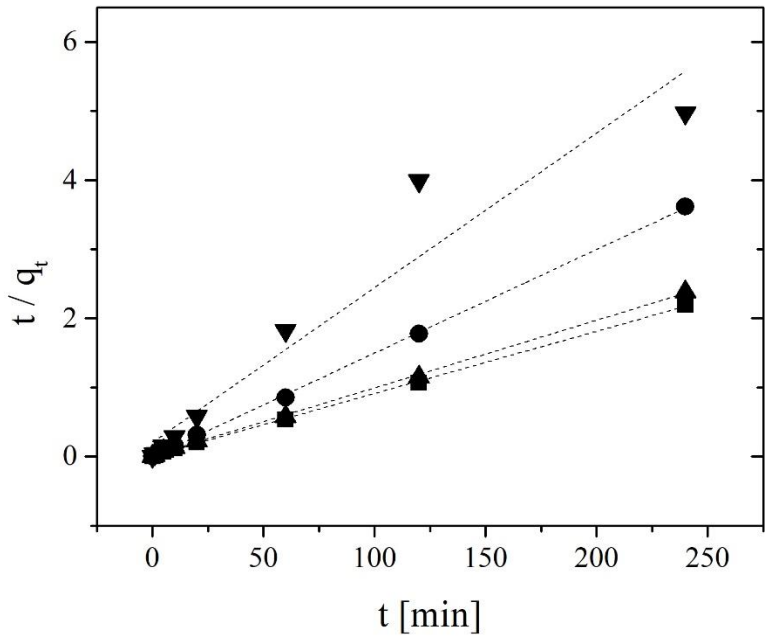

Figure 6.10: Pseudo Second Order plot for (■) Fe^{3+} in $Fe_{Ø}$ systems, (●) Ni^{2+} in $Ni_{Ø}$ systems (▲) Fe^{3+} in Fe_{Ni} systems, and (▼) Ni^{2+} in Ni_{Fe} systems

The results obtained indicate that the adsorption kinetics of Fe^{3+} among solutions containing Ni^{2+} can be described to some extent with linear PSO. Figures 6.11-6.14 compare PFO and PSO models for Fe and Ni in monometallic and bimetallic systems. However, a comparison among PSO models (see Table 6.6) shows a decrease in R^2 values between the linear and non-linear regression. Tran et al. (2017) proposed that lower R^2 values between linear and non-linear regression indicates that an undefined transport phenomena might be influencing the metal adsorption rate. Analysis of monometallic systems show that adsorption of both metals occurs early in the process, and this is in accordance to published data elsewhere (Halder et al., 2016; Sharma et al., 1990). However, once there are two metal ions in a solution, any metal having high affinity towards the resin displaces any low affinity metal adsorbed early in the process (see Section

3.4.2.4 and 4.4.2.3). Accordingly, the amount of Ni^{2+} initially adsorbed decreased over time leading to higher Fe^{3+} adsorption. Nevertheless, metal desorption also occurred for Ni^{2+} in $Ni_{Ø}$ systems and to a lesser extent for Fe^{3+} in Fe_{Ni} and $Fe_{Ø}$. This phenomenon of desorption close to equilibrium is also reported in the literature (Halder et al., 2016; Sharma et al., 1990).

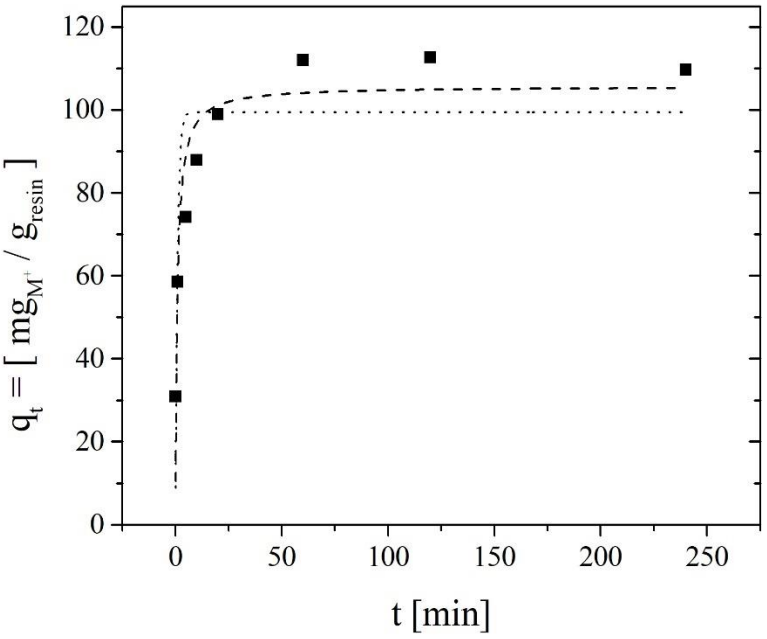

Figure 6.11: Comparison between non-linear PFO (dotted line) and PSO (dashed line) for the description of Fe^{3+} adsorption in $Fe_{Ø}$ systems

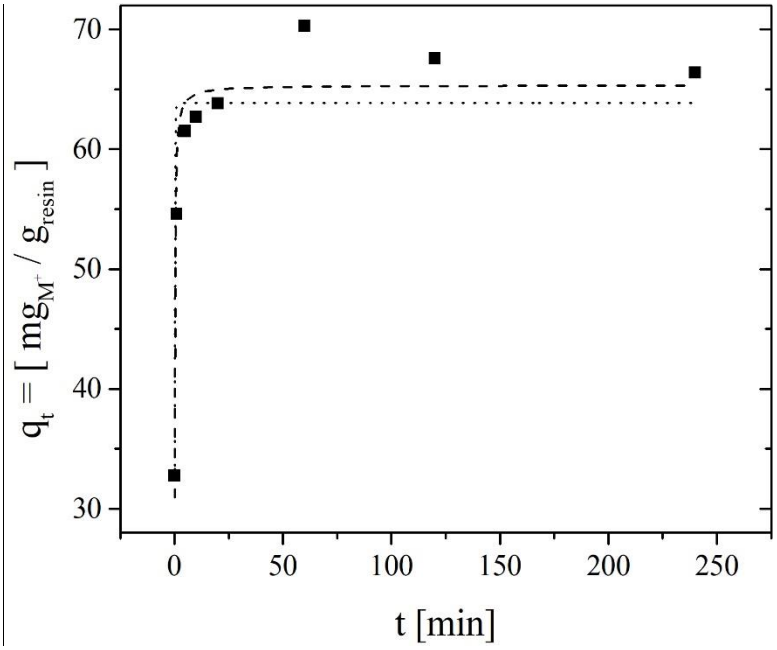

Figure 6.12: Comparison between non-linear PFO (dotted line) and PSO (dashed line) for the description of Ni^{2+} adsorption in $Ni_{Ø}$ systems

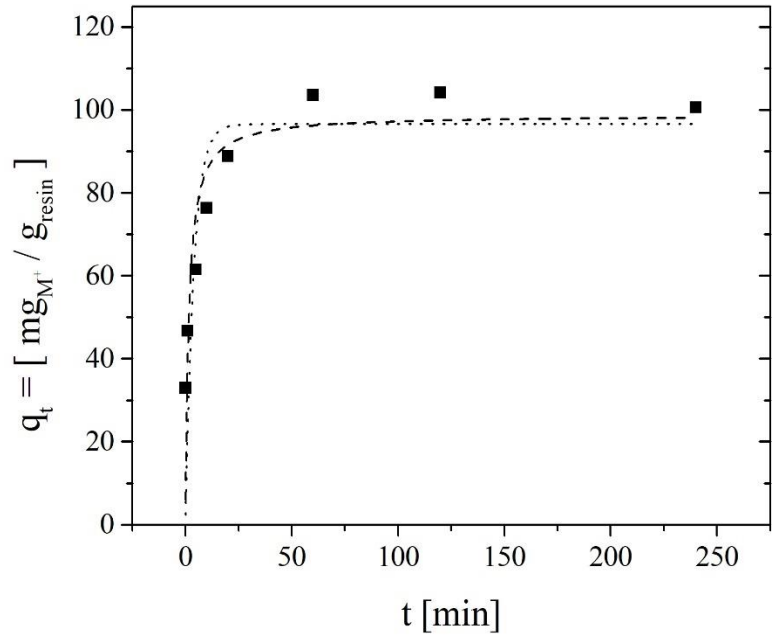

Figure 6.13: Comparison between non-linear PFO (dotted line) and PSO (dashed line) for the description of Fe^{3+} adsorption in Fe_{Ni} systems

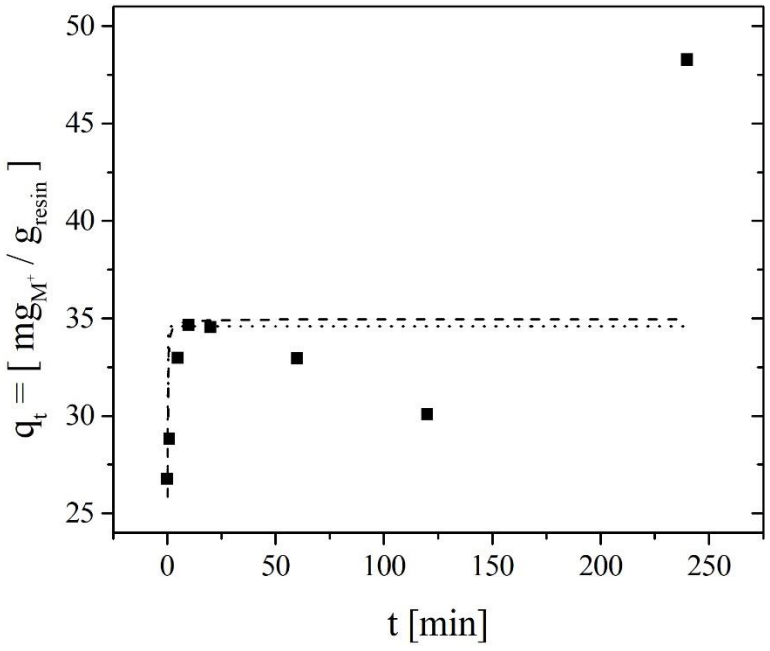

Figure 6.14: Comparison between non-linear PFO (dotted line) and PSO (dashed line) for the description of Ni^{2+} adsorption in Ni_{Fe} systems

Mathematical models such as the Elovich equation include the effect of desorption rates close to equilibrium to achieve greater approximations to the adsorption behavior (Aharoni and Tompkins, 1970). Although initially developed to describe the process of gas adsorption on hygroscopic ore, the Elovich equation is widely used to describe chemisorption that includes near-equilibrium desorption phenomena on aqueous media. The Elovich equation takes the integrated non-linear form as follows:

$$q_t = \frac{1}{\beta}\ln(1 + \alpha\beta t) \qquad \text{Eq. (6.22)}$$

with its respective linear form as:

$$q_t = \frac{1}{\beta}\ln(t) + \frac{1}{\beta}\ln(\alpha\beta) \qquad \text{Eq. (6.23)}$$

where α is the initial rate constant in mg/g·min, β is the desorption constant in mg/g. A plot of q_t versus ln (t) provides the linear equation with a slope of $1/\beta$ and intercept at $1/\beta \cdot \text{Ln}(\alpha \cdot \beta)$. Figure 6.15 includes the linearization of the Elovich equation for Fe^{3+} and Ni^{2+} in mono and bimetallic systems. The correlation R^2 for linear Elovich equation was between 0.88 - 0.90 for Fe^{3+} and 0.46 and 0.85 for Ni^{2+} with β desorption constants of 0.10-0.11 mg Fe^{3+}/g resin-min and 0.20-0.24 mg Ni^{2+}/g resin-min. Elovich model obtained the lowest β values in mono-metallic systems similar to the desorption observed in Figure 6.7. However, the results obtained for the initial rate constant α were well above that observed experimentally reaching orders of several grams of metal adsorbed per gram of resin per minute. Experimentally, the highest adsorption values remained between 0.1 - 0.2 gM^{+}/g resin in periods of 2 h. The Elovich equation determines the initial rate constant by assuming $t >> 1/\alpha \cdot \beta$ (Aharoni and Tompkins, 1970). In other words, the product $\alpha \cdot \beta \cdot t >> 1$ in Equation 6.22 must meet the boundary conditions of $q_t \geq 0$ and $t \geq 0$ (Tran et al., 2017). The results obtained show that the maximum adsorption per gram of resin was on average approximately 60 min. Published literature showed increasing q_t even after 600 min (Juang and Chen, 1997; Wu et al., 2009). It is then possible that at the experimental conditions used, the time necessary to reach equilibrium was not large enough to satisfy the conditions of $t >> 1/\alpha \cdot \beta$ of the simplified Elovich equation. Consequently, the use of Elovich calculation resulted in large initial rate constant. Similarly, it is fair to assume that the adsorption of Fe^{3+} and Ni^{2+} on ion exchange resins does not follow a chemisorption

mechanism. Therefore, estimations with Elovich's equation resulted in low correlation with the experimental data. Since it was not possible to obtain reliable data on the heat of adsorption for Fe^{3+} and Ni^{2+}, it is not possible to confirm that the rate of adsorption is not defined by chemisorption mechanism as suggested by Elovich's equation (Inglezakis and Zorpas, 2012).

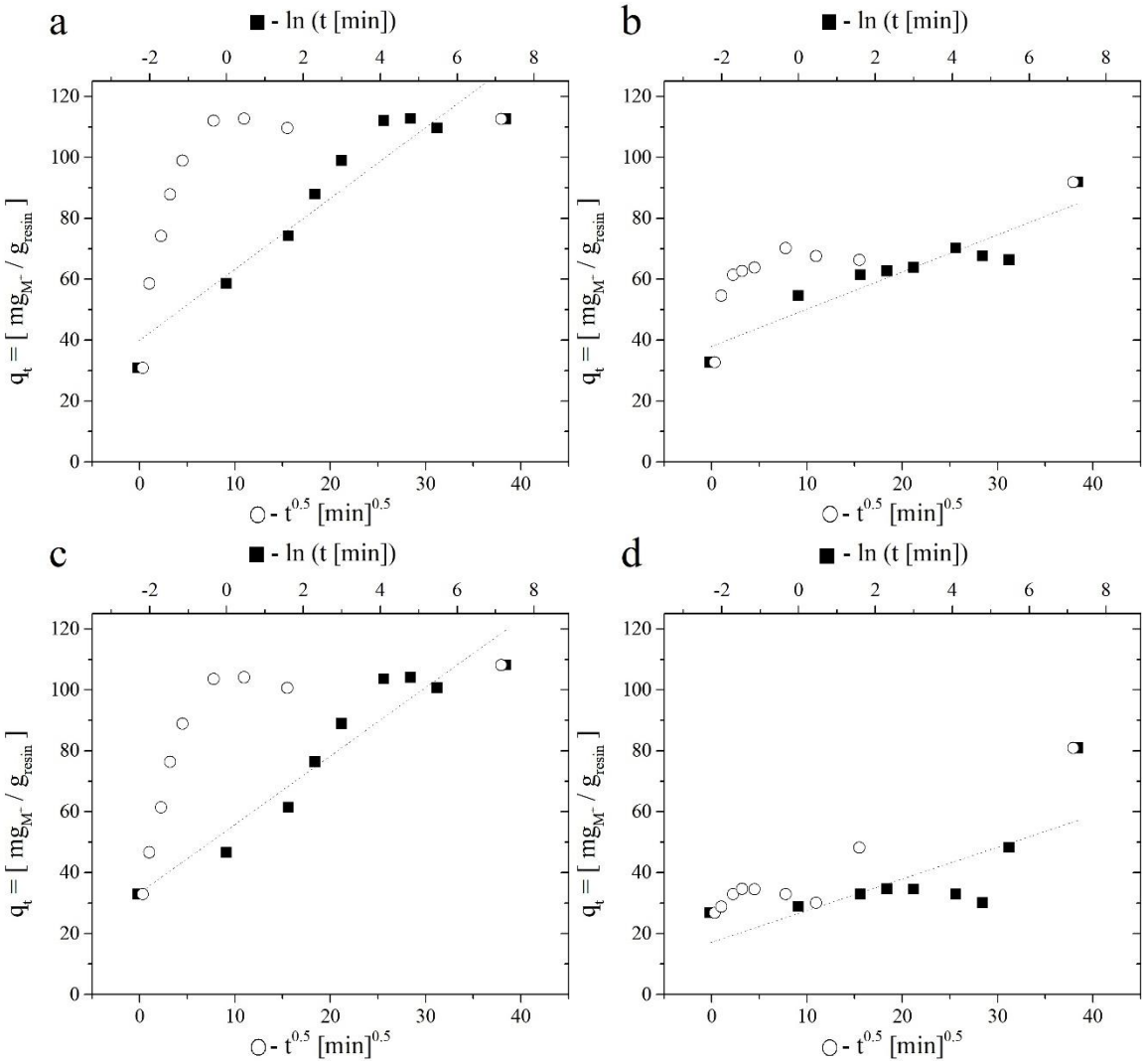

Figure 6.15: Linearization of (■) Elovich and (○) Intraparticle diffusion equation for (a) Fe^{3+} in $Fe_{Ø}$ systems, (b) Ni^{2+} in $Ni_{Ø}$ systems (c) Fe^{3+} in Fe_{Ni} systems, and (d) Ni^{2+} in Ni_{Fe} systems

Given that ion exchange reactions occur within the cross-linked body of the resins, the rate of the adsorption may be dependent on intra-particle diffusion phenomena (IPD). IPD equation confirmed that some type of diffusion phenomena governs the rate of adsorption of Fe^{3+} and Ni^{2+}. IPD has the linear form of:

$$q_t = k_p\sqrt{t} + C \qquad \text{Eq. (6.24)}$$

Where k_p is the rate constant of IDP in mg/g·min$^{0.5}$ and C a constant associated with the thickness of the boundary layer in mg/g. High linear IDP correlations with experimental data with boundary conditions at t = 0 represent characteristic conditions of adsorption governed by intraparticle diffusion. In contrast, if IDP plot shows more than one linear region , then the adsorption process may be related to several types of transport phenomena such as bulk transport, film diffusion, intraparticle diffusion, and or general adsorption (Weber and Smith, 1987). Figure 6.15 shows that none of the linearization of IDP are a straight line towards the origin. Instead, all plots showed discontinuities suggesting other types of transport phenomena involved in the adsorption of Fe^{3+} and Ni^{2+}. However, further experiments are required to identify the types of transport ruling adsorption rates.

Comparisons between PFO, PSO, Elovich, and IDP suggest that PSO maintains the highest correlation between the calculated and experimental data (See Table 6.7). High correlation of PSO with metal adsorption trends was observed by other researchers (Blanchard et al., 1984; Davidescu et al., 2013; Tran et al., 2017). Some scholars suggest that adsorption trends with high correlations to PSO represent mechanisms governed by chemisorption. However, adsorption mechanism cannot be directly assigned based on

observing simple kinetic experiments. Given the three linear regions obtained with IPD is possible to assume that different forms of diffusion may rule the overall adsorption kinetics of Fe^{3+} and Ni^{2+} on ion exchange resins having a combination of phosphonic and sulfonic groups. Further experimentation are required identify the type of diffusion (if any) ruling the adsorption mechanism.

Table 6.7: comparison of R^2 for the linear and non-linear forms of PFO, PSO, Elovich, and IPD equation

System	PFO	NL PFO	PSO	NL PSO	Elovich	IPD
$Fe_{Ø}$	0.9911	0.6817	0.9995	0.8291	0.8813	--
$Ni_{Ø}$	0.4360	0.8215	0.9997	0.9257	0.8501	--
Fe_{Ni}	0.9610	0.5662	0.9992	0.7384	0.9041	--
Ni_{Fe}	-0.0325	0.0425	0.9228	0.0914	0.4568	--

6.5 Conclusion

The high concentrations of the system made it difficult for the calculations of the thermodynamic characteristics of the adsorption of Fe^{3+} and Ni^{2+} in ion exchange resins with a combination of phosphonic and sulfonic groups. However, approximations of the activity coefficients under the experimental conditions were used to obtain qualitative information. The activity coefficients were approximated using the Debye-Huckel limiting Law, Extended Debye Huckel, and Davies equations. Due to the high concentrations of the system, the activity coefficients obtained are below the real values. Therefore, calculations of activity coefficients assuming unity served as a reference for the upper limit conditions.

Results showed that the adsorption of Fe^{3+} in ion exchange resins was favourable. It showed exothermic and exergonic characteristics with positive changes in entropy

obtaining ΔS values ranging from 40 to 220 J/mol·K and ΔH ranging from -27,380 J/mol to -5,760 J/mol. These thermodynamic property trends were maintained regardless of changes in temperature and the presence of Ni^{2+} (ΔS values ranging from 85 to 345 J/mol·K. and ΔH ranging from -52,190 J/mol to -20,530 J/mol). In contrast, the adsorption of Ni^{2+} was only favourable in monometallic $Ni_{Ø}$ systems. Ni^{2+} adsorption in $Ni_{Ø}$ systems presented exothermic and exergonic characteristics with positive changes in entropy (ΔS values ranging from 17 to 88 J/mol·K. and ΔH ranging from -12,690 J/mol to -4,945 J/mol) However, if Fe^{3+} was present in the system, the changes in entropy for Ni^{2+} adsorption tended to negative values while the Gibbs energy were positive (ΔS values ranging from -27 to 87 J/mol·K. and ΔH ranging from -8,249 J/mol to 5850 J/mol), that is the adsorption was not favourable. These observations were confirmed by the low adsorption percentages of Ni^{2+} in Ni_{Fe} systems compared to those obtained in $Ni_{Ø}$ systems.

The results obtained with the PFO and PSO models for the reaction kinetics were in accordance with other results found in the literature. In general, PSO had a higher correlation than PFO. Nonetheless, the degree of correlation decreased between PSO in linear and non-linear form suggesting that the adsorption rate may be governed by unknown transport phenomena not described by the model. It is possible that the discrepancies of all the reaction kinetic models are due to high concentrations of the system. Since it was not possible to obtain reliable data for the heat of adsorption, it was not possible to identify chemisorption or physisorption as main adsorption mechanism. However, due to the low correlation of Elovich equations it was possible to assume that adsorption on ion exchange resins are not due chemisorption. Data fitting with IPD

equation suggests that metal adsorption by cation exchange resins is governed by more than one transport phenomenon. To determine the transport phenomena governing the reaction kinetics, further experiments are recommended.

Chapter 7 Future studies and conclusions

7.1 Future Studies

7.1.1 Adsorption mechanism

The determination of Fe and Ni adsorption mechanism on resins containing a combination of phosphonic and sulfonic groups helps on the identification of better conditions for separation yield improvements. The heat of adsorption, adsorption energy, and the reaction kinetic model that best describes the adsorption process can predict the type of reaction mechanism. Since it was not possible to obtain reliable data on the heat of adsorption or adsorption energy for Fe^{3+} and Ni^{2+}, it is not possible to suggest the mechanism ruling the adsorption of Fe^{3+} on resins with a combination of phosphonic and sulfonic groups. Table 7.1 include a summary of the parameters commonly observed on studies for different types of adsorption mechanisms in aqueous media. Aside the difficulties in obtaining accurate thermodynamic information, kinetic models like PSO or Elovich equation failed to describe the adsorption behavior. Kinetic models like IPD suggested that the adsorption mechanism might include several types of unknown of transport phenomena (See Section 6.4.2).

Studies to obtain close approximations of thermodynamic equilibrium constant of adsorption reactions at high electrolyte concentrations could clarify the reaction mechanism. For this, Pitzer equations and Monte Carlo simulations are recommended for

the calculation of activity coefficients of electrolyte concentrations as high as 6.0 M (Abbas and Ahlberg, 2019). Additionally, column experiment could aid to address the identification of transport phenomena affecting the rate of adsorption (Gao et al., 2018a). Although, the determination of the adsorption mechanism should be confirmed by analytical techniques such as FTIR, SEM, XPS, Raman spectroscopy, TGA/DTA, DSC, Boehm titration, and solution calorimetry.

Table 7.1: Parameter limits for types of adsorption mechanism based on Inglezakis and Zorpas (2012).

	Heat of adsorption (kJ/mol)	**Adsorption energy (kJ/mol)**	**Activation energy (kJ/mol)**
Ion Exchange	<40	8 – 16	24 – 40
Physisorption	40 – 80	< 8	< 40
Chemisorption	>80	> 16	> 40

The initial studies for the determination of adsorption mechanism included the analysis of FTIR spectra of best performer resin (see Figures 7.1–7.3). The identification of characteristic bands of P–O, P=O, S–O, S=O, P–O–H, S–O–H corresponding to the resins with a combination of phosphonic and sulfonic groups (See Figure 3.1 for molecular diagram of the resin) confirmed that the Fe^{3+} adsorption is more than a physisorption mechanism. Table 7.2 includes the characteristic bands of interest for Puromet MTS9570 with the corresponding shifts on wave number for resin before and after adsorption. The peak shifts and the increased intensity of the bands characteristic of the sulfonic (996 cm^{-1}) and phosphonic groups (1668 cm^{-1}) after the sorption process prove that the functional groups are involved in binding of Fe^{3+}. Similar results were obtained by Kołodyńska et al. (2020)

Table 7.2 Some fundamental frequencies for bond assignment deformation of Puromet MTS9570 before and after adsorption in synthetic Fe:Ni leach solution

Bond assignment deformation		Expected band [cm^{-1}]	Observed band Before adsorption [cm^{-1}]	Observed band After adsorption [cm^{-1}]
Aliphatic C–H stretching of CH_2	(Cortina et al., 1994)	2926 - 2920	2911	2924
Aliphatic C–H stretching of CH_3	(Liu et al., 2012)	2865 - 2851	2854	2855
P–O–H stretching	(Kołodyńska et al., 2020)	2280	2290	2292
S–O–H stretching	(Kołodyńska et al., 2020)	2109	2118	2115
P–O–H deformation	(Cortina et al., 1994)	1687	1668	1634
C=C ring stretching	(Cortina et al., 1994)	1490-1452	1484	1484
C–H deformation of CH_3	(Cortina et al., 1994)	1381	1408	1408
P=O stretching	(Cortina et al., 1994)	1228		
P=O stretching	(Kołodyńska et al., 2020)	1132	1123	1131
Sulfates	(Bellamy, 1975)	1130-1080	1077	1073
S=O stretching	(Kołodyńska et al., 2020)	989	996	1019
C-H ring/out of plane deformation	(Bellamy, 1975)	900-860	939	953
C–H out of plane flexion	(Cortina et al., 1994)	832	843	843
Other deformations for P, S			412	426

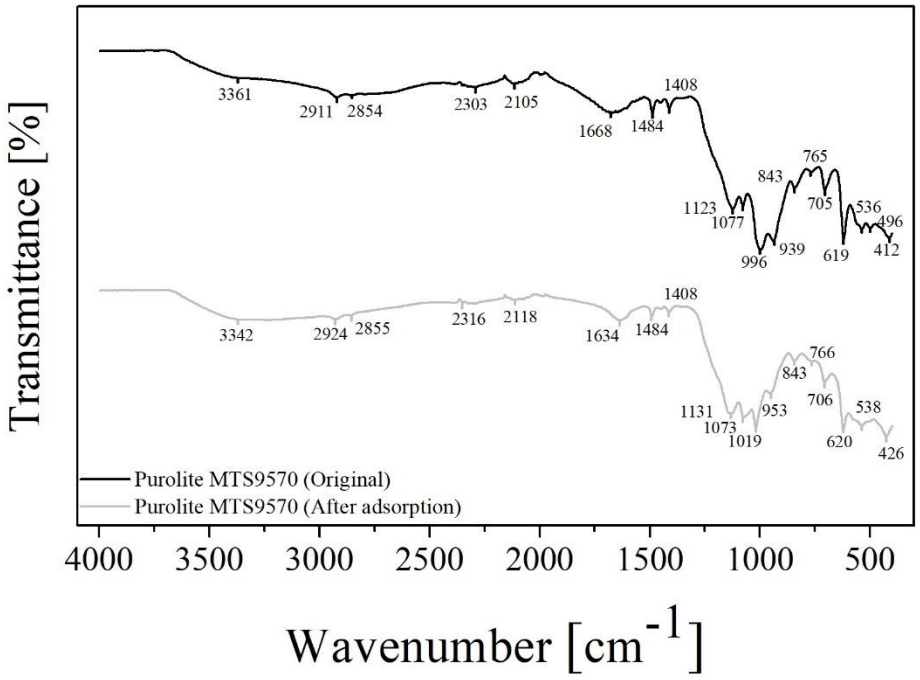

Figure 7.1: FTIR spectra of Puromet MTS9570 (Previously Purolite S957) before and after metal adsorption

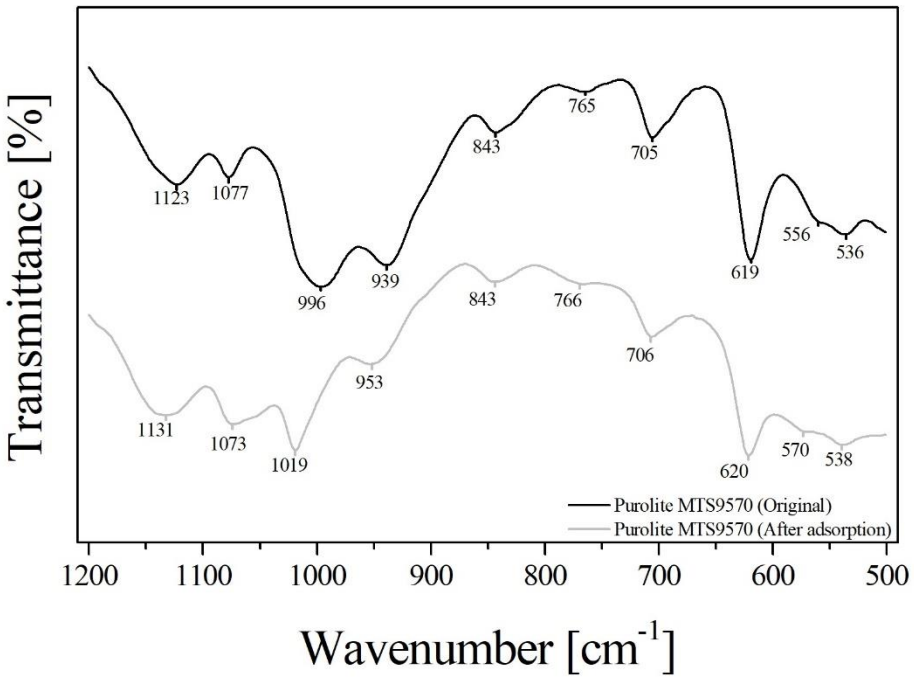

Figure 7.2: FTIR of Puromet MTS9570 before and after metal adsorption on the 500-1200 wavenumber region

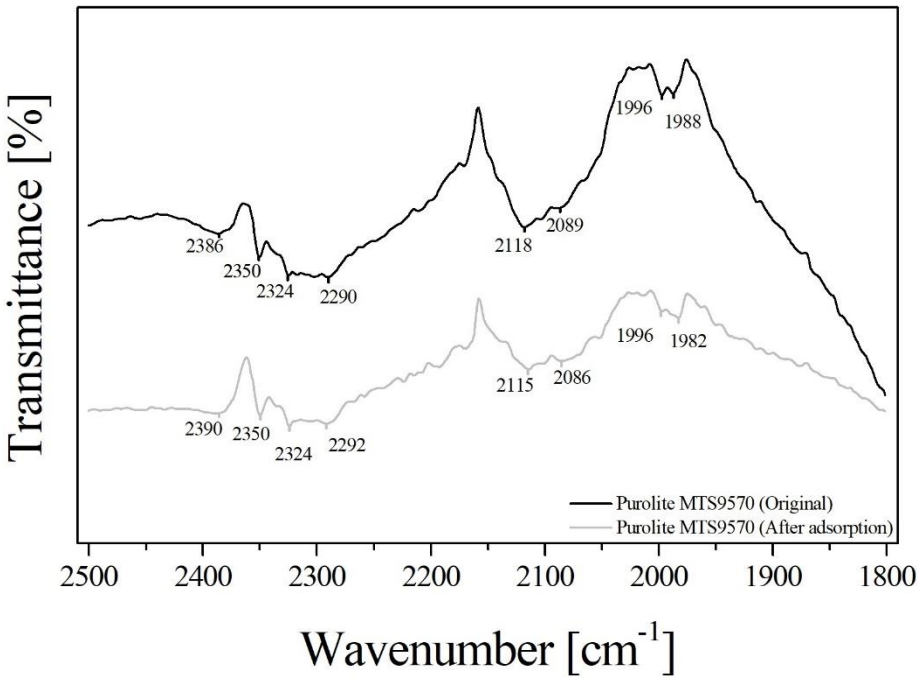

Figure 7.3: FTIR of Puromet MTS9570 before and after metal adsorption on the 1800-2500 wavenumber region

The shifts in wavenumber for the characteristic peaks for phosphonic and sulfonic groups suggest some form of Fe^{3+} bonding with the resin. However, given that resins with a combination of phosphonic and sulfonic groups have chelating and strong cation exchange properties, the shifts in wavenumber cannot confirm the mechanism for Fe^{3+} adsorption. Adsorption of Fe^{3+} could occur through ion exchange, electrostatic interaction, or complexation (Kołodyńska et al., 2020). Further studies on SEM, XPS, Raman spectroscopy, TGA/DTA, DSC, Boehm titration, and solution calorimetry are recommended to clarify the main mechanism for Fe^{3+} adsorption.

7.1.2 Fixed bed column experiments

One of its main advantages of this type of reactors is the option to identify the precise amount of solute required to saturate a determinate amount of resin. Thus, the required volume of solution to reach saturation. Fixed bed systems consist of a cylindrical reactor that contains a static amount of resin that is continuously flowed with a solution containing the solute of interest (See Figure 5.1). This information allows a more accurate determination of adsorption mechanisms and transport phenomena involved in the adsorption and the development of mathematical models to simulate and predict the adsorption behavior reducing the need of experimental work. This allows the study of more variables affecting the adsorption behavior leading to faster optimizations of operating parameters, design, and scale up.

Several mathematical models for dynamic adsorption process have been developed for adsorption of metals in column reactors. Mathematical models require the identification of adsorption mechanism, individual kinetic models for each adsorption step, mass transfer kinetics, and type of transport phenomena involved in adsorption (Gao et al., 2018a). All of this information can be obtained relatively easy through column reactor experimentation. However, extensive experimental work would be required if such information is obtained through batch experiments with stirred reactors as contained in this work.

7.1.3 Accurate determination of thermodynamic information

The high concentrations of the system made it difficult for the calculations of the thermodynamic characteristics of the adsorption of Fe^{3+} and Ni^{2+} in ion exchange resins with a combination of phosphonic and sulfonic groups. For this, Pitzer equations and Monte Carlo simulations are recommended for the calculation of activity coefficients of electrolyte concentrations as high as 6.0 M (Abbas and Ahlberg, 2019). However, both approximation require extensive experimental data, fitting parameters, and substantial computational resources to obtain reliable calculations. Therefore, it is recommended to conduct studies that focus exclusively on the prediction of thermodynamic data on system emulating the conditions of leach liquors of Ni hydrometallurgy plants.

7.1.4 Scale up process

Studies of scale up process can confirm the feasibility of ion exchange for Fe^{3+} removal from concentrated leach liquors in hydrometallurgy plants. Scale up processes have particular conditions hard to emulate in bench scale work. Among them, a rich mix of different metal ions in solution that can compete against Fe^{3+}, solution chemistry, precipitates, and other physical impurities (e.g., sand) that might foul the resin preventing the high yields of Fe^{3+} adsorption observed at bench scale.

Ion exchange at industrial scale mostly focus on the metal recovery of diluted solution. To confirm ion exchange as a potential alternative for Fe^{3+} removal from Ni^{2+} hydrometallurgy plants, resins should perform effectively at solutions of high concentration. To confirm opportunities for Fe^{3+} co-beneficiation whether in RIP (see

Figure 5.2) or in column reactors (See Figure 5.1), it is necessary to confirm best performance conditions of the resins at large scale.

7.1.5 Green chemistry

Different resins containing similar functional groups showed similar adsorption trends. Although the results differed from one another it is possible to assume that this differences are intrinsic to resins specifications and not the functional group. Therefore, it is possible to assume that a functional group could be attached to any substrate, which in consequence would produce similar selectivity trends. This is particularly important for research focused on the development of new biomaterials for metal separation, concentration, and recovery.

There are three major streams in the production of green adsorbents for the separation of heavy metal from liquid media. First, the functionalization of carbon sources such as carbon, biochar, agricultural waste, etc to enhance adsorption characteristics (Gomez et al., 2014). Second, the use of microorganism for the bioaccumulation of the metals (Duprey et al., 2014). Third, the functionalization of natural occurring polysaccharides and other natural resins for ion exchange (Gao et al., 2018b).

Gomez et al., (2014) reported that the xanthate activation of subbituminous coal presented similar Hg, and a slightly lower Cd extraction to extractions obtained by commercial resin DOWEX marathon with SCRs sulfonic groups. Similarly, Xu et al., (2011) prepared anion exchange media by modifying wheat straw for the removal of

phosphorous, nitrogen, chromium, and organic dye from synthetic solutions resembling waste water streams in textile industry.

The modification of microbe's dry membrane to act as an ion exchanger fixating quaternary ammonium groups successfully extracted $Ag(CN)_2^-$ from solutions at pH 9-11 and presented good elution potential (Li et al., 2015). Similarly, genetic modification of E.coli allowed the selective sorption of Ni and Co from solutions with low concentration of metals (i.e.: up to 50 μM) allowing its potential for polluted sites reclamation (Duprey et al., 2014).

Cost-effective adsorbents obtained from various biomass materials and waste bio-products employ the chelating properties of natural occurring resins to remove heavy metals and precious metals (Gao et al., 2018b; O'Connell et al., 2008). Algae, fungi, activated sludge, modified waste cellulose and aquaculture waste provide good chemical stability and adsorption selectivity due to hydroxyl, carboxyl or amino groups in polymer chains. Nevertheless, further improvements are required in order to present a feasible alternative for commercial ion exchange resins.

7.2 Conclusions

Ion exchange resins in batch systems at laboratory scale successfully separated Fe^{3+} from synthetic Ni^{2+} leach solutions at high metal concentrations. The adsorption capabilities and selectivity of Fe^{3+} were evaluated in 16 different functionalities represented in 30 commercial ion exchange resins. The functional groups selected were identified as the most commonly found in commercial resins. The type of resins studied included: (i) strong cationic exchangers containing sulfonic acid groups. (ii) weak cationic exchangers containing carboxylic acid groups. (iii) chelating resins containing N-methylglucamine, amidoxime, iminodiacetic acid, bis-picolylamine, phosphinic, phosphoric, thiol, thiourea, isothiouronium, aminophosphonic acid, and combination of sulfonic and phosphonic acid groups. (iv) mixed bed resins containing a combination of quaternary ammonium and sulfonic acid groups. (v) anion exchange resins containing quaternary ammonium groups employed as control group; and (vi) non-functionalized resins employed as blank experiment.

Selectivity studies in bimetallic systems having equimolar concentration of Fe^{3+} and Ni^{2+} suggested that the functional groups that most favoured Fe^{3+} adsorption were aminophosphonic, a combination of phosphonic and sulfonic groups, iminodiacetic, and methylglucamine groups. Resins with carboxylic acid, quaternary ammonium, and amidoxime groups also showed the potential for selective Fe^{3+} removal but the extent of metal adsorption was substantially lower compared to the best performers. Resin with phosphoric and phosphinic underperformed adsorbing Fe^{3+}. Sulfur containing groups as in Thiol, thiourea, isothiouronium, sulfonic acid, and MBR were not selective for Fe^{3+}

adsorption. Contrarily, resins with bis-pycolilamine showed preference for Ni^{2+} adsorption. Results obtained in bimetallic system were in accordance to those published in literature even if the metal concentration in electrolyte was higher than the concentration commonly studied for ion exchange resins.

Selectivity studies in polymetallic systems having containing 70X excess of Ni^{2+}, close to 25X of Cu^{2+}, and equal concentration of Co^{2+} and Fe^{3+} showed that resins containing phosphoric groups and phosphinic groups achieved the best selectivity. Following were resins with a combination of phosphonic and sulfonic groups, carboxylic acid, quaternary ammonium groups, and MBR. The presence of Cu^{2+} in the system altered the Fe^{3+} selectivity in resins containing aminophosphonic, methylglucamine, and amidoxime groups as showed in bimetallic systems. Although these resins obtained high adsorption of Fe^{3+}, they also allowed substantial base metal co-adsorption, particularly Cu^{2+}. The potential for using resins with aminophosphonic, methylglucamine, and amidoxime for selective Fe^{3+} separations may increase in favourable elution processes. Similar case was observed for resins with iminodiacetic acid groups that obtained high Fe^{3+} adsorptions but the adsorption of Cu^{2+} was higher. Resins with bis-pycolilamine, thiourea, isothiouronium, and thiol showed preference for Cu^{2+} adsorption having close to negligible Fe^{3+} adsorption. Lastly, resins with sulfonic groups that did not show metal preference.

As general trend, the results suggest that those resins containing groups cataloged as hard bases on HSAB theory strongly preferred the adsorption of the hard acid Fe^{3+}, those with borderline characteristics did not show preference for either metal ion, and those with soft characteristics either favoured the borderline acid Ni^{2+} or showed poor metal

adsorption. The results are also in accordance to those currently available in literature, even though the metal separation were conducted at high metal concentration and acidic pH fixed to 1.5.

Metal concentration in electrolyte and solution pH were dominant solution factors affecting the adsorption trends in the bulk of resins tested. Low metal concentration decreased the Fe^{3+} selectivity of the resins. At low metal concentration, resins co-adsorbed high amounts of base metals. If metal concentration remained over 20 g/L, resins obtained low base metal co-adsorptions event at low Fe to Ni concentration ratio. Solution pH above 2.2 also increased base metal co-adsorption s. Meanwhile, pH under 1.0 reduced the extent of metal adsorption. These observations were common for all resins showing that solution pH ranging between 1.0 and 2.2 was the option condition for best Fe^{3+} selectivity. Therefore, its concluded that the difference in selectivity by pH outside the 1.0-2.2 range are due to different metal speciation and resin operation limits.

Variations in temperature between 20°C and 80°C had little effect on the metal adsorption trends as metal selectivity trends remained stable. The ranges of temperature were selected based on the temperature fluctuation throughout hydrometallurgy. Thus, confirming the technical feasibility of ion exchange resin despite the variations in temperature throughout all the hydrometallurgy steps. Adsorption selectivity differed in time, suggesting increased adsorption of Fe^{3+} while decreasing the extent of metal co-adsorption. This observation suggest a base metal displacement by Fe^{3+} confirming its adsorption selectivity.

Semi continuous process at consecutive steps enhanced the amount of Fe^{3+} adsorbed by ion exchange resins. Resins containing a combination of phosphonic and sulfonic groups and N-methylglucamine displayed the best properties for Fe adsorption among resins containing carboxylic acid, phosphoric acid, and quaternary ammonium groups. However, as the adsorption of Fe^{3+} increased with each consecutive step so did the co-adsorption of Ni^{2+} reaching values close to the maximum obtained for Fe^{3+}.

Successful separation of Fe^{3+} from base metal electrolytes at concentration commonly found after PL in hydrometallurgy plants suggest the potential of ion exchange to substitute current iron precipitation processes. However, high adsorption of Fe^{3+} is only part of the process, as resins require efficient elution process to conclude potential of high purity iron sub-production. A series of exploratory elution experiments using H_2SO_4 and HCl at different concentration intended to asses the selective removal of Ni^{2+} from the resin. Resins with a combination of phosphonic and sulfonic groups showed the best Ni^{2+} elution properties. The rest of the resins had relative selectivity for Ni^{2+} or Fe^{3+} elution but underperformed compared to resins with a combination of phosphonic and sulfonic groups. Conversely, resins containing N-methylglucamine had high percentages of metal elution but no selectivity.

Secondary elution tested the viability of Fe^{3+} elution from resins containing phosphonic and sulfonic groups. Eluents containing high concentrations of H_2SO_4 and HCl did not obtained suitable results for Fe^{3+} elution. Instead, the high acid concentration damaged the physical integrity of the resin. The use of complexing agents of carboxyl nature enhanced the Fe^{3+} elution. Eluents composed of EDTA and oxalic acid achieved

reasonable Fe^{3+} removals without affecting the resin structure. EDTA at 5% w/w achieved close to 99% of Fe^{3+} and Ni^{2+} removals while oxalic acid at 10% w/w obtained 67% of Fe^{3+} and 73% Ni^{2+}. Citric acid did not obtain favourable results for Fe^{3+} elution. Although EDTA outperformed oxalic acid, a compromised Fe-EDTA stability resulted in precipitation at the experimental conditions. Therefore, oxalic acid was selected as best eluent. Although, novel research suggest the fabrication of Fe^{3+} nanoparticles capped with EDTA can be employed for important applications such as the treatment of tumor tissues, contrast agents in magnetic resonance imaging, targeted drug delivery, adsorbents, energy conversion and storage, among others suggesting the economic potential of the by products.

Selective recovery of Ni^{2+} during primary elution showed to be time and temperature dependent favouring selectivity at temperatures of 20° C in periods of 30 min. Meanwhile, Fe^{3+} selectivity in secondary elution resulted from temperatures close to 80°C in periods between 60 and 120 min. Elution studies employing resins with quaternary ammonium, phosphoric acid, and aminophosphonic acid groups were unsuccessful using the eluents selected for combination of phosphonic and sulfonic groups. Further studies employing different eluent may obtain satisfactory selective elution for such resins.

The high concentrations of the system made it difficult for the calculations of the thermodynamic characteristics of the adsorption of Fe^{3+} and Ni^{2+} in ion exchange resins with a combination of phosphonic and sulfonic groups. However, approximations of the activity coefficients under the experimental conditions were used to obtain qualitative information. Results showed that the adsorption of Fe^{3+} in ion exchange resins was

favourable. It showed exothermic and exergonic characteristics with positive changes in entropy. These thermodynamic property trends remained constant regardless of the changes in temperature and the presence of Ni^{2+}. In contrast, the adsorption of Ni^{2+} was only favourable in monometallic systems. Ni^{2+} adsorption in systems without Fe^{3+} presented exothermic and exergonic characteristics with positive changes in entropy. However, if Fe^{3+} was present in the system, the changes in entropy for Ni^{2+} adsorption tended to negative values while the Gibbs energy were positive, that is the adsorption was not favourable. These observations confirmed the low adsorption percentages of Ni^{2+} in Ni_{Fe} systems compared to those obtained in $Ni_{Ø}$ systems.

PSO model best described the Fe^{3+} absorption rate among other kinetic models such as PFO, Elovich equation, and IPD. The results obtained were in accordance with other results found in the literature. Nonetheless, the degree of correlation decreased between PSO in linear and non-linear form suggesting that unknown transport phenomena not described by the model impact the adsorption rate. It is possible that the discrepancies of all the reaction kinetic models are due to high concentrations of the system. Since it was not possible to obtain reliable data for the heat of adsorption, it was not possible to identify chemisorption or physisorption as main adsorption mechanism. However, due to the low correlation of Elovich equations it was possible to assume that adsorption on ion exchange resins are not due chemisorption. Data fitting with IPD equation also suggests that metal adsorption by resins with a combination of phosphonic and sulfonic groups is governed by more than one transport phenomenon. To determine the transport phenomena governing the reaction kinetics, further experiments are recommended.

Overall, the results obtained suggest ion exchange as a potential alternative to iron precipitation in nickel purification processes. Given the results obtained at the given experimental conditions, ion exchange could be applicable to process beneficiating Ni from either sulfide or laterite type ores. However, further experimentations among the best performers is essential to conclude potential of high purity iron sub-production. Likewise, further economic studies are required to determine the cost benefit of increased operative cost by ion exchange compared to reduced environmental footprint and reduction of solid handling in Fe^{3+} removal by precipitation following trends of zero waste production and green mining approaches.

References

Abbas, Z., Ahlberg, E., 2019. Activity Coefficients of Concentrated Salt Solutions: A Monte Carlo Investigation. J. Solution Chem. 48, 1222–1243. https://doi.org/10.1007/s10953-019-00905-y

Agatzini-Leonardou, S., Tsakiridis, P.E., Oustadakis, P., Karidakis, T., Katsiapi, A., 2009. Hydrometallurgical process for the separation and recovery of nickel from sulphate heap leach liquor of nickeliferrous laterite ores. Miner. Eng. 22, 1181–1192.

Aghazadeh, M., Karimzadeh, I., Ganjali, M.R., 2017. Ethylenediaminetetraacetic acid capped superparamagnetic iron oxide (Fe3O4) nanoparticles: A novel preparation method and characterization. J. Magn. Magn. Mater. 439, 312–319. https://doi.org/10.1016/j.jmmm.2017.05.042

Aharoni, C., Tompkins, F.C., 1970. Kinetics of Adsorption and Desorption and the Elovich Equation. Adv. Catal. 21, 1–49. https://doi.org/10.1016/S0360-0564(08)60563-5

Akita, S., Maeda, T., Takeuchi, H., 1994. Metal Sorption Characteristics of a Macromolecular Resin Containing D2EHPA. J. Chem. Eng. Japan 27, 126–129.

Akkaya, R., Ulusoy, U., 2008. Adsorptive features of chitosan entrapped in polyacrylamide hydrogel for Pb 2+, UO 2 2+, and Th 4+. J. Hazard. Mater. 151, 380–388.

Alexandratos, S.D., 2007. New polymer-supported ion-complexing agents: Design, preparation and metal ion affinities of immobilized ligands. J. Hazard. Mater. 139, 467–470.

Alexandratos, S.D., 1988. Design and development of polymer-based separations: dual mechanism bifunctional polymers as a new category of metal ion complexing agents with enhanced ionic recognition. Sep. Purif. Methods 17, 67–102.

Alexandratos, S.D., Smith, S.D., 2004. High stability solvent impregnated resins: Metal ion complexation as a function of time. Solvent Extr. ion Exch. 22, 713–720.

Aly, M.M., Hamza, M.F., 2013. A review: studies on uranium removal using different techniques. Overview. J. Dispers. Sci. Technol. 34, 182–213.

Antola, O., Holappa, L., Paschen, P., 1995. Nickel Ore Reduction by Hydrogen and Carbon Monoxide Containing Gases. Miner. Process. Extr. Metall. Rev. 15, 169–179. https://doi.org/10.1080/08827509508914195

Arroyo-Torralvo, F., Rodríguez-Almansa, A., Ruiz, I., González, I., Ríos, G., Fernández-Pereira, C., Vilches-Arenas, L.F., 2017. Optimizing operating conditions in an ion-exchange column treatment applied to the removal of Sb and Bi impurities from an electrolyte of a copper electro-refining plant. Hydrometallurgy 171, 285–297. https://doi.org/10.1016/j.hydromet.2017.06.009

Ay, U., Čundeva, K., Akçin, G., Stafilov, T., Zajkova, V.P., Pavlovska, G., 2004. Cobalt(III) Hexamethylenedithiocarbamate as a New Collector for Flotation Preconcentration of Iron, Nickel, Lead, and Zinc Prior to ETAAS. Anal. Lett. 37, 695–710. https://doi.org/10.1081/AL-120029746

Bachiller, D., Torre, M., Rendueles, M., Dıaz, M., 2004. Cyanide recovery by ion exchange from gold ore waste effluents containing copper. Miner. Eng. 17, 767–774.

Bacon, G., Mihaylov, I., 2002. Solvent extraction as an enabling technology in the nickel industry. J. South. African Inst. Min. Metall. 102, 435–443.

Bari, F., Begum, N., Jamaludin, S.B., Hussin, K., 2009. Extraction and separation of Cu (II), Ni (II) and Zn (II) by sol–gel silica immobilized with Cyanex 272. Hydrometallurgy 96, 140–147.

Bayramoglu, G., Arica, M.Y., Liman, G., Celikbicak, O., Salih, B., 2016. Removal of bisphenol A from aqueous medium using molecularly surface imprinted microbeads. Chemosphere 150, 275–284. https://doi.org/10.1016/j.chemosphere.2016.02.040

Bellamy, L.J., 1975. The Infrared Spectra of Complex Molecules. Halsted Press, a division of John Wiley & Sons, Inc., New York, USA.

Benamor, M., Bouariche, Z., Belaid, T., Draa, M.T., 2008. Kinetic studies on cadmium ions by Amberlite XAD7 impregnated resins containing di (2-ethylhexyl) phosphoric acid as extractant. Sep. Purif. Technol. 59, 74–84.

Benkhedda, K., Larivière, D., Scott, S., Evans, D., 2005. Hyphenation of flow injection on-line preconcentration and ICP-MS for the rapid determination of 226 Ra in natural waters. J. Anal. At. Spectrom. 20, 523–528.

Bhattacharjee, S., Gupta, K.K., Chakravarty, S., Thakur, P., Bhattacharyya, G., 2005. Separation of Iron, Nickel, and Cobalt from Sulphated Leach Liquor of Low Nickel Lateritic Oxide Ore. Sep. Sci. Technol. 39, 413–429. https://doi.org/10.1081/SS-120027566

Blanchard, G., Maunaye, M., Martin, G., 1984. Removal of heavy metals from waters by means of natural zeolites. Water Res. 18, 1501–1507. https://doi.org/10.1016/0043-1354(84)90124-6

Breguncci, V., 2001. Gold recovery from alkaline cyanide solutions by electrochemical elution of strong-base anionic polymeric resins. Miner. Metall. Process. 18, 49–53.

Çetintaş, S., Bingöl, D., 2018. Selective nickel recovery from iron-rich solutions. Sep. Sci. Technol. 53, 559–566. https://doi.org/10.1080/01496395.2017.1391289

Chang, Y., Zhai, X., Li, B., Fu, Y., 2010. Removal of iron from acidic leach liquor of lateritic nickel ore by goethite precipitate. Hydrometallurgy 101, 84–87.

Chiariza, R., Horwitz, E.P., Aleksandratos, S.D., Gula, M.J., 1997. Diphonix® resin: a review of its properties and applications. Sep. Sci. Technol. 32, 1–35.

Chouyyok, W., Pittman, J.W., Warner, M.G., Nell, K.M., Clubb, D.C., Gill, G.A., Addleman, R.S., 2016. Surface functionalized nanostructured ceramic sorbents for the effective collection and recovery of uranium from seawater. Dalt. Trans. 45, 11312–11325.

Colella, M.B., Siggia, S., Barnes, R.M., 1980. Synthesis and characterization of a poly(acrylamidoxime) metal chelating resin. Anal. Chem. 52, 967–972. https://doi.org/10.1021/ac50056a044

Cortina, J.L., Meinhardt, E., Roijals, O., Marti, V., 1998. Modification and preparation of polymeric adsorbents for precious-metal extraction in hydrometallurgical processes. React. Funct. Polym. 36, 149–165.

Cortina, J.L., Miralles, N., Aguilar, M., Sastre, A.M., 1994. SOLVENT IMPREGNATED

RESINS CONTAINING DI-(2-ETHYLHEXYL) PHOSPHORIC ACID. I. PREPARATION AND STUDY OF THE RETENTION AND DISTRIBUTION OF THE EXTRACTANT ON THE RESIN. Solvent Extr. Ion Exch. 12, 349–369.

Cortina, J.L., Miralles, N., Sastre, A.M., Aguilar, M., 1997. Solid-liquid extraction studies of divalent metals with impregnated resins containing mixtures of organophosphorus extractants. React. Funct. Polym. 32, 221–229.

Cortina, J.L., Miralles, N., Sastre, A.M., Aguilar, M., 1995. Solid-liquid extraction studies of Zn (II), Cu (II) and Cd (II) from chloride media with impregnated resins containing mixtures of organophosphorus compounds immobilized on to Amberlite XAD2. Hydrometallurgy 37, 301–322.

Cortina, J.L., Miralles, N., Sastre, A.M., Aguilar, M., Profumo, A., Pesavento, M., 1993. Solvent-impregnated resins containing di-(2, 4, 4-trimethylpentyl) phosphinic acid II. Study of the distribution equilibria of Zn (II), Cu (II) and Cd (II). React. Polym. 21, 103–116.

Dabrowski, A., Hubicki, Z., Podkościelny, P., Robens, E., 2004. Selective removal of the heavy metal ions from waters and industrial wastewaters by ion-exchange method. Chemosphere 56, 91–106.

Dai, X., Breuer, P.L., Jeffrey, M.I., 2010. Comparison of activated carbon and ion-exchange resins in recovering copper from cyanide leach solutions. Hydrometallurgy 101, 48–57.

Dai, X., Simons, A., Breuer, P., 2012. A review of copper cyanide recovery technologies for the cyanidation of copper containing gold ores. Miner. Eng. 25, 1–13.

Davidescu, C.M., Ciopec, M., Negrea, A., Popa, A., Lupa, L., Dragan, E.S., Ardelean, R., Ilia, G., Iliescu, S., 2013. Synthesis, characterization, and Ni(II) ion sorption properties of poly(styrene-co-divinylbenzene) functionalized with aminophosphonic acid groups. Polym. Bull. 70, 277–291. https://doi.org/10.1007/s00289-012-0801-3

Dicinoski, G.W., 2000. Novel resins for the selective extraction of gold from copper rich ores. South African J. Chem. 53.

Dingman Jr, J.F., Gloss, K.M., Milano, E.A., Siggia, S., 1974. Concentration of heavy metals by complexation on dithiocarbamate resins. Anal. Chem. 46, 774–777.

Diniz, C. V, Ciminelli, V.S.T., Doyle, F.M., 2005. The use of the chelating resin Dowex M-4195 in the adsorption of selected heavy metal ions from manganese solutions. Hydrometallurgy 78, 147–155.

Diniz, C. V, Doyle, F.M., Ciminelli, V.S.T., 2002. Effect of pH on the adsorption of selected heavy metal ions from concentrated chloride solutions by the chelating resin Dowex M-4195. Sep. Sci. Technol. 37, 3169–3185.

Diniz, C. V, Doyle, P.M., Martins, A.H., 2000. Uptake of heavy metals by chelating resins from acidic manganese chloride solution. Miner. Metall. Process. 17, 217–222.

Dizge, N., Keskinler, B., Barlas, H., 2009. Sorption of Ni (II) ions from aqueous solution by Lewatit cation-exchange resin. J. Hazard. Mater. 167, 915–926.

Drozdzak, J., Leermakers, M., Gao, Y., Phrommavanh, V., Descostes, M., 2015. Evaluation and application of Diffusive Gradients in Thin Films (DGT) technique using Chelex®-100, Metsorb^{TM} and Diphonix® binding phases in uranium mining environments. Anal. Chim. Acta 889, 71–81.

Duprey, A., Chansavang, V., Frémion, F., Gonthier, C., Louis, Y., Lejeune, P., Springer, F., Desjardin, V., Rodrigue, A., Dorel, C., 2014. “NiCo Buster”: engineering E. coli for fast and efficient capture of cobalt and nickel. J. Biol. Eng. 8, 19.

DybczyŃski, R., Hubicki, Z., Kulisa, K., 1988. ION EXCHANGE BEHAVIOUR OF 23 ELEMENTS AND AMPHOTERIC PROPERTIES OF CHELATING RESIN DUOLITE ES 346 CONTAINING AMIDOXIME GROUPS. Solvent Extr. Ion Exch. 6, 699–724. https://doi.org/10.1080/07366298808917961

Dyson, N.F., Scott, T.R., 1976. Acid leaching of nickel sulphide concentrates. Hydrometallurgy 1, 361–372. https://doi.org/10.1016/0304-386X(76)90037-2

Fakhar, I., Yamin, B.M., Hasbullah, S.A., 2017. A comparative study of the metal binding behavior of alanine based bis-thiourea isomers. Chem. Cent. J. 11, 76.

Fedyukevich, V.A., Kubyshkin, S.A., Blokhin, A.A., Sukharzhevskii, S.M., Vorob’ev-Desyatovskii, N. V, 2015. Use of ion-exchange resins to deal with the effect of preg-robbing of gold in the course of cyanide leaching. Russ. J. Appl. Chem. 88, 250–258.

Fedyukevich, V.A., Vorob’ev-Desyatovskii, N. V, 2016. Advantages and disadvantages of various kinds of adsorbents used in industrial extraction of [Au (CN) 2. Russ. J. Appl. Chem. 89, 577–582.

Fernando, K., Tran, T., Laing, S., Kim, M.J., 2002. The use of ion exchange resins for the treatment of cyanidation tailings part 1—process development of selective base metal elution. Miner. Eng. 15, 1163–1171.

Flett, D.S., 2004. Cobalt-nickel separation in hydrometallurgy: a review. Chem. Sustain. Dev. 12, 81–91.

Free, M.L., 2013. Hydrometallurgy: fundamentals and applications. John Wiley & Sons.

Galán, B., Castañeda, D., Ortiz, I., 2005. Removal and recovery of Cr (VI) from polluted ground waters: a comparative study of ion-exchange technologies. Water Res. 39, 4317–4324.

Gao, X., Hu, Y., Guo, T., Ye, X., Li, Q., Guo, M., Liu, H., Wu, Z., 2013. Comparative Study of the Competitive Adsorption of Mg, Ca and Sr Ions onto Resins. Adsorpt. Sci. Technol. 31, 45–58.

Gao, X., Zhang, Y., Zhao, Y., 2018a. Modelling and experimental investigation of the adsorption breakthrough behaviors of Pd (II) and Cu (II) by ETA microspheres. J. Chem. Technol. Biotechnol. 93, 3526–3534. https://doi.org/10.1002/jctb.5725

Gao, X., Zhang, Y., Zhao, Y., 2018b. Zinc oxide templating of porous alginate beads for the recovery of gold ions. Carbohydr. Polym. 200, 297–304. https://doi.org/10.1016/j.carbpol.2018.07.097

Gibert, O., Valderrama, C., Peterkova, M., Cortina, J.L., 2010. Evaluation of selective sorbents for the extraction of valuable metal ions (Cs, Rb, Li, U) from reverse osmosis rejected brine. Solvent Extr. Ion Exch. 28, 543–562.

Glover, M.R.L., Young, B.D., Bryson, A.W., 1990. Modelling the binary adsorption of gold and zinc cyanides onto a strong-base anion exchange resin. Int. J. Miner. Process. 30, 217–228.

Gode, F., Pehlivan, E., 2003. A comparative study of two chelating ion-exchange resins for the removal of chromium(III) from aqueous solution. J. Hazard. Mater. 100, 231–243. https://doi.org/10.1016/S0304-3894(03)00110-9

Gomez, L.M., Colpas-Castillo, F., Fernandez-Maestre, R., 2014. Cation exchange for mercury and cadmium of xanthated, sulfonated, activated and non-treated subbituminous coal, commercial activated carbon and commercial synthetic resin: effect of pre-oxidation on xanthation of subbituminous coal. Int. J. Coal Sci. Technol. 1, 235–240.

Grosse, A.C., Dicinoski, G.W., Shaw, M.J., Haddad, P.R., 2003. Leaching and recovery of gold using ammoniacal thiosulfate leach liquors (a review). Hydrometallurgy 69, 1–21.

Guo, H., Zhang, S., Kou, Z., Zhai, S., Ma, W., Yang, Y., 2015. Removal of cadmium(II) from aqueous solutions by chemically modified maize straw. Carbohydr. Polym. 115, 177–185. https://doi.org/10.1016/j.carbpol.2014.08.041

Gupta, V.K., Singh, P., Rahman, N., 2004. Adsorption behavior of Hg (II), Pb (II), and Cd (II) from aqueous solution on Duolite C-433: a synthetic resin. J. Colloid Interface Sci. 275, 398–402.

Haas, K.L., Franz, K.J., 2009. Application of metal coordination chemistry to explore and manipulate cell biology. Chem. Rev. 109, 4921–4960.

Halder, G., Khan, A.A., Dhawane, S., 2016. Fluoride Sorption Onto a Steam-Activated Biochar Derived From *Cocos nucifera* Shell. CLEAN - Soil, Air, Water 44, 124–133. https://doi.org/10.1002/clen.201400649

Harland, C.E., 1994. Ion exchange: theory and practice. Royal society of Chemistry.

Hawari, A.H., Mulligan, C.N., 2006. Biosorption of lead(II), cadmium(II), copper(II) and nickel(II) by anaerobic granular biomass. Bioresour. Technol. 97, 692–700.

https://doi.org/10.1016/j.biortech.2005.03.033

He, X., Fang, Z., Jia, J., Ma, L., Li, Y., Chai, Z., Chen, X., 2016. Study on the treatment of wastewater containing Cu (II) by D851 ion exchange resin. Desalin. Water Treat. 57, 3597–3605.

Helfferich, F.G., 1962. Ion exchange. Courier Corporation.

Ho, Y.S., McKay, G., 1998. A Comparison of chemisorption kinetic models applied to pollutant removal on various sorbents. Process Saf. Environ. Prot. 76, 332–340. https://doi.org/10.1205/095758298529696

Horwitz, E.P., Chiarizia, R., Dietz, M.L., 1997. Dipex: A new extraction chromatographic material for the separation and preconcentration of actinides from aqueous solution. React. Funct. Polym. 33, 25–36.

Hubicki, Z., 1986. Purification of nickel sulfate using chelating ion exchangers and weak-base anion exchangers. Hydrometallurgy 16, 361–375. https://doi.org/10.1016/0304-386X(86)90010-1

Hubicki, Z., Wójcik, G., 2004. Studies of the selective removal of microquantities of platinum (IV) ions from model chloride solutions onto ion exchangers containing functional tertiary amine and polyamine groups. Adsorpt. Sci. Technol. 22, 627–637.

Hubicki, Z., Wołowicz, A., 2009. A comparative study of chelating and cationic ion exchange resins for the removal of palladium (II) complexes from acidic chloride media. J. Hazard. Mater. 164, 1414–1419.

Iglesias, M., Antico, E., Salvado, V., 1999. Recovery of palladium (II) and gold (III) from diluted liquors using the resin duolite GT-73. Anal. Chim. Acta 381, 61–67.

INCO, 2006. Voisey's Bay - Newest Jewel in Inco's Crown. Int. Min. 7–8.

Inglezakis, V.J., Zorpas, A.A., 2012. Heat of adsorption, adsorption energy and activation energy in adsorption and ion exchange systems. Desalin. Water Treat. 39, 149–157. https://doi.org/10.1080/19443994.2012.669169

Izaki, M., 2010. Electrodeposition of iron and iron alloys. Mod. Electroplat. 5.

Jermakowicz-Bartkowiak, D., Kolarz, B.N., Serwin, A., 2005. Sorption of precious metals from acid solutions by functionalised vinylbenzyl chloride–acrylonitryle–divinylbenzene copolymers bearing amino and guanidine ligands. React. Funct. Polym. 65, 135–142.

Jing, X., Liu, F., Yang, X., Ling, P., Li, L., Long, C., Li, A., 2009. Adsorption performances and mechanisms of the newly synthesized N, N′-di (carboxymethyl) dithiocarbamate chelating resin toward divalent heavy metal ions from aqueous media. J. Hazard. Mater. 167, 589–596.

Juang, R.-S., 1999. Preparation, properties and sorption behavior of impregnated resins containing acidic organophosphorus extractants, in: PROC NATL SCI COUNC REPUB CHINA PART A PHYS SCI ENG. pp. 353–364.

Juang, R.S., Chen, M.L., 1997. Application of the Elovich Equation to the Kinetics of Metal Sorption with Solvent-Impregnated Resins. Ind. Eng. Chem. Res. 36, 813–820. https://doi.org/10.1021/ie960351f

Jurrius, Y., Sole, K.C., Hardwick, E., 2014. Removal of copper and zinc from a cobalt electrolyte by ion exchange at Kamoto Copper Company ' s Luilu plant, in: Hydrometallurgy 2014 : Proceedings of the 7th International Symposium on

Hydrometallurgy. Vol 2. Canadian Institute of Mining, Metallurgy and Petroleum, Victoria BC, Canada, pp. 281–295.

Kabay, N., Demircioğlu, M., Yaylı, S., Günay, E., Yüksel, M., Sağlam, M., Streat, M., 1998. Recovery of uranium from phosphoric acid solutions using chelating ion-exchange resins. Ind. Eng. Chem. Res. 37, 1983–1990.

Kabay, N., Egawa, H., 1994. Chelating Polymers for Recovery of Uranium from Seawater∗. Sep. Sci. Technol. 29, 135–150.

Kagaya, S., Gemmei-Ide, M., Inoue, Y., 2014. Chelating Resins, in: Encyclopedia of Polymeric Nanomaterials. Springer Berlin Heidelberg, Berlin, Heidelberg, pp. 1–10. https://doi.org/10.1007/978-3-642-36199-9_206-1

Kaušpėdienė, D., Snukiškis, J., Gefenienė, A., 1998. Simultaneous purification of sewage from Cd (II) and nonionic surfactant with cation exchanger. J. Radioanal. Nucl. Chem. 229, 129-A133.

Kerr, A., 2008. Mineral Commodities of Newfoundland and Labrador -Nickel. St. John's, NL, Canada.

Kholkin, A.I., Pashkov, G.L., Belova, V. V., 2000. Binary extraction in hydrometallurgy. Miner. Process. Extr. Metall. Rev. 21, 217–248. https://doi.org/10.1080/08827500008914169

Kiefer, R., Höll, W.H., 2001. Sorption of heavy metals onto selective ion-exchange resins with aminophosphonate functional groups. Ind. Eng. Chem. Res. 40, 4570–4576.

Kielland, J., 1937. Individual Activity Coefficients of Ions in Aqueous Solutions. J. Am. Chem. Soc. 59, 1675–1678. https://doi.org/10.1021/ja01288a032

Kim, S.J., Lim, K.H., Park, Y.G., Kim, J.H., Cho, S.Y., 2001. Simultaneous removal and recovery of cadmium and cyanide ions in synthetic wastewater by ion exchange. Korean J. Chem. Eng. 18, 686–691.

Koivula, R., Lehto, J., Pajo, L., Gale, T., Leinonen, H., 2000. Purification of metal plating rinse waters with chelating ion exchangers. Hydrometallurgy 56, 93–108.

Kołodyńska, D., Fila, D., Hubicki, Z., 2020. Evaluation of possible use of the macroporous ion exchanger in the adsorption process of rare earth elements and heavy metal ions from spent batteries solutions. Chem. Eng. Process. - Process Intensif. 147, 107767. https://doi.org/10.1016/j.cep.2019.107767

Kononova, O.N., Kholmogorov, A.G., Danilenko, N. V, Goryaeva, N.G., Shatnykh, K.A., Kachin, S. V, 2007. Recovery of silver from thiosulfate and thiocyanate leach solutions by adsorption on anion exchange resins and activated carbon. Hydrometallurgy 88, 189–195.

Korkisch, J., 1988. CRC Handbook of Ion Exchange Resins. CRC Press.

Kotze, M., Green, B., Mackenzie, J., Virnig, M., 2005. Resin-in-pulp and resin-in-solution. Dev. Miner. Process. 15, 603–635.

Kramer, J., Dhladhla, N.E., Koch, K.R., 2006. Guanidinium functionalised silica-based anion exchangers significantly improve the selectivity of platinum group metal recovery from process solutions. Sep. Purif. Technol. 49, 181–185.

Kurama, H., Çatalsarik, T., 2000. Removal of zinc cyanide from a leach solution by an anionic ion-exchange resin. Desalination 129, 1–6.

Kusku, O., Rivas, B.L., Urbano, B.F., Arda, M., Kabay, N., Bryjak, M., 2014. A

comparative study of removal of Cr (VI) by ion exchange resins bearing quaternary ammonium groups. J. Chem. Technol. Biotechnol. 89, 851–857.

Lagergren, S., 1898. About the theory of so-called adsorption of soluble substances. K. Sven. Vetensk. Handl. 4, 1–39.

Lashley, M.A., Mehio, N., Nugent, J.W., Holguin, E., Do-Thanh, C.-L., Bryantsev, V.S., Dai, S., Hancock, R.D., 2016. Amidoximes as ligand functionalities for braided polymeric materials for the recovery of uranium from seawater. Polyhedron 109, 81–91. https://doi.org/10.1016/J.POLY.2016.01.026

Lawrance, G.A., 2013. Introduction to coordination chemistry. John Wiley & Sons.

Leao, V.A., Ciminelli, V.S.T., Costa, R. de S., 1998. Cyanide recycling using strong-base ion-exchange resins. JOM J. Miner. Met. Mater. Soc. 50, 66–69.

Lee, S.-K., Lee, U.-H., 2016. Adsorption and desorption property of iminodiacetate resin (Lewatit® TP207) for indium recovery. J. Ind. Eng. Chem. 40, 23–25.

Lezzi, A., Cobianco, S., 1994. Chelating resins supporting dithiocarbamate and methylthiourea groups in adsorption of heavy metal ions. J. Appl. Polym. Sci. 54, 889–897.

Li, T., Guo, C., Xie, T., Zhou, C., Zhang, Y., 2015. Preparation of quaternary ammonium–Chlorella vulgaris and its adsorption of Ag (CN) 2−. Water Sci. Technol. 72, 1437–1445.

Littlejohn, P., Vaughan, J., 2014. Selective elution of nickel and cobalt from iminodiacetic acid cation exchange resin using ammoniacal solutions. Hydrometallurgy 141, 24–30. https://doi.org/10.1016/j.hydromet.2013.10.009

Liu, H., Li, F., Xu, B., Zhang, G., Han, F., Zhou, Y., Xin, X., Xu, B., 2012. Synthesis, Characterization and Properties of New Lauryl Amidopropyl Trimethyl Ammoniums. J. Surfactants Deterg. 15, 709–713. https://doi.org/10.1007/s11743-012-1350-3

Liu, Y., 2009. Is the free energy change of adsorption correctly calculated? J. Chem. Eng. Data 54, 1981–1985. https://doi.org/10.1021/je800661q

Lukey, G.C., Van Deventer, J.S.J., Chowdhury, R.L., Shallcross, D.C., 1999. The effect of salinity on the capacity and selectivity of ion exchange resins for gold cyanide. Miner. Eng. 12, 769–785.

Lukey, G.C., Van Deventer, J.S.J., Shallcross, D.C., 2000. The effect of functional group structure on the elution of metal cyanide complexes from ion-exchange resins. Sep. Sci. Technol. 35, 2393–2413.

Lv, R., Hu, Y., Jia, Z., Li, R., Zhang, X., Liu, J., Fan, C., Feng, J., Zhang, L., Wang, Z., 2019. Removal of Fe3+ and Al3+ ions from phosphoric acid–nitric acid solutions with chelating resins. Hydrometallurgy 188, 194–200. https://doi.org/10.1016/j.hydromet.2019.07.005

Manov, G.G., Bates, R.G., Hamer, W.J., Agree, S.F., 1943. Values of the Constants in the Debye—Hückel Equation for Activity Coefficients. J. Am. Chem. Soc. 65, 1765–1767. https://doi.org/10.1021/ja01249a028

Maranon, E., Suárez, F., Alonso, F., Fernández, Y., Sastre, H., 1999. Preliminary study of iron removal from hydrochloric pickling liquor by ion exchange. Ind. Eng. Chem. Res. 38, 2782–2786.

Martell, A.E., Hancock, R.D., 2013. Metal complexes in aqueous solutions. Springer

Science & Business Media.

McKevitt, B., Dreisinger, D., 2012. Development of an engineering model for nickel loading onto an iminodiacetic resin for resin-in-pulp applications: Part I—Method development and discussion of rate limiting factors. Hydrometallurgy 121, 35–44.

McKevitt, B., Dreisinger, D., 2009. A comparison of various ion exchange resins for the removal of ferric ions from copper electrowinning electrolyte solutions part I: Electrolytes containing no other impurities. Hydrometallurgy 98, 116–121. https://doi.org/10.1016/j.hydromet.2009.04.008

Mensah-Biney, R., Reid, K.J., Hepworth, M.T., 1995. The loading capacity of selected cation exchange resins and activated carbons for gold-thiourea complex. Miner. Eng. 8, 125–146.

Meshram, P., Abhilash, Pandey, B.D., 2019. Advanced Review on Extraction of Nickel from Primary and Secondary Sources. Miner. Process. Extr. Metall. Rev. 40, 157–193. https://doi.org/10.1080/08827508.2018.1514300

Miesiac, I., 2005. Removal of zinc (II) and iron (II) from spent hydrochloric acid by means of anionic resins. Ind. Eng. Chem. Res. 44, 1004–1011.

Monhemius, A., 2016. THE IRON ELEPHANT: A Brief History of Hydrometallurgists' Struggles with Element No. 26. XXVIII Int. Miner. Process. Congr.

Monteagudo, J.M., Ortiz, M.J., 2000. Removal of inorganic mercury from mine waste water by ion exchange. J. Chem. Technol. Biotechnol. 75, 767–772.

Moosavirad, S.M., Sarikhani, R., Shahsavani, E., Mohammadi, S.Z., 2015. Removal of some heavy metals from inorganic industrial wastewaters by ion exchange method. J.

Water Chem. Technol. 37, 191–199.

Mudd, G.M., 2010. Global trends and environmental issues in nickel mining: Sulfides versus laterites. Ore Geol. Rev. 38, 9–26.

Müller, G., Janošková, K., Bakalár, T., Cakl, J., Jiránková, H., 2012. Removal of Zn (II) from aqueous solutions using Lewatit S1468. Desalin. Water Treat. 37, 146–151.

Nagib, S., Inoue, K., Yamaguchi, T., Tamaru, T., 1999. Recovery of Ni from a large excess of Al generated from spent hydrodesulfurization catalyst using picolylamine type chelating resin and complexane types of chemically modified chitosan. Hydrometallurgy 51, 73–85.

National Resources Canada, 2020. Nickel facts [WWW Document]. Nat. Resour. Canada. URL https://www.nrcan.gc.ca/our-natural-resources/minerals-mining/minerals-metals-facts/nickel-facts/20519 (accessed 2.2.20).

Navarro, R., Gallardo, V., Saucedo, I., Guibal, E., 2009. Extraction of Fe (III) from hydrochloric acid solutions using Amberlite XAD-7 resin impregnated with trioctylphosphine oxide (Cyanex 921). Hydrometallurgy 98, 257–266.

Nayl, A.A., 2010. Extraction and separation of Co(II) and Ni(II) from acidic sulfate solutions using Aliquat 336. J. Hazard. Mater. 173, 223–230. https://doi.org/10.1016/j.jhazmat.2009.08.072

Nickel Institute, 2018. About nickel [WWW Document]. Nickel Inst. URL https://nickelinstitute.org/about-nickel/ (accessed 2.2.20).

Nikoloski, A.N., Ang, K.-L., 2014. Review of the application of ion exchange resins for the recovery of platinum-group metals from hydrochloric acid solutions. Miner.

Process. Extr. Metall. Rev. 35, 369–389.

Nikoloski, A.N., Ang, K.-L., Li, D., 2015. Recovery of platinum, palladium and rhodium from acidic chloride leach solution using ion exchange resins. Hydrometallurgy 152, 20–32.

NIST, 2013. Critically Selected Stability Constants of Metal Complexes [WWW Document]. Crit. Sel. Stab. Constants Met. Complexes Database Version 8.0. URL https://www.nist.gov/srd/nist46 (accessed 1.28.20).

Nomngongo, P.N., Ngila, J.C., Kamau, J.N., Msagati, T.A.M., Marjanovic, L., Moodley, B., 2013. Pre-concentration of trace elements in short chain alcohols using different commercial cation exchange resins prior to inductively coupled plasma-optical emission spectrometric detection. Anal. Chim. Acta 787, 78–86.

O'Connell, D.W., Birkinshaw, C., O'Dwyer, T.F., 2008. Heavy metal adsorbents prepared from the modification of cellulose: A review. Bioresour. Technol. 99, 6709–6724.

Okewole, A.I., Antunes, E., Nyokong, T., Tshentu, Z.R., 2013. The development of novel nickel selective amine extractants: 2, 2′-Pyridylimidazole functionalised chelating resin. Miner. Eng. 54, 88–93.

Parus, A., Wieszczycka, K., Olszanowski, A., 2010. Solvent extraction of iron (III) from chloride solutions in the presence of copper (II) and zinc (II) using hydrophobic pyridyl ketoximes. Sep. Sci. Technol. 46, 87–93.

Pearson, R.G., 1963. Hard and soft acids and bases. J. Am. Chem. Soc. 85, 3533–3539.

Petersková, M., Valderrama, C., Gibert, O., Cortina, J.L., 2012. Extraction of valuable metal ions (Cs, Rb, Li, U) from reverse osmosis concentrate using selective sorbents.

Desalination 286, 316–323.

Podkościelna, B., Kołodyńska, D., 2013. A new type of cation-exchange polymeric microspheres with pendant methylenethiol groups. Polym. Adv. Technol. 24, 866–872.

Rahman, L., Sarkar, S.M., Yusoff, M.M., Abdullah, H., 2016. Efficient removal of transition metal ions using poly(amidoxime) ligand from polymer grafted kenaf cellulose †. https://doi.org/10.1039/c5ra18502e

Rengaraj, S., Yeon, J.W., Kim, Y., Jung, Y., Ha, Y.K., Kim, W.H., 2007. Adsorption characteristics of Cu(II) onto ion exchange resins 252H and 1500H: Kinetics, isotherms and error analysis. J. Hazard. Mater. 143, 469–477. https://doi.org/10.1016/j.jhazmat.2006.09.064

Rivas, B.L., Maturana, H.A., Villegas, S., 2000. Adsorption behavior of metal ions by amidoxime chelating resin. J. Appl. Polym. Sci. 77, 1994–1999. https://doi.org/10.1002/1097-4628(20000829)77:9<1994::AID-APP15>3.0.CO;2-P

Riveros, P.A., 2010. The removal of antimony from copper electrolytes using amino-phosphonic resins: Improving the elution of pentavalent antimony. Hydrometallurgy 105, 110–114.

Riveros, P.A., 2004. The extraction of Fe (III) using cation-exchange carboxylic resins. Hydrometallurgy 72, 279–290.

Rodrigues, A.E., 1986. Ion exchange: science and technology. Springer Science & Business Media.

Rosato, L., Harris, G.B., Stanley, R.W., 1984. Separation of nickel from cobalt in sulphate

medium by ion exchange. Hydrometallurgy 13, 33–44.

Saha, B., Iglesias, M., Dimming, I.W., Streat, M., 2000. Sorption of trace heavy metals by thiol containing chelating resins. Solvent Extr. Ion Exch. 18, 133–167.

Sahu, K.K., Das, R.P., 2000. Mixed solvent systems for the extraction and stripping of iron(III) from concentrated acid chloride solutions. Metall. Mater. Trans. B Process Metall. Mater. Process. Sci. 31, 1169–1174. https://doi.org/10.1007/s11663-000-0003-5

Salvestrini, S., Leone, V., Iovino, P., Canzano, S., Capasso, S., 2014. Considerations about the correct evaluation of sorption thermodynamic parameters from equilibrium isotherms. J. Chem. Thermodyn. 68, 310–316. https://doi.org/10.1016/j.jct.2013.09.013

Sharma, Y.C., Gupta, G.S., Prasad, G., Rupainwar, D.C., 1990. Use of wollastonite in the removal of Ni(II) from aqueous solutions. Water. Air. Soil Pollut. 49, 69–79. https://doi.org/10.1007/BF00279511

Silva, R.A., Hawboldt, K., Zhang, Y., 2018. Application of resins with functional groups in the separation of metal ions/species–a review. Miner. Process. Extr. Metall. Rev. 39, 395–413. https://doi.org/10.1080/08827508.2018.1459619

Silva, R.A., Zhang, Y., Hawboldt, K., James, L., Saunders, W., 2018. Selective Separation of Iron from Simulated Nickel Leach Solutions Using Ion Exchange Technology, in: Extraction 2018. Springer, pp. 2161–2172.

Silva, R.A., Zhang, Y., Hawboldt, K., James, L.A., 2019. Study on Iron-nickel Separation Using Ion Exchange Resins with Different Functional Groups for Potential Iron Sub-

production. Miner. Process. Extr. Metall. Rev. 1–15. https://doi.org/https://doi.org/10.1080/08827508.2019.1678155

Skoog, D.A., West, D.M., Holler, F.J., Crouch, S.R., 2014. Fundamentals of Analytical Chemistry, Ninth Editio, Cengage Learning.

Smith, A.G., Tasker, P.A., White, D.J., 2003. The structures of phenolic oximes and their complexes. Coord. Chem. Rev. 241, 61–85.

Smith, R.M., Martell, A.E., 1987. Critical stability constants, enthalpies and entropies for the formation of metal complexes of aminopolycarboxylic acids and carboxylic acids. Sci. Total Environ. 64, 125–147. https://doi.org/10.1016/0048-9697(87)90127-6

Sole, K., Mooiman, M., Edmundhardwick, 2016. Present and future applications of ion exchange in hydrometallurgy: An overview. IEX 2016.

Sole, K.C., Mooiman, M.B., Hardwick, E., 2018. Ion exchange in hydrometallurgical processing: an overview and selected applications. Sep. Purif. Rev. 47, 159–178.

Soylak, M., Elci, L., 1997. Preconcentration and separation of trace metal ions from sea water samples by sorption on amberlite XAD-16 after complexation with sodium diethyl dithiocarbamate. Int. J. Environ. Anal. Chem. 66, 51–59.

Srivastava, S., Rao, G.N., 1990. Separation of palladium (II) from transition elements by using an ion-exchange salicylaldoxime-formaldehyde resin. Analyst 115, 1607–1609.

Stefan, D.S., Meghea, I., 2014. Mechanism of simultaneous removal of Ca 2+, Ni 2+, Pb 2+ and Al 3+ ions from aqueous solutions using Purolite® S930 ion exchange resin. Comptes Rendus Chim. 17, 496–502.

Tran, H.N., You, S.J., Chao, H.P., 2016. Effect of pyrolysis temperatures and times on the

adsorption of cadmium onto orange peel derived biochar. Waste Manag. Res. 34, 129–138. https://doi.org/10.1177/0734242X15615698

Tran, H.N., You, S.J., Hosseini-Bandegharaei, A., Chao, H.P., 2017. Mistakes and inconsistencies regarding adsorption of contaminants from aqueous solutions: A critical review. Water Res. https://doi.org/10.1016/j.watres.2017.04.014

Van Deventer, J., 2011. Selected ion exchange applications in the hydrometallurgical industry. Solvent Extr. Ion Exch. 29, 695–718.

Van Nguyen, N., Lee, J., Jha, M.K., Yoo, K., Jeong, J., 2009. Copper recovery from low concentration waste solution using Dowex G-26 resin. Hydrometallurgy 97, 237–242.

Vasiliu, S., Bunia, I., Racovita, S., Neagu, V., 2011. Adsorption of cefotaxime sodium salt on polymer coated ion exchange resin microparticles: Kinetics, equilibrium and thermodynamic studies. Carbohydr. Polym. 85, 376–387. https://doi.org/10.1016/j.carbpol.2011.02.039

Vaughan, J., Dieters, C., Fu, W., Byrne, K., 2016a. Properties of Lewatit® TP272, a commercial solvent impregnated cation exchange resin for cobalt recovery. Miner. Eng. 88, 2–8. https://doi.org/10.1016/J.MINENG.2015.07.005

Vaughan, J., Dieters, C., Fu, W., Byrne, K., 2016b. Properties of Lewatit® TP272, a commercial solvent impregnated cation exchange resin for cobalt recovery. Miner. Eng. 88, 2–8.

Virolainen, S., Heinonen, J., Paatero, E., 2013. Selective recovery of germanium with N-methylglucamine functional resin from sulfate solutions. Sep. Purif. Technol. 104, 193–199.

Virolainen, S., Laatikainen, M., Sainio, T., 2015. Ion exchange recovery of rhenium from industrially relevant sulfate solutions: Single column separations and modeling. Hydrometallurgy 158, 74–82.

Wachinski, A.M., 2016. Environmental Ion Exchange: Principles and Design. Crc Press.

Wade, L.J., 2006. Organic Chemistry, Chapter 19th: Amines, 6th ed, Pearson Prentice Hall.

Walsh, D.J., Crosby, P., Dalton, R.F., 1983. Metal specific hydroxyoxime ion-exchange resins. Polymer (Guildf). 24, 423–427.

Wang, K., Li, J., McDonald, R.G., Browner, R.E., 2011. The effect of iron precipitation upon nickel losses from synthetic atmospheric nickel laterite leach solutions: statistical analysis and modelling. Hydrometallurgy 109, 140–152.

Weber, W.J., Smith, E.H., 1987. Simulation and design models for adsorption processes. Environ. Sci. Technol. 21, 1040–1050. https://doi.org/10.1021/es00164a002

Whittington, B.I., Muir, D., 2000. Pressure Acid Leaching of Nickel Laterites: A Review. Miner. Process. Extr. Metall. Rev. 21, 527–599. https://doi.org/10.1080/08827500008914177

Wójcik, G., Neagu, V., Bunia, I., 2011. Sorption studies of chromium (VI) onto new ion exchanger with tertiary amine, quaternary ammonium and ketone groups. J. Hazard. Mater. 190, 544–552.

Wołowicz, A., Hubicki, Z., 2012. The use of the chelating resin of a new generation Lewatit MonoPlus TP-220 with the bis-picolylamine functional groups in the removal of selected metal ions from acidic solutions. Chem. Eng. J. 197, 493–508.

Wu, F.C., Tseng, R.L., Juang, R.S., 2009. Characteristics of Elovich equation used for the

analysis of adsorption kinetics in dye-chitosan systems. Chem. Eng. J. 150, 366–373. https://doi.org/10.1016/j.cej.2009.01.014

Xu, X., Gao, B.-Y., Yue, Q.-Y., Zhong, Q.-Q., Li, Q., 2011. Preparation of new types of anion exchange resins from agricultural by-products and their utilization in the removal of various toxic anions from solutions. Chem. Eng. J. 167, 104–111.

YABUTANI, T., SUMI, H., NAKAMURA, T., AKATSUKI, S., THUY, L.T.X., 2012. Multielemental Elution Behavior of Metal Ions Adsorbed on Iminodiacetic Acid Chelating Resin by Using Hydrogen Peroxide as an Eluent. Anal. Sci. 28, 463–468. https://doi.org/10.2116/analsci.28.463

Yoshimura, K., Miyazaki, Y., Ota, F., Matsuokaa, S., Sakashitac, H., 1998. Complexation of boric acid with the N-methyl-D-glucamine group in solution and in crosslinked polymer. J. Chem. Soc., Faraday T rans 94, 683–689.

Zaganiaris, E.J., 2013. Ion exchange resins and adsorbents in chemical processing. BoD-Books on Demand.

Zagorodni, A.A., 2006. Ion exchange materials: properties and applications. Elsevier.

Zhang, P., Guo, Q., Wei, G., Qu, J., Qi, T., 2015. Precipitation of α-Fe 2 O 3 and recovery of Ni and Co from synthetic laterite-leaching solutions. Hydrometallurgy 153, 21–29.

Zhang, X., Zhou, K., Lei, Q., Xing, Y., Peng, C., Chen, W., 2021. Stripping of Fe(III) from Aliquat 336 by NaH2PO4: implication for rare-earth elements recovery from red mud. Sep. Sci. Technol. 56, 301–309. https://doi.org/10.1080/01496395.2020.1713814

Zhang, Y., Liu, Q., Li, L., 2016. Removal of iron from sythetic copper leach solution using a hydroxy-oxime chelating resin. Hydrometallurgy 164, 154–158.

https://doi.org/10.1016/J.HYDROMET.2016.06.004

Zhu, X., Alexandratos, S.D., 2005. Affinity and selectivity of immobilized N-methyl-d-glucamine for mercury (II) ions. Ind. Eng. Chem. Res. 44, 7490–7495.